Cardiovascular Psychiatry and Neurology

Blood-Brain Barrier Breakdown and Blood-Brain Communication in Neurological and Psychiatric Diseases

Guest Editors: Alon Friedman and Daniela Kaufer

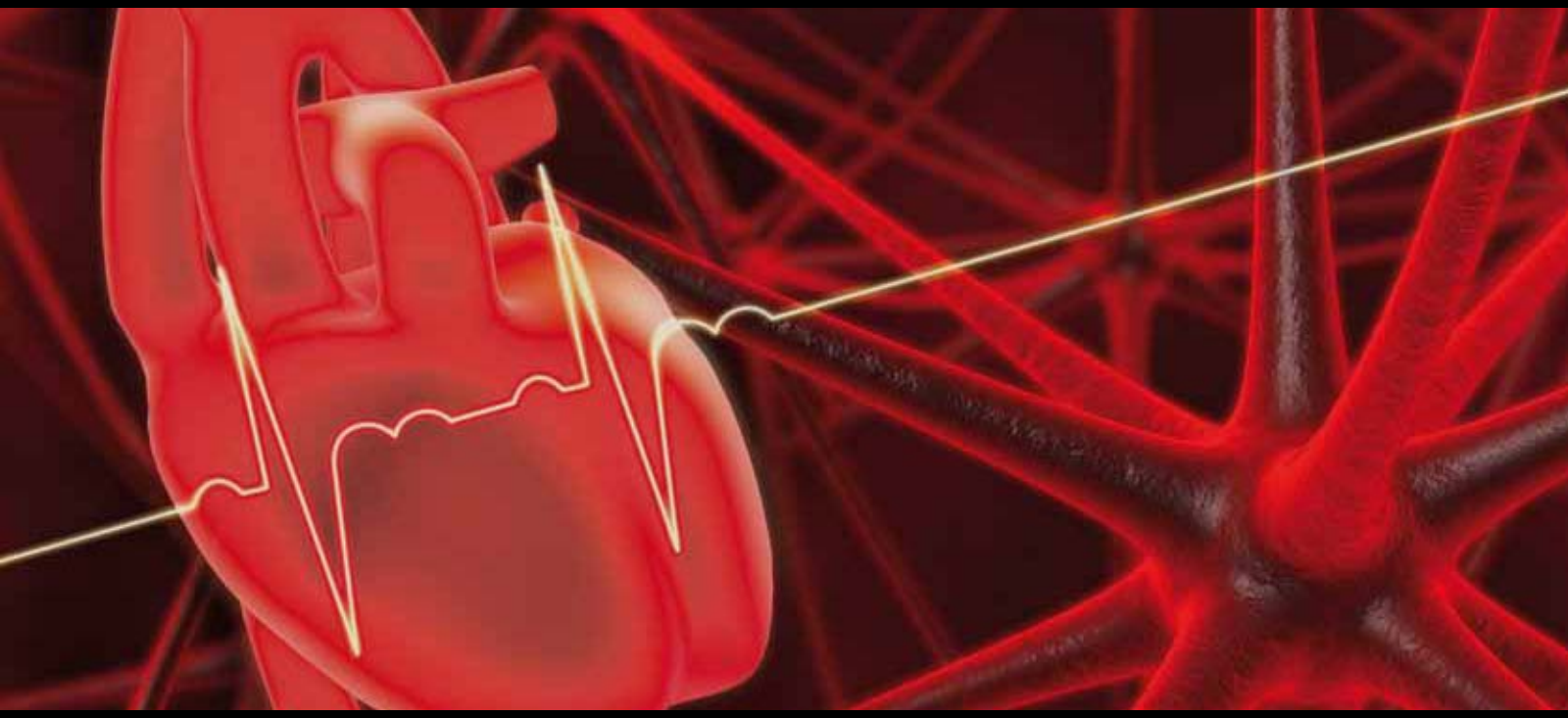

Blood-Brain Barrier Breakdown and Blood-Brain Communication in Neurological and Psychiatric Diseases

Cardiovascular Psychiatry and Neurology

Blood-Brain Barrier Breakdown and Blood-Brain Communication in Neurological and Psychiatric Diseases

Guest Editors: Alon Friedman and Daniela Kaufer

Editorial Board

Contents

Hindawi Publishing Corporation
Cardiovascular Psychiatry and Neurology
Volume 2011, Article ID 431470, 2 pages
doi:10.1155/2011/431470

Editorial

Blood-Brain Barrier Breakdown and Blood-Brain Communication in Neurological and Psychiatric Diseases

Alon Friedman[1] and Daniela Kaufer[2]

[1] *Department of Physiology and Biomedical Engineering, Faculty of Health Sciences and Zlotowski Center for Neuroscience, Ben-Gurion University of the Negev, Beer-Sheva 84105, Israel*
[2] *Department of Integrative Biology and Helen Wills Neuroscience Institute, University of California, Berkeley, CA 94720-3140, USA*

Correspondence should be addressed to Alon Friedman, alonf@bgu.ac.il

Received 26 April 2011; Accepted 26 April 2011

More than a century ago, Paul Ehrlich demonstrated in a set of dye experiments the lack of permeability of intracerebral vessels to albumin-binding dyes and therefore postulated a barrier between blood and neuronal tissue. Indeed, transport across the blood-brain barrier (BBB) is tightly regulated by at least four different cells that comprise the brain microvasculature: the endothelial cell and highly specific tight junctions between them, the pericytes which share with the endothelial cells a common capillary basement membrane, the astrocytic foot processes which cover the capillaries, and nerve endings which innervate the vessels. Importantly, dysfunction of the BBB occurs during numerous common neurological diseases, including stroke, epilepsy, trauma, tumors, and infectious and degenerative diseases. While it has been long recognized that BBB dysfunction is associated with brain diseases, only recently it has been suggested to play a role in the pathogenesis of neuronal networks dysfunction and degeneration. In this special issue clinical and experimental evidence for the involvement of BBB dysfunction in the pathogenesis of seizures and epilepsy (N. Marchi et al. "*the etiological role of blood-brain barrier dysfunction in seizure disorders*" and L. M. Gibson et al. in "*Occult cerebrovascular disease and lateonset epilepsy: could loss of neurovascular unit integrity be a viable model?*"), posttraumatic epilepsy (O. Tomkins et al. in "*Blood-brain barrier breakdown following traumatic brain injury: a possible role in posttraumatic epilepsy*"), Alzheimer's diseases (V. C. Anderson et al. in "*The blood-brain barrier and microvascular water exchange in Alzheimer's disease*"), and psychiatric disorders (Y. Serlin et al. in "*Vascular pathology and blood-brain barrier disruption in cognitive and psychiatric complications of type 2 diabetes mellitus*") is given. Experimental evidence points to the mechanisms involved, which most importantly seems to include astroglial activation and disturbance of the extracellular milieu, specifically altered homeostasis of water and electrolytes (V. C. Anderson et al. in "*The blood-brain barrier and microvascular water exchange in Alzheimer's disease*"). In addition, immune response and inflammation seems to have closed bidirectional interactions with disturbed BBB permeability (H. B. Stolp et al. in "*Effects of neonatal systemic inflammation on blood-brain barrier permeability and behaviour in juvenile and adult rats,*" A. S. Haqqani and D. B. Stanimirovic in "*Intercellular interactomics of human brain endothelial cells and Th17 lymphocytes: a novel strategy for identifying therapeutic targets of CNS inflammation,*" and A. R. Friedman et al. in "*Elucidating the complex interactions between stress and epileptogenic pathways*").

The accumulating experimental evidence for BBB involvement in the pathogenesis and progression of these common neurological diseases raises important unresolved questions of how similar vascular dysfunction can lead to wide range of neurological symptoms and signs. While the answers to these key questions are not yet known, papers in this special issue tackle some of the potential variables including the localization, extent, and duration of BBB dysfunction (Y. Serlin et al. in "*Vascular pathology and blood-brain barrier disruption in cognitive and psychiatric complications of type 2 diabetes mellitus*"), the time point during development (H. B. Stolp et al. in "*Effects of neonatal systemic inflammation on blood-brain barrier permeability and*

behaviour in juvenile and adult rats") and aging (L. M. Gibson et al. in "*Occult cerebrovascular disease and late-onset epilepsy: could loss of neurovascular unit integrity be a viable model?*") in which disturbance occurs, and the interaction with confounding factors such as stress in early life or in adulthood (A. R. Friedman et al. in "*Elucidating the complex interactions between stress and epileptogenic pathways*"). These open questions raise the need for the development of new methods for the study of BBB dysfunction exvivo—as described by R. Kovács and colleagues (in "*Slice cultures as a model to study neurovascular coupling and blood brain barrier in vitro*"). Furthermore, it becomes clear that methods for the quantitative and reliable evaluation of BBB permeability are lacking. In this respect, new imaging approaches in experimental animals (D. Jorks et al. in "*A novel algorithm for the assessment of blood-brain barrier permeability suggests that brain topical application of endothelin-1 does not cause early opening of the barrier in rats*") and in humans (O. Tomkins et al. in "*Blood-brain barrier breakdown following traumatic brain injury: a possible role in posttraumatic epilepsy*" and V. C. Anderson et al. in "*The blood-brain barrier and microvascular water exchange in Alzheimer's disease*") are presented as part of the ongoing effort to allow the diagnosis, followup, and evaluation of the integrity of the neurovascular unit and BBB functions. Finally, the new concepts and mechanisms described recently in the literature highlight the neurovascular unit including specifically brain vessels and immune system as new therapeutic targets for the prevention and treatment of neurological diseases. Novel approaches for the identification of new targets based on complex genomic, proteomic, and interactomics tools are presented by A. S. Haqqani and D. B. Stanimirovic (in "*Intercellular interactomics of human brain endothelial cells and Th17 lymphocytes: a novel strategy for identifying therapeutic targets of CNS inflammation*").

Alon Friedman
Daniela Kaufer

Hindawi Publishing Corporation
Cardiovascular Psychiatry and Neurology
Volume 2011, Article ID 469046, 10 pages
doi:10.1155/2011/469046

Research Article

Effects of Neonatal Systemic Inflammation on Blood-Brain Barrier Permeability and Behaviour in Juvenile and Adult Rats

H. B. Stolp,[1,2] P. A. Johansson,[1,3] M. D. Habgood,[1] K. M. Dziegielewska,[1] N. R. Saunders,[1] and C. J. Ek[1]

[1] *Department of Pharmacology, University of Melbourne, Medical Building 181, Parkville VIC 3010, Australia*
[2] *Department of Physiology, Anatomy and Genetics, University of Oxford, Oxford OX13QX, UK*
[3] *Institute of Stem Cell Research, Helmholtz Zentrum München, 85764 Neuherberg, Germany*

Correspondence should be addressed to C. J. Ek, cjek@unimelb.edu.au

Received 11 August 2010; Revised 9 January 2011; Accepted 18 January 2011

Academic Editor: Alon Friedman

Several neurological disorders have been linked to inflammatory insults suffered during development. We investigated the effects of neonatal systemic inflammation, induced by LPS injections, on blood-brain barrier permeability, endothelial tight junctions and behaviour of juvenile (P20) and adult rats. LPS-treatment resulted in altered cellular localisation of claudin-5 and changes in ultrastructural morphology of a few cerebral blood vessels. Barrier permeability to sucrose was significantly increased in LPS treated animals when adult but not at P20 or earlier. Behavioural tests showed that LPS treated animals at P20 exhibited altered behaviour using prepulse inhibition (PPI) analysis, whereas adults demonstrated altered behaviour in the dark/light test. These data indicate that an inflammatory insult during brain development can change blood-brain barrier permeability and behaviour in later life. It also suggests that the impact of inflammation can occur in several phases (short- and long-term) and that each phase might lead to different behavioural modifications.

1. Introduction

Human data related to disorders such as autism, schizophrenia, and cerebral palsy indicate that a period of infection/inflammation during specific stages of brain development may act as a triggering insult [1–4]. In animal experimental studies, inflammation induced during the early postnatal period in rodents has been associated with increased blood-brain barrier permeability [5], white matter damage [6–13], ventricular enlargement [9, 14], and reduced neuron numbers in regions of the hippocampus and cerebellum [15, 16]. In addition, in animals exposed to inflammation *in utero* or during early postnatal life, long-term behavioural alterations such as deficits in prepulse inhibition test [17, 18], motor behaviour [19], and learning and memory [19, 20] have also been reported. However, the biological mechanisms involved in these pathologies are still not understood. To date there are no studies that directly investigated possible links between changes in blood-brain barrier permeability and behavioural alterations in animals exposed to an inflammatory mediator during early stages of brain development.

In this study, we have investigated possible correlations between some behavioural tests and blood-brain barrier morphology and permeability in adolescent and adult rats that were exposed to a prolonged inflammatory stimulus (LPS-injections) as neonates. To examine possible cellular mechanisms behind the alteration in blood-brain barrier permeability, the distribution of claudin-5, a key tight junction protein shown to directly affect barrier permeability [21, 22], was visualised by immunocytochemistry and electron microscopy was used to study the ultrastructure of brain blood vessels in these animals.

2. Materials and Methods

2.1. Animal Model. All experiments were approved by the University of Melbourne Animal Ethics Committee according to NH&MRC guidelines. Sprague-Dawley rats were

sourced from the Breeding Research Facility at University of Melbourne and all animals were kept under similar condition in standard animal cages with sawdust bedding, free access to food (Specialty feed rat pellets)/water, and under controlled environment (12 h day/light cycle, 20-21°C and 50–60% relative humidity). During the light period, the illumination in the room was >350 lux (1 meter above ground) and background noise due to air-conditioning was about 55 dB.

Newborn rats were given five 0.2 mg/kg intraperitoneal (i.p.) injections of lipopolysaccharide (LPS, *E. coli* 055:B5) or equal volume of sterile saline (control animals) at postnatal day 0 (P0), 2, 4, 6, and 8, to produce a prolonged period of inflammation over the postnatal period [11]. Litters were marked and equally divided into saline- and LPS-treated cohorts, including both male and female animals. During the period of treatment (P0–P8), LPS-injected animals had a significantly lower body weight compared to saline-injected controls. At P8 LPS-treated pups weighed 18.1 ± 0.6 g compared to 22.8 ± 0.7 g for controls (mean ± SEM; $n = 29$ for each group). The body weight was still lower at P20 in LPS-injected animals (controls 65 ± 2 g, 56 ± 2 g for LPS-treated animals; $^{***}P = .0003$, $n = 20$ for each group), whereas no significant difference was found in adults (controls 224 ± 14 g, LPS-treated animals 239 ± 16 g; $P = .51$, $n = 11$ for each group).

Animals were left until either P20 or adulthood for behavioural testing; blood-brain barrier permeability measurements were made at P9 and P20 (we have previously published adult sucrose permeability data [11]), claudin-5 immunocytochemistry was performed at P9, P20 and adult; ultrastructural examination of cerebral blood vessels was carried out on adult material only.

2.2. Behavioural Tests. All behavioural tests were performed at the Integrative Neuroscience Facility, Howard Florey Institute. Animals were acclimatised to the facility for a week before testing and 1-2 day recovery periods were allowed between each set of tests. The first two tests were conducted at P20 ($n = 35$, 2 days following weaning) and in adult animals ($n = 16$), whereas the last two tests (Open field, Morris water maze) were carried out in adults only, as P20 animals were too young to cooperate. Different cohorts of animals were tested at P20 and as adults to avoid influences in adult responses due to previous exposure to behavioural testing conditions. Rats were tested in random order and under similar environmental conditions to those under which they were normally kept unless specifically stated below.

2.2.1. Prepulse Inhibition and Acoustic Startle Response. For this test the animal was placed in a 9 cm diameter cylinder on a movement-sensitive platform inside a sound-attenuating box with a background sound level of 70 dB. Over 40 minutes a programme of randomly ordered sound stimuli, with 25 second intervals, was given. These included the 115 dB, 40 msec startle stimuli either by itself or preceded by a 100 msec weak prepulse nonstartling stimulus at 74, 78, or 86 dB (i.e., 4, 8 and 16 dB above background), and no stimuli periods. The same programme of sound stimuli was used for each animal. The startle response (a jumping reflex that lasts for less than one second) was measured by STARTLE software.

2.2.2. Light/Dark Test. Animals were placed in a 40 × 40 cm arena, divided into a light (750 lux) and dark (no light) half by a Perspex insert, with a Tru scan locomotor system (light sensors measuring movement in the vertical and horizontal planes) and Tru scan software for live data recording and analysis. After 10 minutes the session was stopped and the animal was returned to its cage. The movement of the animal was analysed including the latency of the first entry and number of entries into the light half.

2.2.3. Open Field Exploration Test. The general locomotor activity of the adult animals was determined in open field exploration. Animals were placed in a 40 × 40 cm arena setup with a Tru scan locomotor system and Tru scan software for live data recording and analysis. After 1 hour the session was stopped and the animal returned to its cage. Analysis of movement, detected by the Tru Scan locomotor system, was conducted for horizontal and vertical planes as well as the movement of the animal along the margins or the centre of the arena.

2.2.4. Morris Water Maze. A circular water maze pool (2 m diameter) was filled to a depth of 30 cm with 25°C water and enough nontoxic paint to make the water opaque. A circular 15 cm diameter platform was submerged 1 cm below the water level in one quadrant of the pool. The animal was placed in the water in a random quadrant and allowed 2 minutes to find the platform. The time to find the platform was recorded. The animal was left for 30 seconds on the platform before being removed, dried and placed under a warming lamp before repeating the test with the same platform location, but the animal entering the pool in a different quadrant. The testing procedure was repeated daily until the animals showed no improvement in the time taken to find the platform. For a final test, the platform was removed and the animal was introduced to the pool for 1 minute. The frequency and duration the animal spent in the platform zone (the zone where the platform used to be) were measured.

2.3. Blood-Brain Barrier Permeability. Brain/plasma sucrose concentration ratios were measured as an index of blood-brain barrier permeability in animals that had been injected with either LPS or saline as neonates (see above). Due to the small size of P9 animals, different methods were used to estimate concentration ratios at younger (P9) and older (P20) ages ($n = 6$ for each age group and treatment).

In P9 animals, serial blood sampling is not possible therefore, in order to obtain proper steady state concentration ratios, nephrectomy was performed under isoflurane (3%) anaesthesia before an i.p. injection (6 μL/g body weight) of 1 μCi ^{14}C-sucrose (Amersham, CFB146). Animals regained consciousness and were kept under a heat-lamp at 28°C. Three hours after the sucrose injection, when concentration

ratios achieve a near to steady state level [23], the animals were terminally anaesthetised with halothane and blood and brains collected. Plasma was separated by centrifugation. The brain was divided into cerebral hemispheres, midbrain, cerebellum and brainstem and frozen before further processing.

In P20 rats serial blood sampling was possible, and was used to construct the plasma radioactivity curve following radiolabel injection [11]. In anaesthetised animals, the left femoral vein and artery were cannulated, and 2 μCi (P20) of ^{14}C-sucrose was injected (6 μL/g body weight) via the venous cannula, followed by an equal volume of saline. Blood was collected (60–80 μL) from the arterial cannula into heparinised glass capillaries every 5 minutes until the end of the experiment (30 minutes) and plasma separated by centrifugation. Immediately after the last blood sample was collected the heart was transected to prevent further circulation of the tracer and the brain dissected out. The brain was divided into the cerebral hemispheres, midbrain, cerebellum and brainstem and frozen.

Soluene-350 (0.5 mL, Packard Biosciences) was added to each vial with brain tissue and left for 48 hours at 37°C to completely solubilise the tissue. Following this, 4.5 mL of scintillation fluid (Ultra Gold, Packard Biosciences) was added to all vials with brain or plasma samples. The radioactivity in each vial was determined by liquid scintillation counting (1409 DSA, Wallac) and expressed as dpm/μg sample. Brain/plasma sucrose concentration ratios were calculated as has been described before [11]. We have previously measured permeability in adult animals using the same treatment protocol and methods as for P20 animals [11], and data are presented along with the results from this study.

2.4. Claudin-5 Immunocytochemistry. LPS or saline-injected animals at P9, P20 and adult were terminally anaesthetised with inhaled isoflurane (P9) or i.p. Nembutal (P20 and adults; 0.1-0.2 mL/100 g, Rhone Merieux) before perfusion through the aorta with heparinised phosphate buffered saline (PBS, pH 7.4) followed by 4% paraformaldehyde in 0.1 M phosphate buffer (pH 7.4). Brains were removed from the skull, postfixed in Bouin's fixative for 24 hours and processed and sectioned for histology. Briefly, tissue was dehydrated through increasing concentrations of ethanol, cleared in chloroform and embedded in paraffin wax. Sections were cut coronally with a thickness of 5 μm on a Bright rotary microtome (Leica) [5, 11].

Claudin-5 protein was detected in paraffin embedded tissue sections using the PAP method of immunohistochemistry. Sections were dewaxed, rehydrated and incubated in Peroxidase Blocker followed by Protein Blocker (1 hour each; Blockers sourced from DAKO). Sections were exposed to the primary antibody, mouse anticlaudin-5 (Zymed, diluted 1 : 200) overnight at 4°C. Secondary rabbit antimouse antibody and mouse-PAP (DAKO) were used following standard procedures [11] and sections developed for approximately 5 minutes using the DAB+ kit (DAKO). Between each incubation step, sections were washed 3 × 5 minutes with PBS-Tween20 (pH 7.4). Controls included incubating slides with one of the antibodies omitted and were always blank.

Immunocytochemical distribution of claudin-5 in microvessels was determined under light microscope to be either "junctional" or "cytoplasmic" as described previously [11]. The proportion of vessels with either appearance in the cortex and white matter (corpus callosum and external capsule) was determined and scored by the same blinded observer (KMD, 3–6 sections were counted per brain, $n = 3$ brains in each group).

2.5. Electron Microscopy. For morphological examination of blood vessels with an electron microscope tissue was collected from adult rats exposed to either LPS or saline as neonates (n = 3-4 for each group). Animals were anaesthetised as described above and perfused transcardially with 50 mL heparinised phosphate buffered saline followed by 200 mL solution of 2% paraformaldehyde/2.5% glutaraldehyde in phosphate buffer (0.1 M, pH 7.3). Several tissue blocks (up to 1 mm^{3}a piece) were cut from different parts of the corpus callosum and external capsule from each animal and postfixed overnight in the same fixative. Tissue was washed in sodium cacodylate buffer (0.1 M, pH 7.3, 3 × 20 minutes) before processing with a 2% osmium tetroxide/1% potassium ferricyanide solution followed by uranyl acetate treatment. Tissue was dehydrated in increasing concentrations of acetone and embedded in Araldite Epon. Ultrathin sections were cut with a Reichard UltraE microtome and contrasted with uranyl acetate and lead citrate. Thirty to fifty blood vessels from each tissue block were examined under a Phillips CM10 electron microscope to determine their ultrastructure with special focus on the integrity of tight junctions.

2.6. Statistical Analysis. Comparisons between saline-(control) and LPS-(experimental) injected animals were made using regression analysis for the prepulse inhibition test. For all other data, differences between control and experimental animal groups were compared for statistical significance using Student's t-tests with corrections for multiple comparisons. A P-value of less than .05 was considered significant in all cases.

3. Results

3.1. Behavioural Tests. The effect of systemic inflammation during early postnatal development of the rat on behaviour in later life was determined using behavioural tests previously shown to be associated with early life exposure to inflammation, such as anxiety (light/dark test) and altered prepulse inhibition (PPI) as well as general tests of motor behaviour and learning.

3.1.1. Prepulse Inhibition and Acoustic Startle Response. Acoustic startle response and prepulse inhibition were measured as part of one test. No significant difference in acoustic startle response was observed between LPS-treated or control animals at either P20 or adult (data not shown). However, a significant decrease in prepulse startle inhibition was observed in LPS-treated animals at P20 (linear regression

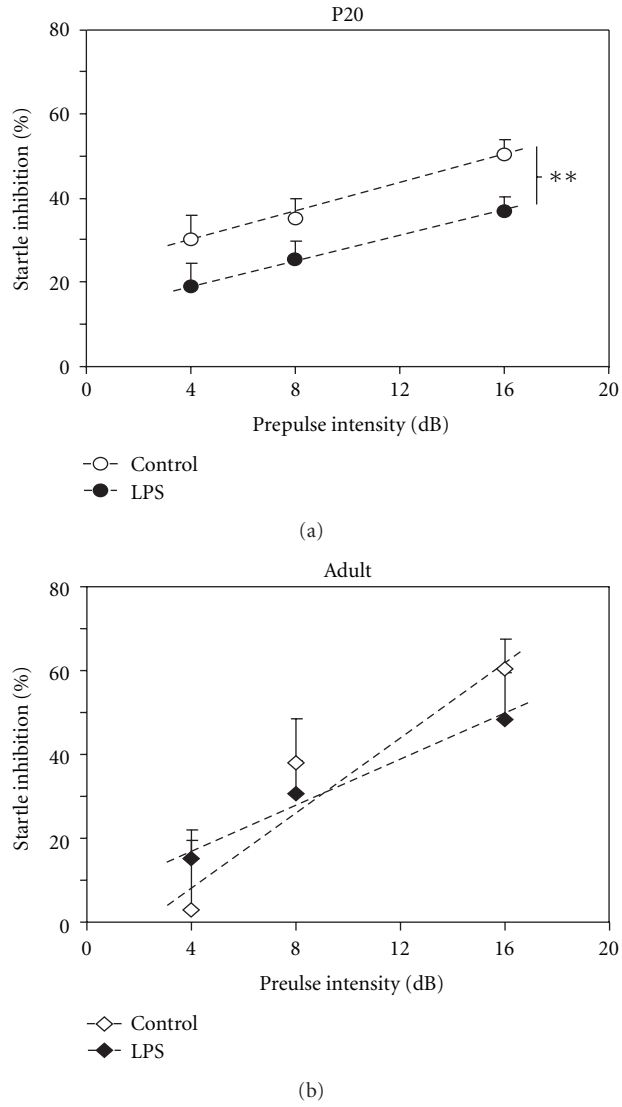

Figure 1: The sensory motor gaiting of animal cohorts was tested using the prepulse inhibition paradigm. Animals were exposed to a 115 dB stimulus either alone or with a 4, 8 or 16 dB prepulse. The presence of a prepulse inhibits the startle response produced by the 115 dB stimulus alone. Data are presented as percent startle inhibition (mean ± SEM) for each prepulse intensity. At P20 (a), animals exposed to LPS had reduced startle inhibition compared to saline-injected age-matched controls ($^{**}P < .01$, linear regression analyses; $n = 29$). Adult animals (b) showed no significant difference between groups of animals although there was a trend toward reduced startle inhibition at 16 dB prepulse in LPS-treated animals ($n = 8$ for each data point).

analysis, $^{**}P < .01$, Figure 1(a)). In adult animals there was a trend towards a decreased prepulse inhibition at the higher prepulse intensity (16 dB), the difference was not statistically significant (Figure 1(b)).

3.1.2. Light/Dark Test. P20 LPS-treated animals showed a small but significant decrease in their total moves in the Light/Dark test ($^{*}P = .02$, Figure 2(a)) compared to those treated with saline. However, no changes in their entrance into the light half of the apparatus, the time spent in the light half or the latency to enter the light half was detected (Figures 2(b) and 2(c)). In contrast, in adult animals LPS treatment resulted in significantly increased entries into the light half of the apparatus as well as earlier entry and more time spent in the light half of the chamber (Figures 2(b) and 2(c)). They also showed generally more exploratory behaviour, as indicated by increased vertical plane entries (Figure 2(b)).

Table 1: Brain/plasma sucrose concentration ratios.

Age	Control	LPS
P9	12.5 ± 0.6 ($n = 6$)	11.9 ± 1.6 ($n = 6$)
P20	2.6 ± 0.2 ($n = 6$)	2.1 ± 0.1 ($n = 6$)
Adult	2.3 ± 0.4^ ($n = 7$)	4.2 ± 0.5*^ ($n = 7$)

Note: P9 ratios were from nephrectomised awake animals 3 hours after an i.p. injection, whereas ratios in older animals were 30 min ratios in anaesthetised animals after an i.v. injection. Data are mean ± SEM, $^{*}P < .05$ from control, ^ data published previously [11].

3.1.3. Open Field Exploration Test. LPS-treated adult rats showed no difference from control animals in any of the parameters analysed such as the total number of moves (884 ± 62 versus 895 ± 60), time (sec) moving (1321 ± 127 versus 1383 ± 136), or in their velocity (cm/sec, 1522 ± 209 versus 1508 ± 223).

3.1.4. Morris Water Maze. Adult animals exposed to LPS during their early postnatal development showed no significant differences in behaviour from the saline-injected controls in the Morris Water Maze, with no changes in the time taken to learn the location of a submerged platform or their exploratory behaviour when the platform was removed (Figures 3(a) and 3(b)).

3.2. Blood-Brain Barrier Permeability. Results from permeability studies performed in this paper are only valid within each age group and cannot be directly compared between P9 and older animals since different methods were used at different ages to determine brain/plasma sucrose concentration ratios (see Methods). Results are presented in Table 1. At P9 and P20 there was no significant difference in permeability of the blood-brain barrier between the LPS and saline-treated groups of animals. At P9 the brain/plasma sucrose concentration ratios of control animals were 12.5 ± 0.6% (mean ± SEM) compared to 11.9 ± 1.6% in LPS-treated animals ($P = .8$). At P20 the brain/plasma sucrose concentration ratios in controls were 2.6 ± 0.2% compared to 2.1 ± 0.1% ($P = .1$) in LPS-treated animals (see Table 1). In contrast, in adult animals we have shown previously [11] there is a significant increase in the brain/plasma sucrose concentration ratios following early postnatal LPS treatment (4.2 ± 0.5% in LPS-treated animals compared to 2.5 ± 0.4% for controls, $^{*}P < .05$).

3.3. Claudin-5 Immunocytochemistry. Claudin-5 is so far the only tight junction protein that has been experimentally

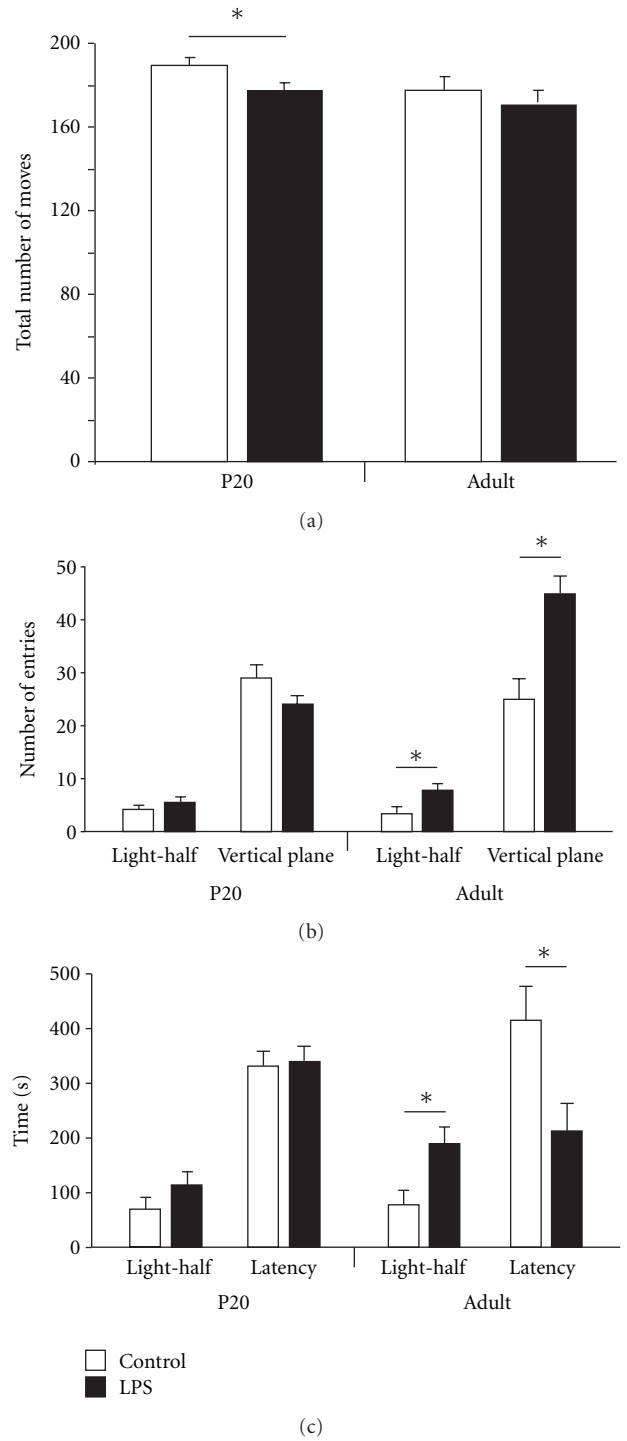

Figure 2: The behaviour of P20 and adult animals in a stressful environment was determined in an arena where half was brightly lit and the other half was dark and enclosed. Total moves (a) and entries into the light half and the vertical plane were determined (b), as well as time spent in the light half and latency (c). P20 animals exposed to LPS during postnatal development showed a small but significant decrease in total movement in this apparatus, but otherwise showed no changes compared to saline-injected controls ($n = 8$ for each group). Adult animals treated with LPS showed increased exploratory behaviour with increased time and entries into the light half of the arena, reduced latency to enter the light half and increased vertical plane entries ($^*P < .05$, data are mean ± SEM, $n = 8$ for each group).

shown to directly affect the permeability of the blood-brain barrier [22], therefore its distribution was investigated using immunocytochemistry on paraffin-embedded brain sections (see Methods) and the results are illustrated and summarised in Figure 4. In saline-injected control animals at all ages studied (P9, P20 and adult), claudin-5 immunohistochemistry showed a typical cell-to-cell junction distribution pattern (Figures 4(a) and 4(c)) in approximately 80–100% of vessels (indicated as ++++ in Figure 4(e)) within the cortex and white matter while in the remaining cerebral blood vessels distribution of the claudin-5 immunoreactivity appeared more cytoplasmic. Distribution of claudin-5 immunoreactivity in brains from all LPS-treated animals showed a distinct shift, typically exhibiting less junctional staining and a relatively more cytoplasmic distribution (see Figures 4(b), 4(d), and 4(e)).

3.4. Ultrastructure of Cerebral Blood Vessels. The ultrastructure of blood vessels, and specifically tight junctions, in the white matter (external capsule and corpus callosum) was examined. Tissue was compared from adult control animals and adult animals that had been exposed to LPS during development. All vessels examined from control brains appeared to have a normal ultrastructure, with little perivascular space, close association of astrocytic end feet, well defined basement membrane (Figure 5(a)) and obvious tight junctions between the intercellular clefts of apposing endothelial cells (Figure 5(c)). Most vessels in white matter from LPS-treated animals were not obviously different from control brains (Figure 5(b)). Tight junctions were apparent at cell-cell contacts (Figure 5(d)), as were the associations with the surrounding structures. However, in 2 out of 50 vessels in sections from the LPS-treated animals, ultrastructural abnormalities were observed (Figure 5(e)). In these vessels the lumen was convoluted and there was an apparent disruption of the perivascular space. Despite this, the structure of the tight junctions associated with these unusual vessels appeared to be normal (Figure 5(f)).

4. Discussion

Increasing evidence, both clinical and experimental, indicates that an early inflammatory insult can affect brain development and behaviour later in life. The aim of this study was to determine whether there is a correlation between changes in the permeability properties of the blood-brain barrier induced by a period of neonatal inflammation and later behaviour using the rat as an experimental model.

4.1. Blood-Brain Barrier Permeability and Behaviour. In the present model of early life inflammation some alterations in blood-brain barrier function and white matter damage have previously been reported. These include short-term changes in blood-brain barrier permeability to protein in young pups and long-term changes to small molecular weight molecules in adult animals exposed to prolonged inflammation during development [11]. The present study determined that this long-term permeability change develops sometime after 3

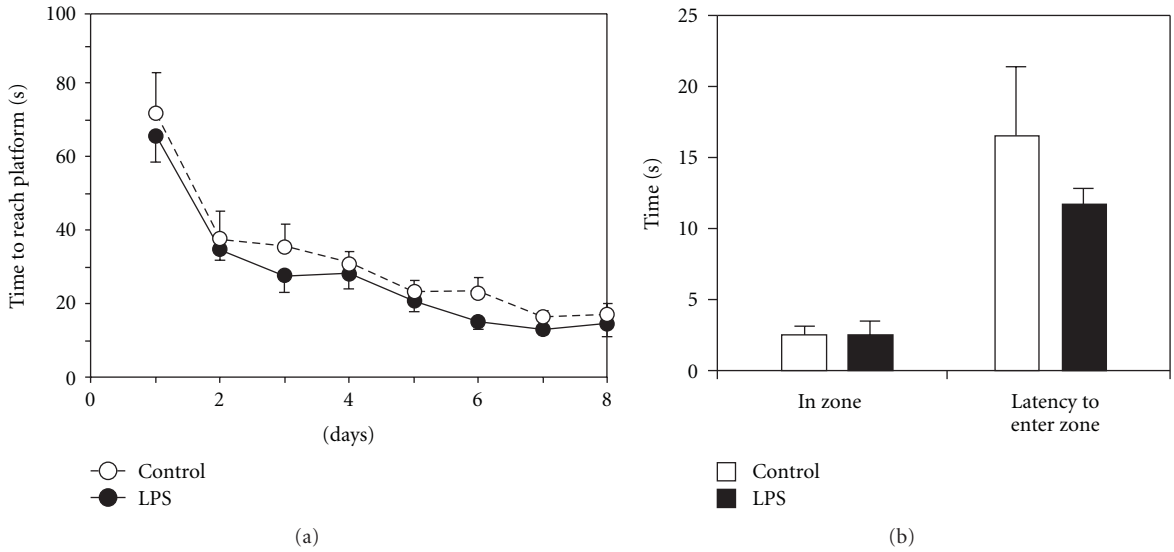

Figure 3: Adult animals treated with either saline or LPS during the postnatal period were tested for their ability to learn and remember and their general locomotor activity in the Morris Water Maze. No difference was observed between saline- and LPS-treated animals for any of the measured parameters. Data are mean ± SEM, $n = 8$ for each group.

weeks of age, as animals tested at P20 showed no significant change in the permeability of the blood-brain barrier to sucrose (Table 1). Interestingly, changes in blood vessel tight junction distribution preceded long-term alterations in both blood-brain barrier permeability and behaviour.

It has previously been hypothesised that this alteration in function of the blood-brain barrier in the adult may contribute to inflammation-induced behavioural changes such as altered prepulse inhibition (PPI). The results from the current study suggest that changes in PPI occur prior to the long-term change in barrier function to small molecules, however they may relate to damage resulting from the transient increase in protein permeability and white matter volume reduction that occurs up to P9 [11].

One of the major behavioural modifications observed in the present study was a change in sensory-motor gaiting, demonstrated by PPI test in juvenile rats, but not in adults following an early inflammatory insult (Figure 1). Changes in PPI have been reported in several studies that examined effects of systemic inflammation during fetal or early postnatal stages of brain development, however, some results have been conflicting. Fortier and colleagues [17] found that LPS administered to pregnant mice during mid to late gestation resulted in reduced PPI in offspring when adult, whereas polyI:C, which is used to mimic viral infections, did not. In contrast, higher doses of polyI:C at comparable ages of gestation have been found to result in altered PPI in a separate study [24]. Similarly, Fortier et al. [17] suggested that inflammation at very early stages of gestation (GD10-11) in the mouse did not cause changes in the PPI response of the adult offspring, while an earlier study by Shi et al. [18] indicated that inflammation-induced either by viral infection or injection of the polyI:C viral mimic at GD9.5 did in fact result in a reduced PPI response in adult offspring. These discrepancies could be due to the different doses of polyI:C used, particularly as inflammation has been associated with increased serum cortisol concentration in the perinatal period [25], which in turn has been found to alter PPI in a dose-specific manner [26]. This suggests that these two systems may interact to produce widely different results depending on the magnitude of the initial insult. Therefore, while changes in PPI are now frequently seen in models of early life inflammatory challenge, the long-term behavioural outcome is dependent on many factors, including dose of inflammatory agent and gestational age at time of insult. The present study supports the recent finding of Ibi et al. [27] that neonatal inflammation, in comparison to inflammation during gestation, also results in long-term alteration in the PPI response. It also supports the hypothesis of Wolff and Bilkey [24] that PPI deficits are distinguishable in juvenile animals.

Behavioural changes seen at P20 for PPI may continue into adulthood although in this study the difference between the two treatment groups was no longer statistically significant (Figure 1). LPS challenged animals did however show a significant behavioural change in the Light/Dark test compared to saline-treated animals when adult (Figure 2). In contrast, in animals tested at P20 there was no significant difference for this test between control and LPS-injected animals suggesting that the effect seen in adult animals may take a longer period to develop and is not manifested until later in life. However, it may be that this is not an appropriate test for such juvenile animals, as many of them (both saline- and LPS-injected) did not enter the light area of the arena at all during the testing period.

The results of the Light/Dark test obtained for adult animals were different from what might have been expected from clinical disease associations [28, 29] and some previous studies. Fetal exposure to inflammation (via the dam) in the C57 mouse produced long-term anxiety-like behaviour on

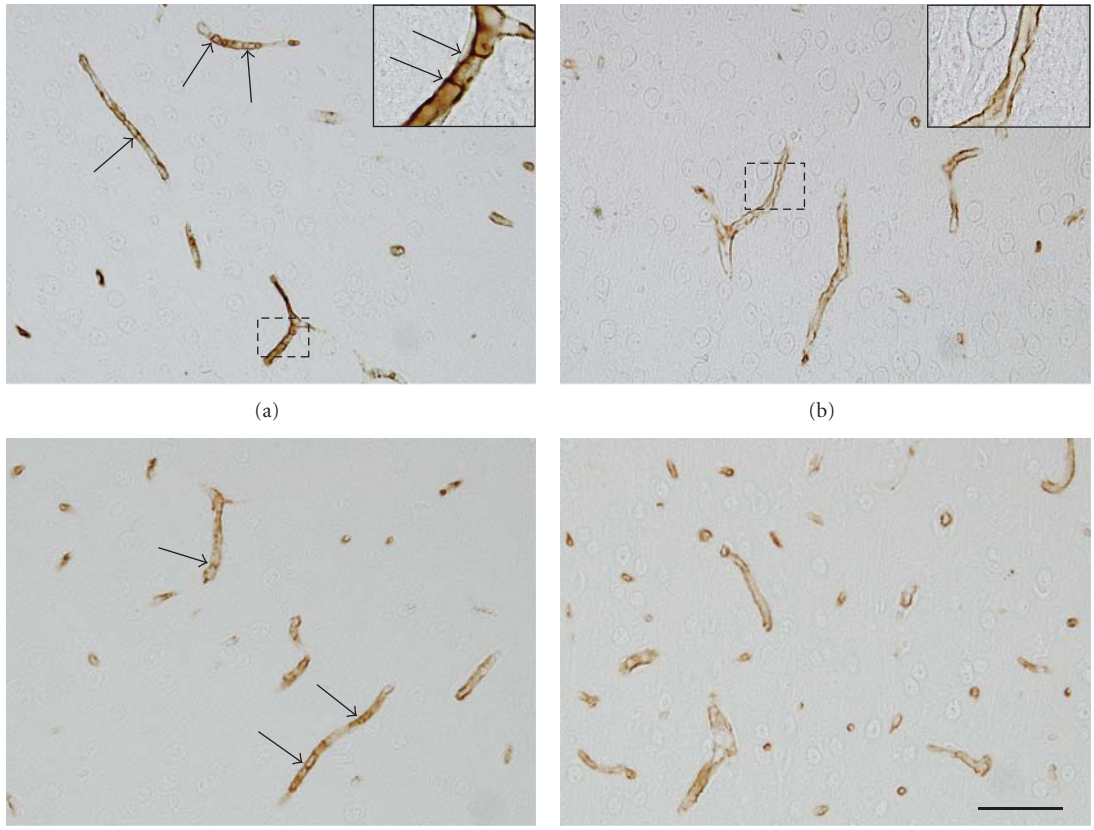

(a) (b) (c) (d)

Distribution	P9		P20		Adult	
	Control	LPS	Control	LPS	Control	LPS
Junctional	++++	++	++++	++	++++	++
Cytoplasmic	–	+++	+	+++	++	+++

(e)

Figure 4: Claudin-5 immunoreactivity was detected on the endothelial cells of brain microvessels. In P9 (a) and adult (c) control brains, claudin-5 (brown reaction product) appears to be continuous along the length of the microvessels and to form a distinct pattern consistent with its location at cell-to-cell junctions (higher magnification in insert in (a)). In P9 (b) and adult (d) animals treated with LPS during the first 8 days of life a proportion of vessels in the brain (see also (e)) showed an altered distribution of claudin-5, with a fainter immunoreactivity and more diffuse staining pattern apparently in the cytoplasm (see insert for cellular distribution pattern in insert in (b)). Scale bar = 50 μm. Inserts show magnification of regions indicated by box in (a) and (b). (e) illustrates a relative proportion of cerebral blood vessels displaying claudin-5 immunoreactivity that was observed as "junctional" or cytoplasmic (see Methods). This showed that there is a shift towards cytoplasmic staining of claudin-5 in LPS-treated animals at all ages. $n = 3$ for each group.

the elevated plus maze [30]. However, a study of inflammation in the postnatal rat (P7-28) did not show any increased anxiety-like behaviour on the same apparatus [31, 32]. The reduced light avoidance exhibited by the LPS-treated animals in the present study (Figure 2) does not appear to be due to reduced sensory input. Animals receiving LPS-injections during infancy responded normally to visual and auditory stimuli in the Morris Water Maze and PPI. It therefore seems that much of the apparent conflict in results so far reported in the literature may reflect differences in timing of inflammation during development, the degree of inflammatory insult, the method of inducing it and perhaps the species.

LPS-treated animals showed no difference in their behaviour compared to saline-injected control animals for either the open field or the Morris Water Maze, indicating that not all aspects of behaviour are affected as a result of inflammatory insult during early postnatal development.

4.2. Tight Junctions. We examined tight junctions both morphologically under the electron microscope and molecularly using claudin-5 immunoreactivity. Tight junctions located

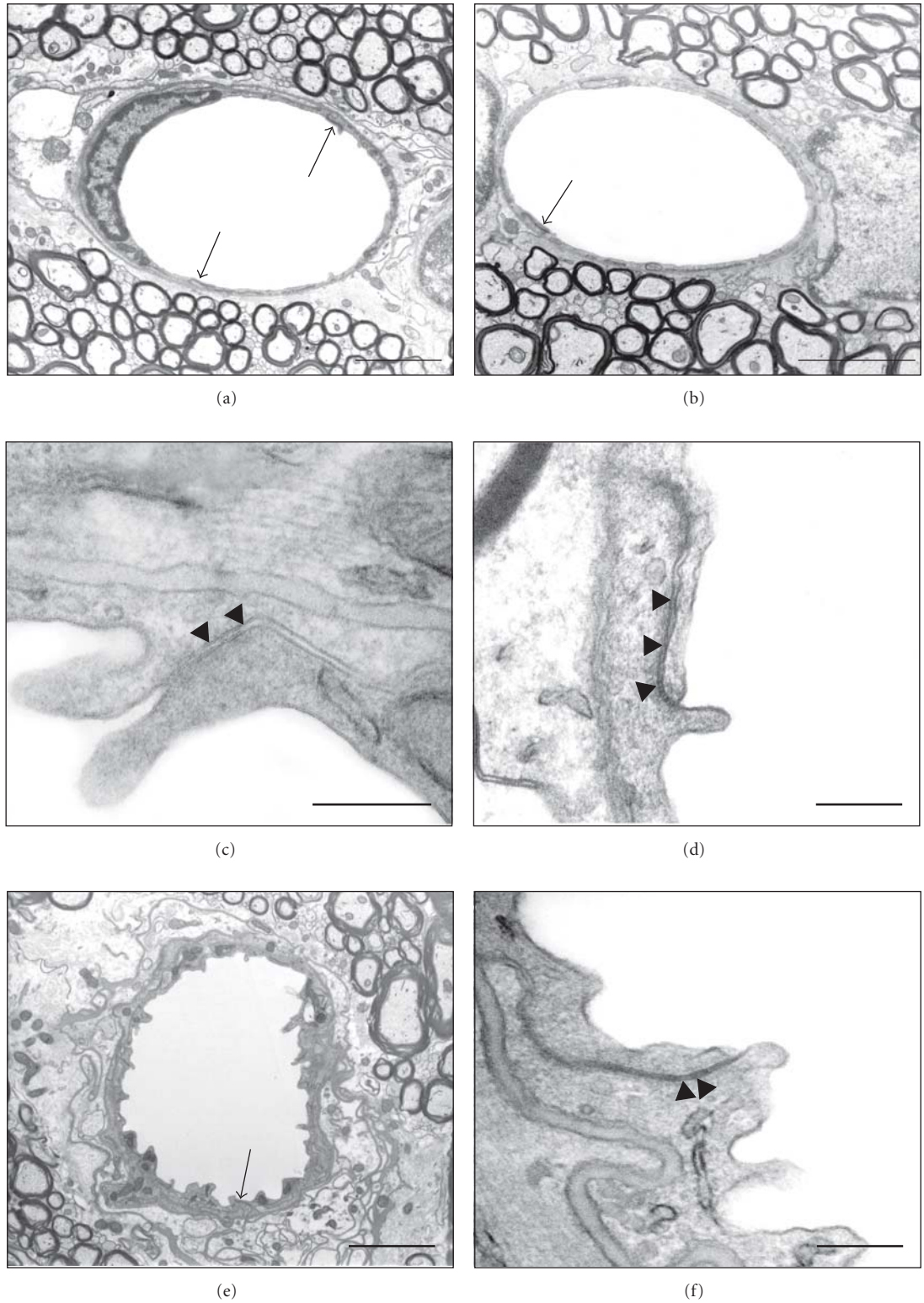

Figure 5: Electronmicrographs of blood vessels in the external capsule of adult control and LPS-treated rats. Most blood vessels appear identical in control (a) and LPS-treated animals (b), arrows indicate tight junctions. At higher magnification the tight junctions are visible and these look normal in LPS-treated animals (d) compared to control animals (c) with several fusions points (arrowheads) along the intercellular cleft. A small proportion of cerebral capillaries in LPS-treated animals appeared abnormal with convoluted lumen and poorly structured perivascular space (e). In these vessels the tight junction (arrow in (e)) still appeared normal and at higher magnification the characteristic fusion points were visible within the tight junction (arrowheads in (f)). Scale bars: 3 μm in (a), (b), (e); 200 nm in (c), (d), (f).

between endothelial cells of cerebral blood vessels are the structural basis for the blood-brain barriers that normally severely restrict paracellular permeability from blood into brain [33]. The present study of blood vessel ultrastructure in the white matter of adult animals exposed to LPS early in development showed no apparent alteration in the structure of tight junctions with several "kissing points" visible as an indicator of closely apposed membranes.

However, while examining these junctions we found a small number of the blood vessels that did appear to have gross ultrastructural abnormalities (Figure 5). The gross ultrastructural changes observed in these vessels are not dissimilar to those observed in animal models of pericyte deficiency [34] where increased permeability of the blood-brain barrier was observed. Although the proportion of these abnormal vessels was low this does not rule out their potential to influence blood-brain barrier permeability. Due to the normally extremely low permeability of cerebral blood vessels, a few vessels with altered permeability could significantly contribute to the overall properties of the blood-brain barrier. Although the tight junctions in all vessels appeared to be normal (including those in the abnormal vessels, Figure 5), the functionality of these tight junctions can only be confirmed using electron denser tracers [35]. Sucrose permeability was increased throughout the cortex in these animals, indicating that other low molecular weight molecules, such as some drugs or heavy metals, may have prolonged access to the brain, potentially contributing to long-term damage of the brain.

The tight junctions are composed of a number of proteins that are thought to have different roles in relation to paracellular permeability. Disruption of these proteins has been associated with alterations in blood-brain barrier permeability [36–38] and the expression of, for example, claudin-5 can be regulated through protein kinase C by the actions of a number of cytokines [39]. Molecular alterations of the tight junction proteins may lead to increased permeability even without ultrastructurally altering the junctions. In a claudin-5 knockout mouse no overt morphological abnormalities in the blood vessels were found despite a size selective increase in blood-brain barrier permeability [22]; however, as this study did not include EM immunocytochemistry it is not clear what was the cellular route (paracellular or transcellular) responsible for the observed increase in barrier permeability to small molecules that was observed. Although there is a link between altered claudin-5 distribution and an increase in sucrose permeability in adults in the present study (Table 1), the results from younger animals show that LPS treatment can also cause an altered distribution of claudin-5 protein immunoreactivity that is not associated with changes in sucrose permeability. In order to understand these differences we need a better understanding of the molecular functions of tight junction proteins as well as the changes of these proteins that may occur in response to LPS treatment.

In conclusion, the present results demonstrate that a period of prolonged systemic inflammation in the neonatal rat can cause a multitude of modifications that manifest in later life, ranging from alterations in behaviour, changes in blood-brain barrier permeability and in structure of some cerebral blood vessels. The results also show that these changes develop at different times after the initiating inflammatory insult and are not always temporally correlated. The results from the present study are suggestive of a two-phase progression model: a first wave of damage (i.e., acute blood-brain barrier disruption and white matter damage [11]) that causes early changes in blood vessel morphology/composition and early behavioural alterations and a second phase of damage, induced by the adult-onset increase in blood-brain barrier permeability, that produces the later behavioural changes.

Acknowledgments

This work was supported by an NHMRC project grant. H. B. Stolp, M. D. Habgood, K. M. Dziegielewska, N. R. Saunders, and C. J. Ek are members of the Neurobid Consortium, funded by the NHMRC and European Union Seventh Framework Programme (FP7/2007-2013) under Grant agreement no. HEALTH-F2-2009-241778.

References

[1] A. S. Brown, "Prenatal infection as a risk factor for schizophrenia," *Schizophrenia Bulletin*, vol. 32, no. 2, pp. 200–202, 2006.

[2] K. B. Nelson and R. E. Willoughby, "Infection, inflammation and the risk of cerebral palsy," *Current Opinion in Neurology*, vol. 13, no. 2, pp. 133–139, 2000.

[3] C. A. Pardo and C. G. Eberhart, "The neurobiology of autism," *Brain Pathology*, vol. 17, no. 4, pp. 434–447, 2007.

[4] H. B. Stolp and K. M. Dziegielewska, "Review: role of developmental inflammation and blood-brain barrier dysfunction in neurodevelopmental and neurodegenerative diseases," *Neuropathology and Applied Neurobiology*, vol. 35, no. 2, pp. 132–146, 2009.

[5] H. B. Stolp, K. M. Dziegielewska, C. J. Ek et al., "Breakdown of the blood-brain barrier to proteins in white matter of the developing brain following systemic inflammation," *Cell and Tissue Research*, vol. 320, no. 3, pp. 369–378, 2005.

[6] T. Debillon, C. Gras-Leguen, S. Leroy, J. Caillon, J. C. Rozé, and P. Gressens, "Patterns of cerebral inflammatory response in a rabbit model of intrauterine infection-mediated brain lesion," *Developmental Brain Research*, vol. 145, no. 1, pp. 39–48, 2003.

[7] F. H. Gilles, D. R. Averill, and C. S. Kerr, "Neonatal endotoxin encephalopathy," *Annals of Neurology*, vol. 2, no. 1, pp. 49–56, 1977.

[8] C. Mallard, A. K. Welin, D. Peebles, H. Hagberg, and I. Kjellmer, "White matter injury following systemic endotoxemia or asphyxia in the fetal sheep," *Neurochemical Research*, vol. 28, no. 2, pp. 215–223, 2003.

[9] Y. Pang, Z. Cai, and P. G. Rhodes, "Disturbance of oligodendrocyte development, hypomyelination and white matter injury in the neonatal rat brain after intracerebral injection of lipopolysaccharide," *Developmental Brain Research*, vol. 140, no. 2, pp. 205–214, 2003.

[10] C. I. Rousset, S. Chalon, S. Cantagrel et al., "Maternal exposure to LPS induces hypomyelination in the internal capsule and programmed cell death in the deep gray matter in newborn rats," *Pediatric Research*, vol. 59, no. 3, pp. 428–433, 2006.

[11] H. B. Stolp, K. M. Dziegielewska, C. J. Ek, A. M. Potter, and N. R. Saunders, "Long-term changes in blood-brain barrier permeability and white matter following prolonged systemic inflammation in early development in the rat," *European Journal of Neuroscience*, vol. 22, no. 11, pp. 2805–2816, 2005.

[12] X. Wang, G. Hellgren, C. Löfqvist et al., "White matter damage after chronic subclinical inflammation in newborn mice," *Journal of Child Neurology*, vol. 24, no. 9, pp. 1171–1178, 2009.

[13] G. Loron, P. Olivier, H. See et al., "Ciprofloxacin prevents myelination delay in neonatal rats subjected to E. coli sepsis," *Annals of Neurology*. In press.

[14] L. W. Fan, Y. Pang, S. Lin, P. G. Rhodes, and Z. Cai, "Minocycline attenuates lipopolysaccharide-induced white matter injury in the neonatal rat brain," *Neuroscience*, vol. 133, no. 1, pp. 159–168, 2005.

[15] U. Meyer, M. Nyffeler, A. Engler et al., "The time of prenatal immune challenge determines the specificity of inflammation-mediated brain and behavioral pathology," *Journal of Neuroscience*, vol. 26, no. 18, pp. 4752–4762, 2006.

[16] L. Shi, S. E. P. Smith, N. Malkova, D. Tse, Y. Su, and P. H. Patterson, "Activation of the maternal immune system alters cerebellar development in the offspring," *Brain, Behavior, and Immunity*, vol. 23, no. 1, pp. 116–123, 2009.

[17] M. E. Fortier, G. N. Luheshi, and P. Boksa, "Effects of prenatal infection on prepulse inhibition in the rat depend on the nature of the infectious agent and the stage of pregnancy," *Behavioural Brain Research*, vol. 181, no. 2, pp. 270–277, 2007.

[18] L. Shi, S. H. Fatemi, R. W. Sidwell, and P. H. Patterson, "Maternal influenza infection causes marked behavioral and pharmacological changes in the offspring," *Journal of Neuroscience*, vol. 23, no. 1, pp. 297–302, 2003.

[19] Y. Pang, L. W. Fan, B. Zheng, Z. Cai, and P. G. Rhodes, "Role of interleukin-6 in lipopolysaccharide-induced brain injury and behavioral dysfunction in neonatal rats," *Neuroscience*, vol. 141, no. 2, pp. 745–755, 2006.

[20] S. D. Bilbo, J. C. Biedenkapp, A. Der-Avakian, L. R. Watkins, J. W. Rudy, and S. F. Maier, "Neonatal infection-induced memory impairment after lipopolysaccharide in adulthood is prevented via caspase-1 inhibition," *Journal of Neuroscience*, vol. 25, no. 35, pp. 8000–8009, 2005.

[21] K. Morita, H. Sasaki, M. Furuse, and S. Tsukita, "Endothelial claudin: claudin-5/TMVCF constitutes tight junction strands in endothelial cells," *Journal of Cell Biology*, vol. 147, no. 1, pp. 185–194, 1999.

[22] T. Nitta, M. Hata, S. Gotoh et al., "Size-selective loosening of the blood-brain barrier in claudin-5-deficient mice," *Journal of Cell Biology*, vol. 161, no. 3, pp. 653–660, 2003.

[23] C. J. Ek, M. D. Habgood, K. M. Dziegielewska, A. Potter, and N. R. Saunders, "Permeability and route of entry for lipid-insoluble molecules across brain barriers in developing Monodelphis domestica," *Journal of Physiology*, vol. 536, no. 3, pp. 841–853, 2001.

[24] A. R. Wolff and D. K. Bilkey, "Immune activation during mid-gestation disrupts sensorimotor gating in rat offspring," *Behavioural Brain Research*, vol. 190, no. 1, pp. 156–159, 2008.

[25] R. E. Fisher, N. A. Karrow, M. Quinton et al., "Endotoxin exposure during late pregnancy alters ovine offspring febrile and hypothalamic-pituitary-adrenal axis responsiveness later in life," *Stress*, vol. 13, no. 4, pp. 334–342, 2010.

[26] S. L. Kjær, G. Wegener, R. Rosenberg, S. P. Lund, and K. S. Hougaard, "Prenatal and adult stress interplay—behavioral implications," *Brain Research*, vol. 1320, pp. 106–113, 2010.

[27] D. Ibi, T. Nagai, Y. Kitahara et al., "Neonatal polyI:C treatment in mice results in schizophrenia-like behavioral and neurochemical abnormalities in adulthood," *Neuroscience Research*, vol. 64, no. 3, pp. 297–305, 2009.

[28] N. Davies, A. Russell, P. Jones, and R. M. Murray, "Which characteristics of schizophrenia predate psychosis?" *Journal of Psychiatric Research*, vol. 32, no. 3-4, pp. 121–131, 1998.

[29] M. Weinstock, "Alterations induced by gestational stress in brain morphology and behaviour of the offspring," *Progress in Neurobiology*, vol. 65, no. 5, pp. 427–451, 2001.

[30] G. Hava, L. Vered, M. Yael, H. Mordechai, and H. Mahoud, "Alterations in behavior in adult offspring mice following maternal inflammation during pregnancy," *Developmental Psychobiology*, vol. 48, no. 2, pp. 162–168, 2006.

[31] S. J. Spencer, J. G. Heida, and Q. J. Pittman, "Early life immune challenge—effects on behavioural indices of adult rat fear and anxiety," *Behavioural Brain Research*, vol. 164, no. 2, pp. 231–238, 2005.

[32] S. J. Spencer, S. Martin, A. Mouihate, and Q. J. Pittman, "Early-life immune challenge: defining a critical window for effects on adult responses to immune challenge," *Neuropsychopharmacology*, vol. 31, no. 9, pp. 1910–1918, 2006.

[33] T. S. Reese and M. J. Karnovsky, "Fine structural localization of a blood-brain barrier to exogenous peroxidase," *Journal of Cell Biology*, vol. 34, no. 1, pp. 207–217, 1967.

[34] P. Lindahl, B. R. Johansson, P. Levéen, and C. Betsholtz, "Pericyte loss and microaneurysm formation in PDGF-B-deficient mice," *Science*, vol. 277, no. 5323, pp. 242–245, 1997.

[35] C. J. Ek, K. M. Dziegielewska, H. Stolp, and N. R. Saunders, "Functional effectiveness of the blood-brain barrier to small water-soluble molecules in developing and adult opossum (*Monodelphis domestica*)," *Journal of Comparative Neurology*, vol. 496, no. 1, pp. 13–26, 2006.

[36] N. S. Harhaj and D. A. Antonetti, "Regulation of tight junctions and loss of barrier function in pathophysiology," *International Journal of Biochemistry and Cell Biology*, vol. 36, no. 7, pp. 1206–1237, 2004.

[37] M. A. Petty and E. H. Lo, "Junctional complexes of the blood-brain barrier: permeability changes in neuroinflammation," *Progress in Neurobiology*, vol. 68, no. 5, pp. 311–323, 2002.

[38] B. Engelhardt and L. Sorokin, "The blood-brain and the blood-cerebrospinal fluid barriers: function and dysfunction," *Seminars in Immunopathology*, vol. 31, no. 4, pp. 497–511, 2009.

[39] Y. Sonobe, H. Takeuchi, K. Kataoka et al., "Interleukin-25 expressed by brain capillary endothelial cells maintains blood-brain barrier function in a protein kinase Cε-dependent manner," *Journal of Biological Chemistry*, vol. 284, no. 46, pp. 31834–31842, 2009.

Hindawi Publishing Corporation
Cardiovascular Psychiatry and Neurology
Volume 2011, Article ID 615829, 9 pages
doi:10.1155/2011/615829

Hypothesis

The Blood-Brain Barrier and Microvascular Water Exchange in Alzheimer's Disease

Valerie C. Anderson,[1] David P. Lenar,[1] Joseph F. Quinn,[2] and William D. Rooney[3]

[1] *Department of Neurological Surgery, Oregon Health & Science University, 3181 SW Sam Jackson Park Road, Portland, OR 97239, USA*
[2] *Department of Neurology, Oregon Health & Science University, Portland, OR 97239, USA*
[3] *Advanced Imaging Research Center, Oregon Health & Science University, Portland, OR 97239, USA*

Correspondence should be addressed to Valerie C. Anderson, andersov@ohsu.edu

Received 2 September 2010; Accepted 12 February 2011

Academic Editor: Daniela Kaufer

Alzheimer's disease (AD) is the most common form of dementia in the elderly. Although traditionally considered a disease of neurofibrillary tangles and amyloid plaques, structural and functional changes in the microvessels may contribute directly to the pathogenesis of the disease. Since vascular dysfunction often precedes cognitive impairment, understanding the role of the blood-brain barrier (BBB) in AD may be key to rational treatment of the disease. We propose that water regulation, a critical function of the BBB, is disturbed in AD and results in abnormal permeability and rates of water exchange across the vessel walls. In this paper, we describe some of the pathological events that may disturb microvascular water exchange in AD and examine the potential of a relatively new imaging technique, dynamic contrast-enhanced MRI, to quantify water exchange on a cellular level and thus serve as a probe of BBB integrity in AD.

1. Introduction

Alzheimer's disease (AD) is the most common form of irreversible dementia in the elderly and accounts for more than 30% of all cases in adults over the age of 80 [1]. Pathologically, the disease is characterized by amyloid deposits, neurofibrillary tangles, and neuronal loss in specific brain regions. Vascular involvement is not part of the diagnostic criteria. Nevertheless, factors that modify vascular risk, including hypertension, diabetes, and hypercholesterolemia, are among the most consistently identified risk factors for the disease. Moreover, profound alterations in cerebrovascular ultrastructure and function have been identified in AD [2, 3]. Since the microvessels are the key site for nutrient and oxygen exchange between the brain and circulating blood, it is likely that processes that disturb capillary physiology or alter brain microcirculation are of major importance for the pathogenesis of AD [4–6].

Morphologically, brain capillaries consist of a layer of endothelial cells that line the luminal surface, pericytes, and an outer basal membrane (Figure 1). In contrast to most of the peripheral endothelia, endothelial cells in the CNS form tight, unfenestrated junctions that restrict paracellular diffusion of water, ions, and large molecules. Since other mechanisms by which blood-borne substances cross into the brain (e.g., carrier-mediated active or facilitated transport, pinocytosis) are limited, these tight junctions limit the diffusion of blood-borne solutes into the brain and are the foundation of the Blood-Brain Barrier (BBB) [7]. In addition to the endothelium, the functional integrity of the barrier is also critically dependent on the basal lamina, pericytes, and surrounding astroglia. The basal lamina provides structural support for the endothelium, signals cell-cell interactions, and separates the endothelium and pericytes from the surrounding extracellular (interstitial) spaces. The pericytes, closely associated with the abluminal surface of the basal membrane, likely play a role in regulating microvascular blood flow and vascular remodeling [2]. Finally, the perivascular astrocyte end-feet which ensheathe the outer surface of the microvessels are of major importance in induction and

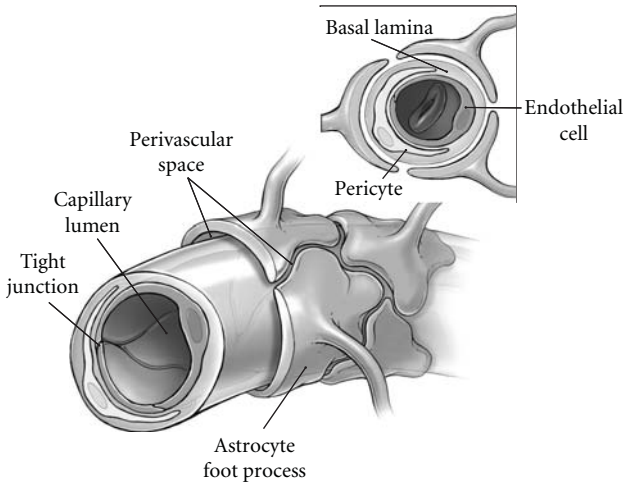

Figure 1: Schematic diagram of the Blood-Brain Barrier. Interstitial fluid flows along perivascular drainage pathways defined by the abluminal capillary surface and astrocyte end-feet, which ensheathe the vessels.

maintenance of the tight junctions, neurovascular coupling, and fluid balance [8, 9].

Approximately 90% of the blood volume in the brain is water, and its exchange into and out of the blood is also tightly regulated by the BBB. As in the periphery, water in the CNS is highly compartmentalized and is present in all brain compartments: intracellular and interstitial fluids, blood, and CSF. Increasing evidence suggests that functional interactions between the cellular components of the BBB—the endothelium, basal lamina, and pericytes—in addition to the astroglial end-feet collectively regulate water exchange between compartments, capillary blood volume, and permeability. We hypothesize that microvascular water exchange is disturbed in the AD brain as a result of an incompetent BBB and is reflected in abnormal intercompartmental water exchange. In this paper, we will provide the rationale for our hypothesis and suggest a quantitative experimental approach, dynamic contrast-enhanced magnetic resonance imaging (DCE-MRI), by which we have recently begun to test this hypothesis in individuals with early cognitive changes.

2. The Pathophysiology of Water Regulation in Alzheimer's Disease

The morphological footprint of BBB disturbances in AD is clear. In the basal membrane, substantial thickening and stiffening is observed in 90% of AD cases [10]. Macroscopically, the capillaries appear thin and fragmented [11]. Overall density tends to be reduced, especially in important cortical and hippocampal regions, and remaining vessels are more tortuous. In addition, the endothelium is frequently atrophic or swollen, and physical coupling to the surrounding glia is often disrupted [12]. Moreover, the number of tight junctions per unit of vessel length is reduced throughout the brain [13–15] with metabolic regulation of remaining tight junctions likely compromised by decreased, mitochondrial density [14]. On a molecular level, the cell adhesion activity of occludin and claudins, integral member proteins localized exclusively to tight junctions, is decreased and accumulation of collagen deposits, proteoglycans, laminins, and other components of the basal matrix is frequently noted [16–18].

Despite the overwhelming abnormalities in capillary structure and function, studies to define the temporal association of microvascular changes with disease severity and progression have not been done in humans, and the extent to which BBB changes are likely to be symptomatic of or causal to the disease remains unclear. Contributing to the uncertainty is the variety of pathological environments present in the AD brain. We expect that BBB function is most likely disturbed as the result of multiple pathologic processes, each of which may influence water exchange at the BBB, as discussed briefly in the following.

2.1. Cerebral Amyloid Angiopathy (CAA). Amyloid-β peptides (Aβ) are derived from proteolytic cleavage of the transmembrane amyloid precursor protein (APP) and vary in length from 39–43 amino acids [19]. In AD, deposits of Aβ characteristically accumulate in the parenchyma as plaques. However, deposition of insoluble Aβ in the vessel walls and interstitial spaces (as cerebral amyloid angiopathy (CAA)) occurs in nearly all individuals with AD [20]. Vascular Aβ deposits are not always found in association with AD, but, when they are found, they exhibit several important differences from non-AD CAA [21]. In particular, the deposits are most commonly associated with the capillaries, where they attach to basal lamina and frequently occlude the lumen and/or protrude into the interstitial space [22–24]. In addition, the deposits are enriched in A$\beta_{1–42}$, the specific isoforms of Aβ found in neuritic plaques [25].

Increasing evidence suggests that these deposits may affect BBB function in AD [26, 27]. In culture, exposure of cortical microvessels to A$\beta_{1–42}$ directly damages the endothelium, resulting in an abnormal plasma membrane pattern, reduced expression of tight junction protein complexes, and increased permeability [28]. *In vivo*, there is clear evidence that vascular A$\beta_{1–42}$ deposits are associated with microhemorrhages. In the human AD brain, both microhemorrhages and A$\beta_{1–42}$ deposits are found close to or encircling microvessels, show densities that covary throughout the brain, and contain both blood- and vessel-derived proteins (fibrinogen, von Willebrand factor, collagen VI) [29]. Moreover, recent studies in APP transgenic mice have shown that increased vascular A$\beta_{1–42}$ levels are associated with decreased capillary density and abnormal basement membrane protein composition, providing evidence that A$\beta_{1–42}$ accumulation is sufficiently destructive to cause loss of vessels *in vivo* [30]. Finally, on a macroscopic scale, CAA-associated A$\beta_{1–42}$ deposits essentially recapitulate the perivascular drainage pathways [31, 32]. Thus, A$\beta_{1–42}$ deposits build up around the same abluminal surfaces along which interstitial fluid is cleared, impeding diffusion of fluids and further compromising the BBB's ability to regulate water effectively.

2.2. Inflammation. Blood-Brain Barrier function may also be affected by the inflammatory environment of AD microvessels [33]. Endothelial cells and astrocytes are activated during inflammatory CNS disease and express a variety of angiogenic mediators that affect BBB permeability, as demonstrated in other experimental models. For example, in experimental allergic encephalopathy, vascular endothelial growth factor (VEGF-A) localized in reactive astrocytes is upregulated and decreases expression of tight junction proteins, converting the microvessels into permeable fenestrated capillaries [34]. Importantly, affected vessels are no more permeable to proteins and macromolecules than those with tight junctions but are much more permeable to water.

In AD, many microvessels express the same growth factors, proteases, and proteins that typically characterize an angiogenic response. However, the extent to which expression of these factors is related to angiogenesis is unclear [35–37]. APP transgenic mice overexpressing Aβ exhibit impaired angiogenesis [38]. In the human AD brain, both microvascular density [11, 39] and reduced blood volume [40–42] are commonly observed. It is possible that the growth factors and other markers typical of an angiogenic response may in fact mediate an inflammatory one in the context of the increased Aβ levels that characterize the AD brain, with direct effects on the BBB. Consistent with this, Aβ has been shown to stimulate expression and activation of metalloproteases that degrade a wide variety of extracellular matrix components, resulting in loss of tight junctions and BBB integrity [36, 43].

2.3. Aquaporins. In addition to inflammatory mediators, astrocytes in the brain express aquaporin-4 (AQP4), one of the family of water channels found in plasma membranes throughout the body [44–48]. Functionally, aquaporins regulate transmembrane water permeability in response to osmotic gradients. In the brain, AQP4 is localized to tissue-fluid interfaces: in the glia limitans (pia-subarachnoid CSF), the ependyma (ependymal lining-ventricular CSF), and at the BBB in the astrocyte foot processes and, to a lesser extent, the endothelium [48]. The expression of AQP4 specifically at the borders of fluid-filled compartments suggests an important role of these channels in water homeostasis, a role now confirmed by many groups [45, 49–52].

While evidence linking aquaporins with fluid regulation in conditions associated with brain edema is now substantial, the effect of neurodegenerative disease on aquaporins and the consequences to BBB function remain to be defined [44]. At present, the extent to which AQP4 pathophysiology contributes to structural abnormalities in the BBB has not been established [53, 54]. Nevertheless, Wilcock et al. have recently found that AQP4 localization to the perivascular end-feet is significantly reduced in APP transgenic mice with high vascular Aβ, as is the density of astrocyte end-feet in close contact with vessel wall [55]. That only minimal changes were observed in APP transgenics with low Aβ load suggests that aquaporin function may be altered at the BBB in AD and may be a consequence of Aβ deposition in the microvessels.

3. Dynamic Contrast-Enhanced Magnetic Resonance Imaging (DCE-MRI)

The experimental index of BBB integrity has traditionally been based on the exclusion of blood-borne molecules (e.g., albumin or horseradish peroxidase) for which BBB transport mechanisms are poor. In the case of albumin, a 70 kDa serum protein, the albumin transporter is nearly absent in brain endothelium, while horseradish peroxidase is rarely found in the parenchyma due to the absence of pinocytotic vesicles [4, 56]. The presence of low molecular weight dyes in the cerebrospinal fluid (CSF) after intravenous injection has also been used to probe BBB compromise. While methodologically simpler, these experiments can be difficult to interpret as details related to dye stability, binding mechanisms, and specific effects on vascular morphology are generally lacking. Nevertheless, an age-related increase in Evans blue and carboxyfluorescein has been observed in the cortex of APP transgenic mice overexpressing Aβ following rapid intraperitoneal injection [57]. Importantly, changes in permeability appeared in young mice, *before* Aβ deposition, consistent with BBB changes early in the disease process. However, findings have not been universal and in double transgenics overexpressing APP and presenilin 1, part of the γ-secretase complex responsible for APP cleavage, bolus infusion of neither albumin nor ^{125}I-insulin showed increased permeability compared to age-matched controls [58].

Assessment of BBB function in AD patients has been limited for the most part to analysis of cerebrospinal fluid (CSF) content. Here, too, data are conflicting, and albumin levels significantly different from those of age-matched controls have not been consistently identified [59, 60]. Nevertheless, an increased CSF-albumin index has been reported in subsets of AD patients by several groups [60]. Additionally, Bowman et al. recently found a significant correlation of CSF-albumin index with the rate of disease progression in a subset of patients with mild-to-moderate AD [61]. This finding suggests that BBB dysfunction may increase the rate of disease progression in at least some AD patients.

In contrast to this more traditional approach, dynamic MRI techniques provide quantitative measures of BBB integrity based on changes in the water proton (^1H_2O) longitudinal or transverse relaxation rate constants, R_1 and R_2^*, respectively, during bolus passage of a low molecular weight paramagnetic contrast reagent (CR). Dynamic susceptibility contrast (DSC) MRI, is based on measurement of R_2^* ($= 1/T_2^*$) effects and has been used by many groups to characterize perfusion changes in the AD brain [62–65]. R_2^* effects can be exquisitely sensitive to pathophysiological changes, but their interpretation on a molecular level can be challenging. Changes in R_2^* are strongly influenced by bulk magnetic susceptibility effects. These effects are long range and vary depending on the size, shape, and orientation of the local magnetic field [66]. As a result, susceptibility effects not only cross tissue compartment boundaries but vary substantially on the histological scale, which is small with respect to an MRI voxel [67–69]. Susceptibility effects,

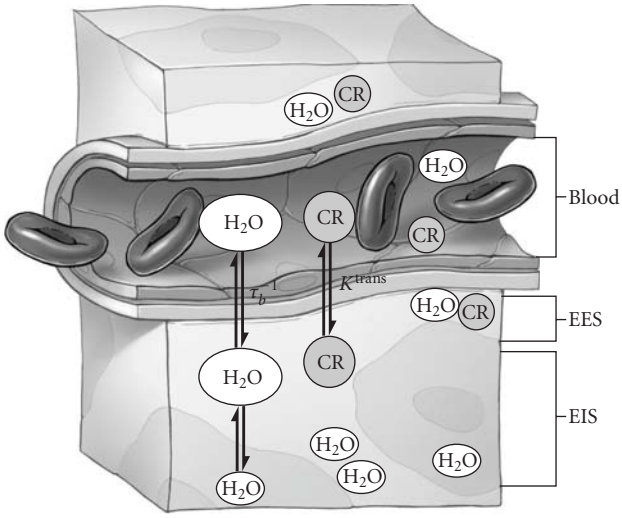

Figure 2: Schematic diagram of the three-compartment model of tissue. EES: extravascular extracellular space; EIS: extravascular intracellular space; τ_b^{-1}: unidirectional rate constant for water extravasation; K^{trans}: pseudo-first-order rate constant for CR extravasation.

therefore, can make analytical interpretation of DSC-MRI problematic and result in large errors in pharmacokinetic estimates derived from DSC measurements [70]. In contrast, DCE-MRI is based on R_1 ($= 1/T_1$) changes. These occur from direct contact of ^1H_2O to CR and are not influenced by bulk magnetic susceptibility [71]. As a result, the ^1H_2O R_1 value in a given compartment is unaffected by CR in an adjacent compartment except by intercompartment ^1H_2O exchange. Thus, R_1 changes during bolus CR passage can be interpreted analytically to provide a quantitative measure of intercompartmental water dynamics. Changes in tissue water compartmentalization have been shown to be an extremely sensitive and early indicator of BBB breakdown in multiple sclerosis, tumors, and other pathologies [72–74].

The accuracy of DCE-MRI parameters depends critically on the pharmacokinetic model used to fit the tissue R_1 changes (ΔR_{1t}) after CR injection. To a first approximation, biological tissue can be described by three compartments: blood, extravascular extracellular (EES), and extravascular intracellular space (EIS) (Figure 2). In each compartment, CR and ^1H_2O are assumed to be well mixed. In healthy brain, ^1H_2O (which forms the basis for the MR signal) occupies and exchanges between all three compartments, while low molecular weight contrast reagents do not permeate cell membranes and are restricted to the plasma and EES [67–69]. Immediately after injection, CR is confined to the plasma and greatly increases the R_1 of ^1H_2O in the blood, R_{1b}(^1H_2O exchange between erythrocytes and plasma is fast on the MR timescale, and the amount of ^1H_2O in blood can be modeled using the hematocrit volume fraction) [75]. Over time, CR diffuses through the vessel wall and increases the R_1 of ^1H_2O in the extravascular space. Thus, the mathematical relationship between R_{1b} and R_{1t} depends not only on the kinetics of compartmental ^1H_2O exchange but also on the rate at which CR leaks through the vessel wall (K^{trans}) [76].

In the limit of small K^{trans} ($< 10^{-4}\,min^{-1}$), as is the case for studies of normal and near-normal BBB permeability, a model with only two compartments is sufficient to describe transendothelial ^1H_2O exchange. In this two-site model, it is assumed that CR is initially confined to the blood plasma and that ^1H_2O freely exchanges between the plasma and a combined (EES and EIS) extravascular space. Since most of the ^1H_2O MRI signal originates from the extravascular space (in white matter, the blood ^1H_2O signal is less than 2% of the total signal), it is further assumed that R_{1t} exhibits single exponential behavior. At early times after CR administration, the time dependence of R_{1t} changes depend primarily on changes in R_{1b}, and hence on the concentration of CR in the blood (CR_b); $[CR_b]$ is a fictious concentration since CR distributes only into the plasma, so it is useful to recast this in terms of $[CR_p]$:

$$R_{1b}(t) = r_1[CR_b](t) + R_{1b0} = r_1\,(1-h)\left[CR_p\right](t) + R_{1b0}, \tag{1}$$

where r_1 is the longitudinal relaxivity of CR, R_{1b0} is the R_1 of blood ^1H_2O before CR injection and h is the hematocrit.

CR extravasation also contributes to the time dependence of ΔR_{1t}, and this is accounted for by a time-varying extravascular R_1 ($\equiv R_{1e}$) component. As CR permeates the BBB, it passes into the EES (see Figure 2). If K^{trans} is small, though, CR never achieves sufficient concentration to drive the EIS-EES water exchange. Under these conditions, the linear relationship of (2) applies. Here, $[CR_{EES}]$ is the concentration of CR in the EES. Under these conditions, the time dependence of $[CR_{EES}]$, and hence R_{1e}, is determined by the Kety-Schmidt integral rate law [72, 79, 80]. Manipulation of these two equations yields the (nonlinear) relationship between R_{1b} and R_{1t} for two-site transendothelial exchange shown in (3) [67–69]. Fits of R_{1b} and R_{1t} to (3) yield not only v_b, the cerebral blood volume ($v_b = p_b f_w$, where f_w is the tissue volume accessible to mobile solutes (ca. 0.8)), but τ_b^{-1}, the rate constant for water extravasation. τ_b^{-1} and the related permeability-surface area product of water, P_wS ($= v_b/\tau_b$), represent quantitative measures of capillary water permeability and are direct measures of BBB integrity. Here we assume that $r1$ is independent of compartment:

$$R_{1e}(t) = r_1 v_e[CR_{EES}](t) + R_{1e0}, \tag{2}$$

where v_e is the extravascular extracellular volume fraction and R_{1e0} is the R_1 of the extravascular ^1H_2O before CR injection and without transendothelial exchange,

$$R_{1t}(t) = \frac{1}{2}\left\{\left[R_{1b}(t) + R_{1e} + \tau_b^{-1} + \frac{p_b}{\tau_b(1-p_b)}\right] - \left[\left(R_{1e} - R_{1b}(t) - \tau_b^{-1} + \frac{p_b}{\tau_b(1-p_b)}\right)^2 + \frac{4p_b}{\tau_b^2(1-p_b)}\right]^{1/2}\right\}, \tag{3}$$

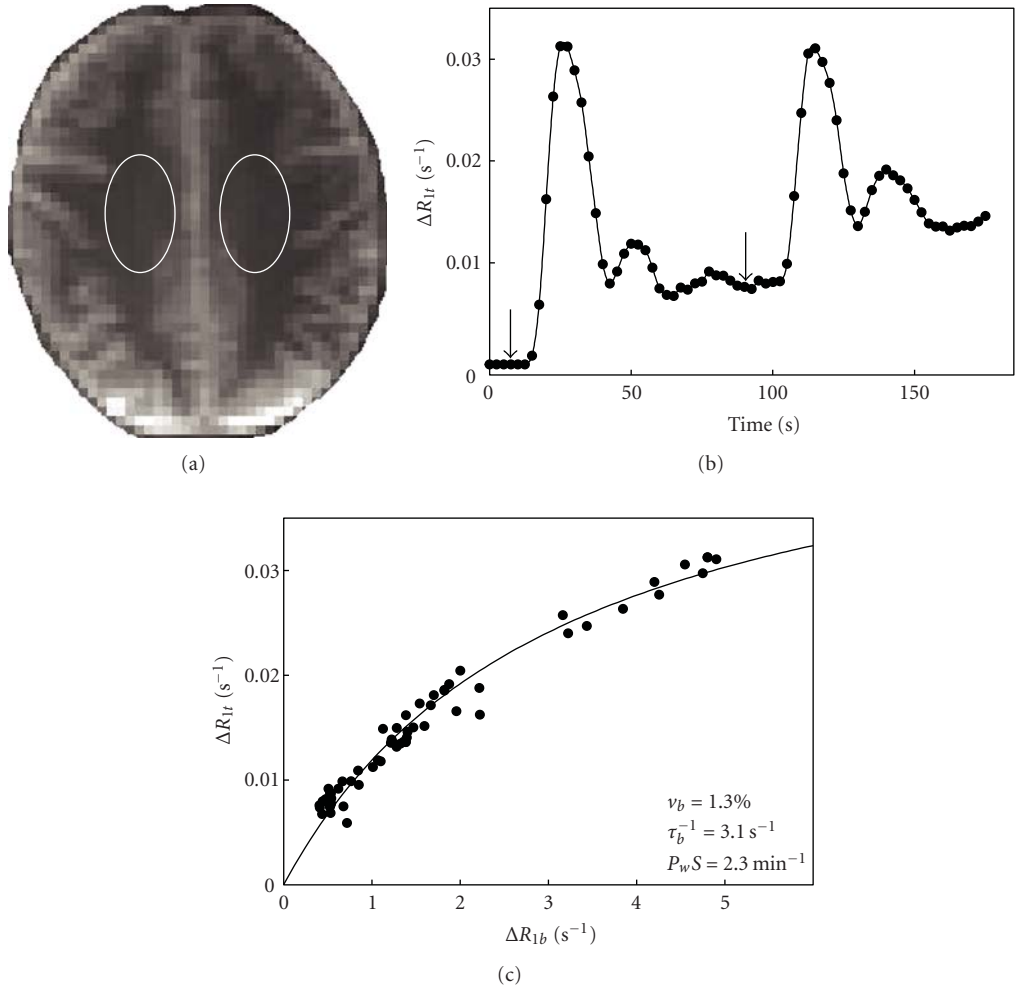

FIGURE 3: DCE-MRI region of interest (ROI) analysis in the centrum semiovale (CSO) of a 73-year-old healthy female. (a) Axial T_1-weighted (turboFLASH) images were collected on a Siemens 7 T system with 8-channel phased array transmit/receive head coil; selected ROI shown in white. (b) Plot of pre-post contrast R_{1t} (ΔR_{1t}) versus time. Images were collected immediately preceding two 0.05 mmol/kg bolus injections of gadoteridol and every 2.5 seconds over the next 175 sec. R_{1t} values were calculated at each time point by fitting the signal intensity curves to a standard two-parameter single exponential inversion recovery equation [77]. (c) ΔR_{1t} plotted as a function of ΔR_{1b}. Changes in the blood signal, ΔR_{1b}, were determined from an ROI placed entirely in the sagittal sinus. The solid line represents the best fit of the data to (3). Resultant estimates of ν_b, τ_b^{-1}, and P_wS are also shown.

where R_{1t0}, R_{1b0} are the R_1 of tissue and blood, respectively, before CR injection, R_{1e} is the R_1 of extravascular water in the absence of transendothelial exchange, τ_b is the average intravascular lifetime, and p_b is the mole fraction of blood water.

Previous DCE-MRI studies in AD individuals have found minimal disruption of the BBB [81, 82]. However, these studies are limited by the relatively low field strength (1.5 T) of the measurements and the lack of pharmacokinetic modeling. The real power of DCE to probe BBB disturbances, particularly in the context of a relatively intact barrier, is most evident at high field, where the increased signal-to-noise and reduced CR detection threshold yields significantly better precision and accuracy of pharmacokinetic estimates. Figure 3 shows a representative 7 T DCE-MRI study performed recently in our laboratory. Fitting to (3) yields values of τ_b^{-1} and ν_b in the centrum semiovale that are in close agreement with those reported previously [83, 84]. Application of (3) on a pixel-wise basis results in parametric maps like the ones shown in Figure 4(a) [78]. As far as we are aware, this is the first map of the water permeability surface area product (P_wS) produced using dynamic MR techniques in an individual with early AD, and underscores the power of DCE to visualize even subtle changes in BBB water permeability (Figure 4(b)).

It should be noted that use of (3) can lead to large errors in parametric estimates if ^1H_2O exchange across the BBB or extravascular cell membranes (i.e., between EES and EIS in Figure 2) is slow on the timescale of DCE measurements [85]. In either of these situations, abstraction of accurate parameters requires a three-compartment model and a more comprehensive pharmacokinetic treatment. Such a model

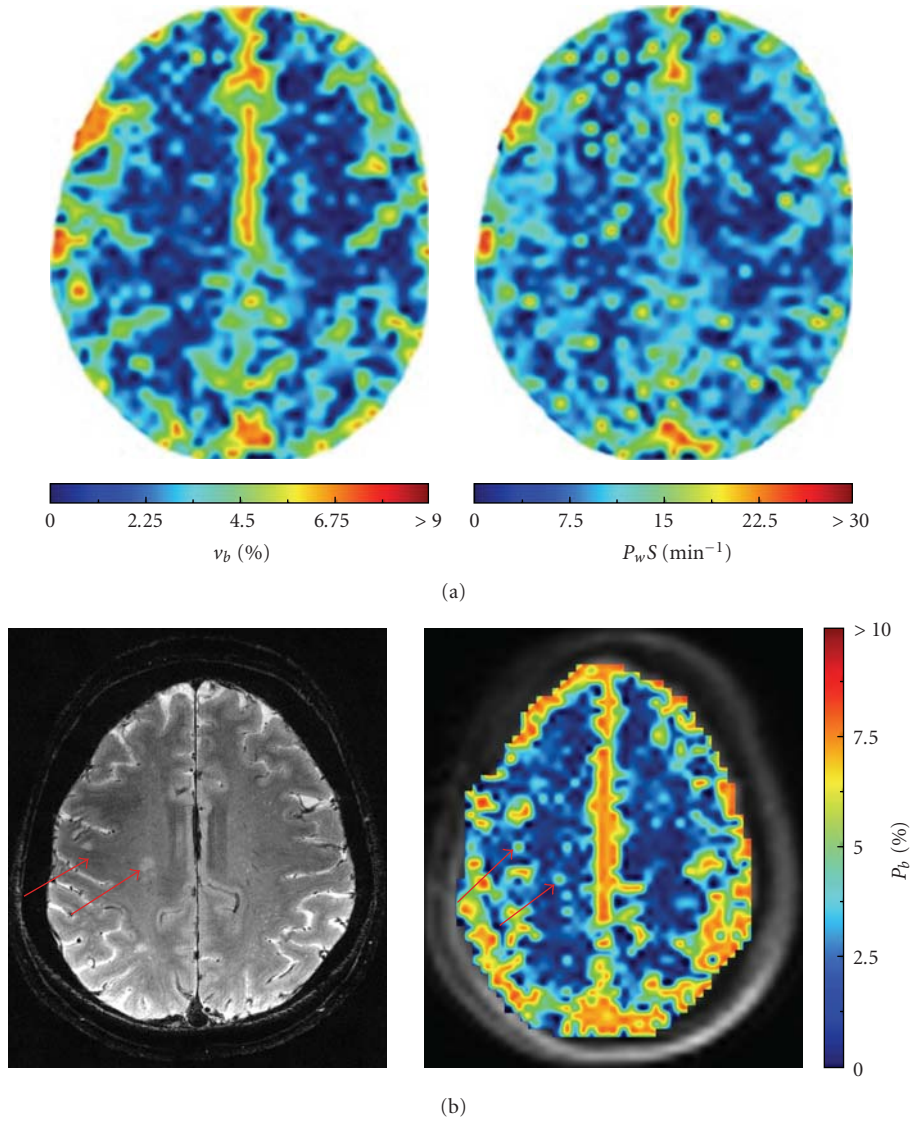

Figure 4: 7 T (a) DCE-MRI maps of blood volume (v_b) and water permeability (P_wS) in a superior slice from a 71-year-old female with early AD [78]. (b) T_2-weighted spin echo image and corresponding p_b map from a healthy 70-year-old female. Arrows indicate hyperintense white matter regions (15–23 mm^2) visible on both the T_2 image and corresponding parametric map.

has been developed by Li et al. and is currently being applied in our laboratory [76].

4. Conclusion

The BBB plays a critical role in water homeostasis in the brain. Although the mechanism remains to be determined, converging evidence suggests that AD pathophysiology may disturb the BBB and disrupt intercompartmental water exchange. DCE-MRI is an extremely powerful and sensitive probe of water dynamics in the living brain. Pharmacokinetic modeling provides quantitative estimates of blood volume, vascular permeability, and rates of transendothelial water exchange. We expect that DCE-MRI studies, particularly at high field, will play a key role in unlocking the contribution of BBB dysfunction to the pathophysiology of AD.

Acknowledgments

The authors wish to thank Andy Rekito for assistance with illustrations. This work was supported by Grants from the National Institute on Aging (K25 AG033638 and P30 AG08017) and the Oregon Partnership for Alzheimer's Research.

References

[1] A. J. Bastos Leite, P. Scheltens, and F. Barkhof, "Pathological aging of the brain: an overview," *Topics in Magnetic Resonance Imaging*, vol. 15, no. 6, pp. 369–389, 2004.

[2] B. V. Zlokovic, "Neurovascular mechanisms of Alzheimer's neurodegeneration," *Trends in Neurosciences*, vol. 28, no. 4, pp. 202–208, 2005.

[3] C. Iadecola and P. B. Gorelick, "Converging pathogenic mechanisms in vascular and neurodegenerative dementia," *Stroke*, vol. 34, no. 2, pp. 335–337, 2003.

[4] A. S. Lossinsky and R. R. Shivers, "Structural pathways for macromolecular and cellular transport across the blood-brain barrier during inflammatory conditions. Review," *Histology and Histopathology*, vol. 19, no. 2, pp. 535–564, 2004.

[5] P. Ballabh, A. Braun, and M. Nedergaard, "The blood-brain barrier: an overview: structure, regulation, and clinical implications," *Neurobiology of Disease*, vol. 16, no. 1, pp. 1–13, 2004.

[6] N. J. Abbott, "Evidence for bulk flow of brain interstitial fluid: significance for physiology and pathology," *Neurochemistry International*, vol. 45, no. 4, pp. 545–552, 2004.

[7] E. A. Neuwelt, N. H. Greig, C. Raffel et al., "Mechanisms of disease: the blood-brain barrier," *Neurosurgery*, vol. 54, no. 1, pp. 131–142, 2004.

[8] S. W. Lee, W. J. Kim, Y. K. Choi et al., "SSeCKS regulates angiogenesis and tight junction formation in blood-brain barrier," *Nature Medicine*, vol. 9, no. 7, pp. 900–906, 2003.

[9] N. J. Abbott, L. Rönnbäck, and E. Hansson, "Astrocyte-endothelial interactions at the blood-brain barrier," *Nature Reviews Neuroscience*, vol. 7, no. 1, pp. 41–53, 2006.

[10] D. R. Thal, E. Ghebremedhin, M. Orantes, and O. D. Wiestler, "Vascular pathology in Alzheimer disease: correlation of cerebral amyloid angiopathy and arteriosclerosis/lipohyalinosis with cognitive decline," *Journal of Neuropathology and Experimental Neurology*, vol. 62, no. 12, pp. 1287–1301, 2003.

[11] L. Buée, P. R. Hof, and A. Delacourte, "Brain microvascular changes in Alzheimer's disease and other dementias," *Annals of the New York Academy of Sciences*, vol. 826, pp. 7–24, 1997.

[12] E. Farkas and P. G. M. Luiten, "Cerebral microvascular pathology in aging and Alzheimer's disease," *Progress in Neurobiology*, vol. 64, no. 6, pp. 575–611, 2001.

[13] P. A. Stewart, K. Hayakawa, M. A. Akers, and H. V. Vinters, "A morphometric study of the blood-brain barrier in Alzheimer's disease," *Laboratory Investigation*, vol. 67, no. 6, pp. 734–742, 1992.

[14] L. Claudio, "Ultrastructural features of the blood-brain barrier in biopsy tissue from Alzheimer's disease patients," *Acta Neuropathologica*, vol. 91, no. 1, pp. 6–14, 1996.

[15] E. Farkas, G. I. De Jong, E. Apró, R. A. I. De Vos, E. N. H. Jansen Steur, and P. G. M. Luiten, "Similar ultrastructural breakdown of cerebrocortical capillaries in Alzheimer's disease, Parkinson's disease, and experimental hypertension: What is the functional link?" *Annals of the New York Academy of Sciences*, vol. 903, pp. 72–82, 2000.

[16] T. M. Berzin, B. D. Zipser, M. S. Rafii et al., "Agrin and microvascular damage in Alzheimer's disease," *Neurobiology of Aging*, vol. 21, no. 2, pp. 349–355, 2000.

[17] M. O. Romanitan, B. O. Popescu, B. Winblad, O. A. Bajenaru, and N. Bogdanovic, "Occludin is overexpressed in Alzheimer's disease and vascular dementia," *Journal of Cellular and Molecular Medicine*, vol. 11, no. 3, pp. 569–579, 2007.

[18] M. O. Romanitan, B. O. Popescu, T. Spulber et al., "Altered expression of claudin family proteins in Alzheimer's disease and vascular dementia brains," *Journal of Cellular and Molecular Medicine*, vol. 14, no. 5, pp. 1088–1100, 2010.

[19] C. Haass and D. J. Selkoe, "Soluble protein oligomers in neurodegeneration: lessons from the Alzheimer's amyloid β-peptide," *Nature Reviews Molecular Cell Biology*, vol. 8, no. 2, pp. 101–112, 2007.

[20] M. M. Verbeel, R. M. W. de Waal, and H. V. Vinters, *Cerebral Amyloid Angiopathy in Alzheimer's Disease and Related Disorders*, Kluwer Academic Publishers, Dordrecht, The Netherlands, 2000.

[21] D. R. Thal, W. S. T. Griffin, R. A. I. de Vos, and E. Ghebremedhin, "Cerebral amyloid angiopathy and its relationship to Alzheimer's disease," *Acta Neuropathologica*, vol. 115, no. 6, pp. 599–609, 2008.

[22] J. Attems and K. A. Jellinger, "Only cerebral capillary amyloid angiopathy correlates with Alzheimer pathology—a pilot study," *Acta Neuropathologica*, vol. 107, no. 2, pp. 83–90, 2004.

[23] H. Yamaguchi, T. Yamazaki, C. A. Lemere, M. P. Frosch, and D. J. Selkoe, "Beta amyloid is focally deposited within the outer basement membrane in the amyloid angiopathy of Alzheimer's disease: an immunoelectron microscopic study," *American Journal of Pathology*, vol. 141, no. 1, pp. 249–259, 1992.

[24] D. R. Thal, E. Capetillo-Zarate, S. Larionov, M. Staufenbiel, S. Zurbruegg, and N. Beckmann, "Capillary cerebral amyloid angiopathy is associated with vessel occlusion and cerebral blood flow disturbances," *Neurobiology of Aging*, vol. 30, no. 12, pp. 1936–1948, 2009.

[25] A. E. Roher, J. D. Lowenson, S. Clarke et al., "β-Amyloid-(1-42) is a major component of cerebrovascular amyloid deposits: implications for the pathology of Alzheimer disease," *Proceedings of the National Academy of Sciences of the United States of America*, vol. 90, no. 22, pp. 10836–10840, 1993.

[26] R. D. Bell and B. V. Zlokovic, "Neurovascular mechanisms and blood-brain barrier disorder in Alzheimer's disease," *Acta Neuropathologica*, vol. 118, no. 1, pp. 103–113, 2009.

[27] R. O. Carare, M. Bernardes-Silva, T. A. Newman et al., "Solutes, but not cells, drain from the brain parenchyma along basement membranes of capillaries and arteries: significance for cerebral amyloid angiopathy and neuroimmunology," *Neuropathology and Applied Neurobiology*, vol. 34, no. 2, pp. 131–144, 2008.

[28] S. Marco and S. D. Skaper, "Amyloid β-peptide alters tight junction protein distribution and expression in brain microvessel endothelial cells," *Neuroscience Letters*, vol. 401, no. 3, pp. 219–224, 2006.

[29] K. M. Cullen, Z. Kócsi, and J. Stone, "Microvascular pathology in the aging human brain: evidence that senile plaques are sites of microhaemorrhages," *Neurobiology of Aging*, vol. 27, no. 12, pp. 1786–1796, 2006.

[30] C. A. Hawkes, W. Härtig, J. Kacza et al., "Perivascular drainage of solutes is impaired in the ageing mouse brain and in the presence of cerebral amyloid angiopathy," *Acta Neuropathologica*, vol. 121, no. 4, pp. 431–443, 2011.

[31] S. D. Preston, P. V. Steart, A. Wilkinson, J. A. R. Nicoll, and R. O. Weller, "Capillary and arterial cerebral amyloid angiopathy in Alzheimer's disease: defining the perivascular route for the elimination of amyloid β from the human brain," *Neuropathology and Applied Neurobiology*, vol. 29, no. 2, pp. 106–117, 2003.

[32] A. T. Argaw, B. T. Gurfein, Y. Zhang, A. Zameer, and G. R. John, "VEGF-mediated disruption of endothelial CLN-5 promotes blood-brain barrier breakdown," *Proceedings of the National Academy of Sciences of the United States of America*, vol. 106, no. 6, pp. 1977–1982, 2009.

[33] R. Pluta, S. Januszewski, and M. Uamek, "White matter, brain edema, blood brain barrier," *Journal of Cerebral Blood Flow & Metabolism*, vol. 25, p. S251, 2005.

[34] A. T. Argaw, B. T. Gurfein, Y. Zhang, A. Zameer, and G. R. John, "VEGF-mediated disruption of endothelial CLN-5 promotes blood-brain barrier breakdown," *Proceedings of*

the National Academy of Sciences of the United States of America, vol. 106, no. 6, pp. 1977–1982, 2009.

[35] I. Mateo, J. Llorca, J. Infante et al., "Low serum VEGF levels are associated with Alzheimer's disease," *Acta Neurologica Scandinavica*, vol. 116, no. 1, pp. 56–58, 2007.

[36] L. Thirumangalakudi, P. G. Samany, A. Owoso, B. Wiskar, and P. Grammas, "Angiogenic proteins are expressed by brain blood vessels in Alzheimer's disease," *Journal of Alzheimer's Disease*, vol. 10, no. 1, pp. 111–118, 2006.

[37] M. Chiappelli, B. Borroni, S. Archetti et al., "VEGF gene and phenotype relation with Alzheimer's disease and mild cognitive impairment," *Rejuvenation Research*, vol. 9, no. 4, pp. 485–493, 2006.

[38] D. Paris, N. Patel, A. Delledonne, A. Quadros, R. Smeed, and M. Mullan, "Impaired angiogenesis in a transgenic mouse model of cerebral amyloidosis," *Neuroscience Letters*, vol. 366, no. 1, pp. 80–85, 2004.

[39] K. A. Jellinger, "Alzheimer disease and cerebrovascular pathology: an update," *Journal of Neural Transmission*, vol. 109, no. 5-6, pp. 813–836, 2002.

[40] G. J. Harris, R. F. Lewis, A. Satlin et al., "Dynamic susceptibility contrast MRI of regional cerebral blood volume in Alzheimer's disease," *American Journal of Psychiatry*, vol. 153, no. 5, pp. 721–724, 1996.

[41] K. A. Johnson and M. S. Albert, "Perfusion abnormalities in prodromal AD," *Neurobiology of Aging*, vol. 21, no. 2, pp. 289–292, 2000.

[42] A. Bozzao, R. Floris, M. E. Baviera, A. Apruzzese, and G. Simonetti, "Diffusion and perfusion MR imaging in cases of Alzheimer's disease: correlations with cortical atrophy and lesion load," *American Journal of Neuroradiology*, vol. 22, no. 6, pp. 1030–1036, 2001.

[43] S. S. Jung, W. Zhang, and W. E. Van Nostrand, "Pathogenic Aβ induces the expression and activation of matrix metalloproteinase-2 in human cerebrovascular smooth muscle cells," *Journal of Neurochemistry*, vol. 85, no. 5, pp. 1208–1215, 2003.

[44] M. J. Tait, S. Saadoun, B. A. Bell, and M. C. Papadopoulos, "Water movements in the brain: role of aquaporins," *Trends in Neurosciences*, vol. 31, no. 1, pp. 37–43, 2008.

[45] Z. Zador, O. Bloch, X. Yao, and G. T. Manley, "Aquaporins: role in cerebral edema and brain water balance," *Progress in Brain Research*, vol. 161, pp. 185–194, 2007.

[46] P. Agre, S. Nielsen, and O. P. Ottersen, "Towards a molecular understanding of water homeostasis in the brain," *Neuroscience*, vol. 129, no. 4, pp. 849–850, 2004.

[47] P. Agre, "The aquaporin water channels," *Proceedings of the American Thoracic Society*, vol. 3, no. 1, pp. 5–13, 2006.

[48] M. Amiry-Moghaddam and O. P. Ottersen, "The molecular basis of water transport in the brain," *Nature Reviews Neuroscience*, vol. 4, no. 12, pp. 991–1001, 2003.

[49] T. Pannicke, A. Wurm, I. Iandiev et al., "Deletion of aquaporin-4 renders retinal glial cells more susceptible to osmotic stress," *Journal of Neuroscience Research*, vol. 88, no. 13, pp. 2877–2888, 2010.

[50] E. E. Benarroch, "Aquaporin-4, homeostasis, and neurologic disease," *Neurology*, vol. 69, no. 24, pp. 2266–2268, 2007.

[51] T. Eid, T. S. W. Lee, M. J. Thomas et al., "Loss of perivascular aquaporin 4 may underlie deficient water and K homeostasis in the human epileptogenic hippocampus," *Proceedings of the National Academy of Sciences of the United States of America*, vol. 102, no. 4, pp. 1193–1198, 2005.

[52] S. Nag, J. L. Manias, and D. J. Stewart, "Pathology and new players in the pathogenesis of brain edema," *Acta Neuropathologica*, vol. 118, no. 2, pp. 197–217, 2009.

[53] S. Saadoun, M. J. Tait, A. Reza et al., "AQP4 gene deletion in mice does not alter blood-brain barrier integrity or brain morphology," *Neuroscience*, vol. 161, no. 3, pp. 764–772, 2009.

[54] J. Zhou, H. Kong, X. Hua, M. Xiao, J. Ding, and G. Hu, "Altered blood-brain barrier integrity in adult aquaporin-4 knockout mice," *NeuroReport*, vol. 19, no. 1, pp. 1–5, 2008.

[55] D. M. Wilcock, M. P. Vitek, and C. A. Colton, "Vascular amyloid alters astrocytic water and potassium channels in mouse models and humans with Alzheimer's disease," *Neuroscience*, vol. 159, no. 3, pp. 1055–1069, 2009.

[56] P. A. Stewart, "Endothelial vesicles in the blood-brain barrier: are they related to permeability?" *Cellular and Molecular Neurobiology*, vol. 20, no. 2, pp. 149–163, 2000.

[57] M. Ujiie, D. L. Dickstein, D. A. Carlow, and W. A. Jefferies, "Blood-brain barrier permeability precedes senile plaque formation in an Alzheimer disease model," *Microcirculation*, vol. 10, no. 6, pp. 463–470, 2003.

[58] J. F. Poduslo, G. L. Curran, T. M. Wengenack, B. Malester, and K. Duff, "Permeability of proteins at the blood-brain barrier in the normal adult mouse and double transgenic mouse model of Alzheimer's disease," *Neurobiology of Disease*, vol. 8, no. 4, pp. 555–567, 2001.

[59] I. Skoog, A. Wallin, P. Fredman et al., "A population study on blood-brain barrier function in 85-year-olds: relation to Alzheimer's disease and vascular dementia," *Neurology*, vol. 50, no. 4, pp. 966–971, 1998.

[60] A. Algotsson and B. Winblad, "The integrity of the blood-brain barrier in Alzheimer's disease," *Acta Neurologica Scandinavica*, vol. 115, no. 6, pp. 403–408, 2007.

[61] G. L. Bowman, J. A. Kaye, M. Moore, D. Waichunas, N. E. Carlson, and J. F. Quinn, "Blood-brain barrier impairment in Alzheimer disease: stability and functional significance," *Neurology*, vol. 68, no. 21, pp. 1809–1814, 2007.

[62] G. J. Harris, R. F. Lewis, A. Satlin et al., "Dynamic susceptibility contrast MR imaging of regional cerebral blood volume in Alzheimer disease: a promising alternative to nuclear medicine," *American Journal of Neuroradiology*, vol. 19, no. 9, pp. 1727–1732, 1998.

[63] L. C. Maas, G. J. Harris, A. Satlin, C. D. English, R. F. Lewis, and P. F. Renshaw, "Regional cerebral blood volume measured by dynamic susceptibility contrast MR imaging in Alzheimer's disease: a principal components analysis," *Journal of Magnetic Resonance Imaging*, vol. 7, no. 1, pp. 215–219, 1997.

[64] D. Mattia, F. Babiloni, A. Romigi et al., "Quantitative EEG and dynamic susceptibility contrast MRI in Alzheimer's disease: a correlative study," *Clinical Neurophysiology*, vol. 114, no. 7, pp. 1210–1216, 2003.

[65] L. Cavallin, R. Danielsson, A. R. Öksengard et al., "Can dynamic susceptibility contrast magnetic resonance imaging replace single-photon emission computed tomography in the diagnosis of patients with Alzheimer's disease? A pilot study," *Acta Radiologica*, vol. 47, no. 9, pp. 977–985, 2006.

[66] B. F. Kjølby, L. Østergaard, and V. G. Kiselev, "Theoretical model of intravascular paramagnetic tracers effect on tissue relaxation," *Magnetic Resonance in Medicine*, vol. 56, no. 1, pp. 187–197, 2006.

[67] C. S. Landis, X. Li, F. W. Telang et al., "Determination of the MRI contrast agent concentration time course in vivo following bolus injection: effect of equilibrium transcytolemmal

water exchange," *Magnetic Resonance in Medicine*, vol. 44, no. 4, pp. 563–574, 2000.

[68] C. Schwarzbauer, S. P. Morrissey, R. Deichmann et al., "Quantitative magnetic resonance imaging of capillary water permeability and regional blood volume with an intravascular MR contrast agent," *Magnetic Resonance in Medicine*, vol. 37, no. 5, pp. 769–777, 1997.

[69] W. D. Rooney, T. E. Yankeelov, P. K. Coyle et al., "Regional blood volumes and intravascular water lifetimes in human brain," in *Proceedings of the International Society for Magnetic Resonance in Medicine*, vol. 11, p. 2188.

[70] T. H. Jochimsen, R. D. Newbould, S. T. Skare et al., "Identifying systematic errors in quantitative dynamic-susceptibility contrast perfusion imaging by high-resolution multi-echo parallel EPI," *NMR in Biomedicine*, vol. 20, no. 4, pp. 429–438, 2007.

[71] P. Caravan, J. J. Ellison, T. J. McMurry, and R. B. Lauffer, "Gadolinium(III) chelates as MRI contrast agents: Structure, dynamics, and applications," *Chemical Reviews*, vol. 99, no. 9, pp. 2293–2352, 1999.

[72] P. S. Tofts and A. G. Kermode, "Measurement of the blood-brain barrier permeability and leakage space using dynamic MR imaging. 1. Fundamental concepts," *Magnetic Resonance in Medicine*, vol. 17, no. 2, pp. 357–367, 1991.

[73] K. A. Broom, D. C. Anthony, A. M. Blamire et al., "MRI reveals that early changes in cerebral blood volume precede blood-brain barrier breakdown and overt pathology in MS-like lesions in rat brain," *Journal of Cerebral Blood Flow and Metabolism*, vol. 25, no. 2, pp. 204–216, 2005.

[74] T. E. Yankeelov, W. D. Rooney, W. Huang et al., "Evidence for shutter-speed variation in CR bolus-tracking studies of human pathology," *NMR in Biomedicine*, vol. 18, no. 3, pp. 173–185, 2005.

[75] J. H. Lee, D. C. Medina, X. Li et al., "Deuterium quenching of ^1H_2O relaxation in the living rat brain," *Proceedings of the International Society for Magnetic Resonance in Medicine*, vol. 9, p. 529, 2001.

[76] X. Li, W. D. Rooney, and C. S. Springer, "A unified magnetic resonance imaging pharmacokinetic theory: intravascular and extracellular contrast reagents," *Magnetic Resonance in Medicine*, vol. 54, no. 6, pp. 1351–1359, 2005.

[77] P. Gowland and V. Stevenson, "T_1: the longitudinal relaxation time," in *Quantitative MRI of the Brain*, P. S. Tofts, Ed., pp. 111–141, John Wiley & Sons, West Sussex, UK, 2003.

[78] V. C. Anderson, D. P. Lenar, J. F. Quinn, J. A. Kaye, X. Li, and W. D. Rooney, "Quantitative characterization of blood brain barrier permeability in early AD: a pilot 7T DCE-MRI study," in *Proceedings of the International Conference on Alzheimer's Disease*, Honolulu, Hawaii, USA, July 2010.

[79] H. B. W. Larsson, M. Stubgaard, J. L. Frederiksen, M. Jensen, O. Henriksen, and O. B. Paulson, "Quantitation of blood-brain barrier defect by magnetic resonance imaging and gadolinium-DTPA in patients with multiple sclerosis and brain tumors," *Magnetic Resonance in Medicine*, vol. 16, no. 1, pp. 117–131, 1990.

[80] P. S. Tofts, G. Brix, D. L. Buckley et al., "Estimating kinetic parameters from dynamic contrast-enhanced T- weighted MRI of a diffusable tracer: standardized quantities and symbols," *Journal of Magnetic Resonance Imaging*, vol. 10, no. 3, pp. 223–232, 1999.

[81] H. Wang, E. J. Golob, and M. Y. Su, "Vascular volume and blood-brain barrier permeability measured by dynamic contrast enhanced MRI in hippocampus and cerebellum of patients with MCI and normal controls," *Journal of Magnetic Resonance Imaging*, vol. 24, no. 3, pp. 695–700, 2006.

[82] J. M. Starr, A. J. Farrall, P. Armitage, B. McGurn, and J. Wardlaw, "Blood-brain barrier permeability in Alzheimer's disease: a case-control MRI study," *Psychiatry Research*, vol. 171, no. 3, pp. 232–241, 2009.

[83] W. D. Rooney, T. E. Yankeelov, P. K. Coyle, F. W. Telang, and C. S. Springer, "Regional blood volumes and intravascular water lifetimes in human brain," *Proceedings of the International Society for Magnetic Resonance in Medicine*, vol. 11, p. 2188, 2003.

[84] G. C. Newman, E. Delucia-Deranja, A. Tudorica, F. E. Hospod, and C. S. Patlak, "Cerebral blood volume measurements by T_*^2-weighted MRI and contrast infusion," *Magnetic Resonance in Medicine*, vol. 50, no. 4, pp. 844–855, 2003.

[85] C. S. Landis, X. Li, F. W. Telang et al., "Equilibrium transcytolemmal water-exchange kinetics in skeletal muscle in vivo," *Magnetic Resonance in Medicine*, vol. 42, no. 3, pp. 467–478, 1999.

Hindawi Publishing Corporation
Cardiovascular Psychiatry and Neurology
Volume 2011, Article ID 765923, 11 pages
doi:10.1155/2011/765923

Research Article

Blood-Brain Barrier Breakdown Following Traumatic Brain Injury: A Possible Role in Posttraumatic Epilepsy

Oren Tomkins,[1,2] Akiva Feintuch,[3] Moni Benifla,[4] Avi Cohen,[4] Alon Friedman,[1,4,5] and Ilan Shelef[3]

[1] *Departments of Physiology and Neurobiology, Zlotowski Center for Neuroscience, Ben-Gurion University of the Negev, 84105 Beer-Sheva, Israel*
[2] *Department of Ophthalmology, Bnai Zion Medical Center, Haifa, Israel*
[3] *Department of Neuroradiology, Soroka University Medical Center and Zlotowski Center for Neuroscience, Ben-Gurion University of the Negev, Beer-Sheva, Israel*
[4] *Department of Neurosurgery, Soroka University Medical Center and Zlotowski Center for Neuroscience, Ben-Gurion University of the Negev, Beer-Sheva, Israel*
[5] *Department of Biomedical Engineering, Ben-Gurion University of the Negev, Beer-Sheva, Israel*

Correspondence should be addressed to Oren Tomkins, oren.tomkins@gmail.com

Received 30 October 2010; Accepted 2 January 2011

Academic Editor: Daniela Kaufer

Recent animal experiments indicate a critical role for opening of the blood-brain barrier (BBB) in the pathogenesis of post-traumatic epilepsy (PTE). This study aimed to investigate the frequency, extent, and functional correlates of BBB disruption in epileptic patients following mild traumatic brain injury (TBI). Thirty-seven TBI patients were included in this study, 19 of whom suffered from PTE. All underwent electroencephalographic (EEG) recordings and brain magnetic resonance imaging (bMRI). bMRIs were evaluated for BBB disruption using novel quantitative techniques. Cortical dysfunction was localized using standardized low-resolution brain electromagnetic tomography (sLORETA). TBI patients displayed significant EEG slowing compared to controls with no significant differences between PTE and nonepileptic patients. BBB disruption was found in 82.4% of PTE compared to 25% of non-epileptic patients ($P = .001$) and could be observed even years following the trauma. The volume of cerebral cortex with BBB disruption was significantly larger in PTE patients ($P = .001$). Slow wave EEG activity was localized to the same region of BBB disruption in 70% of patients and correlated to the volume of BBB disrupted cortex. We finally present a patient suffering from early cortical dysfunction and BBB breakdown with a gradual and parallel resolution of both pathologies. Our findings demonstrate that BBB pathology is frequently found following mild TBI. Lasting BBB breakdown is found with increased frequency and extent in PTE patients. Based on recent animal studies and the colocalization found between the region of disrupted BBB and abnormal EEG activity, we suggest a role for a vascular lesion in the pathogenesis of PTE.

1. Introduction

Traumatic brain injury (TBI) is a common cause of mortality and morbidity with an occurrence of approximately 200 cases per 100,000 people a year. It is also a known major risk factor for focal epilepsy [1]. The incidence of post-traumatic epilepsy (PTE) ranges from 2–50% in different studies, accounting for approximately 20% of symptomatic epilepsies [1–6]. Seizures may occur immediately following the trauma, though PTE usually develops several months and even years later. While immediate post-traumatic seizures may be successfully treated with antiepileptic drugs [7], the mechanisms underlying the development of PTE remain unknown with no means for preventing it [8].

The central nervous system is protected by the function of the blood-brain barrier (BBB), which regulates the passage of blood constituents in and out of the brain extracellular space. It has been previously suggested that an increase in BBB permeability may be associated with the pathogenesis of neurological disorders [9–11]. However, only recent animal experiments directly showed that primary prolonged opening of the BBB leads to the development of delayed, long-lasting epileptiform activity [12]. Furthermore, it has been suggested that the most common serum protein, albumin,

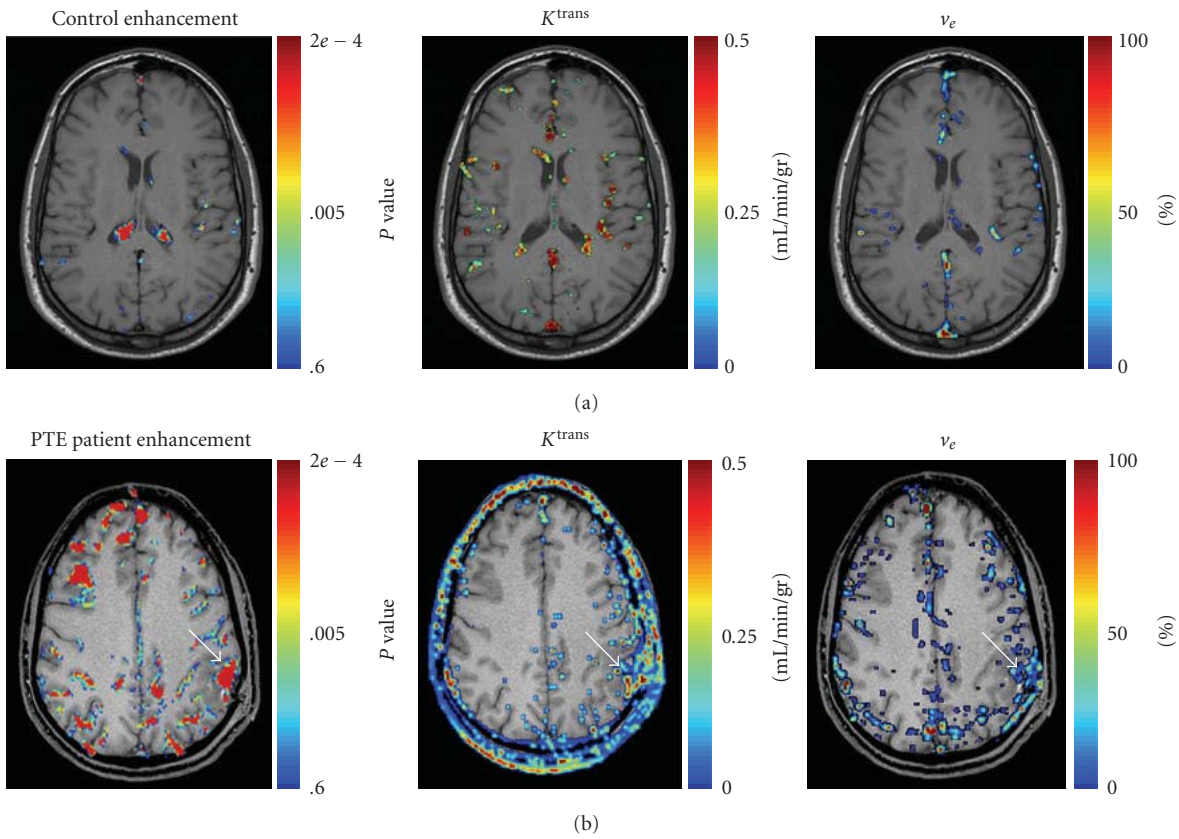

Figure 1: Imaging modalities allow for BBB permeability evaluation and quantification. (a) Control subject: no BBB disruption is observed within the brain parenchyma (areas of significant differences are found in blood vessels, sinuses and the choroid plexus). Increased BBB permeability (K^{trans}) and extravascular volume (v_e) are also localized to those same structures. (b) A 28-year-old PTE patient 10 days following TBI. A region of increased BBB permeability is detected over the left parietal lobe in both methods (arrows).

may underlie astrocytic activation and dysfunction, further leading to neuronal hypersynchrony (i.e., *epileptogenesis*) and accumulated neuronal loss [13, 14]. While previous clinical studies showed that altered permeability is observed in neurological patients [15–18], little data exists on the frequency, extent and significance of enhanced BBB permeability in epileptic patients [19]. The aim of the present study was to characterize the frequency of long-lasting increases in BBB permeability following head trauma and explore correlations with the extent of cerebral lesions, EEG abnormalities, and the presence of post-traumatic epilepsy. Part of this study has been published as a short report [20].

2. Materials and Methods

2.1. Patient Selection. The study protocol was approved by the Soroka Medical Center Medical Ethics Board and Helsinki Committee (NIH clinical trial registration: NCT00419874). Patients were included in the study if they were referred to the tertiary center's outpatient clinic following hospitalization due to TBI, most often with significant symptoms. Thirty-seven head trauma patients (11 women, 26 men) aged 10–68 years (26.89 ± 2.43), who were examined during the years 2005–2007 were included in this study (Table 1). Patients were included if, at the time of enrollment, they were more than one week after TBI (28.81 ± 8.81, median= 3 months), were fully conscious, and with mild to no neurological impairment. All patients were healthy prior to the traumatic brain injury with no history of neurological or psychiatric disorders. Eighteen patients had been involved in moving vehicle accidents, 7 had fallen, and 12 were hit by a blunt instrument (hammer, door, fist, etc.). Most patients ($n = 34$, 91.89%) suffered from mild TBI according to a Glasgow coma score (GSC) of >13 upon admission (in 88% the documented score was 15). A short period of unconsciousness lasting up to several minutes was noted in 13 patients, and 3 patients suffered from loss of consciousness lasting several days. In the 21 remaining patients, no period of unconsciousness was reported. All patients made a good recovery before being enrolled in the study.

Nineteen patients were diagnosed as suffering from PTE with partial seizures (in 11 patients, secondary generalization was reported). A diagnosis of PTE was given to patients that presented with at least one delayed epileptic seizure (more than a week after the trauma). The non-epileptic TBI patients ($n = 18$) mainly suffered from headaches ($n = 15$, 83.33%), cognitive impairment ($n = 2$, 11.11%), mild motor

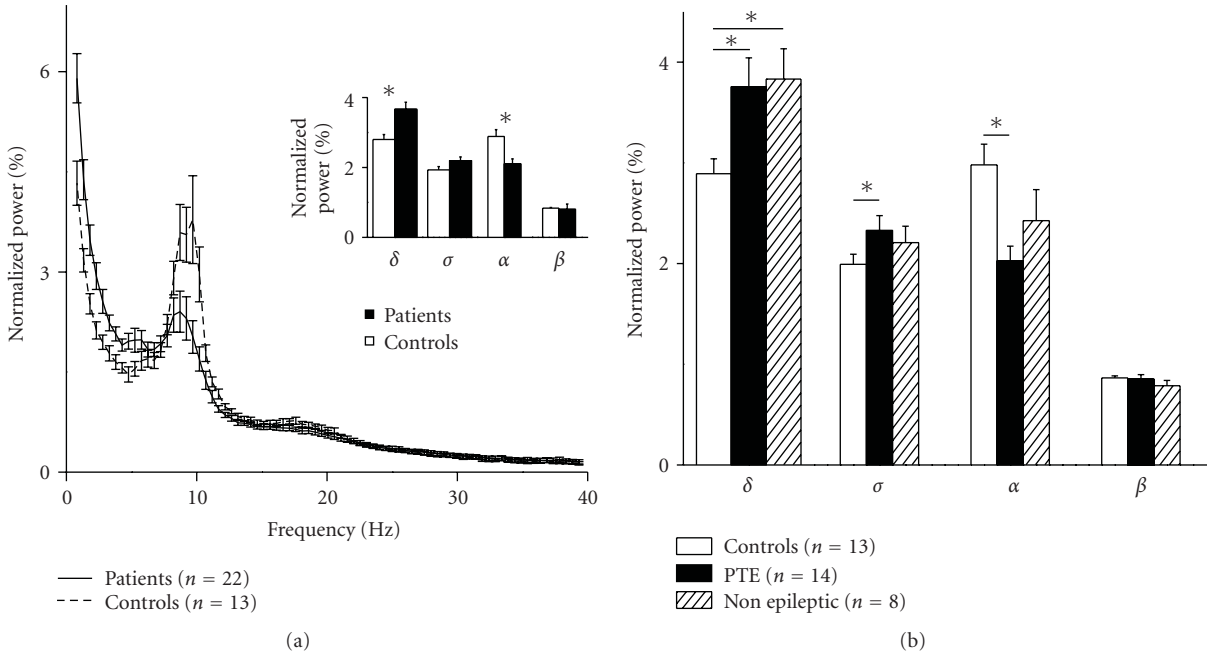

Figure 2: Abnormal qEEG in TBI patients. (a) Average normalized power spectrum representation of all TBI patients and controls that underwent qEEG. Note the significant increase in delta power and the decrease in the alpha band in TBI patients compared to controls (inset). (b) Power spectrum averages of patient subgroups according to the occurrence of seizures. While both the PTE and the non-epileptic group had elevated delta power compared to controls, only PTE patients had a significant reduction of alpha and increase of theta power. *= $P < .05$.

dysphasia ($n = 1$, 5.56%), or an acute stress reaction ($n = 1$, 5.56%). Both the PTE and non-epileptic groups were similar in age (27.05 ± 3.78 and 26.72 ± 3.14 years, resp., $P = .95$) and gender (7 women and 12 men, and 4 women and 14 men, resp., $P = .33$). A third group, consisting of 13 healthy adult volunteers (5 women and 8 men, aged 34.77 ± 2.47 years) with no history of brain injury or neurological disease, served as a control for the quantitative electroencephalography (qEEG) studies. A fourth group of 8 healthy adult volunteers (3 women and 5 men, aged 29.57 ± 0.48) underwent bMRI scans for normal BBB function measurements.

2.2. Quantitative Electroencephalography. qEEG recordings were carried out using a clinical 128 channel digital EEG acquisition unit (CEEGRAPH IV, Bio-logic Systems Corp., Mundelein, Illinois), with a digitization rate of 256 Hz. Twenty-three conventional AgCl surface electrodes were placed according to the international 10–20 electrode system, with additional electrodes placed at both ear lobes. Scalp electrode impedances were kept below 10 kΩ. The band pass was set at 0.1 to 100 Hz. EEG data was visually inspected, and 50–80 seconds of artifact-free, closed eye data were extracted for quantitative analysis. Fast Fourier transform (FFT) was applied to the EEG waveforms recorded from each electrode of each subject. A periodogram was used to calculate the average power spectrum. The EEG was then clinically interpreted by a physician unaware of the study. For each subject, the average value for the discrete frequency bands (delta 1.5–4 Hz, theta 4.5–7.5 Hz, alpha 8–12 Hz, beta 13–30 Hz) was normalized to each subject's own total power of the 1.5–40 Hz frequency spectrum (values are represented as % of the total electrode power).

2.3. Magnetic Resonance Imaging. MRI scans were performed using a 1.5 Tesla machine (Intera, Philips Medical Systems, Best, the Netherlands). For BBB integrity evaluations, images were collected before and following the peripheral administration of the contrast medium Magnetol® (Gadolinium-DTPA (Gd-DTPA) 0.5 M, 0.1 mmol/kg) (Soreq Radiopharmaceuticals, Israel), as described below.

2.4. BBB Integrity Evaluation. Two independent methods were used in the present study to estimate BBB permeability: (1) a semiquantitative method was used to detect and calculate the volume of BBB disrupted cortex; (2) a dynamic method was used for measuring the relative change in BBB disrupted volume with time.

2.4.1. The Semi-Quantitative Evaluation of BBB Permeability. (Figure 1(a))—Axial T1-weighted spin-echo images were obtained (582/15/1 [TR/TE/NEX], section thickness, 5 mm; intersection gap, 1 mm; matrix, 256 × 256) were performed before and following the peripheral addministration of Gd-DTPA. Using a manual anatomical landmark identification method [21], we paired matching brain images before and after the administration of Gd-DTPA. Image analysis was performed on matching images in the dicom format. Using a field of view of 230 × 230 mm resulted in a resolution of

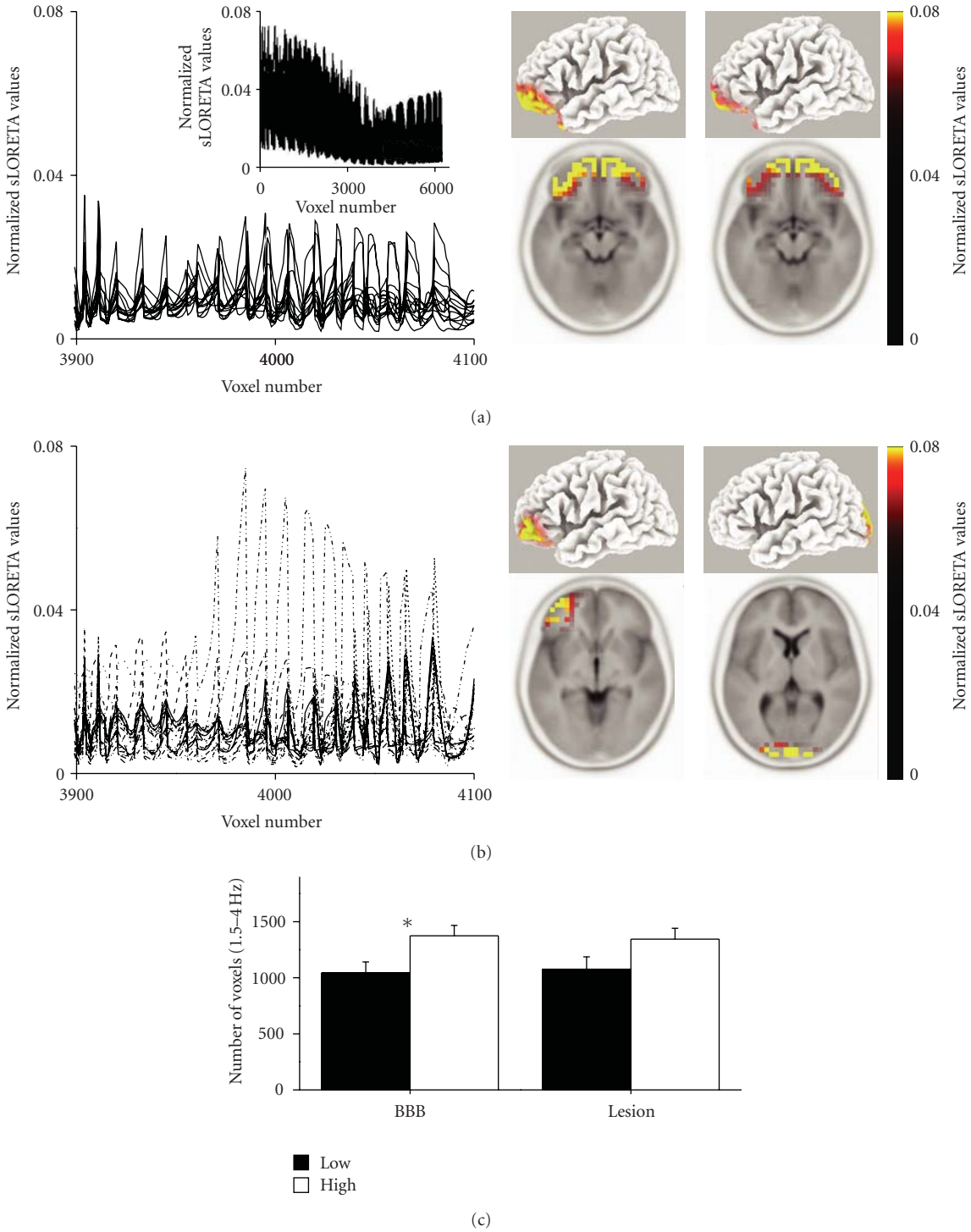

Figure 3: The extent of qEEG slowing in PTE patients correlates with BBB disruption. (a) An enlarged region of normalized sLORETA values for the delta band in voxels number 3900–4100 from healthy controls. The entire normalized sLORETA for the delta band is shown in the inset, as are 2 examples of signal localization to the frontal midline region. (b) The PTE population displayed marked variability among the same voxels, and maximal signal localization was varied according to the site of injury. (c) The volume of cortex with abnormal cortical activity according to sLORETA between patients with the bottom (black) and top (white) half volume of BBB disruption or cortical lesion. Note that patients with a larger volume of BBB disruption also had a significantly larger volume of dysfunctional cortex. *= $P < .05$.

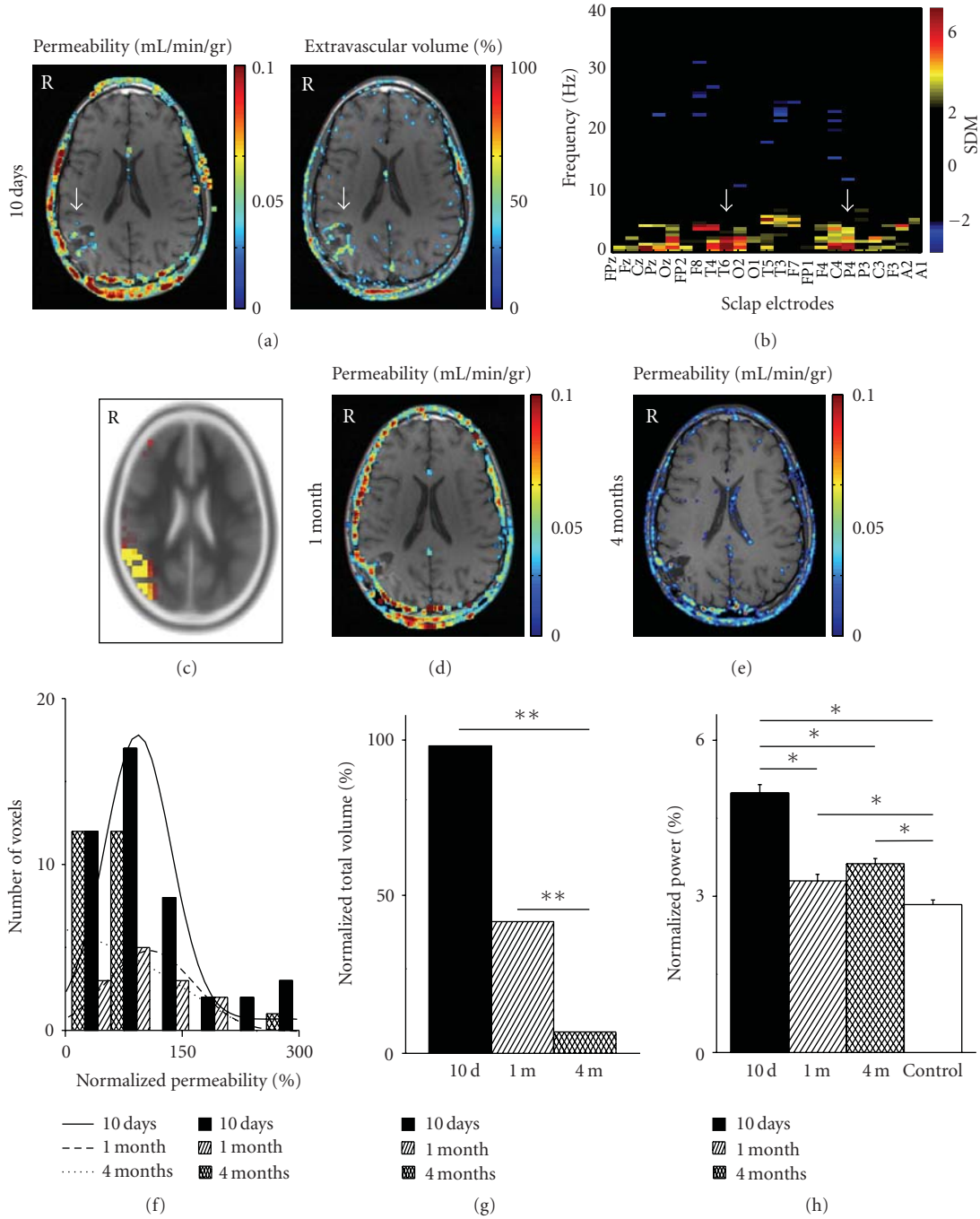

Figure 4: Abnormal EEG slowing localizes to region of BBB disruption in a 15-year-old PTE patient one month following mild TBI (see text for details). (a) BBB evaluation 10 days after the event revealed a focal area of increased BBB permeability (left, arrow, Brodmann area 40), surrounded by an increase of extravascular volume (right, arrow). (b) Representation of the EEG recording with the x-axis representing the 23 different electrodes, the y-axis the frequencies at 0.5 Hz intervals, and the colour coding the number of standard deviations from the average control EEG. Note the increased power in the delta range over the right temporoparietal electrodes (arrows). (c) sLORETA localized the delta activity to the right parietal region (Brodmann area 40). Repeated MRI scans 1 (d) and 4 months (e) following the trauma revealed a resolution of the BBB lesion. (f) Histogram representation of the permeability values surrounding the cortical lesion (normalized to the average value of the contralateral hemisphere). (g) Four months after the trauma there is a significant decrease in the permeability values, as well as in the extravascular volume. (h) Quantification of the average delta power shows a significant reduction in delta wave activity as time progresses, though remaining significantly increased compared to controls even 4 months after the event and resolution of the BBB lesion. * = $P < .05$, ** = $P < .0001$.

Table 1: Patient characteristics. Thirty-seven patients with TBI were enrolled in this study. Eighteen patients presented at our outpatient clinic with general complaints such as headaches and were included in the non-epileptic group. Nineteen patients presented with seizures and were included in the PTE patient group. sLORETA localization to Brodmann areas of abnormal EEG activity and enhancement is presented in parentheses.

#	Age	Symptoms	Abnormal enhancement	EEG interpretation
1	22	Acute stress reaction	No disruption	—
2	24	Cognitive impairment	Rt. frontal (47)	Normal
3	37	Headaches	No disruption	—
4	49	Headaches	No disruption	—
5	19	Headaches	—	Normal
6	25	Headaches	No disruption	Normal
7	27	Headaches	No disruption	—
8	17	Headaches	No disruption	—
9	25	Headaches	No disruption	Normal
10	17	Headaches	No disruption	—
11	22	Headaches	No disruption	—
12	46	Headaches	Rt. parietal (38)	—
13	13	Headaches	Rt. Parieto-occipital (18)	Normal (18Rt)
14	23	Headaches	—	Normal
15	13	Headaches	—	Normal
16	62	Headaches	No disruption	—
17	18	Headaches	No disruption	—
18	22	Motor Aphasia, Rt. Central Facialis	Lt. parietal (9)	Lt. fronto- parietal delta activity (9)
19	34	Behavioral Changes, Susp. Temporal seizures	Rt. temporal (21)	Rt. fronto-temporal delta activity (21)
20	29	Seizures	—	Normal
21	12	Seizures	—	Lt. temporal delta activity (47)
22	23	Seizures	Lt. parietal (40)	Lt. parietal epileptiform focus (47)
23	62	Seizures	Lt. parietal (2)	—
24	15	Seizures	Rt. parietal (40)	Rt. Temporo-parietal epileptiform activity (40)
25	10	Seizures	No disruption	Lt. frontal delta activitv 01)
26	18	Seizures	Rt. temporo-occipital (37)	Rt. Temporal teta activitv (38)
27	18	Seizures	Rt. parietal (40)	—
28	37	Seizures	Rt. temporal (47)	Rt. Temporal epileptiform focus (47)
29	68	Seizures+ Rt. Hemiparesis	Lt. parietal (3)	—
30	17	Seizures	No disruption	Normal
31	15	Seizures	—	Lt. temporo-parietal delta activity (38)
32	49	Seizures	No disruption	Normal
33	28	Seizures	Lt. parietal (40)	Lt. temporo-parietal epileptiform activity (19)
34	17	Seizures	Lt. fronto-parietal (8)	Lt. frontal delta activity (47)
35	23	Seizures	Rt. parietal (40)	—
36	16	Seizures	Lt. parietal (40)	—
37	23	Seizures	—	Lt. fronto-temporal epileptiform activity (11)

0.81 mm^2/pixel, or 12.92 mm^2/population group. Matching populations were compared to detect changes in signal intensity. These were inspected for either differences in percent enhancement (pertaining to the presence of the contrast agent), or for statistical significance (using Student's t-test). In order to detect abnormal penetration of contrast agent through the BBB, we set the "detection threshold" to >20% increase in signal intensity (i.e., >2 standard deviations from the normal parenchymal mean). The Bonferroni correction for multiple simultaneous statistical tests was applied for the statistical calculations. Changes in signal enhancement were considered to be due to BBB disruption if they occurred within the brain parenchyma.

2.4.2. Dynamic Evaluation of BBB Permeability. (Figure 1(b))—The imaging protocol for this contrast-enhanced studies was modified according to published methods [22]. Four consecutive 3D RF spoiled T1 weighted field echo acquisitions with an array of flip angles ($\alpha = 2°, 10°, 20°, 35°$) were performed to allow calculation of T1 maps. The third sequence was then repeated ($n = 80$) to produce a T1 weighted dynamic data set with a time resolution of

5.5 seconds and a duration of approximately 10 minutes. Contrast agent was given as an intravenous bolus injection over a period of 4 seconds following the fifth dynamic scan. Maps of proton density M_0 and intrinsic longitudinal relaxation rate ($R10 = 1/T10$) were calculated. 4D (x, y, z, t) postinjection longitudinal relaxation rate [$R1(t)$] maps were calculated for each T1 weighted dynamic phase using signal intensity data from pre- and postcontrast T1 field echo images [$S(t) - S(0)$]. 4D Gd-DTPA concentrations [$C(t)$] maps were then calculated from the 4D $R1(t)$ maps:

$$C(t) = \frac{(R1(t) - R10)}{r_1}, \quad (1)$$

where $r1$ is the relaxivity of Gd-DTPA determined experimentally. $r_1 = 4.39$ [$s^{-1}mM^{-1}$] (at 37°C and at 1.5 T). The time course of the intravascular contrast concentration was used to calculate an effective vascular input function (VIF). Maps of $R10$, $C(t)$, and the VIF were then used to calculate the volume transfer constant between blood plasma and extravascular extracellular space (EES)—K^{trans}, and the volume of extravascular extracellular space per unit volume of tissue—v_e, on a pixel by pixel basis using a standard compartmental model. Using this model, the time course of contrast agent concentration in tissue can be described by the following equation:

$$C_t(t) = K^{\text{trans}}\left(C_p(t) \otimes \exp\left(-k_{\text{ep}} \cdot t\right)\right) \quad (2)$$

$C_t(t)$ represents the tracer concentration in the tissue at time t, $C_p(t)$ the tracer concentration in blood plasma at time t, $k_{\text{ep}} = K^{\text{trans}}/v_e$ the rate constant between EES and blood plasma and $\otimes$ denotes convolution. Resulting images represent BBB permeability (defined as $K^{\text{trans}}[\text{min}^{-1}] = \text{PS}\rho$ where PS[mL min^{-1} gr^{-1}] is the permeability of a surface area product per unit mass of tissue, and ρ [g ml^{-1}] is the density of tissue) and the volume fraction of the EES (expressed as the volume of contrast agent per volume of pixel, and therefore represented as percentage).

Normalization of the quantified permeability values was performed to the average value of the contralateral uninvolved hemisphere.

2.5. Calculating Lesion and BBB Disrupted Volume and Location. Measuring the size of the cortical lesion and BBB disrupted area was performed using MATLAB (version 7.1) on images obtained through the semi-quantitative evaluation. For lesion volume measurements, T1 MRI images before contrast agent administration were used. An experienced neuroradiologist identified the location of the parenchymal lesion in all slices, and the number of pixels was counted. BBB disruption volume was performed on the same slices where the lesion was identified. Using the signal enhancement results for those slices, the number of pixels with enhancement above 20% was counted. Lesion and BBB-disrupted volumes are displayed in cm^3.

For quantifying BBB permeability, values of all pixels within a region of interest were collected using the dynamic method and a frequency distribution was calculated. The extravascular volume of the contrast agent (v_e) was quantified by calculating the sum of values within the region of interest. Localization of the cortical and BBB lesions according to Brodmann areas was performed by manual anatomical registration to the digitized Talairach brain atlas.

2.6. Statistical Analysis. The nonparametric Mann-Whitney U test was used for evaluating statistical significance of the differences in the power spectrum between controls and the patient groups, the change in cortical lesion and BBB disrupted volumes compared to neuronal dysfunction as measured by qEEG, and for changes in permeability, extravascular volume, and delta band power with time. The χ^2 Pearson's test was used for evaluating the frequency of abnormal qEEG activity, and cortical lesions between the PTE and non-epileptic groups. Correlations between BBB disruption or lesion size and the volume of dysfunctional cortex were performed using the Student's t-test. All results are presented as mean ± SEM.

3. Results

3.1. Lasting BBB Disruption in TBI Patients. 30 patients underwent bMRI scans (15 PTE and 15 non-epileptic) and the images were evaluated for parenchymal lesions and disruption volumes. In the healthy control group ($n = 8$), significant enhancement was only observed in blood vessels and regions known to lack a BBB (Figure 1(a) and also see [15]). In contrast, 16 TBI patients (53.3%) showed parenchymal regions with enhanced signal indicating BBB disruption (Figure 1(b)). In 15 of these patients (93.8%) the disrupted BBB was located in cortical regions surrounding old contusions (and with no involvement of more distant cortical regions), suggesting a local trauma-related mechanism. In a single patient BBB disruption was detected in a parietal region, but no concomitant cortical lesion was found in any sequences including T2*.

BBB disruption was identified up to several months following the traumatic event (19.4 ± 9.4, median = 2.5 months), with a delay of 1.5–11 years in 4 patients. Cortical lesions were found in the parietal ($n = 11$, 68.8%), temporal ($n = 3$, 18.8%), frontal ($n = 1$, 6.3%), and occipital ($n = 1$, 6.3%) regions. The average lesion volume was $6.0 \pm 1.7\ \text{cm}^3$ and the average volume of cortex with disrupted BBB was $5.9 \pm 1.6\ \text{cm}^3$. Although PTE patients were more likely to have a lesion diagnosed on their MRI scans than non-epileptic patients (83.3 versus 38.9%, $P = .006$), there was no significant difference with respect to the size of the lesion (6.6 ± 1.9 versus $5.3 \pm 2.8\ \text{cm}^3$, $P = .19$). Conversely, PTE patients were more likely to have BBB disruption than non-epileptic patients (82.4 versus 25%, $P = .001$), and the volume of BBB disruption was significantly larger (9.8 ± 2.6 versus $1.7 \pm 0.6\ \text{cm}^3$, $P = .001$).

3.2. EEG Analysis in Post-Traumatic Patients. EEG recordings were performed on 22 TBI patients 10 days–11 years (median= 3 months) after the trauma. Abnormal EEG slowing or interictal epileptiform activity was detected in

78.6% (11 of 14) of the PTE patients and in 12.5% (1 of 8) of the non-epileptic group ($P = .006$). Comparison of FFT spectral analysis between the TBI patients and the healthy control group revealed a significant increase in delta power among the TBI patients (3.7 ± 0.2 versus $2.8 \pm 0.2\%$, for patients vs. controls, resp.; $P = .002$) and a significant decrease in the alpha band power (2.1 ± 0.1 versus $2.9 \pm 0.2\%$, $P = .005$, Figure 2(a)). The significant increase in delta power was similar in both the PTE ($3.68 \pm 0.28\%$) and non-epileptic patients ($3.76 \pm 0.29\%$). In contrast, only the PTE group showed a significantly reduced alpha (1.99 ± 0.14 and $2.83 \pm 0.15\%$, $P = .01$) and elevated theta power (2.28 ± 0.14 and $1.93 \pm 0.09\%$, $P = .04$, Figure 2(b)) compared to the controls.

3.3. BBB Breakdown and Source Localization of Abnormal EEG Patterns. The spatial relationship between BBB disruption and abnormal cortical function was assessed by localizing the cortical sources of pathological slow delta activity using sLORETA. In healthy individuals (control group), the voxels generating delta activity were consistently localized to medial frontal and interhemispheric cortical structures (Figure 3(a)). In contrast, TBI patients displayed a high variability for the maximal activity region (Figure 3(b)). 10 TBI patients with identified BBB disruption underwent EEG recordings. In 7 of them, sLORETA localized the source for abnormal delta to the same Brodmann area as that of the BBB disruption.

The volume of cortex with slow delta activity was estimated by counting the number of voxels one standard deviation away from the average control value. This was significantly greater among TBI patients with a large BBB disrupted lesion than patients with small lesions (1042.6 ± 5.3 versus 1373.6 ± 4.13 voxels, $P = .03$, Figure 3(c)), suggesting a close relationship between increased BBB permeability and cortical dysfunction. No significant difference was found in relation to the size of the anatomical cortical lesion (1075.7 ± 6 versus 1344.6 ± 4.3 voxels, $P = .09$).

3.4. BBB Breakdown and EEG Followup with Time: A Case Description. In three patients, we performed repeated bMRI and EEG studies to underscore the dynamic relations between abnormal BBB permeability and cortical dysfunction. One such patient with post-traumatic BBB opening and PTE is presented here in more detail (Figure 4): a 15-year-old boy was admitted two hours after a blunt head injury during a moving vehicle accident, causing a short (minutes) episode of unconsciousness. Upon admission, he was conscious and a full neurological examination was normal (GCS = 15). A brain computed tomography (bCT) scan showed an open depressed right parietal skull fracture, and a right parietal subarachnoid hemorrhage with no mass effect. The depressed fracture was elevated under general anesthesia. The patient was discharged with no complications on day 5. A repeated bCT scan that was performed on day 7 revealed absorption of the hemorrhage with good positioning of the fractured bone. Ten days after the trauma he had a partial seizure consisting of involuntary movements on his left hand and was therefore readmitted. A bMRI scan revealed a small right parietal hemorrhagic contusion. Dynamic BBB analysis detected increased permeability with a larger area of extravascular permeation around the contused brain (Figure 4(a)). qEEG recordings showed increased slow wave activity (1–6 Hz) over the right temporoparietal electrodes (Figure 4(b)). Interictal spikes were observed during his recording and localized to the right temporo-parietal region by sLORETA (Brodmann area 40, Figure 4(c)). He was released under medical treatment with Sodium Valporate. Subsequent MRI scans and qEEG recordings (performed on the same day, ca. 24 hours after previous antiepileptic medication) were conducted one and four months later. MRI scans revealed a persistent, though smaller area of BBB disruption over the same region (Figures 4(d) and 4(e)). Quantification of the imaging data revealed that the pattern of the normalized permeability shifted towards lower permeability values between day 10 and four months ($P < .0001$, Figure 4(f)). In parallel, the contrast agent extravascular volume also diminished, reflecting a smaller area of BBB disruption ($P < .0001$, Figure 4(g)). Quantitative EEG evaluation showed that the power of the delta band similarly diminished with time. It is interesting to note that 4 months after the trauma, while the extravascular volume of the contrast agent returned to control values (compared to the contralateral hemisphere) the delta power remained significantly higher than that of the control population ($P = .007$, Figure 4(h)—see below).

4. Discussion

In this study, we investigated anatomical and functional characteristics from symptomatic patients following mild to moderate head trauma. In 37 TBI patients, we used two different quantitative methods for evaluating BBB permeability as well as EEG spectral analysis with a source localization method. We found that TBI patients show (1) a lasting focal increase in BBB permeability in up to 70% of TBI patients; (2) increased EEG slowing (compared to healthy controls) which seems to originate from a focal cortical region; (3) a good spatial correlation between the BBB lesion and the presumed source for abnormal neuronal (qEEG) activity; (4) a correlation between the size of the BBB disrupted region, but *not* the anatomical lesion, with the extent of neuronal dysfunction, and (5) patients with PTE have a higher likelihood to show abnormal BBB permeability and of a larger cortical area compared to post-traumatic patients without epilepsy. It is important to note that our study suffers from a significant "selection bias" as patients were recruited from a tertiary outpatient clinic seeing patients that were hospitalized due to TBI and referred due to significant symptomatology. Therefore, they do not reflect the true prevalence of PTE in this patient population. The relatively high rate of BBB disruption noted in our study may also reflect this selection bias. In addition, the use of our quantitative imaging methods may have increased the sensitivity of BBB breakdown measurements which would not be identified using other methods.

4.1. Cortical Dysfunction in TBI Patients. In accordance with earlier studies [16, 23–25], we find that patients with mild to moderate TBI commonly have abnormal EEG recordings. Interestingly, although PTE patients were more likely to have interictal sharp activity on their EEG than non-epileptic post-traumatic patients, quantitative analyses did not reveal significant differences between the two groups. EEG slowing most likely reflects dysfunction of the cortical network and neuronal hypersynchronization [26]. Indeed, while different animal models for brain injury consistently revealed electrophysiological evidence for neuronal hyperexcitability and hypersynchronicity [12–14, 27–30], only rarely have behavioral manifestations of seizures been reported [31, 32]. This stresses the well-known observation that neuronal hypersynchrony (and slowing) does not always manifest clinically as convulsions [33], probably depending on the cortical region involved. The lack of differences found between qEEG analysis in our PTE and non-epileptic symptomatic patients may arise from the fact that these groups indeed share a common path, that is, very similar pathologic neuronal dysfunction presenting with different phenotypes. Further research into the differences between these groups is needed to address this issue.

4.2. BBB Disruption May Lead to Cortical Dysfunction. Recent work has shown that abnormal slow wave cortical activity following traumatic head injury can be localized to a focal region related to the site of trauma [16, 34, 35]. Considering that an average calculation of the delta band amplitude from all electrodes may yield little information (since the source of abnormal activity is not equally distributed in all scalp electrodes, but related to the site of injury), we used sLORETA to calculate the distribution of the delta band in 6239 voxels representing the entire cerebral cortex gray matter. As expected, there was a high variability in EEG current density distribution in PTE patients when compared to healthy controls, probably reflecting focal, trauma-related brain dysfunction (Figure 3). sLORETA localized the site of maximal delta wave activity in close proximity to the MR-defined cortical lesion, suggesting a causative relationship. This implies that EEG slowing is probably due to focal cortical generators (which differ in location between patients) rather than a single common "pathological" generator or general diffuse cortical slowing, as one would expect in the case of a general stress-dependent mechanism or lesion in deeper brain structures like the thalamus or brain stem [34, 35]. Although a correlation was found between the size of the BBB lesion and the volume of cortical dysfunction, no such relationship was found with the size of the anatomical lesion. This may reflect the fact that following trauma, the contused brain starts undergoing a rapid process of neuronal necrosis and gliosis and therefore is not the source of abnormal neuronal activity. However, the surrounding nonnecrotic tissue remains functional and may be exposed to abnormal conditions that impact on its normal neuronal behavior. This implies that other unknown trauma-related processes may be at the basis of cortical dysfunction. Indeed, animal studies show that cortical hyperexcitability develops in regions surrounding the site of direct trauma [36–38].

Based on the following observations, this study supports the supposition that lasting BBB disruption is related to the emergence of neocortical dysfunction: (1) both BBB disruption and the estimated source of pathological delta wave activity were colocalized in the cerebral cortex. (2) The greater the volume of BBB disruption the larger the area of cortical dysfunction. (3) In select cases, BBB disruption and cortical dysfunction resolve simultaneously. We cannot however rule out that abnormal neural activity causes alterations in the permeability of the local vascular bed, or that both result directly from trauma but by different mechanisms. The observation that increased BBB permeability is noted in some patients despite apparently complete medical control of seizures supports the hypothesis that the vascular pathology is not a direct result of the pathological neuronal discharge. Our hypothesis is also strongly supported by recent animal experiments demonstrating that BBB breakdown or direct exposure of the cerebral cortex to serum albumin induces activation of astrocytes, reduced buffering of extracellular potassium leading to neuronal hyperexcitability [13]. Perfusion MRI studies were not performed as part of our routine protocol, thus we cannot entirely exclude increased local cerebral blood flow as an underlying or additional source for the observed enhancement. However, this is unlikely, since no enhancement is usually observed in patients with focal epilepsy from other causes (data not shown).

Finally, this preliminary study calls for prospective human studies which are required to elucidate the prevalence of BBB breakdown in TBI patients using sensitive imaging modalities and the possible causative relationship between early breakdown of the BBB and the development of PTE.

5. Conclusion

Our study, for the first time, shows that quantitative and repeated measurements of BBB permeability in human patients are possible using routine imaging techniques with postprocessing. This provides powerful tools for evaluating the extent of dysfunction and outcome in patients suffering BBB disruption. Furthermore, we suggest that such procedures may correlate with cortical function and serve as follow-up measures in neurological patients. As observed in the present study, this might be especially useful for patients with TBI, but could also assist following recovery from other pathologies associated with increased BBB permeability (e.g., tumors, stroke, multiple sclerosis, and infectious diseases). It remains unclear as to what extent such dynamic measures of brain vascular bed permeability will be valuable in predicting the natural course of common neurological diseases.

Acknowledgments

This paper was supported by the Sonderforschungsbereich TR3 (AF) and the Israeli Science Foundation (566/07, Alon Friedman). The authors would like to thank Asi Kreh for his assistance with the MRI studies.

References

[1] J. F. Annegers, J. D. Grabow, R. V. Groover, E. R. Laws Jr., L. R. Elveback, and L. T. Kurland, "Seizures after head trauma: a population study," *Neurology*, vol. 30, no. 7, pp. 683–689, 1980.

[2] J. F. Annegers, W. A. Hauser, S. P. Coan, and W. A. Rocca, "A population-based study of seizures after traumatic brain injuries," *The New England Journal of Medicine*, vol. 338, no. 1, pp. 20–24, 1998.

[3] B. T. Desai, S. Whitman, R. Coonley Hoganson, T. E. Coleman, G. Gabriel, and J. Dell, "Seizures and civilian head injuries," *Epilepsia*, vol. 24, no. 3, pp. 289–296, 1983.

[4] W. F. Caveness, A. M. Meirowsky, B. L. Rish et al., "The nature of posttraumatic epilepsy," *Journal of Neurosurgery*, vol. 50, no. 5, pp. 545–553, 1979.

[5] I. Asikainen, M. Kaste, and S. Sarna, "Early and late posttraumatic seizures in traumatic brain injury rehabilitation patients: brain injury factors causing late seizures and influence of seizures on long-term outcome," *Epilepsia*, vol. 40, no. 5, pp. 584–589, 1999.

[6] A. M. Salazar, B. Jabbari, and S. C. Vance, "Epilepsy after penetrating head injury. I. Clinical correlates: a report of the Vietnam Head Injury Study," *Neurology*, vol. 35, no. 10, pp. 1406–1414, 1985.

[7] N. R. Temkin, S. S. Dikmen, A. J. Wilensky, J. Keihm, S. Chabal, and H. R. Winn, "A randomized, double-blind study of phenytoin for the prevention of post-traumatic seizures," *The New England Journal of Medicine*, vol. 323, no. 8, pp. 497–502, 1990.

[8] N. Garga and D. H. Lowenstein, "Posttraumatic epilepsy: a major problem in desperate need of major advances," *Epilepsy Currents*, vol. 6, no. 1, pp. 1–5, 2006.

[9] A. Minagar, W. Jy, J. J. Jimenez, and J. S. Alexander, "Multiple sclerosis as a vascular disease," *Neurological Research*, vol. 28, no. 3, pp. 230–235, 2006.

[10] B. V. Zlokovic, "Neurovascular mechanisms of Alzheimer's neurodegeneration," *Trends in Neurosciences*, vol. 28, no. 4, pp. 202–208, 2005.

[11] A. R. Tunkel and W. M. Scheld, "Pathogenesis and pathophysiology of bacterial meningitis," *Annual Review of Medicine*, vol. 44, pp. 103–120, 1993.

[12] E. Seiffert, J. P. Dreier, S. Ivens et al., "Lasting blood-brain barrier disruption induces epileptic focus in the rat somatosensory cortex," *Journal of Neuroscience*, vol. 24, no. 36, pp. 7829–7836, 2004.

[13] S. Ivens, D. Kaufer, L. P. Flores et al., "TGF-β receptor-mediated albumin uptake into astrocytes is involved in neocortical epileptogenesis," *Brain*, vol. 130, no. 2, pp. 535–547, 2007.

[14] O. Tomkins, O. Friedman, S. Ivens et al., "Blood-brain barrier disruption results in delayed functional and structural alterations in the rat neocortex," *Neurobiology of Disease*, vol. 25, no. 2, pp. 367–377, 2007.

[15] O. Tomkins, D. Kaufer, A. Korn et al., "Frequent blood-brain barrier disruption in the human cerebral cortex," *Cellular and Molecular Neurobiology*, vol. 21, no. 6, pp. 675–691, 2001.

[16] A. Korn, H. Golan, I. Melamed, R. Pascual-Marqui, and A. Friedman, "Focal cortical dysfunction and blood-brain barrier disruption in patients with postconcussion syndrome," *Journal of Clinical Neurophysiology*, vol. 22, no. 1, pp. 1–9, 2005.

[17] J. P. Dreier, K. Jurkat-Rott, G. G. Petzold et al., "Opening of the blood-brain barrier preceding cortical edema in a severe attack of FHM type II," *Neurology*, vol. 64, no. 12, pp. 2145–2147, 2005.

[18] J. D. Huber, R. D. Egleton, and T. P. Davis, "Molecular physiology and pathophysiology of tight junctions in the blood -brain barrier," *Trends in Neurosciences*, vol. 24, no. 12, pp. 719–725, 2001.

[19] D. Shlosberg, M. Benifla, D. Kaufer, and A. Friedman, "Blood-brain barrier breakdown as a therapeutic target in traumatic brain injury," *Nature Reviews Neurology*, vol. 6, no. 7, pp. 393–403, 2010.

[20] O. Tomkins, I. Shelef, I. Kaizerman et al., "Blood-brain barrier disruption in post-traumatic epilepsy," *Journal of Neurology, Neurosurgery and Psychiatry*, vol. 79, no. 7, pp. 774–777, 2008.

[21] J. B. A. Maintz and M. A. Viergever, "A survey of medical image registration," *Medical Image Analysis*, vol. 2, no. 1, pp. 1–36, 1998.

[22] X. P. Zhu, K. L. Li, I. D. Kamaly-Asl et al., "Quantification of endothelial permeability, leakage space, and blood volume in brain tumors using combined T1 and T2* contrast-enhanced dynamic MR imaging," *Journal of Magnetic Resonance Imaging*, vol. 11, no. 6, pp. 575–585, 2000.

[23] N. A. Shaw, "The neurophysiology of concussion," *Progress in Neurobiology*, vol. 67, no. 4, pp. 281–344, 2002.

[24] M. R. Watson, G. W. Fenton, R. J. McClelland, J. Lumsden, M. Headley, and W. H. Rutherford, "The post-concussional state: neurophysiological aspects," *British Journal of Psychiatry*, vol. 167, pp. 514–521, 1995.

[25] R. Diaz-Arrastia, M. A. Agostini, A. B. Frol et al., "Neurophysiologic and neuroradiologic features of intractable epilepsy after traumatic brain injury in adults," *Archives of Neurology*, vol. 57, no. 11, pp. 1611–1616, 2000.

[26] F. Ferrillo, M. Beelke, and L. Nobili, "Sleep EEG synchronization mechanisms and activation of interictal epileptic spikes," *Clinical Neurophysiology*, vol. 111, no. 2, supplement, pp. S65–S73, 2000.

[27] V. Santhakumar, A. D. H. Ratzliff, J. Jeng, Z. Toth, and I. Soltesz, "Long-term hyperexcitability in the hippocampus after experimental head trauma," *Annals of Neurology*, vol. 50, no. 6, pp. 708–717, 2001.

[28] K. M. Jacobs, B. J. Hwang, and D. A. Prince, "Focal epileptogenesis in a rat model of polymicrogyria," *Journal of Neurophysiology*, vol. 81, no. 1, pp. 159–173, 1999.

[29] D. A. Prince and G. F. Tseng, "Epileptogenesis in chronically injured cortex: in vitro studies," *Journal of Neurophysiology*, vol. 69, no. 4, pp. 1276–1291, 1993.

[30] S. N. Hoffman, P. A. Salin, and D. A. Prince, "Chronic neocortical epileptogenesis in vitro," *Journal of Neurophysiology*, vol. 71, no. 5, pp. 1762–1773, 1994.

[31] R. D'Ambrosio, J. P. Fairbanks, J. S. Fender, D. E. Born, D. L. Doyle, and J. W. Miller, "Post-traumatic epilepsy following fluid percussion injury in the rat," *Brain*, vol. 127, no. 2, pp. 304–314, 2004.

[32] R. D'Ambrosio, J. S. Fender, J. P. Fairbanks et al., "Progression from frontal-parietal to mesial-temporal epilepsy after fluid percussion injury in the rat," *Brain*, vol. 128, no. 1, pp. 174–188, 2005.

[33] J. A. Hartings, A. J. Williams, and F. C. Tortella, "Occurrence of nonconvulsive seizures, periodic epileptiform discharges, and intermittent rhythmic delta activity in rat focal ischemia," *Experimental Neurology*, vol. 179, no. 2, pp. 139–149, 2003.

[34] O. J. Andy, "Post concussion syndrome: brainstem seizures, a case report," *Clinical EEG Electroencephalography*, vol. 20, no. 1, pp. 24–34, 1989.

[35] J. F. Soustiel, H. Hafner, A. V. Chistyakov, A. Barzilai, and M. Feinsod, "Trigeminal and auditory evoked responses in minor head injuries and post-concussion syndrome," *Brain Injury*, vol. 9, no. 8, pp. 805–813, 1995.

[36] K. M. Jacobs, M. J. Gutnick, and D. A. Prince, "Hyperexcitability in a model of cortical maldevelopment," *Cerebral Cortex*, vol. 6, no. 3, pp. 514–523, 1996.

[37] W. H. Hoffman and L. B. Haberly, "Kindling-induced epileptiform potentials in piriform cortex slices originate in the underlying endopiriform nucleus," *Journal of Neurophysiology*, vol. 76, no. 3, pp. 1430–1438, 1996.

[38] K. M. Jacobs, K. D. Graber, V. N. Kharazia, I. Parada, and D. A. Prince, "Postlesional epilepsy: the ultimate brain plasticity," *Epilepsia*, vol. 41, no. 6, supplement, pp. S153–S161, 2000.

Hindawi Publishing Corporation
Cardiovascular Psychiatry and Neurology
Volume 2011, Article ID 482415, 9 pages
doi:10.1155/2011/482415

Review Article

The Etiological Role of Blood-Brain Barrier Dysfunction in Seizure Disorders

Nicola Marchi,[1,2,3] William Tierney,[2] Andreas V. Alexopoulos,[3] Vikram Puvenna,[2] Tiziana Granata,[4] and Damir Janigro[1,2,3,5]

[1] *Department of Molecular Medicine, Cleveland Clinic Foundation, NB-20 LRI 9500 Euclid Avenue, Cleveland, OH 44195, USA*
[2] *Department of Cell Biology, Cleveland Clinic Foundation, NB-20 LRI 9500 Euclid Avenue, Cleveland, OH 44195, USA*
[3] *Epilepsy Center, Cleveland Clinic Foundation, NB-20 LRI 9500 Euclid Avenue, Cleveland, OH 44195, USA*
[4] *Division of Child Neurology, Carlo Besta Neurological Institute, 20133 Milan, Italy*
[5] *Cerebrovascular Center, Cleveland Clinic Foundation, NB-20 LRI 9500 Euclid Avenue, Cleveland, OH 44195, USA*

Correspondence should be addressed to Nicola Marchi, marchin@ccf.org and Damir Janigro, janigrd@ccf.org

Received 10 November 2010; Accepted 28 January 2011

Academic Editor: Alon Friedman

A wind of change characterizes epilepsy research efforts. The traditional approach, based on a neurocentric view of seizure generation, promoted understanding of the neuronal mechanisms of seizures; this resulted in the development of potent antiepileptic drugs (AEDs). The fact that a significant number of individuals with epilepsy still fail to respond to available AEDs restates the need for an alternative approach. Blood-brain barrier (BBB) dysfunction is an important etiological player in seizure disorders, and combination therapies utilizing an AED in conjunction with a "cerebrovascular" drug could be used to control seizures more effectively than AED therapy alone. The fact that the BBB plays an etiologic role in other neurological diseases will be discussed in the context of a more "holistic" approach to the patient with epilepsy, where comorbidity variables are also encompassed by drug therapy.

1. Introduction

The blood-brain barrier (BBB) is a system of capillary endothelial cells that protects the brain from harmful substances present in the blood stream, while supplying the brain with the nutrients required for proper function [1–3]. The capillary endothelium is characterized by the presence of tight junctions, lack of fenestrations, and minimal pinocytotic vesicles. In particular, tight junctions between endothelial cells form a barrier, which selectively excludes most blood-borne substances from entering the brain, protecting it from systemic influences. The BBB is anatomically and functionally associated with brain parenchymal cells. The distance between a BBB capillary and neurons is of few micrometers while the overall surface of exchange between the BBB and the brain parenchyma reaches 20 m^2 in the adult human brain [4]. In short, the extent and complexity of the cerebrovascular interface together with the anatomical proximity of BBB vessels and neurons are highly suggestive of an active role in brain disease. In addition to the structural integrity of the BBB, there exists an enzymatic surveillance system that metabolizes drugs and other compounds bypassing the structural barrier. Recently, a strong effect of these enzymes on antiepileptic drugs (AED) metabolism has been shown in human epileptic brain [5].

Failure of the BBB has been traditionally considered the result of brain diseases (e.g., brain tumors, seizures, central nervous system infections, multiple sclerosis). As a result, the potential for a therapeutic approach to restore BBB functions has been overlooked for a more traditional neuronal take of brain pharmacology. The latter approach has been only partially successful, as evidenced by the persistent clinical burden represented by drug-resistant brain diseases [6, 7]. Most animal models of neurological disorders are based on the fact that brain neurons are the sole origin of the disorder and therefore the chief targets, while a possible role for the cerebral vasculature is often overlooked (Figure 1).

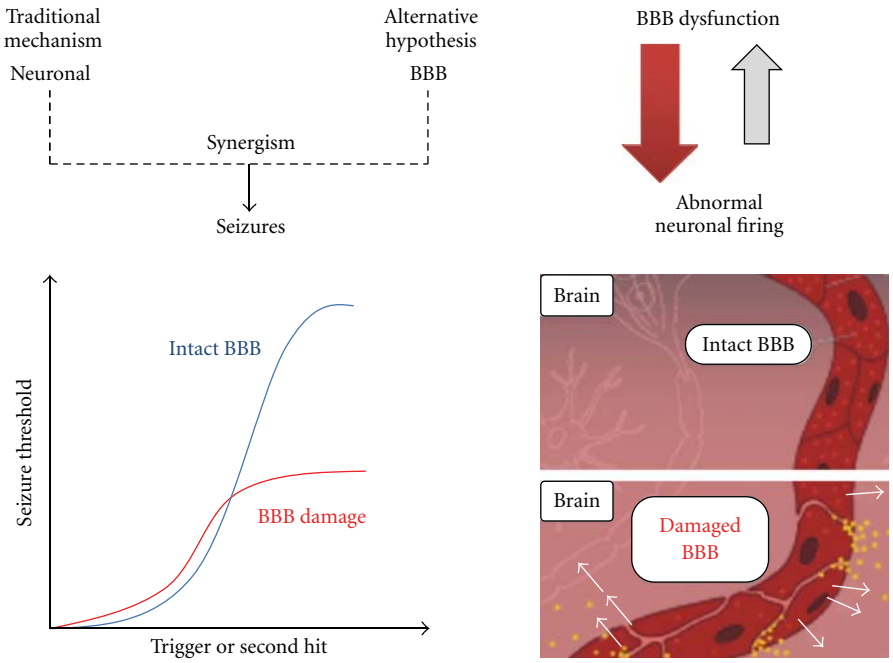

Figure 1: Seizure generation based on cerebrovascular events. Traditionally, the main and leading hypothesis to explain seizures consisted of abnormal neuronal wiring and excitability. While evidence of this is undisputed, the alternative/complementary hypothesis also adds to the mix pre-existing leakage of the BBB, which generates a decrease in seizure threshold. According to this hypothesis BBB leakage decreases seizure threshold independent of the fact that such leakage is associated with or a result of the seizure itself (blue versus red idealized traces). In other words, and based on the results by Friedman's Group, traumatically induced BBB disruption (BBBD) lowers seizure threshold. Others (e.g., Marchi et al.) have shown that BBBD alone is sufficient to provoke a seizure in a nonepileptic animal. While the contribution of BBB dysfunction to seizures has been demonstrated, the exact mechanisms (e.g., brain entry of peripherally circulating molecules, *yellow dots* in the cartoon) remain unclear.

2. Astrocytes and the Blood-Brain Barrier

Glial cells are numerically the predominant cell type in the brain, and the glial/neuron ratio increases dramatically with brain complexity and size [8]. Astrocytes, a specific subtype of glial cells play an important role in regulating cerebral ion homeostasis, transmitter regulation, maintenance of the blood-brain barrier (BBB), and structural, as well as metabolic, support of neuronal cells, for example, by providing the glucose-lactate shuttle [8, 9]. At the vascular level, astrocytes extend larger processes also known as "end-feet" whose terminations cover 99% of the abluminal vascular surface of capillaries, arterioles, and venules present in the cerebrovascular network. At the brain microcapillary level, these cells become one of the main building blocks of the BBB, a highly specialized dynamic and functional interface between the blood and the brain that plays a primary role in controlling and modulating the homeostasis of the central nervous system (CNS).

3. Blood-Brain Barrier Function: Unless You Can Measure, You Cannot Study It

One of the problems of BBB research has been the lack of reliable methods to measure BBB intactness [10, 11]. "Opening" of the BBB provides molecules normally present in blood with open passage into the CNS. Proteins normally present in blood are free to diffuse into the CNS, and in turn, molecules and protein normally present in high concentrations in the CNS are free to diffuse into the blood. These peripheral markers of BBB opening can be detected in the blood in order to evaluate the permeability characteristics of the BBB at any given time. In brief, such markers should have low or undetectable plasma levels in normal subjects and have a higher concentration in the CSF than in plasma [10, 11]. These proteins should be normally blocked by the BBB and exhibit flux across the BBB during barrier damage. Several proteins, including S100β, neuron-specific enolase (NSE), and glial fibrillary acidic protein (GFAP), have been evaluated for this purpose, but only S100β meets all the above-mentioned characteristics [10, 11]. The fact that serum S100β can be used as marker of BBB integrity is not necessarily in disagreement with the notion that S100β is also a marker of brain damage, since both phenomena (BBB failure and brain damage) are temporally and topographically associated. In general, changes in S100β correlate well with radiological indexes of BBB function, such as signal changes on MRI [12, 13].

These methodological aspects of BBB measurements are crucial to our understanding of the relative contribution of the BBB to seizure development. Seizures and epilepsy are commonly observed in conjunction with stroke, traumatic brain injury and CNS infections, all conditions known to result in compromised BBB function. A point of debate is

whether the compromised integrity of the BBB may be a *prodromic* component of the etiology of epilepsy secondary to such pathologies (Figure 1). In support of this hypothesis is the fact that BBB damage after acute head trauma is a well-known pathologic finding in both animal and human studies. BBB disruption may persist for weeks to years after the injury and may colocalize with the area of abnormal EEG activity [14–16]. The increased interest in osmotic opening of the BBB as a viable mechanism of increased drug delivery to the brain provides an opportunity to explore the connection between BBB opening and seizures in a controlled clinical environment. Osmotic opening of the BBB by vascular infusion of a hyperosmolar bolus of mannitol is mediated by vasodilatation and shrinkage of capillary endothelial cells. Cell shrinkage results in widening of the interendothelial tight junctions to an estimated radius of 200 Å [17]. The permeability effect is largely reversed within minutes. In rodents, porcine and humans loss of BBB integrity by intra-arterial hyperosmotic mannitol has been shown to rapidly lead to EEG changes consistent with epileptic seizures [18–20], that is, spike/wave complexes interspersed with decreased EEG voltage. These studies demonstrate a correlation between the extent of acute BBB openings, as evaluated by imaging and serum S100β levels, and development of seizures.

Another example of S100β application is shown in Figure 2(a). We measured S100β serum levels to establish a temporal relation between a BBB score and seizure development. We collected blood from patients with drug-resistant epilepsy before, during, and immediately after an ictal event. Patients were continuously monitored by EEG. We found that S100β serum levels were elevated at the time of seizures compared to postictal, interictal levels (Figure 2(a)). The latter finding has several implications and represents the first attempt to monitor BBB status during a specific interictal-ictal-interictal transition.

A profound remodeling of the cerebral vasculature associated with leakage and extravasation of serum proteins, consequently with spontaneous seizures, is observed in rodent models of temporal lobe epilepsy. Moreover, it was recently demonstrated that angiogenesis occurs in human TLE (as well as in rodent models of TLE) as a consequence of seizures [22]. In particular upregulation of VEGF in neurons, accompanied by an increase in vascular density, has been described after acute, short- or long-lasting seizures. Once initiated, the angiogenic processes increase progressively, even in the absence of seizure activity, as observed during the latent period (e.g., in pilocarpine-treated rats), or after single short seizures induced by electro-convulsive shock. Conversely, it has also been repeatedly shown that BBB leakage promotes seizures or epileptogenesis [19, 23, 24]. Whatever the temporal relationship between BBB leakage and seizures, it is clear that the epileptic brain is characterized by an abnormal blood-brain interface (Figure 1).

Controversial is the use of imaging techniques to detect BBB damage. The presence of brain edema can be evaluated by MRI. Specifically, structural changes at a cellular level can be assessed by diffusion-weighted imaging (DWI), which calculates the extent of passive water motion or diffusivity (apparent diffusion coefficient, ADC). Curiously, contradictory data have been obtained when evaluating the changes in brain water perfusion in rodent models and in patients with epilepsy [25–28]. DWI analysis in animal studies has demonstrated an early and transient decrease of water diffusivity during provoked status epilepticus or sustained seizures. Peri-ictal and postictal human studies, using DWI or diffusion tensor imaging (DTI), have also shown transiently decreased local diffusivity in some cases [25–28].

4. The Blood-Brain Barrier and Ictogenesis

While epilepsies affect approximately 1% of the population, seizures may occur sporadically in a much larger number of subjects [29]. Historically, a *neurocentric* philosophy has dominated the study of epilepsy and seizures, and only recently the research field has considered the fact that the cerebral vasculature is in fact intimately involved in the maintenance of proper neuronal activity and pathogenesis of seizures (Figure 1). BBB damage can occur as result of pathological events initiated "outside the brain," such as stroke, peripheral inflammation, iatrogenic vascular manipulations, hypertension, heat, and blood hyperosmolarity. The latter are clinically associated with adverse neurological consequences such as cognitive impairment, psychiatric disturbances, and seizures. Evidence indicates that, within the periphery-brain axis, the BBB represents the key player in translating peripheral/vascular pathological events into a neuronal pathological signal, such as seizures. Perhaps the first question we must ask relates to the timing of BBB damage in relation to seizure occurrence: which comes first? Does BBB damage initiate seizures or vice versa? In experimental models of epilepsy, seizures are commonly induced by manipulation of neuronal receptors or by a kindling process. Under these conditions, neuronal death, reactive gliosis, and increased BBB permeability have been predominantly considered as the consequences of seizures [30]. This approach, and the subsequent interpretation of data, has detracted importance from the etiological role of the BBB in epilepsies and, for the most part, has impeded development of alternative pharmacological targets. Seizures are a result of a shift in the normal balance of excitation and inhibition within the brain. Given the numerous players controlling neuronal activity, it is not surprising that many different ways exist to perturb this normal balance, thus triggering seizures. Extravasation of serum albumin in the brain parenchyma was proposed as a mechanism contributing to ictogenesis and epileptogenesis in condition of damaged BBB. Direct brain exposure to serum albumin is associated with downregulation of inward-rectifying potassium (Kir 4.1) channels in astrocytes, resulting in reduced buffering capacity [31].

An important corollary of the BBB-centric hypothesis is the fact that interictal-to-ictal transitions may be caused by cycles of BBB openings. Patients with epilepsy have seizures intermittently, and, depending on the underlying cause, many patients are seizure-free for months. The sporadic appearance of seizures implies that there are

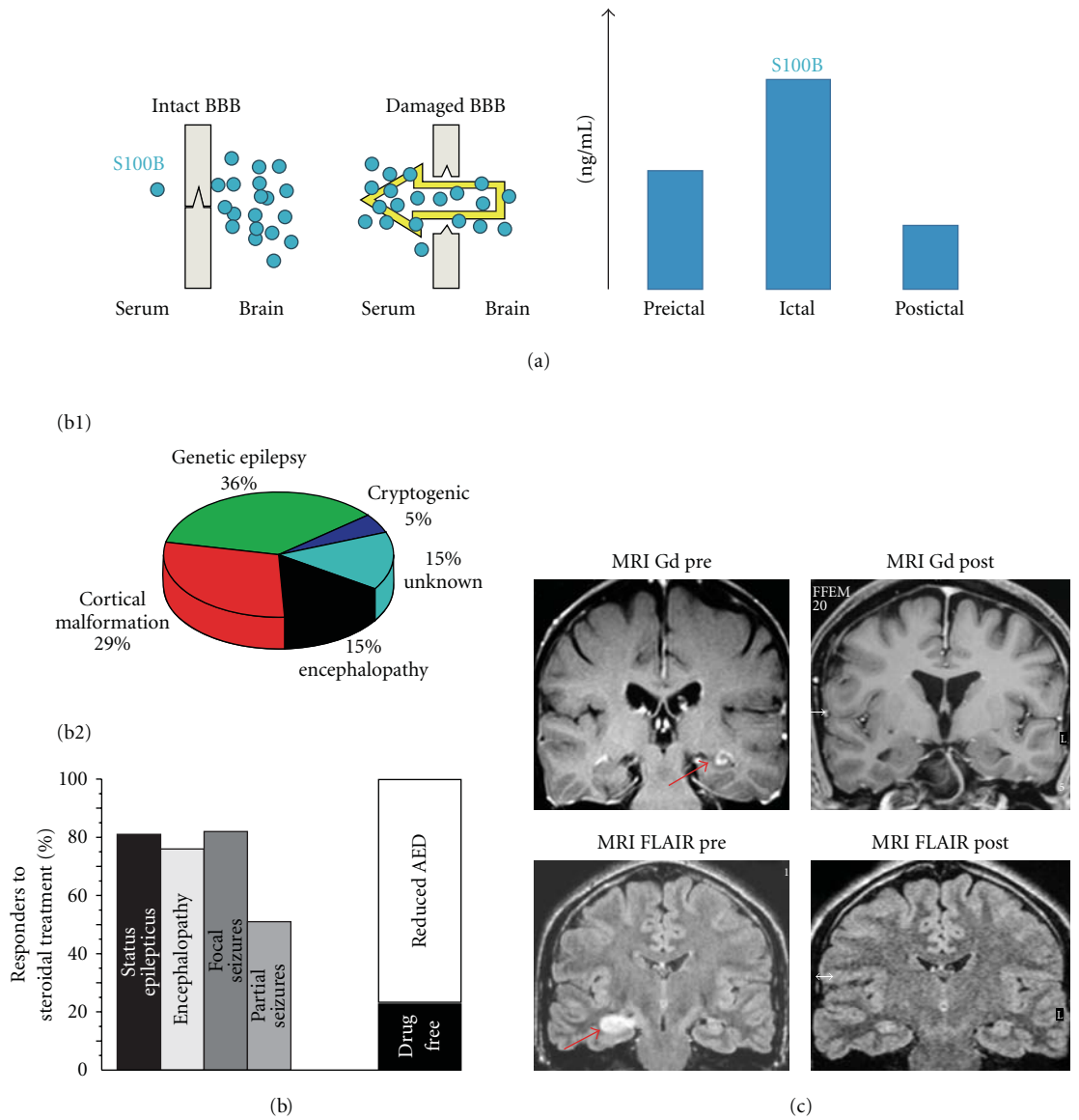

Figure 2: (a) Evidence in support of a link between blood-brain barrier failure and seizures in human subjects shows the rational for the use of serum S100β as a surrogate marker of BBBD. Extensive literature cited in this paper explains in further detail how this test is interpreted. The data presented herein refers to preliminary findings obtained in a cohort of subjects in the EEG monitoring unit. These subjects were continuously monitored for EEG changes suggestive of seizures. Serum samples were taken interictally, ictally, while another sample was taken postictally after approximately 3 hours. Note the increase of ictal S100β as indication of blood-brain barrier opening in these subjects. (b) Efficacy of glucocorticosteroids in a cohort of pediatric drug resistant epileptic subjects. The etiology of seizures that responded to steroids is shown in the pie chart in B1, while B2 shows the efficacy of anti-inflammatory treatment. (c) Note that discrete regions of the brain appear to have developed abnormal signal on contrast enhanced (Gd) or FLAIR sequences (see also [21]). Note that, in the MRI scans shown, the efficacy of steroids on seizures was paralleled by changes possibly associated with improved blood-brain barrier function ($n = 2$ patients).

precipitating factors inducing seizures in these patients. Seizure precipitating factors include psychological or physical stress, sleep deprivation, hormonal changes associated with the menstrual cycle, or exposure to toxic substances and certain medications [29]. All of these factors have been shown to be associated with compromised BBB permeability [30]. Severe head trauma is associated with a damaged BBB and with high risk of epilepsy [15]. The propensity of severe trauma leading to development of epilepsy suggests that brain injury results in long-lasting, pathologic changes in the brain that change a normal neural network into a hyperexcitable one. Furthermore, it is reasonable to predict that BBB damage could be sufficient to turn a "silent" brain malformation into an active one, allowing for the development of recurrent seizures and drug resistance. Pre-existing abnormalities in cortical development may contribute to the

occurrence of seizures in response to a vascular challenge (*two-hit hypothesis,* Figure 1).

5. Interplay between Seizures, Blood-Brain Barrier, and White Blood Cells

Experimental evidence has indicated a role of brain inflammation in epilepsy [32]. It is important to underscore that any inflammatory process, either of peripheral or brain origin, includes early vascular damage, fundamental to the propagation and maintenance of inflammation. Thus, inflammatory process follows traditional pathophysiological sequelae and is accompanied by dilation and increased permeability of blood vessels. It is surprising that, when dealing with seizure disorders, this definition is often forgotten and parenchymal cells are considered to be sole players in the inflammatory process.

As stated above, experimental evidence supports the role of intravascular inflammation in seizure disorders. Recently, the involvement of circulating immune cells, their interaction with the BBB, and seizure propensity have been recently investigated [33]. Concordant data have been obtained using models of peripheral inflammation, such as experimental colitis, or the systemic administration of the cholinergic agonist pilocarpine [34–37]. Activation of circulating white blood cells (WBCs) was observed in animals prior to the development of seizures. In particular, pilocarpine induced acute intravascular proinflammatory changes leading to BBB leakage. In addition, loss of BBB function could be triggered by systemic proinflammatory events occurring in response to seizure activity and activation of the hypothalamic-pituitary-adrenal axis. Recently, a profound postictal change in the immune cell composition of peripheral blood in epileptics was reported [38]. In particular, NK and T CD8+ cell count was elevated. This is suggestive of the involvement of the immune axis mediated by the mesial-sympathetic connections. Based on this evidence, one may envision a model where bidirectional flux of neuroimmune information travels from and to the CNS to involve systemic organs. Departure from this equilibrium may favor seizures.

An additional piece to the puzzle is whether or not transmigration of WBCs occurs during epileptogenesis or acute and chronic seizures. While studies have demonstrated the proseizure effect of BBB-WBCs interaction, it is not clear whether WBCs need to invade the brain to produce an epileptogenic effect. Recent evidence has provided somehow contractor results. However, it is possible that the apparent discrepancy between reports resides in the terminology used to indicate the anatomical location of cells and their quantification. For instance, WBC brain invasion was considered to occur even when a small number of WBCs ($\sim$1 cells/10 mm^2 of brain tissue) were found in the parenchyma of epileptic human brains [33]. Our recent data showed WBC accumulation mainly at the intra- and perivascular compartments of the BBB in rodent model of seizures and brains resected from epileptic subjects [20]. Moreover, when detected in the brain parenchyma, WBC presence was limited to a specific subpopulation [39]. In particular, granulocytes appeared transiently in rat brain during epileptogenesis while monocytes/macrophages were present in the hippocampus until chronic seizures developed. B- and T-lymphocytes and NK cells were negligible [39]. The presence of brain WBC also depended on the model of seizure used. In general, it appears that a limited number of WBCs home into the brain parenchyma, while most of the WBCs are segregated to the perivascular BBB space. This is in agreement with the fact that WBC vascular extravasation under *sterile* conditions (e.g., absence of pathogens as in most of the epilepsies) is an uncommon event. The possibility also exists that WBC brain extravasation could be a reversible event. In other words, it might be that cells "extravasate" and then rapidly return into the blood stream. However, further studies are needed to rule out this possibility. Nevertheless, activated intravascular T-cells and granulocytes/monocytes can produce proinflammatory factors that, upon reaching the brain, could stimulate microglia and astrocytes causing a local inflammatory response.

While WBC brain infiltrates are found in selected seizure disorders where a clear antigenic component is present (e.g., Rasmussen's encephalitis, [40, 41]), we now propose immunologic mechanisms of seizures applicable to a larger number of epilepsies where autoimmunity is not present. In other words, we suggest that, upon activation, WBCs act at the BBB and reside in the proximity of the vasculature without further entry into the brain parenchyma. Under these circumstances, the endpoint facilitating seizures is BBB damage regardless of subsequent WBC involvement. Whether the perivascular homing of leukocytes will lead to a more robust disruption of the BBB is possible but not yet certain. This hypothesis stems from the fact that the majority of seizure disorders are not associated with any brain immunological signature, therefore "no brain" needs to be identified and "neutralized" by the WBCs.

6. Restoring Cerebrovascular Integrity to Prevent or Reduce Seizures

Given the considerations listed above, it becomes plausible that BBB repair may be of antiseizure value. If BBB damage promotes seizures, then prophylactic control of the events leading to cerebrovascular failure should be effective in preventing or reducing seizures. Preservation of BBB integrity may represent a complementary pharmacological approach to the use of neuron-targeting AEDs. Glucocorticosteroids (GCs), acting on the classic proinflammatory target and on the cerebrovasculature, may thus become clinically useful in preventing or reducing seizure occurrence (Figure 2 and [21]).

We have recently obtained evidence supporting the effectiveness of adjunctive GCs treatment in children with intractable epilepsy; we intentionally excluded those syndromes known to be responsive to GCs and ACTH (L-G, L-K, West or Rasmussen's). GCs were beneficial regardless of the pathology and epileptic syndrome (Figure 2(c)). Similar results were obtained using the pilocarpine model of status epilepticus. We found that BBB integrity was preserved in rats pretreated with anti-inflammatory agents [21]. Preliminary results also showed that FLAIR hyperintensities

were attenuated in patients who responded to CG therapy, suggesting that FLAIR is a surrogate radiologic index of BBB damage (Figure 2(b)). A comprehensive study needs to be performed in order to prove this.

The efficacy of glucocorticosteroids in reducing drug-resistant seizures remains, however, controversial. A Cochrane review suggests that steroids lack efficacy [42]. The latter study was based on a relatively small population of subjects and derived from meta-analysis of a single trial. Moreover, only ACTH was used, leaving out the use of commonly prescribed corticosteroids. In contrast, recent reports have suggested the efficacy of add-on glucocorticosteroids in pediatric forms of epilepsy [43–46]. While no conclusive studies are yet available, our recent published data [21] and preliminary data in Figure 2 provided an indication of the efficacy of glucocorticosteroids in drug-resistant pediatric seizures. We would also like to underscore that BBB damage is observed independently of the species and the type of seizures. BBB damage, as evaluated by albumin leakage, is comparable regardless of means to induce seizures [20, 23, 47, 48]. Thus, if BBB failure is a trigger of chronic as well as spontaneous, unprovoked, or iatrogenic seizures then BBB repair may impact seizure burden regardless of whether therapy is applied prophylactically or after epileptogenesis is completed. Moreover, BBB damage during epileptogenesis was found and was similar to BBB damage observed in acute animal experiments or chronic patient samples [20, 23, 47, 48].

7. Do We Need Better Experimental Models to Develop Better AEDs?

While all epilepsies are characterized by recurrent seizures, profound etiological and pathophysiological differences exist between them. These differences are often overlooked when planning laboratory experiments. Experimental models of epilepsy were originally created as drug screening tools, and a reproducible number of seizures were therefore a desirable goal. The use of these experimental models has then been expanded to the understanding of mechanisms of epileptogenesis and drug resistance. This leap has reduced a variety of clinical epileptic syndromes to a few simplistic models, disregarding the complex actuality of the epilepsies. The question remains of how to develop an appropriate experimental model able to mimic a specific epileptic syndrome. Basic research relies on models of epilepsy characterized by a rapid onset of generalized seizures, leading over time to spontaneous seizures. While these models have generated important mechanistic insights of neuronal transmission, basic science research needs to generate better models to bring the development of new therapeutic options onto a more clinically applicable level.

There are several clinically relevant models of neonatal brain disease spanning from rodent models with genetic defects or k.o. animals, models of epigenetic inheritance, or models based on insertion of chromosomal material. Teratogen exposure (drugs and/or environmental poisons), maternal trauma, infection, and stroke are all factors that might interfere with the normal progression of brain development and give rise to aberrant patterns of cortical structure. Acquired cortical dysplasia appears to result from a progressive process (i.e., that may continue beyond the time of insult), affecting not only the primary region of lesion but also surrounding "normal" tissue [49, 50].

Malformations of cortical development (MCD) are often observed in clinical cases of drug-resistant epilepsy. Dysplastic regions are characterized by aberrant neuronal and vascular architecture. Brain regions affected by neurovascular dysplasia have a lower seizure threshold compared to normal brain [51–55]. While cortical dysplasia is a common clinical correlate of earlyonset epilepsies, it is difficult to study the basic mechanisms linking dysplastic lesions to epileptogenesis in human tissue. Models such as the methylazoxymethanol (MAM) exposed rat were until recently believed to cause MCD by a neurotoxic action. MAM is a DNA alkylating agent. Injection (i.p.) of MAM acetate into pregnant rats at day 14/15 of gestation (E14, E15) exposes the fetuses to an agent that disrupts cell proliferation at a time when neocortical and hippocampal neurons and glia are being formed [56, 57]. The most salient result of this manipulation is cortical thinning and the generation of cortical heterotopias. A number of laboratories have shown that MAM animals have lower seizure thresholds than normal controls in response to a variety of epileptogenic agents (flurothyl, hyperthermia, kindling, etc.; [58]). Studies have also suggested that these animals have behavioral impairments [59]. The main pathology that MAM recapitulates is microcephaly [60].

Recent findings, however, have shown a remarkable toxicity of MAM towards endothelial cells and presence of dimorphic and leaky BBB vessels [56]. In this scenario the significance of *BBB damage* does not only refer to iatrogenic manipulation or traumatic events, but rather expands to various pathological changes leading to loss of fundamental BBB features, including selective permeability. In many ways, this is conceptually analogous to "membrane integrity" in cells, where small damage to membrane lipids may compromise a variety of cellular functions. Recently it has been shown that the toxins thalidomide (THAL) or MAM causes postnatal brain maldevelopment and hyperexcitability associated to abnormal vascular trunks [61] (Figure 3). In addition to seizures, prenatal exposure to THAL, valproic acid alone, or in combination with other agents [49] produces a spectrum of psychiatric and behavioral traits that are consistent with the clinical presentation of neonatal seizures and subsequent development of life-long neurological diseases. Why this occurs is not fully understood, but our previous and current results suggest that THAL and MAM, given at E15, (1) cause a transient reduction of VEGF signaling resulting in limited angiogenic potential at a time when cortical development is maximal, and (2) aborted angiogenesis results in persistence of abnormal vascular profiles [49, 61, 62], leaky BBB vessels causing brain edema at birth, increased expression of water channels, and decreased expression and function of BBB tight junctions [49, 61, 62]; (3) the combined effects of edema and BBB leakage lead to improper development and positioning of parenchymal brain cells (Figure 3), which, finally, may cause seizures and permanent brain rewiring.

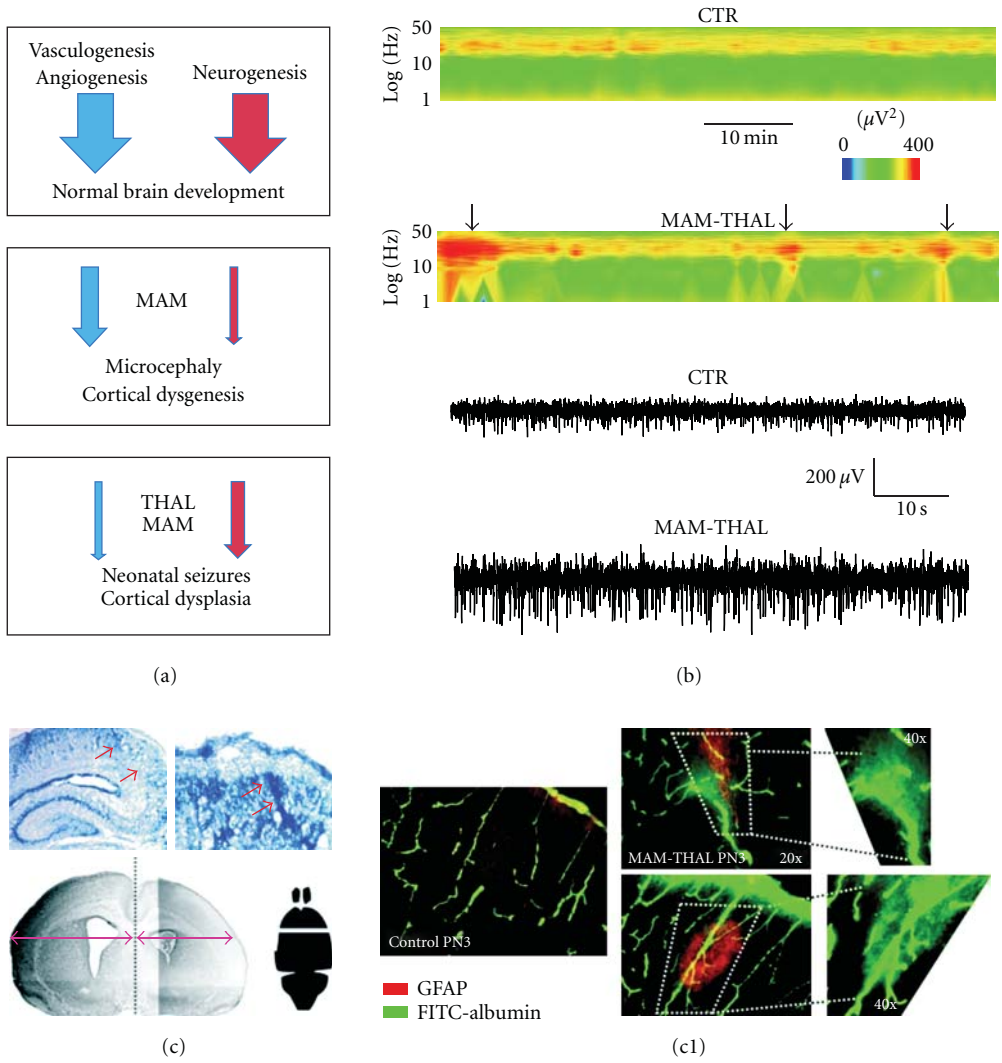

Figure 3: Leakage of the BBB is associated with neonatal seizures. (a) Summary of the neurovascular changes induced by prenatal exposure to MAM and/or THAL. (b) Seizures in neonatal THAL-MAM rats displayed on a joint time-frequency plot. Note also the traces recorded by the scalp electrode. (c) Loss of selective BBB permeability is associated to brain edema and hemispheric asymmetry in THAL-MAM rats. *Red arrows* point to region of disrupted cytoarchitecture due to vascular edema. (c1) FITC-albumin is used to indicate loss of BBB integrity.

Remarkably, in a subset of THAL-MAM new born rats, epileptic fits were recorded (Figure 3).

8. Final Remarks

The BBB has been historically studied as a "pharmacokinetic" obstacle to brain drug delivery. However, cerebrovascular failure has been recently proposed to have an etiological role in brain diseases that have been traditionally considered *neuronal in nature*, among all seizure disorders. Based on available evidence, we discussed the role of BBB failure in the initiation and sustaining of seizures and epilepsies and discussed whether a realistic clinical opportunity for BBB drugs exists. Evidence suggests that such a clinical opportunity does exist for drug-resistant forms of epilepsy, where traditional neuronal AEDs fail to control seizure, allowing for a complementary *cerebrovascular* therapeutic option.

Acknowledgments

Support is by R01 NS060881 (to AJ), the Cleveland Clinic-Swedish Satellite Laboratory Feasibility Project, Federal Appropriation Washington State and R01 NS43284, R01 NS38195, R21 HD057256 to D. Janigro.

References

[1] G. A. Grant and D. Janigro, "The blood-brain barrier," in *Youmans Neurological Surgery*, H. R. Winn, Ed., vol. 1, Saunders, Philadelphia, Pa, USA, 2010.

[2] N. J. Abbott, "Astrocyte-endothelial interactions and blood-brain barrier permeability," *Journal of Anatomy*, vol. 200, no. 6, pp. 629–638, 2002.

[3] N. J. Abbott, L. Ronnback, and E. Hansson, "Astrocyte-endothelial interactions at the blood-brain barrier," *Nature Reviews Neuroscience*, vol. 7, no. 1, pp. 41–53, 2006.

[4] B. V. Zlokovic, "The Blood-Brain Barrier in Health and Chronic Neurodegenerative Disorders," *Neuron*, vol. 57, no. 2, pp. 178–201, 2008.

[5] C. Ghosh, J. Gonzalez-Martinez, M. Hossain et al., "Pattern of P450 expression at the human blood-brain barrier: roles of epileptic condition and laminar flow," *Epilepsia*, vol. 51, no. 8, pp. 1408–1417, 2010.

[6] S. M. Sisodiya, W. R. Lint, B. N. Harding, M. V. Squier, and M. Thom, "Drug resistance in epilepsy: human epilepsy," *Novartis Foundation Symposium*, vol. 243, pp. 167–179, 2002.

[7] S. M. Sisodiya, "Mechanisms of antiepileptic drug resistance," *Current Opinion in Neurology*, vol. 16, no. 2, pp. 197–201, 2003.

[8] N. A. Oberheim, T. Takano, X. Han et al., "Uniquely hominid features of adult human astrocytes," *Journal of Neuroscience*, vol. 29, no. 10, pp. 3276–3287, 2009.

[9] P. J. Magistretti and L. Pellerin, "Cellular basis of brain energy metabolism and their relevance to brain imaging-evidence for a prominent role for astrocytes," *Cerebral Cortex*, vol. 5, pp. 301–306, 1995.

[10] N. Marchi, P. Rasmussen, M. Kapural et al., "Peripheral markers of brain damage and blood-brain barrier dysfunction," *Restorative Neurology and Neuroscience*, vol. 21, no. 3-4, pp. 109–121, 2003.

[11] N. Marchi, M. Cavaglia, V. Fazio, S. Bhudia, K. Hallene, and D. Janigro, "Peripheral markers of blood-brain barrier damage," *Clinica Chimica Acta*, vol. 342, no. 1-2, pp. 1–12, 2004.

[12] A. A. Kanner, N. Marchi, V. Fazio et al., "Serum S100β: a noninvasive marker of blood-brain barrier function and brain lesions," *Cancer*, vol. 97, no. 11, pp. 2806–2813, 2003.

[13] M. Kapural, L. Krizanac-Bengez, G. Barnett et al., "Serum S-100β as a possible marker of blood-brain barrier disruption," *Brain Research*, vol. 940, no. 1-2, pp. 102–104, 2002.

[14] G. A. Grant and D. Janigro, "The blood-brain barrier," in *Youmans Neurological Surgery*, H. R. Winn, Ed., vol. 1, pp. 153–174, Saunders, Philadelphia, Pa, USA, 2004.

[15] A. Korn, H. Golan, I. Melamed, R. Pascual-Marqui, and A. Friedman, "Focal cortical dysfunction and blood-brain barrier disruption in patients with postconcussion syndrome," *Journal of Clinical Neurophysiology*, vol. 22, no. 1, pp. 1–9, 2005.

[16] R. H. Schmidt and M. S. Grady, "Regional patterns of blood-brain barrier breakdown following central and lateral fluid percussion injury in rodents," *Journal of Neurotrauma*, vol. 10, no. 4, pp. 415–430, 1993.

[17] R. A. Kroll and E. A. Neuwelt, "Outwitting the blood-brain barrier for therapeutic purposes: osmotic opening and other means," *Neurosurgery*, vol. 42, no. 5, pp. 1083–1100, 1998.

[18] C. Fieschi, G. L. Lenzi, and E. Zanette, "Effects on EEG of the osmotic opening of the blood-brain barrier in rats," *Life Sciences*, vol. 27, no. 3, pp. 239–243, 1980.

[19] N. Marchi, L. Angelov, T. Masaryk et al., "Seizure-promoting effect of blood-brain barrier disruption," *Epilepsia*, vol. 48, no. 4, pp. 732–742, 2007.

[20] N. Marchi, Q. Teng, C. Ghosh et al., "Blood-brain barrier damage, but not parenchymal white blood cells, is a hallmark of seizure activity," *Brain Research*, vol. 1353, pp. 176–186, 2010.

[21] N. Marchi, A. Batra, Q. Fan et al., "Antagonism of peripheral inflammation prevents status epilepticus," *Neurobiology of Disease*, vol. 33, no. 2, pp. 171–271, 2009.

[22] V. Rigau, M. Morin, M. C. Rousset et al., "Angiogenesis is associated with blood-brain barrier permeability in temporal lobe epilepsy," *Brain*, vol. 130, no. 7, pp. 1942–1956, 2007.

[23] E. Seiffert, J. P. Dreier, S. Ivens et al., "Lasting blood-brain barrier disruption induces epileptic focus in the rat somatosensory cortex," *Journal of Neuroscience*, vol. 24, no. 36, pp. 7829–7836, 2004.

[24] E. A. Van Vliet, A. S. da Costa, S. Redeker, R. Van Schaik, E. Aronica, and J. A. Gorter, "Blood-brain barrier leakage may lead to progression of temporal lobe epilepsy," *Brain*, vol. 130, no. 2, pp. 521–534, 2007.

[25] V. Alvarez, P. Maeder, and A. O. Rossetti, "Postictal blood-brain barrier breakdown on contrast-enhanced MRI," *Epilepsy and Behavior*, vol. 17, no. 2, pp. 302–303, 2010.

[26] C. Amato, M. Elia, S. A. Musumeci, P. Bisceglie, and M. Moschini, "Transient MRI abnormalities associated with partial status epilepticus: a case report," *European Journal of Radiology*, vol. 38, no. 1, pp. 50–54, 2001.

[27] M. G. Lansberg, M. W. O'Brien, A. M. Norbash, M. E. Moseley, M. Morrell, and G. W. Albers, "MRI abnormalities associated with partial status epilepticus," *Neurology*, vol. 52, no. 5, pp. 1021–1027, 1999.

[28] K. M. Tan, J. W. Britton, J. R. Buchhalter et al., "Influence of subtraction ictal SPECT on surgical management in focal epilepsy of indeterminate localization: a prospective study," *Epilepsy Research*, vol. 82, no. 2-3, pp. 190–193, 2008.

[29] W. A. Hauser, "Epidemiology of acute symptomatic seizures," in *Epilepsy: A Comprehensive Textbook*, G. Engel and T. A. Pedley, Eds., pp. 71–75, Lippincott Williams and Wilkins, Philadelphia, Pa, USA, 2008.

[30] E. Oby and D. Janigro, "The blood-brain barrier and epilepsy," *Epilepsia*, vol. 47, no. 11, pp. 1761–1774, 2006.

[31] S. Ivens, D. Kaufer, L. P. Flores et al., "TGF-β receptor-mediated albumin uptake into astrocytes is involved in neocortical epileptogenesis," *Brain*, vol. 130, no. 2, pp. 535–547, 2007.

[32] A. Vezzani and T. Granata, "Brain inflammation in epilepsy: experimental and clinical evidence," *Epilepsia*, vol. 46, no. 11, pp. 1724–1743, 2005.

[33] P. F. Fabene, G. N. Mora, M. Martinello et al., "A role for leukocyte-endothelial adhesion mechanisms in epilepsy," *Nature Medicine*, vol. 14, no. 12, pp. 1377–1383, 2008.

[34] G. Akhan, F. Andermann, and M. J. Gotman, "Ulcerative colitis, status epilepticus and intractable temporal seizures," *Epileptic Disorders*, vol. 4, no. 2, pp. 135–137, 2002.

[35] Z. L. Chen and S. Strickland, "Neuronal death in the hippocampus is promoted by plasmin-catalyzed degradation of laminin," *Cell*, vol. 91, no. 7, pp. 917–925, 1997.

[36] N. Marchi, E. Oby, N. Fernandez et al., "*In vivo* and *in vitro* effects of pilocarpine: relevance to ictogenesis," *Epilepsia*, vol. 48, no. 10, pp. 1934–1946, 2007.

[37] R. Scheid and N. Teich, "Neurologic manifestations of ulcerative colitis," *European Journal of Neurology*, vol. 14, no. 5, pp. 483–492, 2007.

[38] S. Bauer, M. Köller, S. Cepok et al., "NK and CD4+ T cell changes in blood after seizures in temporal lobe epilepsy," *Experimental Neurology*, vol. 211, no. 2, pp. 370–377, 2008.

[39] T. Ravizza, B. Gagliardi, F. Noé, K. Boer, E. Aronica, and A. Vezzani, "Innate and adaptive immunity during epileptogenesis and spontaneous seizures: evidence from experimental models and human temporal lobe epilepsy," *Neurobiology of Disease*, vol. 29, no. 1, pp. 142–160, 2008.

[40] T. Granata, G. Gobbi, R. Spreafico et al., "Rasmussen's encephalitis: early characteristics allow diagnosis," *Neurology*, vol. 60, no. 3, pp. 422–425, 2003.

[41] T. Granata, "Rasmussen's syndrome," *Neurological Sciences*, vol. 24, no. 4, pp. S239–S243, 2003.

[42] N. A. Gayatri, C. D. Ferrie, and H. Cross, "Corticosteroids including ACTH for childhood epilepsy other than epileptic spasms," *Cochrane Database of Systematic Reviews*, no. 1, article CD005222, 2007.

[43] T. Araki, H. Otsubo, Y. Makino et al., "Efficacy of dexamathasone on cerebral swelling and seizures during subdural grid EEG recording in children," *Epilepsia*, vol. 47, no. 1, pp. 176–180, 2006.

[44] R. Gupta and R. Appleton, "Corticosteroids in the management of the paediatric epilepsies," *Archives of Disease in Childhood*, vol. 90, no. 4, pp. 379–384, 2005.

[45] D. B. Sinclair, "Prednisone therapy in pediatric epilepsy," *Pediatric Neurology*, vol. 28, no. 3, pp. 194–198, 2003.

[46] H. Verhelst, P. Boon, G. Buyse et al., "Steroids in intractable childhood epilepsy: clinical experience and review of the literature," *Seizure*, vol. 14, no. 6, pp. 412–421, 2005.

[47] N. Marchi, Q. Teng, M. T. Nguyen et al., "Multimodal investigations of trans-endothelial cell trafficking under condition of disrupted blood-brain barrier integrity," *BMC Neuroscience*, vol. 11, article 34, 2010.

[48] E. Van Vliet, E. Aronica, S. Redeker et al., "Selective and persistent upregulation of mdr1b mRNA and P-glycoprotein in the parahippocampal cortex of chronic epileptic rats," *Epilepsy Research*, vol. 60, no. 2-3, pp. 203–213, 2004.

[49] Q. Y. Fan, S. Ramakrishna, N. Marchi, V. Fazio, K. Hallene, and D. Janigro, "Combined effects of prenatal inhibition of vasculogenesis and neurogenesis on rat brain development," *Neurobiology of Disease*, vol. 32, no. 3, pp. 499–509, 2008.

[50] M. Marin-Padilla, "Perinatal brain damage, cortical reorganization (acquired cortical dysplasias), and epilepsy," *Advances in Neurology*, vol. 84, pp. 153–172, 2000.

[51] M. E. Calcagnotto, M. F. Paredes, and S. C. Baraban, "Heterotopic neurons with altered inhibitory synaptic function in an animal model of malformation-associated epilepsy," *Journal of Neuroscience*, vol. 22, no. 17, pp. 7596–7605, 2002.

[52] N. Chevassus-Au-Louis, P. Congar, A. Represa, Y. Ben-Ari, and J. L. Gaïarsa, "Neuronal migration disorders: heterotopic neocortical neurons in ca1 provide a bridge between the hippocampus and the neocortex," *Proceedings of the National Academy of Sciences of the United States of America*, vol. 95, no. 17, pp. 10263–10268, 1998.

[53] N. Chevassus-Au-Louis, A. Rafiki, I. Jorquera, Y. Ben-Ari, and A. Represa, "Neocortex in the hippocampus: an anatomical and functional study of CA1 heterotopias after prenatal treatment with methylazoxymethanol in rats," *Journal of Comparative Neurology*, vol. 394, no. 4, pp. 520–536, 1998.

[54] N. Chevassus-au-Louis, I. Jorquera, Y. Ben-Ari, and A. Represa, "Abnormal connections in the malformed cortex of rats with prenatal treatment with methylazoxymethanol may support hyperexcitability," *Developmental Neuroscience*, vol. 21, no. 3–5, pp. 385–392, 1999.

[55] R. Matsumoto, M. Kinoshita, J. Taki et al., "In vivo epileptogenicity of focal cortical dysplasia: a direct cortical paired stimulation study," *Epilepsia*, vol. 46, no. 11, pp. 1744–1749, 2005.

[56] S. Bassanini, K. Hallene, G. Battaglia et al., "Early cerebrovascular and parenchymal events following prenatal exposure to the putative neurotoxin methylazoxymethanol," *Neurobiology of Disease*, vol. 26, no. 2, pp. 481–495, 2007.

[57] G. Battaglia, S. Pagliardini, L. Saglietti et al., "Neurogenesis in cerebral heterotopia induced in rats by prenatal methylazoxymethanol treatment," *Cerebral Cortex*, vol. 13, no. 7, pp. 736–748, 2003.

[58] S. C. Baraban and P. A. Schwartzkroin, "Flurothyl seizure susceptibility in rats following prenatal methylazoxymethanol treatment," *Epilepsy Research*, vol. 23, no. 3, pp. 189–194, 1996.

[59] M. Di Luca, F. Merazzi, P. N. E. De Graan et al., "Selective alteration in B-50/GAP-43 phosphorylation in brain areas of animals characterized by cognitive impairment," *Brain Research*, vol. 607, no. 1-2, pp. 329–332, 1993.

[60] C. Colacitti, G. Sancini, S. DeBiasi et al., "Prenatal methylazoxymethanol treatment in rats produces brain abnormalities with morphological similarities to human developmental brain dysgeneses," *Journal of Neuropathology and Experimental Neurology*, vol. 58, no. 1, pp. 92–106, 1999.

[61] K. L. Hallene, E. Oby, B. J. Lee et al., "Prenatal exposure to thalidomide, altered vasculogenesis, and CNS malformations," *Neuroscience*, vol. 142, no. 1, pp. 267–283, 2006.

[62] N. Marchi, G. Guiso, S. Caccia et al., "Determinants of drug brain uptake in a rat model of seizure-associated malformations of cortical development," *Neurobiology of Disease*, vol. 24, no. 3, pp. 429–442, 2006.

Hindawi Publishing Corporation
Cardiovascular Psychiatry and Neurology
Volume 2011, Article ID 461263, 8 pages
doi:10.1155/2011/461263

Review Article

Elucidating the Complex Interactions between Stress and Epileptogenic Pathways

Aaron R. Friedman,[1] Luisa P. Cacheaux,[1] Sebastian Ivens,[2,3] and Daniela Kaufer[1,4]

[1] *Department of Integrative Biology, University of California-Berkeley, Berkeley, CA 94720-3140, USA*
[2] *Institute of Neurophysiology, Charité University Medicine, 10117 Berlin, Germany*
[3] *Department of Psychiatry and Psychotherapy, Charité University Medicine, 10117 Berlin, Germany*
[4] *Helen Wills Neuroscience Institute, University of California-Berkeley, Berkeley, CA 94720-3140, USA*

Correspondence should be addressed to Daniela Kaufer, danielak@berkeley.edu

Received 13 November 2010; Accepted 22 January 2011

Academic Editor: Alon Friedman

Clinical and experimental data suggest that stress contributes to the pathology of epilepsy. We review mechanisms by which stress, primarily via stress hormones, may exacerbate epilepsy, focusing on the intersection between stress-induced pathways and the progression of pathological events that occur before, during, and after the onset of epileptogenesis. In addition to this temporal nuance, we discuss other complexities in stress-epilepsy interactions, including the role of blood-brain barrier dysfunction, neuron-glia interactions, and inflammatory/cytokine pathways that may be protective or damaging depending on context. We advocate the use of global analytical tools, such as microarray, in support of a shift away from a narrow focus on seizures and towards profiling the complex, early process of epileptogenesis, in which multiple pathways may interact to dictate the ultimate onset of chronic, recurring seizures.

1. Introduction

In clinical studies of epilepsy patients, stress is the most frequently self-reported trigger of seizures—higher than other precipitants such as sleep deprivation, fatigue, diet, or even missed medication [1–3]. In prospective study, increased severity of self-reported stress/anxiety also correlates with increased risk of subsequent seizure [4]. These studies, derived from the first-hand experience of those who suffer from epilepsy, set the stage for a wealth of experimental data indicating that stress may impact and exacerbate epilepsy in at least four contexts: (1) life stress, particularly early life stress, may create a vulnerability for the incidence of epilepsy; (2) stress may play a role in the etiology of symptomatic epilepsy by exacerbating the causal event, such as traumatic brain injury, stroke, or status epilepticus; (3) stress may play a role in the process of epileptogenesis—the "silent period" that follows initial injury and is characterized by progressive cellular and network changes thought to underlie the ultimate onset of chronic seizures; (4) stress may increase the frequency or severity of seizures after epilepsy onset. In this paper, we focus on the molecular pathways by which stress and epilepsy may converge. We emphasize the nuance and complexity of these pathways, noting that the role of particular molecules can vary from neuroprotective to destructive, depending on context. To highlight this complexity, we discuss the signaling pathways that are initiated following blood-brain barrier dysfunction and emphasize neural-glia interactions. Finally, in light of the complex interplay of pathways that affect epilepsy, we advocate strategies for "global" characterization of epilepsy pathology to complement the single pathway investigation typically favored by inference-guided experimentation.

2. Mechanisms by Which Stress May Create Vulnerability to Epilepsy

In addition to the immediate physiological "stress response," stressful incidents, particularly early in life, can cause long-term changes in the organism that create vulnerability for a variety of diseases [5, 6]. This concept of stress-induced

vulnerability has not been frequently applied to epilepsy, despite evidence that many persistent changes induced by stress are likely to affect mechanisms of epilepsy. Perhaps most importantly, early life stress can cause long-lasting alterations in the regulation of the hypothalamic-pituitary adrenal (HPA) axis [7], which controls the release of stress hormones (glucocorticoids; GCs). These alterations, which are effected by cognitive mechanisms (neural plasticity in reinforcing stress-responsive networks [8, 9]) and genetic transcriptional mechanisms (classical and epigenetic regulation of genes controlling the HPA axis [10, 11]), lead to adult animals that have an impaired stress response to aversive stimuli, including increase in stress hormone release and impairment of HPA negative feedback [12]. Thus, all aspects of the stress response that may directly exacerbate epilepsy (described in subsequent sections) are likely to be particularly potent in individuals that have experienced early life stress. For example, early life stress affects adult induction of immune and inflammatory pathways [13, 14], which have been implicated in neural damage in epilepsy. Similarly, early life stress decreases the expression of brain-derived neurotrophic factor (BDNF) in the adult brain [15–17], which is a critical mediator of neuroprotection across epilepsy models.

Early life stress may also have a profound impact on the development of white matter in the brain. Preliminary work in our lab and others indicates that stress may increase or decrease myelination, depending on developmental stage and other unknown factors (unpublished data and [18]). These paradoxical findings are echoed by the literature showing that GCs induce *in vitro* oligodendrocyte precursor cells (OPCs) to differentiate into mature oligodendrocytes [19–21] and promote oligodendrocyte survival [22], yet total removal of GCs by adrenalectomy results in hypermyelination [23] while prenatal GC treatment delays myelination in sheep [24]. If early life stress does result in delayed and/or hypomyelination, it would constitute a startling and underappreciated similarity to a variety of seizure syndromes. Delayed myelination is a hallmark of infantile spasms [25] and other seizure disorders [26], and several genetic hypomyelination disorders or manipulations include severe seizure symptoms [27, 28]. In these models, treatment is associated with white matter recovery: amino acid supplement of patients with a serine biosynthesis disorder resulted in restoration of white matter and major seizure reduction [29, 30]. Pharmacologically (L-allylglycine, bicuculline, and kainic acid) or electrically induced seizures also cause demyelination [31, 32], and alterations of white matter have been associated with both symptomatic and idiopathic epilepsy [33–35] and with hippocampal sclerosis [36]. Indeed, while glia have received a surge of recent interest for causal roles in epilepsy, this attention has focused almost exclusively on astrocytes. Possible roles for oligodendrocytes remain largely uninvestigated.

Direct investigation of early life stress on subsequent epilepsy is sparse, but there have been at least a few studies in rodents. One study subjected pups to maternal separation (MS) or normal rearing and then induced status epilepticus (SE) by lithium-pilocarpine at P16 and assessed subsequent advent of behavioral seizures in adulthood. Only one normally reared rat showed adult spontaneous recurrent seizures (SRS), whereas all 8 rats from the MS group developed SRS [37], though it is not clear if this difference can be attributed to a persistent "vulnerability" created by MS or to a more immediate effect of the MS stress on severity of induced SE. Another group subjected rats to MS or mild handling and assessed seizure induction by amygdala kindling subsequently in adulthood. MS rats required significantly less stimulation for seizure induction [38]. Gendered analysis indicates that this effect may only hold true for female rats [39]—an interesting finding given the well-known effects of sex hormones both on stress response and on epilepsy [9, 40–42]. A similar study showed that chronic GC supplement in adult adrenalectomized rats also accelerated the rate of amygdala kindling [43], indicating that interactions between GCs and seizure threshold may be generalized outside of the early life period.

The limited available direct evidence, as well as general observations of persistent changes mediated by early life stress, indicates that it could cause a life-long vulnerability for subsequent epilepsy. Given that the factors that govern whether or not epileptogenesis occurs after traumatic injury are poorly understood, the role of early life stress vulnerability deserves more in-depth study.

3. Mechanisms by Which Stress May Exacerbate Etiological Incidents

The most common form of symptomatic epilepsy involves a precipitating traumatic incident—an initial prolonged seizure (SE), stroke, traumatic brain injury, or infection/fever—that is followed by onset of epilepsy after a delay of months to years. A wealth of evidence indicates that damage suffered during such incidents and possibly also the induction of repair mechanisms constitute the first steps of epileptogenesis. Can activation of stress pathways during etiological incidents exacerbate damage or otherwise contribute to the proximate steps of epileptogenesis?

One of the common occurrences across different types of precipitating incidents is immediate neurological injury and cell death. GCs exacerbate such neural injury. For example, viral vector blockade of glucocorticoid receptors (GR) during kainic acid (KA) treatment (used to induce SE and associated excitotoxic cell death) significantly reduced the size of the ensuing hippocampal lesion and also significantly reduced cell death in KA-treated neural cell culture cotreated with GCs [44]. The damaging effects of GCs appear to be at least partially dependent on their downregulation of BDNF, as exogenous BDNF also attenuates the *in vitro* cell death. GC induction of proinflammatory pathways (discussed in Section 4) also plays a major role by leading to excitotoxic cell death [45]. Similarly, stress treatment prior to stroke (via the middle cerebral artery occlusion model) increases levels of pro-inflammatory TNF-α and Il-1β, causing more extensive cell death in the infarct [46, 47]

Breakdown of the blood-brain barrier (BBB) is also common across etiological incidents. Research in our lab and in our collaborator's has shown that BBB disruption

allows serum albumin to enter the brain and activate the transforming growth factor beta receptor (TGF-βR) signaling pathway in astrocytes, ultimately inducing epileptiform activity and spontaneous seizures. Blockade of the TGF-βR prevents albumin-induced signaling, epileptiform activity, and reduces seizures detected by EEG monitoring ([48–50] and unpublished data). Interestingly, stress also disrupts the BBB [51–53] and thus may directly contribute to postinjury BBB leakiness, likely through induction of pro-inflammatory pathways [54].

4. Mechanisms by Which Stress May Contribute to Epileptogenesis

Beyond the proximate precipitating incident, the process of epileptogenesis occurs over a period of weeks to years and is marked by a somewhat stereotypical progression of restructuring events that precede the onset of chronic spontaneous seizures [55, 56]. The role of astrocytes in this process has come to be one of the most studied frontiers in epilepsy research, due to the effects of activated astrocytes and gliosis on regulating excitability via extracellular ions and neurotransmitters, and to the association of glial scars with hippocampal sclerosis [57, 58]. Pro-inflammatory cytokine pathways are common mediators of astrocyte activation and epileptogenesis across epilepsy models. For example, albumin activation of the TGF-β pathway in astrocytes leads to the induction of pro-inflammatory and cytokine pathways including NF-κB [48]. Similarly, pilocarpine-induced SE causes an increase in leukocyte adhesion molecules and local leukocyte recruitment, a critical first step in the induction of the pro-inflammatory immune response [59]. In both cases, blockade of this initial pro-inflammatory event prevents subsequent onset of epileptic activity. While GCs are generally thought of as anti-inflammatory, and indeed often used as therapeutic peripheral anti-inflammatory agents, they actually have pro-inflammatory roles within brain [60]. Indeed, stress increases the expression or activity of a number of mediators of inflammation in the brain, including NF-κB, TNF-α, IL-1α, IL-1β, prostaglandins, and free radicals such as NO [45, 61–63] via both catecholamines and GCs [60, 64]. Thus, stress would be expected to enhance pro-inflammatory pathways that are major aspects of epileptogenesis.

Aberrant neurogenesis in the hippocampus is also a hallmark of epileptogenesis [65, 66], including the ectopic migration of new neurons into the hilus. Stress and GCs influence the proliferation, differentiation, and survival of neural stem cells in the hippocampus [67–69]. Generally, stress decreases neurogenesis at both proliferation and survival stages [69], but also decreases the percentage of precursor cells that adopt a neural cell fate (unpublished data). It is unknown how or if stress effects on neurogenesis may interact with aberrant neurogenesis during epileptogenesis.

5. Mechanisms by Which Stress May Exacerbate the Frequency or Severity of Seizures

After the progression of epileptogenesis and the onset of epilepsy, patients experience spontaneous recurrent seizures that vary in frequency and severity. As mentioned in the introduction of this paper, stress is the major self-reported precipitant affecting seizure frequency. In support of these clinical studies, stress pathways have been shown to promote neural activity in a variety of ways, suggesting that stress may directly contribute to the hyperexcitability that causes spontaneous seizures. Corticotropin-releasing hormone (CRH)—which is released in the brain as the first step of the stress hormone response—causes an increase in neural discharge and modulates glutamatergic transmission [70–72]. While CRH acts directly on a variety of neural receptors [71, 73], it also ultimately induces release of GCs from the adrenal glands. GCs themselves increase the release of excitatory glutamate [74], while stress paradigms similarly induce an increase in extracellular glutamate and aspartate [75]. Excitatory actions of GCs can be mediated by fast-acting protein mechanisms [76–78] as well as the classical delayed (transcriptional) effects of GR, which have been shown to modulate calcium currents in particular [79, 80].

6. Complexity in Epileptogenic Pathways and Experimental Implications

We see from the above that stress pathways converge with a variety of other signaling pathways associated with epilepsy, including regulators of excitotoxic cell death, myelination, inflammation, astrocytic activation, and neurogenesis. The nature of this interaction depends on the timing of stress relative to the progression of epilepsy. However, a variety of other variable factors make these pathway interactions quite complex. Firstly, it should be noted that many events associated with epileptogenesis, such as inflammation, gliosis, and neurogenesis, are frequently assumed to be pathological. Equally plausible in many cases is that these pathways may represent (failed) attempts of neuroprotection and recovery. Stress itself is often conceptualized as having an "inverted U-shaped" effect on a given task or output, with extremely low or high amounts of GCs being "detrimental" but moderate amounts being "beneficial." Furthermore, it is widely recognized that the effects of stress may vary depending on task or context. For example, early life stress is detrimental by many metrics, but may also lead to a blunting of inflammatory response that is protective in terms of epilepsy vulnerability [60]. This type of nuanced analysis must be applied when considering the effect of stress on epilepsy (protective and detrimental effects of stress on epilepsy are reviewed in depth by [81]); it would also be well applied to epileptic pathways in themselves. Inflammation, reactive astrocytes, and neurogenesis in particular have been alternately described as protective or pathological. The specific effects of these mechanisms may vary depending on severity of injury (i.e., protective after mild precipitating brain trauma, but overexpressed and damaging after severe brain injury) or on the specific stage of epileptogenesis.

Similarly, it is important to consider that most of these mechanisms are investigated in the context of "strong inference" type experimentation, wherein a specific pathway is genetically or pharmacologically manipulated, and specific

Figure 1: Transcriptional analysis of GC-responsive genes that are modulated by albumin treatment. Arrays from three animals that were sacrificed 24 hours after albumin treatment [48] were reanalyzed to identify genes that are modulated by both stress and the model of albumin-induced epileptogenesis. *Genes mentioned in text.

outputs such as cell death or seizure onset are interpreted as markers of pathology. In taking a step back to a more global view of epilepsy, we emphasize that a large number of molecular mechanisms are in play at any given moment, interacting in complex ways. What is the net output, for example, when pathways known to be neuroprotective, and others known to cause neural damage, are induced at the same time?

To address such complexity in epileptogenic mechanisms, we advocate the use of global analytical tools such as microarrays. While microarrays are frequently used as a discovery tool, they may also be used in a much more targeted fashion to characterize global events surrounding a specific mechanism. For example, we used microarrays to characterize the transcriptional profile that follows albumin binding to TGF-βRs, showing that this proximal event triggers a cascade that is highly similar to TGF-β signaling induced by the endogenous ligand TGF-β1, including a number of pro-inflammatory outputs [48]. Such transcriptional profiles are being gathered for a variety of epilepsy models by the Consortium for Epilepsy Microarray (Raymond Dingledine, personal communication), and used to define the common set of genes that are modulated across different models of epilepsy, as well as clarify interacting mechanisms and beneficial/detrimental effects. To demonstrate the utility of this approach, we reanalyzed our previous array data from rats treated with albumin, focusing on a subset of genes identified as "core GC responsive genes" by the Microarray Consortium (Figure 1). This allowed us to delineate the numerous transcriptional intersections between stress and our epilepsy model. Of particular note, in context of the mechanisms discussed in this paper, is synergistic modulation of pro-inflammatory cytokine pathways by both albumin treatment and GCs, including chemokine (C-C motif) ligand 2 (Ccl2), interleukin-6 (Il6), tumor necrosis factor (Tnf), and interleukin-1 beta (Il1b). We look forward to future use of these microarray resources, which will elucidate the common pathways in various types of epileptogenesis and allow for nuanced analysis of exacerbating risk factors, such as stress.

7. Conclusions

Stress may create vulnerability to epilepsy prior to etiological incidents, as well as exacerbate epileptogenesis following traumatic injury. While potential effects of stress on neural injury are well understood, the ways in which early life stress may create vulnerability for epilepsy, particularly in regard to possible roles for white matter, represent an unknown frontier for future research. While seizures continue to be the defining aspect of epilepsy, nuanced and global analysis of the complex events that occur during epileptogenesis may offer greater insight into the progression of, and possible therapeutic interventions against, epilepsy.

Acknowledgments

The authors thank Raymond Dingledine for providing array data for GC-responsive genes. D. Kaufer is supported by the NIH (R01NS066005), the CURE Foundation, the Binational US-Israel Foundation, and the Mary Elizabeth Rennie Epilepsy Foundation.

References

[1] J. Dionisio and W. O. Tatum, "Triggers and techniques in termination of partial seizures," *Epilepsy and Behavior*, vol. 17, no. 2, pp. 210–214, 2010.

[2] M. M. Frucht, M. Quigg, C. Schwaner, and N. B. Fountain, "Distribution of seizure precipitants among epilepsy syndromes," *Epilepsia*, vol. 41, no. 12, pp. 1534–1539, 2000.

[3] M. R. Sperling, C. A. Schilling, D. Glosser, J. I. Tracy, and A. A. Asadi-Pooya, "Self-perception of seizure precipitants and their relation to anxiety level, depression, and health locus of control in epilepsy," *Seizure*, vol. 17, no. 4, pp. 302–307, 2008.

[4] S. R. Haut, C. B. Hall, J. Masur, and R. B. Lipton, "Seizure occurrence: precipitants and prediction," *Neurology*, vol. 69, no. 20, pp. 1905–1910, 2007.

[5] J. P. Shonkoff, W. T. Boyce, and B. S. McEwen, "Neuroscience, molecular biology, and the childhood roots of health disparities: building a new framework for health promotion and disease prevention," *Journal of the American Medical Association*, vol. 301, no. 21, pp. 2252–2259, 2009.

[6] D. D. Francis, "Conceptualizing child health disparities: a role for developmental neurogenomics," *Pediatrics*, vol. 124, no. 3, supplement, pp. S196–S202, 2009.

[7] B. S. McEwen, "Understanding the potency of stressful early life experiences on brain and body function," *Metabolism*, vol. 57, no. 2, pp. S11–S15, 2008.

[8] B. S. McEwen, "Physiology and neurobiology of stress and adaptation: central role of the brain," *Physiological Reviews*, vol. 87, no. 3, pp. 873–904, 2007.

[9] B. S. McEwen, "Stress, sex, and neural adaptation to a changing environment: mechanisms of neuronal remodeling," *Annals of the New York Academy of Sciences*, vol. 1204, supplement, pp. E38–E59, 2010.

[10] C. F. Gillespie, J. Phifer, B. Bradley, and K. J. Ressler, "Risk and resilience: genetic and environmental influences on development of the stress response," *Depression and Anxiety*, vol. 26, no. 11, pp. 984–992, 2009.

[11] D. Francis, J. Diorio, D. Liu, and M. J. Meaney, "Nongenomic transmission across generations of maternal behavior and stress responses in the rat," *Science*, vol. 286, no. 5442, pp. 1155–1158, 1999.

[12] M. J. Meaney, J. Diorio, D. Francis et al., "Early environmental regulation of forebrain glucocorticoid receptor gene expression: implications for adrenocortical responses to stress," *Developmental Neuroscience*, vol. 18, no. 1-2, pp. 49–72, 1996.

[13] D. L. Bellinger, C. Lubahn, and D. Lorton, "Maternal and early life stress effects on immune function: relevance to immunotoxicology," *Journal of Immunotoxicology*, vol. 5, no. 4, pp. 419–444, 2008.

[14] A. Danese, C. M. Pariante, A. Caspi, A. Taylor, and R. Poulton, "Childhood maltreatment predicts adult inflammation in a life-course study," *Proceedings of the National Academy of Sciences of the United States of America*, vol. 104, no. 4, pp. 1319–1324, 2007.

[15] N. Bazak, N. Kozlovsky, Z. Kaplan et al., "Pre-pubertal stress exposure affects adult behavioral response in association with changes in circulating corticosterone and brain-derived neurotrophic factor," *Psychoneuroendocrinology*, vol. 34, no. 6, pp. 844–858, 2009.

[16] M. Lippmann, A. Bress, C. B. Nemeroff, P. M. Plotsky, and L. M. Monteggia, "Long-term behavioural and molecular alterations associated with maternal separation in rats," *European Journal of Neuroscience*, vol. 25, no. 10, pp. 3091–3098, 2007.

[17] T. L. Roth, F. D. Lubin, A. J. Funk, and J. D. Sweatt, "Lasting Epigenetic Influence of Early-Life Adversity on the BDNF Gene," *Biological Psychiatry*, vol. 65, no. 9, pp. 760–769, 2009.

[18] A. M. Karssen, S. Her, J. Z. Li et al., "Stress-induced changes in primate prefrontal profiles of gene expression," *Molecular Psychiatry*, vol. 12, no. 12, pp. 1089–1102, 2007.

[19] B. A. Barres, M. A. Lazar, and M. C. Raff, "A novel role for thyroid hormone, glucocorticoids and retinoic acid in timing oligodendrocyte development," *Development*, vol. 120, no. 5, pp. 1097–1108, 1994.

[20] R. P. Gobert, L. Joubert, M. L. Curchod et al., "Convergent functional genomics of oligodendrocyte differentiation identifies multiple autoinhibitory signaling circuits," *Molecular and Cellular Biology*, vol. 29, no. 6, pp. 1538–1553, 2009.

[21] L. Joubert, I. Foucault, Y. Sagot et al., "Chemical inducers and transcriptional markers of oligodendrocyte differentiation," *Journal of Neuroscience Research*, vol. 88, no. 12, pp. 2546–2557, 2010.

[22] S. A. Mann, B. Versmold, R. Marx et al., "Corticosteroids reverse cytokine-induced block of survival and differentiation of oligodendrocyte progenitor cells from rats," *Journal of Neuroinflammation*, vol. 5, article no. 39, 2008.

[23] J. S. Meyer and K. R. Fairman, "Early adrenalectomy increases myelin content of the rat brain," *Brain Research*, vol. 349, no. 1-2, pp. 1–9, 1985.

[24] W. L. Huang, C. G. Harper, S. F. Evans, J. P. Newnham, and S. A. Dunlop, "Repeated prenatal corticosteroid administration delays myelination of the corpus callosum in fetal sheep," *International Journal of Developmental Neuroscience*, vol. 19, no. 4, pp. 415–425, 2001.

[25] S. Saltik, N. Kocer, and A. Dervent, "Magnetic resonance imaging findings in infantile spasms: etiologic and pathophysiologic aspects," *Journal of Child Neurology*, vol. 18, no. 4, pp. 241–246, 2003.

[26] L. B. Jardim, R. F. Pires, C. E. Martins et al., "Pyridoxine-Dependent seizures associated with white matter abnormalities," *Neuropediatrics*, vol. 25, no. 5, pp. 259–261, 1994.

[27] J. Silva, S. Sharma, B. Hughes, Y. E. Yu, and J. K. Cowell, "Homozygous inactivation of the Lgi1 gene results in hypomyelination in the peripheral and central nervous systems," *Journal of Neuroscience Research*, vol. 88, no. 15, pp. 3328–3336, 2010.

[28] Y. E. Yu, L. Wen, J. Silva et al., "Lgi1 null mutant mice exhibit myoclonic seizures and CA1 neuronal hyperexcitability," *Human Molecular Genetics*, vol. 19, no. 9, pp. 1702–1711, 2010.

[29] T. J. De Koning, M. Duran, L. Van Maldergem et al., "Congenital microcephaly and seizures due to 3-phosphoglycerate dehydrogenase deficiency: outcome of treatment with amino acids," *Journal of Inherited Metabolic Disease*, vol. 25, no. 2, pp. 119–125, 2002.

[30] T. J. de Koning, J. Jaeken, M. Pineda, L. Van Maldergem, B. T. Poll-The, and M. S. Van der Knaap, "Hypomyelination and reversible white matter attenuation in 3-phosphoglycerate dehydrogenase deficiency," *Neuropediatrics*, vol. 31, no. 6, pp. 287–292, 2000.

[31] A. G. Chapman, E. Westerberg, M. Premachandra, and B. S. Meldrum, "Changes in regional neurotransmitter amino acid levels in rat brain during seizures induced by L-allylglycine, bicuculline, and kainic acid," *Journal of Neurochemistry*, vol. 43, no. 1, pp. 62–70, 1984.

[32] S. Meier, A. U. Bräuer, B. Heimrich, R. Nitsch, and N. E. Savaskan, "Myelination in the hippocampus during development and following lesion," *Cellular and Molecular Life Sciences*, vol. 61, no. 9, pp. 1082–1094, 2004.

[33] C. Kendal, I. Everall, C. Polkey, and S. Al-Sarraj, "Glial cell changes in the white matter in temporal lobe epilepsy," *Epilepsy Research*, vol. 36, no. 1, pp. 43–51, 1999.

[34] E. Hutchinson, D. Pulsipher, K. Dabbs et al., "Children with new-onset epilepsy exhibit diffusion abnormalities in cerebral white matter in the absence of volumetric differences," *Epilepsy Research*, vol. 88, no. 2-3, pp. 208–214, 2010.

[35] T. Wang, L. Jia, B. Lv et al., "Human Ermin (hErmin), a new oligodendrocyte-specific cytoskeletal protein related to epileptic seizure," *Brain Research*, vol. 1367, pp. 77–84, 2011.

[36] L. A. Mitchell, A. S. Harvey, L. T. Coleman, S. A. Mandelstam, and G. D. Jackson, "Anterior temporal changes on MR images of children with hippocampal sclerosis: an effect of seizures on the immature brain?" *American Journal of Neuroradiology*, vol. 24, no. 8, pp. 1670–1677, 2003.

[37] M. C. Lai, C. C. Lui, S. N. Yang, J. Y. Wang, and L. T. Huang, "Epileptogenesis is increased in rats with neonatal isolation and early-life seizure and ameliorated by MK-801: a long-term MRI and histological study," *Pediatric Research*, vol. 66, no. 4, pp. 441–447, 2009.

[38] N. C. Jones, G. Kumar, T. J. O'Brien, M. J. Morris, S. M. Rees, and M. R. Salzberg, "Anxiolytic effects of rapid amygdala kindling, and the influence of early life experience in rats," *Behavioural Brain Research*, vol. 203, no. 1, pp. 81–87, 2009.

[39] M. Salzberg, G. Kumar, L. Supit et al., "Early postnatal stress confers enduring vulnerability to limbic epileptogenesisy," *Epilepsia*, vol. 48, no. 11, pp. 2079–2085, 2007.

[40] C. A. Frye, "Effects and mechanisms of progestogens and androgens in ictal activity," *Epilepsia*, vol. 51, supplement 3, pp. 135–140, 2010.

[41] H. E. Scharfman and N. J. MacLusky, "The influence of gonadal hormones on neuronal excitability, seizures, and epilepsy in the female," *Epilepsia*, vol. 47, no. 9, pp. 1423–1440, 2006.

[42] G. J. Ter Horst, R. Wichmann, M. Gerrits, C. Westenbroek, and Y. Lin, "Sex differences in stress responses: focus on ovarian hormones," *Physiology and Behavior*, vol. 97, no. 2, pp. 239–249, 2009.

[43] T. R. Taher, M. Salzberg, M. J. Morris, S. Rees, and T. J. O'Brien, "Chronic low-dose corticosterone supplementation enhances acquired epileptogenesis in the rat amygdala kindling model of TLE," *Neuropsychopharmacology*, vol. 30, no. 9, pp. 1610–1616, 2005.

[44] D. Kaufer, W. O. Ogle, Z. S. Pincus et al., "Restructuring the neuronal stress response with anti-glucocorticoid gene delivery," *Nature Neuroscience*, vol. 7, no. 9, pp. 947–953, 2004.

[45] K. Dinkel, A. MacPherson, and R. M. Sapolsky, "Novel glucocorticoid effects on acute inflammation in the CNS," *Journal of Neurochemistry*, vol. 84, no. 4, pp. 705–716, 2003.

[46] J. R. Caso, I. Lizasoain, P. Lorenzo, M. A. Moro, and J. C. Leza, "The role of tumor necrosis factor-alpha in stress-induced worsening of cerebral ischemia in rats," *Neuroscience*, vol. 142, no. 1, pp. 59–69, 2006.

[47] J. R. Caso, M. A. Moro, P. Lorenzo, I. Lizasoain, and J. C. Leza, "Involvement of IL-1β in acute stress-induced worsening of cerebral ischaemia in rats," *European Neuropsychopharmacology*, vol. 17, no. 9, pp. 600–607, 2007.

[48] L. P. Cacheaux, S. Ivens, Y. David et al., "Transcriptome profiling reveals TGF-β signaling involvement in epileptogenesis," *Journal of Neuroscience*, vol. 29, no. 28, pp. 8927–8935, 2009.

[49] Y. David, L. P. Cacheaux, S. Ivens et al., "Astrocytic dysfunction in epileptogenesis: consequence of altered potassium and glutamate homeostasis?" *Journal of Neuroscience*, vol. 29, no. 34, pp. 10588–10599, 2009.

[50] S. Ivens, D. Kaufer, L. P. Flores et al., "TGF-β receptor-mediated albumin uptake into astrocytes is involved in neocortical epileptogenesis," *Brain*, vol. 130, no. 2, pp. 535–547, 2007.

[51] H. S. Sharma, J. Cervos-Navarro, and P. K. Dey, "Increased blood-brain barrier permeability following acute short-term swimming exercise in conscious normotensive young rats," *Neuroscience Research*, vol. 10, no. 3, pp. 211–221, 1991.

[52] D. Shlosberg, M. Benifla, D. Kaufer, and A. Friedman, "Blood-brain barrier breakdown as a therapeutic target in traumatic brain injury," *Nature Reviews Neurology*, vol. 6, pp. 393–403, 2010.

[53] A. Friedman, D. Kaufer, J. Shemer, I. Hendler, H. Soreq, and I. Tur-Kaspa, "Pyridostigmine brain penetration under stress enhances neuronal excitability and induces early immediate transcriptional response," *Nature Medicine*, vol. 2, no. 12, pp. 1382–1385, 1996.

[54] P. Esposito, D. Gheorghe, K. Kandere et al., "Acute stress increases permeability of the blood-brain-barrier through activation of brain mast cells," *Brain Research*, vol. 888, no. 1, pp. 117–127, 2001.

[55] F. E. Dudek and T. P. Sutula, "Epileptogenesis in the dentate gyrus: a critical perspective," *Progress in Brain Research*, vol. 163, pp. 755–773, 2007.

[56] N. C. de Lanerolle and T. S. Lee, "New facets of the neuropathology and molecular profile of human temporal lobe epilepsy," *Epilepsy and Behavior*, vol. 7, no. 2, pp. 190–203, 2005.

[57] G. Seifert, G. Carmignoto, and C. Steinhäuser, "Astrocyte dysfunction in epilepsy," *Brain Research Reviews*, vol. 63, no. 1-2, pp. 212–221, 2010.

[58] N. C. de Lanerolle, T. S. Lee, and D. D. Spencer, "Astrocytes and epilepsy," *Neurotherapeutics*, vol. 7, pp. 424–438, 2010.

[59] P. F. Fabene, G. N. Mora, M. Martinello et al., "A role for leukocyte-endothelial adhesion mechanisms in epilepsy," *Nature Medicine*, vol. 14, no. 12, pp. 1377–1383, 2008.

[60] S. F. Sorrells, J. R. Caso, C. D. Munhoz, and R. M. Sapolsky, "The stressed CNS: when glucocorticoids aggravate inflammation," *Neuron*, vol. 64, no. 1, pp. 33–39, 2009.

[61] J. L. M. Madrigal, O. Hurtado, M. A. Moro et al., "The increase in TNF-α levels is implicated in NF-κB activation and inducible nitric oxide synthase expression in brain cortex after immobilization stress," *Neuropsychopharmacology*, vol. 26, no. 2, pp. 155–163, 2002.

[62] J. L.M. Madrigal, M. A. Moro, I. Lizasoain et al., "Inducible nitric oxide synthase expression in brain cortex after acute restraint stress is regulated by nuclear factor κB-mediated mechanisms," *Journal of Neurochemistry*, vol. 76, no. 2, pp. 532–538, 2001.

[63] J. L. M. Madrigal, M. A. Moro, I. Lizasoain et al., "Induction of cyclooxygenase-2 accounts for restraint stress-induced oxidative status in rat brain," *Neuropsychopharmacology*, vol. 28, no. 9, pp. 1579–1588, 2003.

[64] B. García-Bueno, J. L. M. Madrigal, B. G. Pérez-Nievas, and J. C. Leza, "Stress mediators regulate brain prostaglandin synthesis and peroxisome proliferator-activated receptor-γ activation after stress in rats," *Endocrinology*, vol. 149, no. 4, pp. 1969–1978, 2008.

[65] R. Kuruba, B. Hattiangady, and A. K. Shetty, "Hippocampal neurogenesis and neural stem cells in temporal lobe epilepsy," *Epilepsy and Behavior*, vol. 14, no. 1, supplement, pp. 65–73, 2009.

[66] H. E. Scharfman and D. P. McCloskey, "Postnatal neurogenesis as a therapeutic target in temporal lobe epilepsy," *Epilepsy Research*, vol. 85, no. 2-3, pp. 150–161, 2009.

[67] M. Joëls, "Role of corticosteroid hormones in the dentate gyrus," *Progress in Brain Research*, vol. 163, pp. 355–370, 2007.

[68] D. T. Balu and I. Lucki, "Adult hippocampal neurogenesis: regulation, functional implications, and contribution to disease pathology," *Neuroscience and Biobehavioral Reviews*, vol. 33, no. 3, pp. 232–252, 2009.

[69] C. Mirescu and E. Gould, "Stress and adult neurogenesis," *Hippocampus*, vol. 16, no. 3, pp. 233–238, 2006.

[70] J. B. Aldenhoff, D. L. Gruol, and J. Rivier, "Corticotropin releasing factor decreases postburst hyperpolarizations and excites hippocampal neurons," *Science*, vol. 221, no. 4613, pp. 875–877, 1983.

[71] J. Liu, B. Yu, V. Neugebauer et al., "Corticotropin-releasing factor and urocortin I modulate excitatory glutamatergic synaptic transmission," *Journal of Neuroscience*, vol. 24, no. 16, pp. 4020–4029, 2004.

[72] G. S. Hollrigel, K. Chen, T. Z. Baram, and I. Soltesz, "The proconvulsant actions of corticotropin-releasing hormone in the hippocampus of infant rats," *Neuroscience*, vol. 84, no. 1, pp. 71–79, 1998.

[73] B. Roozendaal, G. Schelling, and J. L. McGaugh, "Corticotropin-releasing factor in the basolateral amygdala enhances memory consolidation via an interaction with the β-adrenoceptor-cAMP pathway: dependence on glucocorticoid receptor activation," *Journal of Neuroscience*, vol. 28, no. 26, pp. 6642–6651, 2008.

[74] B. Moghaddam, M. L. Bolinao, B. Stein-Behrens, and R. Sapolsky, "Glucocorticoids mediate the stress-induced extracellular accumulation of glutamate," *Brain Research*, vol. 655, no. 1-2, pp. 251–254, 1994.

[75] B. Moghaddam, "Stress preferentially increases extraneuronal levels of excitatory amino acids in the prefrontal cortex: comparison to hippocampus and basal ganglia," *Journal of Neurochemistry*, vol. 60, no. 5, pp. 1650–1657, 1993.

[76] E. R. de Kloet, H. Karst, and M. Joëls, "Corticosteroid hormones in the central stress response: quick-and-slow," *Frontiers in Neuroendocrinology*, vol. 29, no. 2, pp. 268–272, 2008.

[77] H. Karst, S. Berger, M. Turiault, F. Tronche, G. Schütz, and M. Joëls, "Mineralocorticoid receptors are indispensable for nongenomic modulation of hippocampal glutamate transmission by corticosterone," *Proceedings of the National Academy of Sciences of the United States of America*, vol. 102, no. 52, pp. 19204–19207, 2005.

[78] H. Karst and M. Joëls, "Corticosterone slowly enhances miniature excitatory postsynaptic current amplitude in mice CA1 hippocampal cells," *Journal of Neurophysiology*, vol. 94, no. 5, pp. 3479–3486, 2005.

[79] D. S. Kerr, L. W. Campbell, O. Thibault, and P. W. Landfield, "Hippocampal glucocorticoid receptor activation enhances voltage-dependent Ca conductances: relevance to brain aging," *Proceedings of the National Academy of Sciences of the United States of America*, vol. 89, no. 18, pp. 8527–8531, 1992.

[80] P. Chameau, Y. Qin, S. Spijker, G. Smit, and M. Joëls, "Glucocorticoids specifically enhance L-type calcium current amplitude and affect calcium channel subunit expression in the mouse hippocampus," *Journal of Neurophysiology*, vol. 97, no. 1, pp. 5–14, 2007.

[81] M. Joëls, "Stress, the hippocampus, and epilepsy," *Epilepsia*, vol. 50, no. 4, pp. 586–597, 2009.

Hindawi Publishing Corporation
Cardiovascular Psychiatry and Neurology
Volume 2011, Article ID 609202, 10 pages
doi:10.1155/2011/609202

Review Article

Vascular Pathology and Blood-Brain Barrier Disruption in Cognitive and Psychiatric Complications of Type 2 Diabetes Mellitus

Yonatan Serlin,[1] Jaime Levy,[2] and Hadar Shalev[3]

[1] *Department of Physiology and Neurobiology, Faculty of Health Sciences, Ben-Gurion University of the Negev, Beer-Sheva 84105, Israel*
[2] *Department of Ophthalmology, Soroka University Medical Center, Ben-Gurion University of the Negev, Beer Sheva 84105, Israel*
[3] *Department of Psychiatry, Soroka University Medical Center, Ben-Gurion University of the Negev, Beer-Sheva 84105, Israel*

Correspondence should be addressed to Hadar Shalev, shalev@bgu.ac.il

Received 20 October 2010; Accepted 28 December 2010

Academic Editor: Daniela Kaufer

Vascular pathology is recognized as a principle insult in type 2 diabetes mellitus (T2DM). Co-morbidities such as structural brain abnormalities, cognitive, learning and memory deficits are also prevailing in T2DM patients. We previously suggested that microvascular pathologies involving blood-brain barrier (BBB) breakdown results in leakage of serum-derived components into the brain parenchyma, leading to neuronal dysfunction manifested as psychiatric illnesses. The current postulate focuses on the molecular mechanisms controlling BBB permeability in T2DM, as key contributors to the pathogenesis of mental disorders in patients. Revealing the mechanisms underlying BBB dysfunction and inflammatory response in T2DM and their role in metabolic disturbances, abnormal neurovascular coupling and neuronal plasticity, would contribute to the understanding of the mechanisms underlying psychopathologies in diabetic patients. Establishing this link would offer new targets for future therapeutic interventions.

1. Introduction: The Vascular Hypothesis

Macro- and microvascular complications involving endothelial dysfunction are central to the pathogenesis and clinical manifestations of type 2 diabetes mellitus (T2DM) [1]. Structural brain abnormalities [2–7] and cognitive, learning and memory deficits were demonstrated in T2DM patients [8–10]. We recently published a hypothesis paper suggesting that a primary vascular pathology involving inflammatory cascade and Blood-Brain Barrier (BBB) breakdown, will result in the leakage of serum-derived vascular components into the brain tissue and may cause brain dysfunction which, under some conditions (extent, duration, and/or location), will result in disturbed thinking processes, mood, and behavior, such as those characterizing psychiatric illnesses [11]. The current postulate focuses on inflammation and molecular mechanisms controlling BBB permeability in T2DM as key contributors to the pathogenesis of mental disorders in diabetic patients and suggests novel targets for the prevention and treatment of cognitive and psychiatric complications.

2. Type 2 Diabetes Mellitus and Vascular Pathology

T2DM is a multifactorial metabolic disorder. The underlying etiology, pathophysiology and complications of diabetes are still being elucidated (for review see [12]). T2DM is characterized by chronic abnormal high blood glucose levels (hyperglycemia), insulin resistance, and a relative insulin secretion defect [13]. Induction of insulin resistance is linked to obesity and activation of neuroendocrine and inflammatory responses [14–16]. Approximately 200 million people worldwide have diabetes and it is estimated that without proper measures to slow the epidemic advance of the disease, by 2025 the number of patients will increase to 333 million [17]. T2DM is recognized as an independent risk

factor for cardiovascular disease (CVD), presenting increased risk of morbidity and mortality from coronary heart disease, congestive heart failure, and stroke [18]. Accumulating clinical data disclose the central role of vascular lesions and inflammation in the pathogenesis of T2DM and associated complications [19]. Diabetic macrovascular complications involve vessel obstructions, such as coronary artery diseases, atherosclerosis, and peripheral vascular diseases. Microvascular pathologies include retinopathy, nephropathy, and neuropathy [20]. Direct damage to small blood vessels, particularly by hyperglycemia, is manifested by endothelial dysfunction, diminished perfusion, abnormal endothelial cell (EC) proliferation and increased vessels permeability [21]. T2DM patients exhibit similar microvascular damage within the central nervous system (CNS) which may result in increased incidence of cognitive deterioration, vascular dementia, lacunar infarcts, hemorrhages and Alzheimer's disease [22].

3. Structure and Function of the Blood-Brain Barrier and Quantification of Its Disruption

First evidences for a barrier preventing the passage of water-soluble dyes from the circulation to the brain tissue and the spinal cord were presented consecutively by Ehrlich, Goldmann and Lewandowsky in the beginning of the 20th century [23]. At the interfaces between the blood and the neural tissue or its fluid spaces exist three barrier layers: (1) the BBB present in the capillaries throughout the brain, formed by highly specialized EC partitioning between the blood and brain interstitial fluid, (2) the choroid plexus epithelium between blood and ventricular cerebrospinal fluid (CSF), and (3) the arachnoid epithelium between the blood and subarachnoid CSF [24]. The BBB components include the EC with their basement membrane, lining the lumen of brain capillaries. EC adjoined by specific protein tight junctions (e.g., claudins, occludins, ZO-1, ZO-2, ZO-3 and cingulin) and display specific transport mechanisms and pinocytic vesicles (for review see [25]). The endothelium is enclosed by brain pericytes and astroglial foot processes which form a third continuous layer that separates these blood vessels from the brain tissue. Jointly, these components form a barrier that hinders the entry of most molecules into the brain, and enable active transportation of penetrated molecules out of the brain. Common brain imaging methods, such as magnetic resonance imaging (MRI), computerized tomography (CT), and single photon emission CT (SPECT) are employed for qualitative evaluation of BBB disruption in patients. Extravascular accumulation of a peripherally administrated nonpermeable contrast agents, indicate BBB breakdown [11]. Several methods for quantification of BBB permeability using dynamic contrast enhanced imaging were developed, although a routine clinical examination is not yet available [26–28]. In the clinical setting, quantitative evaluation of BBB disruption can be held by CSF analysis for serum proteins (e.g., albumin) or plasma analysis of brain constituents (e.g., S100B-brain-specific astrocytic calcium-binding protein) [29].

4. Mechanisms of BBB Breakdown

BBB integrity is altered in diverse pathological conditions. Changes are manifested by disruption of junctional components which result in transbarrier leakage, and BBB activation, which relates to the expression and secretion of immune factors by its cellular components. The underlying molecular changes leading to BBB dysfunction are not completely clear, but may involve amplification of endothelial caveolae leading to transcytosis of plasma proteins [30, 31], decreased expression of junctional adhesion as well as tight junction proteins [32, 33], and increased expression of matrix metalloproteases [34]. Reactive cellular activity in the neurovascular junction has also been observed, including increase in migratory activity of pericytes [35] and the proliferation of blood vessels due to upregulation of vascular endothelial growth factor (VEGF) [36]. BBB opening itself leads to the exposure of the brain tissue to serum-derived (normally nonpermeable) molecules, which serve as signaling mediators for brain repair mechanisms but may also facilitate BBB breakdown. Agents released during inflammation aggravate the penetrability of the brain endothelium. EC bradykinin B2 receptors activation lead to an increase in intracellular $Ca2^{+}$ concentrations [37] and subsequently to activation of endothelial nitric oxide synthase (eNOS) which promotes transient tight junctions opening and increased permeability [38]. Furthermore, bradykinin can activate NF-κB pathway in astrocytes, leading to the release of interleukin-6 (IL-6), which can amplify the effect by acting back on the endothelium [39]. Tumor necrosis factor-α (TNFα) increases BBB permeability by direct action on the endothelium [40] and indirectly via endothelin-1 production and IL-1β release from astrocytes [41]. Mediators released from central and peripheral cellular components and connective tissue following injury, can also affect BBB permeability. For example, histamine and TNFα and interferon-γ released in inflammatory pain can alter brain endothelial permeability [42]. IL-1β release may lead to a decreased concentration or altered localization of the tight junction protein occludin, and thus increases BBB permeability. Metalloproteases causing BBB breakdown are upregulated and released during spreading neuronal depolarization after massive neuronal activation [43].

5. Blood-Brain Barrier Breakdown in Diabetes Mellitus

5.1. Anatomical Changes. Altered BBB structure in diabetic patients is a matter of debate. Several studies have indicated that the BBB integrity is sustained in DM, while others revealed association between DM and increased BBB permeability. Intravital microscopy examination of BBB integrity in diabetic rats using fluorescent-labeled albumin displayed intact BBB [44]. These findings should be interpreted with caution since intravital microscopy for quantification of ligands extravasations through the BBB is often complicated and not specific [45]. Postmortem examination of prefrontal and temporal cortex of diabetic patients together

with immunohistochemical stainings against serum proteins concluded that the BBB is well maintained [46]. In contrast, growing body of evidence propose an opposing notion. Animal models of ischemic injury in diabetic rats demonstrated that hyperglycemia significantly aggravated BBB permeability, edema formation, and neurological manifestations [47, 48]. BBB breakdown after ischemia/reperfusion injury result in extravasation of inflammatory cells and fluid into the brain tissue, and thus suggest that BBB disruption has important role in the pathogenesis of brain damage associated with systemic hyperglycemia. MRI brain imaging following intravenous gadolinium administration identified increased BBB permeability in diabetic patients compared to controls [49]. Antibodies against serum S100B and NSE (CNS proteins) were found to be significantly increased in both type 1 and type 2 diabetic subjects compared to controls, implying that diabetes in humans may be associated with alterations in the integrity of the BBB [50].

5.2. Metabolic Changes. Normal metabolic activity of neural tissue relies on constant glucose delivery. Due to the high metabolic demands, glucose transport from the blood across the BBB into the cells of the brain is mediated by rapid facilitated transport. Glucose transporter proteins (GLUT), particularly GLUT1 and GLUT3 ensure glucose supply. GLUT1 protein is highly expressed at the BBB and GLUT3 is primarily found in neurons. GLUT1 expression is controlled by blood glucose levels, to maintain sufficient distribution for optimal neuronal function [51]. In diabetes, imbalance of glucose metabolism, lead to alterations of glucose transport into the brain. Pardrdige et al. (1990) [52] showed a decrease in GLUT1 expression and activity in diabetic rats thus leading to reduced glucose transport in uncontrolled diabetes. Studies focused on chronic hyperglycemia and increased vascular damage showed that abnormal glucose metabolism results in generation of reactive oxygen species (ROS) followed by oxidative stress, mitochondrial dysfunction and inflammatory response [53, 54]. Hyperglycemia is presumed to play a role in the generation of acute phase proteins and inflammatory response [55]. It correlates with data about reduction of the levels of acute-phase serum proteins by treatments that increase insulin sensitivity and lower blood glucose [56].

5.3. Inflammatory Mechanism: From Diabetic Retinopathy to Brain Pathology

5.3.1. Inflammatory Mechanisms. Inflammatory mechanisms underlying vascular pathology in DM are possibly common to the vasculature in the periphery and CNS. Formation of advanced glycation end products (AGEs) via glycation of blood proteins is a consequence of hyperglycemia, and it results in decreased kidney function and small vessels pathology. AGEs accumulation may induce vascular inflammation by the interactions between AGEs and AGE-specific receptors (RAGE) [57]. AGEs activation of endothelial RAGE promotes upregulation of endothelial adhesion molecules including vascular cell adhesion molecule 1 (VCAM-1) and activates transcription factor nuclear factor-κB (NFκB). The former increases monocyte adhesiveness and vascular permeability while the latter regulates multiple proinflammatory and proatherosclerotic target genes in endothelial and vascular smooth muscle cells as well as in macrophages [58].

5.3.2. Diabetic Retinopathy. Well-established data about retinal vessels pathology in DM is available. Due to the structural similarities between the BBB and the blood-retinal barrier (BRB) and the fact that disruption of the BRB in diabetes is associated with retinopathy, it is logical to assume that altered BBB function in DM patients may also result in brain pathology. Chronic hyperglycemia, hyperlipidemia, and hypertension contribute to the pathogenesis of Diabetic Retinopathy (DR) [59–61]. Diabetic macular edema (DME) found in 29% of patients who had diabetes for $\geq$20 years [62] and is caused by increased level of mediators responsible for retinal vascular permeability as IL-6 and VEGF. These factors promote leakage of intravascular fluid from retinal capillaries into retinal spaces [63]. Further damage arises from retinal EC exposure to AGEs leading to abnormal eNOS expression [64] and induction of VEGF expression [65]. Diabetes may also involve altered retinal blood flow as an outcome of the damage to pericytes enclosing the BRB [66, 67] and correlates with microaneurysm formation. Capillary nonperfusion, EC damage, and vessel occlusions contribute to the retinal microcirculation damage [68]. Capillary occlusion by leukostasis, adherence to the vascular endothelium and cellular degeneration lead to retinal ischemia that stimulates pathologic neovascularization mediated by angiogenic factors (e.g., VEGF) which enhance BRB permeability and result in proliferative diabetic retinopathy (PDR) [69, 70]. During the last years, anti-VEGF drugs, such as ranibizumab (Lucentis) and bevacizumab (Avastin) are injected into the vitreous for the treatment of diabetic macular edema.

5.3.3. BRB Examination as a Window for BBB Condition. As previously described, the vascular hypothesis speculates that BBB disintegration may be involved in the pathogenesis of brain diseases. Diabetes-induced microangiopathy of the kidney and retina are well described in the literature. The detailed pathogenesis of microvascular damage within the CNS is less known, since altered functions of cerebral vessels is concealed and less predictable, while in other tissues vascular impairments are detectable and obvious [71]. The analogy between the BBB and the BRB is the platform for conceptualization that retinal vessels examination can provide a tool for estimation of cerebral vessels status. In the clinical setting, investigation and documentation of the BRB integrity are held routinely in T2DM patients. Ophthalmic fluorescein angiography (FA) includes intravenously administration of fluorescein producing angiographic display that is used to visualize retinal blood flow dynamics while recording the integrity of the BRB. Correlation between FA results and BBB permeability measures utilizing dynamic contrast enhanced imaging (e.g., [26, 72]) is thus essential, in order to point out the mutual relation between the two systems. An important feature should be the ability to quantify BRB

leakage in T2DM patients, and novel imaging methods can be implemented [73]. Future perspectives should focus on developing novel applicable tool for prediction of BBB breakdown via BRB image analysis. A similar conclusion was published recently, following the results of a prospective study using MRI examination and retinal imaging [74]. It has been shown that retinal microvascular abnormalities are associated with emergence of subclinical brain infarcts and white matter lesions, and proposed that retinal vascular imaging may offer a noninvasive tool to investigate cerebral small-vessel disease.

6. Blood-Brain Barrier Breakdown in Psychiatric Diseases

There are evidences linking psychiatric illness with BBB alterations. Quantitative evaluation of BBB disruption utilizes CSF analysis for presence of serum proteins leaked through a permeable barrier, or plasma analysis for molecules found exclusively in the brain (as S100B). Similarly, increase in plasma levels of S100B may reflect increased BBB permeability [29]. CSF/serum albumin ratio was elevated in patients suffering from dementias, in comparison to nondemented individuals [75] and in elderly depressed women compared to women without depression [76]. BBB dysfunction was also shown in schizophrenic patients by measuring increased albumin and IgG CSF levels, with additional correlation between the negative symptomatology to CSF/serum albumin ratio [77, 78]. Bell and Zlokovic (2009) recently reviewed the knowledge about the relation between cerebrovascular dysfunction as BBB disruption and neurovascular uncoupling, to cognitive decline and neurodegenerative changes of Alzheimer's disease [79]. Clinical studies demonstrated increased S100B levels in the serum of patients suffering from acute or chronic schizophrenia [80]. Same serum S100B elevation was observed in patients with major depression, with decrease in serum S100B levels during clinical improvement after antidepressant treatment [81].

7. Comorbidity between Diabetes Mellitus and Psychiatric Disorders

Among DM patients there is a significant and consistent association with presence of elevated depressive symptoms and the prevalence of major depression, compared with the general population [82–85]. Recently published data shows that higher A1C levels are associated with lower cognitive function in individuals with diabetes [86]. Accumulating evidence [9, 10] indicates that in diabetic patients, hyperglycemia and diabetes durations contribute to brain atrophy and increases the risk of cognitive impairment. Increased expression of RAGE in Alzheimer's disease brain, indicates its relevancy in the pathogenesis of neuronal dysfunction and death [87]. Postmortem studies of individuals with Alzheimer's disease attributes to this opinion by demonstrating AGEs within the senile plaques [88, 89]. Indeed, studies suggest that T2DM is associated with an increased risk of Alzheimer disease, vascular dementia and risk for development of cognitive impairment in comparison with the general population [90–92]. Anxiety disorders were also found in high prevalence in diabetic population [93, 94].

8. Inflammation and Psychopathology

Inflammatory processes are central to the pathogenesis of T2DM and contribute to BBB dysfunction. Apart from the pathogenic role of the immune responses, accumulating data indicates that immunologic responses also play a role in depression, neurodegeneration, and deficits in cognitive function. Evidence of an inflammatory response in major depression is present over the last two decades [95]. Recent meta-analysis of 24 studies reinforced the notion about cytokine involvement in depression through activation of the inflammatory response [96]. A thorough review by Maes et al. (2009) [97] elaborates the involvement of inflammatory pathways in depression. Increase in proinflammatory cytokines, such as IL-1β, IL-6, interferon-γ and TNFα, with a relative shortage in the anti-inflammatory cytokine IL-10 was documented in depression. Cytokines produced in the periphery and by neurons and glial cells within the CNS are presumed to be involved in the complex autonomic, neuroendocrine, metabolic and behavioral responses to brain injuries as inflammation, ischemia and stroke [98–100]. As mentioned previously, in T2DM, inflammation of adipose tissue contributes to insulin resistance. Activated macrophages in the adipose tissue are the primary cellular source of proinflammatory cytokines as IL-1β, TNF-α and IL-6. These mediators provide additional links between the participation of immune reaction in T2DM and the brain response. In brain regions lacking intact BBB (i.e., circumventricular organs), cytokines leakage from the blood into the brain parenchyma may lead to activation of macrophages and induction of a proinflammatory cascade. Additionally, without crossing the BBB, cytokines are able to interact with perivascular macrophages (reviewed by [101]). Clinical data from patients with major depression demonstrate increase of inflammatory features among them [102]. Studies pointing out the existence of positive correlations between plasma concentrations of inflammatory mediators and the severity of depressive symptoms are also available [103, 104]. Proinflammatory response induces decreased neurogenesis in depression, which is characterized by decreased brain-derived neurotrophic factor (BDNF), neural cell adhesion molecule (NCAM) and fibroblast growth factor (FGF) [105–107]. Inflammation stimulates release or production of corticotropin releasing hormone (CRF), adrenocorticotropic hormone (ACTH) and cortisol via activation of the hypothalamic-pituitary-adrenal axis (HPA) and cortisol in turn may participate in neural atrophy [108, 109]. Furthermore, inflammatory cytokines as IL-1β, IFNγ, and TNFα cause induction of indoleamine-2,3-dioxygenase (IDO), an enzyme catabolizing tryptophan into neurotoxic metabolites known as TRYCATs. IDO activation is significantly related to inflammatory signs and to the severity of depressive symptoms [110, 111]. Serotonin levels

are affected by inflammation since tryptophan is the precursor of 5-HT. IDO metabolize tryptophan in the kynurenine pathway and therefore less tryptophan is available to synthesize 5-HT. Activation of the brain's microglia by Th1 cytokines, either secreted from activated astrocytes or from the periphery, induces IDO and may thus reduce 5-HT levels and result in depression. Astrocytic activation in the brain, facilitated by BBB disruption in inflammatory condition of T2DM may also alter network properties and neuronal excitability by changing glutamate levels and affecting synaptic plasticity. Cytokines may generate, through the kynurenine pathway, the formation of quinolinic acid—an NMDA receptor (NMDAR) agonist. Microglia are the only cells in the CNS that express the complete enzymatic pathway required for the synthesis of quinolinic acid [112]. Hence, inflammatory mediators acting on microglia will increase the levels of quinolinic acid and will activate NMDA receptors. These findings match with new evidence suggesting that heightened glutamate receptor activity in major depression, can underlie inflammation-associated depressive disorders [113]. In addition, quinolinic acid directly causes release of glutamate [114]. Thus, inflammatory mediators can lead to an environment of excess glutamate. Glutamate receptor activation enhances the effect of BBB breakdown by induction of astrocytic transformation. A vicious cycle of cytokine secretion, microglial activation, and further enhancement of glutamate receptors activation is created (see below). Activated microglial cells are also key contributors to the inflammatory response which occur during chronic neurodegeneration in diseases such as Alzheimer's disease, prion disease and Parkinson's disease [115]. These activated microglia release proinflammatory cytokines which affect injured neurons and may exacerbate lesion size and neuronal loss. Postmortem examination of brain tissue from patients suffered from Alzheimer's disease revealed large numbers of activated microglia associated with the amyloid deposits and in regions of the brain where there is neuronal loss [116]. Metabolic syndrome, T2DM, and decline in cognitive function share common inflammatory markers [117]. Elevated levels of insulin may lead to cognitive decline via the effect of hyperinsulinemia on neuronal metabolism and reduced clearance of β amyloid, a frequent pathologic feature of obesity, metabolic syndrome, DM, and Alzheimer's disease [118]. A Recent study showed decrease in executive and processing function among metabolic syndrome patients [119]. Moreover, patients with impaired insulin function were found to have lower levels of the neurotrophic protein BDNF. Decreases in hippocampal BDNF levels showed association with stress-induced depressive behaviors and conversely, antidepressant treatment enhanced the expression of BDNF [120].

9. BBB Breakdown and Psychopathology

Neuropsychiatric disorders such as depression, mood and anxiety disorders, are associated with cerebrovascular impairments [121]. BBB breakdown will result in induction of signaling pathways leading to transformation and activation of the surroundingcells. We mentioned previously how local inflammatory brain responses following BBB changes influence endothelial and glial cells towards elevation of cytokine expression. It is possible to assume that glial cell activation will also participate in the functional changes occurring in the vascular environment and the adjacent neuropil. Indeed, compromised BBB results in a rapid transformation of the resting astrocytes into their active form in ischemic, inflammatory and traumatic brain injuries. Astrocytic endfeet are considered an integral part of the BBB and surround capillaries in the CNS to regulate the vascular tone [122] and tight junction expression [123]. Experimental evidence suggests that upon BBB breakdown, infiltration of albumin, the most abundant serum protein, into the neuropil may account for the astrocytic transformation via the transforming growth factor beta (TGFβ) signaling pathway. Transformed astrocytes undergoes modification in gene expression that includes the upregulation of GFAP and S100B, downregulation of glutamate transporters, glutamine synthase and the inward rectifying potassium channel ($K_{IR4.1}$), AQP4 and gap junctions' proteins [124, 125]. The subsequent gene expression affects the extracellular environment through increased concentrations of potassium and glutamate causing amplification of neuronal excitability [126]. The participation of calcium metabolism in neurovascular coupling provides a hint for a possible pathologic molecular mechanism that may arise from astrocytic activation. Neuron-to-astrocyte signaling is considered being a key mechanism in functional hyperemia. The resultant increase in extracellular glutamate following astrocytic transformation can activate glutamate receptors (mGluRs) located on astrocytes. It has been shown that the dilation of arterioles triggered by neuronal activity is dependent on glutamate-mediated cytosolic calcium ($[Ca^{2+}]$i) oscillations in astrocytes [127]. Activation of mGluRs and the subsequent elevation in $[Ca^{2+}]$i in astrocytes ultimately creates $[Ca^{2+}]$i increase in the endfeet [128]. Zonta et al. [127] demonstrated that inhibition of astrocytic Ca^{2+}responses resulted in the impairment of activity-dependent vasodilation, whereas selective activation of single astrocytes in close proximity to arterioles triggered vessel relaxation [127]. They further observed that in vivo blockade of glutamate-mediated $[Ca^{2+}]$i elevations in astrocytes reduced hyperemic reaction in the somatosensory cortex during contralateral forepaw stimulation. Excess of extracellular glutamate that leads to activation of mGluRs and the increase of $[Ca^{2+}]$i in the endfeet, initiate the activation of Ca^{2+}-sensitive K^+ channels (BK) and the efflux of K^+. BK channels were proposed to play a role in the K^+ modulation of cerebral blood flow [129]. Extracellular excess of potassium has the potential to generate changes in the vascular tone through activation of inward rectifying K^+ channels (K_{IR}) located in smooth muscle (SMC) layer of vessel [130]. BK channels, expressed abundantly in astrocytic endfeets, exhibit sensitivity to membrane depolarization and intracellular calcium levels. Neuronal stimulation of brain slices produced BK channel-mediated K^+ release in astrocytic endfeets, altered the extracellular K^+($[K^+]$o) level in the perivascular space and generated a signal that produces vasodilatory response

by K_{IR} channels in parenchymal arteriole SMC. The elevation of $[K^+]o$ from 3 mmol/L to 8 mmol/L hyperpolarizes parenchymal arteriolar membranes from −45 to −80 mV, and causes a rapid and profound dilation of isolated pressurized parenchymal arterioles as well as arterioles in brain slices [131]. Thus, astrocytic activation after BBB disruption, subsequent reduction in K^+ buffering and the increase of extracellular glutamate and K^+, elevates the $[K^+]o$ levels. This will consequent in enhancement of the mutual activity of glutamate-mediated $[Ca^{2+}]i$ oscillations in astrocytes, BK activation and vasodilatation through SMC K^+ channels. A direct link between the metabolic state in the brain tissue and astrocyte signaling was recently established [132]. According to our hypothesis, the changes in the perivascular microenvironment and the metabolic dysregulation arising from impairment in cerebrovascular response as disturbed or extensive hyperemia may take part in the mechanisms underlying brain pathologies. Hyperemia in the active regions and hypoperfusion of surrounding areas, under some conditions (extent, duration and location) may result in impaired metabolism, inadequate homeostasis preservation, formation of reactive oxygen species and insufficient removal of toxic metabolites. These insults may participate in the evolvement of cognitive or psychiatric illnesses. Mechanisms of abnormal plasticity are also suspected to participate in the development of mental disturbances following BBB breakdown, glial activation and inflammation, via the effect of excess of glutamate. We hypothesize that diffusion of glutamate and K^+ out of the narrow synaptic cleft will affect neighboring synapses, resulting in a loss of synapse- and pathway-specific plasticity. Astrocyte-mediated plasticity mechanisms utilize glutamate for transient mGluR-dependent neuromodulation. In addition long-term potentiation via NMDAR-independent mechanism showing $Ca2^+$ elevation in astrocytes that modulates transmitter release probability and evokes long-term synaptic plasticity [133]. This control in transmitter release at the synapse and the strengthening of synaptic connectivity may possibly result in synaptic tuning in circuits involved in cognitive processing and the control of limbic system excitability [134]. Formation of new synapses may reduce specificity and is expected to activate larger neuronal networks in response to stimuli. These alterations might be expressed in disturbed thinking processes and extreme mood-related behavioral responses, depending on the involved network.

10. Conclusion

Inflammation and vascular pathology have a significant contribution for the pathogenesis of T2DM complications. Neuropsychiatric disorders are also associated with inflammatory reaction and cerebrovascular impairments. Brain injuries that often involve BBB breakdown and astrocytic response increase the risk for neuropsychiatric sequelae, including personality changes, depression, anxiety, dementia, and perhaps psychosis [135, 136]. T2DM patients show higher susceptibility to cerebrovascular diseases which according to our hypothesis may explain the increased incidence of cognitive deterioration, depression, vascular dementia, lacunar infarcts, hemorrhages and Alzheimer's disease among these patients. Revealing the mechanisms underlying the effects of diabetes on BBB structure and function and understanding the role of inflammation, impaired neurovascular coupling, metabolic defects and altered neuronal plasticity in the neuropsychiatric sequela of T2DM, will create a target for clinical and pharmacologic modalities and a potential platform for future therapeutic intervention.

References

[1] M. Stumvoll, B. J. Goldstein, and T. W. Van Haeften, "Type 2 diabetes: principles of pathogenesis and therapy," *Lancet*, vol. 365, no. 9467, pp. 1333–1346, 2005.

[2] T. Pirttila, R. Jarvenpaa, P. Laippala, and H. Frey, "Brain atrophy on computerized axial tomography scans: interaction of age, diabetes and general morbidity," *Gerontology*, vol. 38, no. 5, pp. 285–291, 1992.

[3] Y. Araki, M. Nomura, H. Tanaka et al., "MRI of the brain in diabetes mellitus," *Neuroradiology*, vol. 36, no. 2, pp. 101–103, 1994.

[4] T. Den Heijer, S. E. Vermeer, E. J. Van Dijk et al., "Type 2 diabetes and atrophy of medial temporal lobe structures on brain MRI," *Diabetologia*, vol. 46, no. 12, pp. 1604–1610, 2003.

[5] B. Van Harten, F. E. De Leeuw, H. C. Weinstein, P. Scheltens, and G. J. Biessels, "Brain imaging in patients with diabetes: a systematic review," *Diabetes Care*, vol. 29, no. 11, pp. 2539–2548, 2006.

[6] S. M. Gold, I. Dziobek, V. Sweat et al., "Hippocampal damage and memory impairments as possible early brain complications of type 2 diabetes," *Diabetologia*, vol. 50, no. 4, pp. 711–719, 2007.

[7] P. L. Yau, D. C. Javier, C. M. Ryan et al., "Preliminary evidence for brain complications in obese adolescents with type 2 diabetes mellitus," *Diabetologia*, vol. 53, no. 11, pp. 2298–2306, 2010.

[8] A. M. Abbatecola and G. Paolisso, "Relationship between baseline glycemic control and cognitive function in individuals with type 2 diabetes and other cardiovascular risk factors: the Action to Control Cardiovascular Risk in Diabetes-Memory in Diabetes (ACCORD-MIND) Trial," *Diabetes Care*, vol. 32, no. 8, p. e102, 2009.

[9] D. G. Bruce, W. A. Davis, G. P. Casey et al., "Predictors of cognitive impairment and dementia in older people with diabetes," *Diabetologia*, vol. 51, no. 2, pp. 241–248, 2008.

[10] A. M. Tiehuis, Y. van der Graaf, F. L. Visseren et al., "Diabetes increases atrophy and vascular lesions on brain MRI in patients with symptomatic arterial disease," *Stroke*, vol. 39, no. 5, pp. 1600–1603, 2008.

[11] H. Shalev, Y. Serlin, and A. Friedman, "Breaching the blood-brain barrier as a gate to psychiatric disorder," *Cardiovascular Psychiatry and Neurology*, vol. 2009, Article ID 278531, 7 pages, 2009.

[12] P. N. Surampudi, J. John-Kalarickal, and V. A. Fonseca, "Emerging concepts in the pathophysiology of type 2 diabetes mellitus," *Mount Sinai Journal of Medicine*, vol. 76, no. 3, pp. 216–226, 2009.

[13] Y. Lin and Z. Sun, "Current views on type 2 diabetes," *Journal of Endocrinology*, vol. 204, no. 1, pp. 1–11, 2010.

[14] K. E. Wellen and G. S. Hotamisligil, "Obesity-induced inflammatory changes in adipose tissue," *Journal of Clinical Investigation*, vol. 112, no. 12, pp. 1785–1788, 2003.

[15] H. Xu, G. T. Barnes, Q. Yang et al., "Chronic inflammation in fat plays a crucial role in the development of obesity-related insulin resistance," *Journal of Clinical Investigation*, vol. 112, no. 12, pp. 1821–1830, 2003.

[16] S. H. Golden, M. Lazo, M. Carnethon et al., "Examining a bidirectional association between depressive symptoms and diabetes," *Journal of the American Medical Association*, vol. 299, no. 23, pp. 2751–2759, 2008.

[17] S. Wild, G. Roglic, A. Green, R. Sicree, and H. King, "Global prevalence of diabetes: estimates for the year 2000 and projections for 2030," *Diabetes Care*, vol. 27, no. 5, pp. 1047–1053, 2004.

[18] J. B. McGill, "Improving microvascular outcomes in patients with diabetes through management of hypertension," *Postgraduate Medicine*, vol. 121, no. 2, pp. 89–101, 2009.

[19] P. M. Ridker, "Inflammatory biomarkers and risks of myocardial infarction, stroke, diabetes, and total mortality: implications for longevity," *Nutrition Reviews*, vol. 65, no. 12, pp. S253–S259, 2007.

[20] P. Geraldes and G. L. King, "Activation of protein kinase C isoforms and its impact on diabetic complications," *Circulation Research*, vol. 106, no. 8, pp. 1319–1331, 2010.

[21] S. I. Yamagishi and T. Imaizumi, "Diabetic vascular complications: pathophysiology, biochemical basis and potential therapeutic strategy," *Current Pharmaceutical Design*, vol. 11, no. 18, pp. 2279–2299, 2005.

[22] M. Ristow, "Neurodegenetive disorders associated with diabetes mellitus," *Journal of Molecular Medicine*, vol. 82, no. 8, pp. 510–529, 2004.

[23] B. T. Hawkins and T. P. Davis, "The blood-brain barrier/neurovascular unit in health and disease," *Pharmacological Reviews*, vol. 57, no. 2, pp. 173–185, 2005.

[24] N. J. Abbott, L. Ronnback, and E. Hansson, "Astrocyte-endothelial interactions at the blood-brain barrier," *Nature Reviews Neuroscience*, vol. 7, no. 1, pp. 41–53, 2006.

[25] B. V. Zlokovic, "The blood-brain barrier in health and chronic neurodegenerative disorders," *Neuron*, vol. 57, no. 2, pp. 178–201, 2008.

[26] P. S. Tofts, G. Brix, D. L. Buckley et al., "Estimating kinetic parameters from dynamic contrast-enhanced T-weighted MRI of a diffusable tracer: standardized quantities and symbols," *Journal of Magnetic Resonance Imaging*, vol. 10, no. 3, pp. 223–232, 1999.

[27] G. Zaharchuk, "Theoretical basis of hemodynamic MR imaging techniques to measure cerebral blood volume, cerebral blood flow, and permeability," *American Journal of Neuroradiology*, vol. 28, no. 10, pp. 1850–1858, 2007.

[28] O. Tomkins, I. Shelef, I. Kaizerman et al., "Blood-brain barrier disruption in post-traumatic epilepsy," *Journal of Neurology, Neurosurgery and Psychiatry*, vol. 79, no. 7, pp. 774–777, 2008.

[29] N. Marchi, P. Rasmussen, M. Kapural et al., "Peripheral markers of brain damage and blood-brain barrier dysfunction," *Restorative Neurology and Neuroscience*, vol. 21, no. 3-4, pp. 109–121, 2003.

[30] S. Nag, R. Venugopalan, and D. J. Stewart, "Increased caveolin-1 expression precedes decreased expression of occludin and claudin-5 during blood-brain barrier breakdown," *Acta Neuropathologica*, vol. 114, no. 5, pp. 459–469, 2007.

[31] S. Nag, J. L. Manias, and D. J. Stewart, "Expression of endothelial phosphorylated caveolin-1 is increased in brain injury," *Neuropathology and Applied Neurobiology*, vol. 35, no. 4, pp. 417–426, 2009.

[32] J. Zhao, A. N. Moore, J. B. Redell, and P. K. Dash, "Enhancing expression of Nrf2-driven genes protects the blood-brain barrier after brain injury," *Journal of Neuroscience*, vol. 27, no. 38, pp. 10240–10248, 2007.

[33] D. Yeung, J. L. Manias, D. J. Stewart, and S. Nag, "Decreased junctional adhesion molecule-A expression during blood-brain barrier breakdown," *Acta Neuropathologica*, vol. 115, no. 6, pp. 635–642, 2008.

[34] T. Higashida, C. W. Kreipke, J. A. Rafols et al., "The role of hypoxia-inducible factor-1alpha, aquaporin-4, and matrix metalloproteinase-9 in blood-brain barrier disruption and brain edema after traumatic brain injury," *Journal of Neurosurgery*, vol. 114, no. 1, pp. 92–101, 2011.

[35] P. Dore-Duffy, C. Owen, R. Balabanov, S. Murphy, T. Beaumont, and J. A. Rafols, "Pericyte migration from the vascular wall in response to traumatic brain injury," *Microvascular Research*, vol. 60, no. 1, pp. 55–69, 2000.

[36] S. Nag, J. L. Takahashi, and D. W. Kilty, "Role of vascular endothelial growth factor in blood-brain barrier breakdown and angiogenesis in brain trauma," *Journal of Neuropathology and Experimental Neurology*, vol. 56, no. 8, pp. 912–921, 1997.

[37] F. Marceau and D. Regoli, "Bradykinin receptor ligands: therapeutic perspectives," *Nature Reviews Drug Discovery*, vol. 3, no. 10, pp. 845–852, 2004.

[38] L. M. F. Leeb-Lundberg, "Bradykinin specificity and signaling at GPR100 and B kinin receptors," *British Journal of Pharmacology*, vol. 143, no. 8, pp. 931–932, 2004.

[39] M. Schwaninger, S. Sallmann, N. Petersen et al., "Bradykinin induces interleukin-6 expression in astrocytes through activation of nuclear factor-κB," *Journal of Neurochemistry*, vol. 73, no. 4, pp. 1461–1466, 1999.

[40] M. A. Deli, L. Descamps, M. P. Dehouck et al., "Exposure of tumor necrosis factor-α to luminal membrane of bovine brain capillary endothelial cells cocultured with astrocytes induces a delayed increase of permeability and cytoplasmic stress fiber formation of actin," *Journal of Neuroscience Research*, vol. 41, no. 6, pp. 717–726, 1995.

[41] N. Didier, I. A. Romero, C. Créminon, A. Wijkhuisen, J. Grassi, and A. Mabondzo, "Secretion of interleukin-1β by astrocytes mediates endothelin-1 and tumour necrosis factor-α effects on human brain microvascular endothelial cell permeability," *Journal of Neurochemistry*, vol. 86, no. 1, pp. 246–254, 2003.

[42] J. D. Huber, R. D. Egleton, and T. P. Davis, "Molecular physiology and pathophysiology of tight junctions in the blood -brain barrier," *Trends in Neurosciences*, vol. 24, no. 12, pp. 719–725, 2001.

[43] Y. Gursoy-Ozdemir, J. Qiu, N. Matsuoka et al., "Cortical spreading depression activates and upregulates MMP-9," *Journal of Clinical Investigation*, vol. 113, no. 10, pp. 1447–1455, 2004.

[44] W. G. Mayhan, "Effect of diabetes mellitus on disruption of the blood-brain barrier during acute hypertension," *Brain Research*, vol. 534, no. 1-2, pp. 106–110, 1990.

[45] M. H. Horani and A. D. Mooradian, "Effect of diabetes on the blood brain barrier," *Current Pharmaceutical Design*, vol. 9, no. 10, pp. 833–840, 2003.

[46] J. Dai, G. F. J. M. Vrensen, and R. O. Schlingemann, "Blood-brain barrier integrity is unaltered in human brain cortex with diabetes mellitus," *Brain Research*, vol. 954, no. 2, pp. 311–316, 2002.

[47] W. D. Dietrich, O. Alonso, and R. Busto, "Moderate hyperglycemia worsens acute blood-brain barrier injury after forebrain ischemia in rats," *Stroke*, vol. 24, no. 1, pp. 111–116, 1993.

[48] H. Kamada, F. Yu, C. Nito, and P. H. Chan, "Influence of hyperglycemia on oxidative stress and matrix metalloproteinase-9 activation after focal cerebral ischemia/reperfusion in rats: relation to blood-brain barrier dysfunction," *Stroke*, vol. 38, no. 3, pp. 1044–1049, 2007.

[49] J. M. Starr, J. M. Wardlaw, K. Ferguson, A. MacLullich, I. J. Deary, and I. Marshall, "Increased blood-brain barrier permeability in type II diabetes demonstrated by gadolinium magnetic resonance imaging," *Journal of Neurology Neurosurgery and Psychiatry*, vol. 74, no. 1, pp. 70–76, 2003.

[50] M. R. Hovsepyan, M. J. Haas, A. S. Boyajyan et al., "Astrocytic and neuronal biochemical markers in the sera of subjects with diabetes mellitus," *Neuroscience Letters*, vol. 369, no. 3, pp. 224–227, 2004.

[51] S. J. Vannucci, E. M. Gibbs, and I. A. Simpson, "Glucose utilization and glucose transporter proteins GLUT-1 and GLUT-3 in brains of diabetic (db/db) mice," *American Journal of Physiology*, vol. 272, no. 2, pp. E267–E274, 1997.

[52] W. M. Pardridge, D. Triguero, and C. R. Farrell, "Downregulation of blood-brain barrier glucose transporter in experimental diabetes," *Diabetes*, vol. 39, no. 9, pp. 1040–1044, 1990.

[53] S. Pennathur and J. W. Heinecke, "Oxidative stress and endothelial dysfunction in vascular disease," *Current Diabetes Reports*, vol. 7, no. 4, pp. 257–264, 2007.

[54] V. B. Schrauwen-Hinderling, M. Roden, M. E. Kooi, M. K. C. Hesselink, and P. Schrauwen, "Muscular mitochondrial dysfunction and type 2 diabetes mellitus," *Current Opinion in Clinical Nutrition and Metabolic Care*, vol. 10, no. 6, pp. 698–703, 2007.

[55] Y. Lin, M. W. Rajala, J. P. Berger, D. E. Moller, N. Barzilai, and P. E. Scherer, "Hyperglycemia-induced production of acute phase reactants in adipose tissue," *Journal of Biological Chemistry*, vol. 276, no. 45, pp. 42077–42083, 2001.

[56] C. L. Scott, "Diagnosis, prevention, and intervention for the metabolic syndrome," *American Journal of Cardiology*, vol. 92, no. 1, pp. 35i–42i, 2003.

[57] R. Meerwaldt, C. J. Zeebregts, G. Navis, J. L. Hillebrands, J. D. Lefrandt, and A. J. Smit, "Accumulation of advanced glycation end products and chronic complications in ESRD treated by dialysis," *American Journal of Kidney Diseases*, vol. 53, no. 1, pp. 138–150, 2009.

[58] R. Piga, Y. Naito, S. Kokura, O. Handa, and T. Yoshikawa, "Short-term high glucose exposure induces monocyte-endothelial cells adhesion and transmigration by increasing VCAM-1 and MCP-1 expression in human aortic endothelial cells," *Atherosclerosis*, vol. 193, no. 2, pp. 328–334, 2007.

[59] R. Klein, B. E. K. Klein, S. E. Moss, M. D. Davis, and D. L. DeMets, "Glycosylated hemoglobin predicts the incidence and progression of diabetic retinopathy," *Journal of the American Medical Association*, vol. 260, no. 19, pp. 2864–2871, 1988.

[60] S. Vitale, M. G. Maguire, R. P. Murphy et al., "Clinically significant macular edema in type I diabetes: incidence and risk factors," *Ophthalmology*, vol. 102, no. 8, pp. 1170–1176, 1995.

[61] R. Klein, B. E. K. Klein, S. E. Moss, and K. J. Cruickshanks, "The wisconsin epidemiologic study of diabetic retinopathy: XVII. The 14- year incidence and progression of diabetic retinopathy and associated risk factors in type 1 diabetes," *Ophthalmology*, vol. 105, no. 10, pp. 1801–1815, 1998.

[62] R. Klein, B. E. K. Klein, and S. E. Moss, "The Wisconsin epidemiologic study of diabetic retinopathy. IV. Diabetic macular edema," *Ophthalmology*, vol. 91, no. 12, pp. 1464–1474, 1984.

[63] C. H. Meyer, "Current treatment approaches in diabetic macular edema," *Ophthalmologica*, vol. 221, no. 2, pp. 118–131, 2007.

[64] U. Chakravarthy, R. G. Hayes, A. W. Stitt, E. McAuley, and D. B. Archer, "Constitutive nitric oxide synthase expression in retinal vascular endothelial cells is suppressed by high glucose and advanced glycation end products," *Diabetes*, vol. 47, no. 6, pp. 945–952, 1998.

[65] M. Lu, M. Kuroki, S. Amano et al., "Advanced glycation end products increase retinal vascular endothelial growth factor expression," *Journal of Clinical Investigation*, vol. 101, no. 6, pp. 1219–1224, 1998.

[66] T. A. Ciulla, A. Harris, P. Latkany et al., "Ocular perfusion abnormalities in diabetes," *Acta Ophthalmologica Scandinavica*, vol. 80, no. 5, pp. 468–477, 2002.

[67] C. Paget, M. Lecomte, D. Ruggiero, N. Wiernsperger, and M. Lagarde, "Modification of enzymatic antioxidants in retinal microvascular cells by glucose or advanced glycation end products," *Free Radical Biology and Medicine*, vol. 25, no. 1, pp. 121–129, 1998.

[68] K. Miyamoto and Y. Ogura, "Pathogenetic potential of leukocytes in diabetic retinopathy," *Seminars in Ophthalmology*, vol. 14, no. 4, pp. 233–239, 1999.

[69] L. P. Aiello, R. L. Avery, P. G. Arrigg et al., "Vascular endothelial growth factor in ocular fluid of patients with diabetic retinopathy and other retinal disorders," *New England Journal of Medicine*, vol. 331, no. 22, pp. 1480–1487, 1994.

[70] J. W. Miller, A. P. Adamis, and L. P. Aiello, "Vascular endothelial growth factor in ocular neovascularization and proliferative diabetic retinopathy," *Diabetes/Metabolism Reviews*, vol. 13, no. 1, pp. 37–50, 1997.

[71] J. D. Huber, "Diabetes, cognitive function, and the blood-brain barrier," *Current Pharmaceutical Design*, vol. 14, no. 16, pp. 1594–1600, 2008.

[72] O. Tomkins, I. Shelef, I. Kaizerman et al., "Blood-brain barrier disruption in post-traumatic epilepsy," *Journal of Neurology, Neurosurgery and Psychiatry*, vol. 79, no. 7, pp. 774–777, 2008.

[73] O. Prager, Y. Chassidim, C. Klein, H. Levi, I. Shelef, and A. Friedman, "Dynamic in vivo imaging of cerebral blood flow and blood-brain barrier permeability," *NeuroImage*, vol. 49, no. 1, pp. 337–344, 2010.

[74] N. Cheung, T. Mosley, A. Islam et al., "Retinal microvascular abnormalities and subclinical magnetic resonance imaging brain infarct: a prospective study," *Brain*, vol. 133, no. 7, pp. 1987–1993, 2010.

[75] I. Skoog, A. Wallin, P. Fredman et al., "A population study on blood-brain barrier function in 85-year-olds: relation to Alzheimer's disease and vascular dementia," *Neurology*, vol. 50, no. 4, pp. 966–971, 1998.

[76] P. Gudmundsson, I. Skoog, M. Waern et al., "The relationship between cerebrospinal fluid biomarkers and depression in elderly women," *American Journal of Geriatric Psychiatry*, vol. 15, no. 10, pp. 832–838, 2007.

[77] N. Muller and M. Ackenheil, "Immunoglobulin and albumin content of cerebrospinal fluid in schizophrenic patients: relationship to negative symptomatology," *Schizophrenia Research*, vol. 14, no. 3, pp. 223–228, 1995.

[78] M. J. Schwarz, M. Ackenheil, M. Riedel, and N. Müller, "Blood-cerebrospinal fluid barrier impairment as indicator for an immune process in schizophrenia," *Neuroscience Letters*, vol. 253, no. 3, pp. 201–203, 1998.

[79] R. D. Bell and B. V. Zlokovic, "Neurovascular mechanisms and blood-brain barrier disorder in Alzheimer's disease," *Acta Neuropathologica*, vol. 118, no. 1, pp. 103–113, 2009.

[80] M. Rothermundt, G. Ponath, T. Glaser, G. Hetzel, and V. Arolt, "S100B serum levels and long-term improvement of negative symptoms in patients with schizophrenia," *Neuropsychopharmacology*, vol. 29, no. 5, pp. 1004–1011, 2004.

[81] M. L. Schroeter, H. Abdul-Khaliq, M. Krebs, A. Diefenbacher, and I. E. Blasig, "Serum markers support disease-specific glial pathology in major depression," *Journal of Affective Disorders*, vol. 111, no. 2-3, pp. 271–280, 2008.

[82] M. De Groot, R. Anderson, K. E. Freedland, R. E. Clouse, and P. J. Lustman, "Association of depression and diabetes complications: a meta-analysis," *Psychosomatic Medicine*, vol. 63, no. 4, pp. 619–630, 2001.

[83] R. J. Anderson, K. E. Freedland, R. E. Clouse, and P. J. Lustman, "The prevalence of comorbid depression in adults with diabetes: a meta-analysis," *Diabetes Care*, vol. 24, no. 6, pp. 1069–1078, 2001.

[84] S. H. Saydah, F. L. Brancati, S. H. Golden, J. Fradkin, and M. I. Harris, "Depressive symptoms and the risk of type 2 diabetes mellitus in a US sample," *Diabetes/Metabolism Research and Reviews*, vol. 19, no. 3, pp. 202–208, 2003.

[85] S. Ali, M. A. Stone, J. L. Peters, M. J. Davies, and K. Khunti, "The prevalence of co-morbid depression in adults with Type 2 diabetes: a systematic review and meta-analysis," *Diabetic Medicine*, vol. 23, no. 11, pp. 1165–1173, 2006.

[86] T. Cukierman-Yaffe, H. C. Gerstein, J. D. Williamson et al., "Relationship between baseline glycemic control and cognitive function in individuals with type 2 diabetes and other cardiovascular rIsk factors the action to control cardiovascular risk in diabetes-memory in diabetes (ACCORD-MIND) trial," *Diabetes Care*, vol. 32, no. 2, pp. 221–226, 2009.

[87] S. D. Yan, X. Chen, J. Fu et al., "RAGE and amyloid-β peptide neurotoxicity in Alzheimer's disease," *Nature*, vol. 382, no. 6593, pp. 685–691, 1996.

[88] K. Horie, T. Miyata, T. Yasuda et al., "Immunohistochemical localization of advanced glycation end products, pentosidine, and carboxymethyllysine in lipofuscin pigments of Alzheimer's disease and aged neurons," *Biochemical and Biophysical Research Communications*, vol. 236, no. 2, pp. 327–332, 1997.

[89] H. Vlassara, R. Bucala, and L. Striker, "Pathogenic effects of advanced glycosylation: biochemical, biologic, and clinical implications for diabetes and aging," *Laboratory Investigation*, vol. 70, no. 2, pp. 138–151, 1994.

[90] E. W. Gregg, K. Yaffe, J. A. Cauley et al., "Is diabetes associated with cognitive impairment and cognitive decline among older women?" *Archives of Internal Medicine*, vol. 160, no. 2, pp. 174–180, 2000.

[91] K. Yaffe, T. Blackwell, A. M. Kanaya, N. Davidowitz, E. Barrett-Connor, and K. Krueger, "Diabetes, impaired fasting glucose, and development of cognitive impairment in older women," *Neurology*, vol. 63, no. 4, pp. 658–663, 2004.

[92] K. V. Allen, B. M. Frier, and M. W. J. Strachan, "The relationship between type 2 diabetes and cognitive dysfunction: longitudinal studies and their methodological limitations," *European Journal of Pharmacology*, vol. 490, no. 1–3, pp. 169–175, 2004.

[93] C. E. Lloyd, P. H. Dyert, and A. H. Barnett, "Prevalence of symptoms of depression and anxiety in a diabetes clinic population," *Diabetic Medicine*, vol. 17, no. 3, pp. 198–202, 2000.

[94] R. J. Anderson, M. De Groot, A. B. Grigsby et al., "Anxiety and poor glycemic control: a meta-analytic review of the literature," *International Journal of Psychiatry in Medicine*, vol. 32, no. 3, pp. 235–247, 2002.

[95] A. Gardner and R. G. Boles, "Beyond the serotonin hypothesis: mitochondria, inflammation and neurodegenera-tion in major depression and affective spectrum disorders," *Progress in Neuro-Psychopharmacology and Biological Psychiatry*. In press.

[96] Y. Dowlati, N. Herrmann, W. Swardfager et al., "A meta-analysis of cytokines in major depression," *Biological Psychiatry*, vol. 67, no. 5, pp. 446–457, 2010.

[97] M. Maes, R. Yirmyia, J. Noraberg et al., "The inflammatory & neurodegenerative (I&ND) hypothesis of depression: leads for future research and new drug developments in depression," *Metabolic Brain Disease*, vol. 24, no. 1, pp. 27–53, 2009.

[98] E. M. Sternberg, "Neural-immune interactions in health and disease," *Journal of Clinical Investigation*, vol. 100, no. 11, pp. 2641–2647, 1997.

[99] C. Woiciechowsky, K. Asadullah, D. Nestler et al., "Sympathetic activation triggers systemic interleukin-10 release in immunodepression induced by brain injury," *Nature Medicine*, vol. 4, no. 7, pp. 808–813, 1998.

[100] N. Vila, J. Castillo, A. Dávalos, and A. Chamorro, "Proinflammatory cytokines and early neurological worsening in ischemic stroke," *Stroke*, vol. 31, no. 10, pp. 2325–2329, 2000.

[101] J. C. O'Connor, D. R. Johnson, and G. G. Freund, "Psychoneuroimmune implications of type 2 diabetes: redux," *Immunology and Allergy Clinics of North America*, vol. 29, no. 2, pp. 339–358, 2009.

[102] C. L. Raison, L. Capuron, and A. H. Miller, "Cytokines sing the blues: inflammation and the pathogenesis of depression," *Trends in Immunology*, vol. 27, no. 1, pp. 24–31, 2006.

[103] A. J. Thomas, S. Davis, C. Morris, E. Jackson, R. Harrison, and J. T. O'Brien, "Increase in interleukin-1β in late-life depression," *American Journal of Psychiatry*, vol. 162, no. 1, pp. 175–177, 2005.

[104] S. Alesci, P. E. Martinez, S. Kelkar et al., "Major depression is associated with significant diurnal elevations in plasma interleukin-6 levels, a shift of its circadian rhythm, and loss of physiological complexity in its secretion: clinical implications," *Journal of Clinical Endocrinology and Metabolism*, vol. 90, no. 5, pp. 2522–2530, 2005.

[105] C. A. Turner, H. Akil, S. J. Watson, and S. J. Evans, "The fibroblast growth factor system and mood disorders," *Biological Psychiatry*, vol. 59, no. 12, pp. 1128–1135, 2006.

[106] H. D. Schmidt and R. S. Duman, "The role of neurotrophic factors in adult hippocampal neurogenesis, antidepressant treatments and animal models of depressive-like behavior," *Behavioural Pharmacology*, vol. 18, no. 5-6, pp. 391–418, 2007.

[107] C. Sandi and R. Bisaz, "A model for the involvement of neural cell adhesion molecules in stress-related mood disorders," *Neuroendocrinology*, vol. 85, no. 3, pp. 158–176, 2007.

[108] M. Maes, E. Bosmans, H. Y. Meltzer, S. Scharpe, and E. Suy, "Interleukin-1β: a putative mediator of HPA axis hyperactivity in major depression?" *American Journal of Psychiatry*, vol. 150, no. 8, pp. 1189–1193, 1993.

[109] I. Goshen, T. Kreisel, O. Ben-Menachem-Zidon et al., "Brain interleukin-1 mediates chronic stress-induced depression in mice via adrenocortical activation and hippocampal neurogenesis suppression," *Molecular Psychiatry*, vol. 13, no. 7, pp. 717–728, 2008.

[110] M. Maes, R. Verkerk, S. Bonaccorso, W. Ombelet, E. Bosmans, and S. Scharpé, "Depressive and anxiety symptoms in the early puerperium are related to increased degradation of tryptophan into kynurenine, a phenomenon which is related to immune activation," *Life Sciences*, vol. 71, no. 16, pp. 1837–1848, 2002.

[111] M. C. Wichers, G. Kenis, G. H. Koek, G. Robaeys, N. A. Nicolson, and M. Maes, "Interferon-α-induced depressive symptoms are related to changes in the cytokine network but not to cortisol," *Journal of Psychosomatic Research*, vol. 62, no. 2, pp. 207–214, 2007.

[112] R. Dantzer, J. C. O'Connor, G. G. Freund, R. W. Johnson, and K. W. Kelley, "From inflammation to sickness and depression: when the immune system subjugates the brain," *Nature Reviews Neuroscience*, vol. 9, no. 1, pp. 46–56, 2008.

[113] N. Müller and M. J. Schwarz, "The immune-mediated alteration of serotonin and glutamate: towards an integrated view of depression," *Molecular Psychiatry*, vol. 12, no. 11, pp. 988–1000, 2007.

[114] E. Fedele and A. C. Foster, "An evaluation of the role of extracellular amino acids in the delayed neurodegeneration induced by quinolinic acid in the rat striatum," *Neuroscience*, vol. 52, no. 4, pp. 911–917, 1993.

[115] V. H. Perry, "The influence of systemic inflammation on inflammation in the brain: implications for chronic neurodegenerative disease," *Brain, Behavior, and Immunity*, vol. 18, no. 5, pp. 407–413, 2004.

[116] S. M. Allan and N. J. Rothwell, "Cytokines and acute neurodegeneration," *Nature Reviews Neuroscience*, vol. 2, no. 10, pp. 734–744, 2001.

[117] S. Craft, "The role of metabolic disorders in Alzheimer disease and vascular dementia: two roads converged," *Archives of Neurology*, vol. 66, no. 3, pp. 300–305, 2009.

[118] J.-S. Roriz, T. M. Sá-Roriz, I. Rosset et al., "(Pre)diabetes, brain aging, and cognition," *Biochimica et Biophysica Acta*, vol. 1792, no. 5, pp. 432–443, 2009.

[119] B. Segura, M. A. Jurado, N. Freixenet, C. Albuin, J. Muniesa, and C. Junqué, "Mental slowness and executive dysfunctions in patients with metabolic syndrome," *Neuroscience Letters*, vol. 462, no. 1, pp. 49–53, 2009.

[120] K. Martinowich, H. Manji, and B. Lu, "New insights into BDNF function in depression and anxiety," *Nature Neuroscience*, vol. 10, no. 9, pp. 1089–1093, 2007.

[121] E. Chemerinski and S. R. Levine, "Neuropsychiatric disorders following vascular brain injury," *Mount Sinai Journal of Medicine*, vol. 73, no. 7, pp. 1006–1014, 2006.

[122] K. M. Dunn and M. T. Nelson, "Potassium channels and neurovascular coupling," *Circulation Journal*, vol. 74, no. 4, pp. 608–616, 2010.

[123] R. F. Haseloff, I. E. Blasig, H. C. Bauer, and H. Bauer, "In search of the astrocytic factor(s) modulating blood-brain barrier functions in brain capillary endothelial cells in vitro," *Cellular and Molecular Neurobiology*, vol. 25, no. 1, pp. 25–39, 2005.

[124] A. Friedman, D. Kaufer, and U. Heinemann, "Blood-brain barrier breakdown-inducing astrocytic transformation: novel targets for the prevention of epilepsy," *Epilepsy Research*, vol. 85, no. 2-3, pp. 142–149, 2009.

[125] L. P. Cacheaux, S. Ivens, Y. David et al., "Transcriptome profiling reveals TGF-β signaling involvement in epileptogenesis," *Journal of Neuroscience*, vol. 29, no. 28, pp. 8927–8935, 2009.

[126] S. Ivens, D. Kaufer, L. P. Flores et al., "TGF-β receptor-mediated albumin uptake into astrocytes is involved in neocortical epileptogenesis," *Brain*, vol. 130, no. 2, pp. 535–547, 2007.

[127] M. Zonta, M. C. Angulo, S. Gobbo et al., "Neuron-to-astrocyte signaling is central to the dynamic control of brain microcirculation," *Nature Neuroscience*, vol. 6, no. 1, pp. 43–50, 2003.

[128] H. R. Parri and V. Crunelli, "The role of Ca^{2+} in the generation of spontaneous astrocytic Ca^{2+} oscillations," *Neuroscience*, vol. 120, no. 4, pp. 979–992, 2003.

[129] D. L. Price, J. W. Ludwig, H. Mi, T. L. Schwarz, and M. H. Ellisman, "Distribution of rSlo Ca^{2+}-activated K^+ channels in rat astrocyte perivascular endfeet," *Brain Research*, vol. 956, no. 2, pp. 183–193, 2002.

[130] H. J. Knot, P. A. Zimmermann, and M. T. Nelson, "Extracellular K^+-induced hyperpolarizations and dilatations of rat coronary and cerebral arteries involve inward rectifier K^+ channels," *Journal of Physiology*, vol. 492, no. 2, pp. 419–430, 1996.

[131] J. A. Filosa, A. D. Bonev, S. V. Straub et al., "Local potassium signaling couples neuronal activity to vasodilation in the brain," *Nature Neuroscience*, vol. 9, no. 11, pp. 1397–1403, 2006.

[132] G. Carmignoto and M. Gómez-Gonzalo, "The contribution of astrocyte signalling to neurovascular coupling," *Brain Research Reviews*, vol. 63, no. 1-2, pp. 138–148, 2010.

[133] G. Perea and A. Araque, "Astrocytes potentiate transmitter release at single hippocampal synapses," *Science*, vol. 317, no. 5841, pp. 1083–1086, 2007.

[134] P. Jourdain, L. H. Bergersen, K. Bhaukaurally et al., "Glutamate exocytosis from astrocytes controls synaptic strength," *Nature Neuroscience*, vol. 10, no. 3, pp. 331–339, 2007.

[135] S. Fleminger, "Long-term psychiatric disorders after traumatic brain injury," *European Journal of Anaesthesiology*, vol. 25, supplement 42, pp. 123–130, 2008.

[136] D. F. Guerreiro, R. Navarro, M. Silva, M. Carvalho, and C. Gois, "Psychosis secondary to traumatic brain injury," *Brain Injury*, vol. 23, no. 4, pp. 358–361, 2009.

Hindawi Publishing Corporation
Cardiovascular Psychiatry and Neurology
Volume 2011, Article ID 130406, 7 pages
doi:10.1155/2011/130406

Hypothesis

Occult Cerebrovascular Disease and Late-Onset Epilepsy: Could Loss of Neurovascular Unit Integrity Be a Viable Model?

Lorna M. Gibson,[1] Stuart M. Allan,[2] Laura M. Parkes,[3] and Hedley C. A. Emsley[4]

[1] *Department of Acute Medicine, Western General Hospital, Edinburgh EH4 2XU, UK*
[2] *Faculty of Life Sciences, University of Manchester, AV Hill Building, Oxford Road, Manchester M13 9PT, UK*
[3] *School of Cancer and Imaging Sciences, University of Manchester, Stopford Building, Oxford Road, Manchester M13 9PT, UK*
[4] *Department of Neurology, Royal Preston Hospital, Fulwood, Preston PR2 9HT, UK*

Correspondence should be addressed to Hedley C. A. Emsley, h.emsley@liv.ac.uk

Received 27 August 2010; Revised 13 December 2010; Accepted 30 December 2010

Academic Editor: Alon Friedman

Late-onset epilepsy (LOE) first occurs after 60 years of age and may be due to occult cerebrovascular disease (CVD) which confers an increased risk of stroke. However, patients with late-onset epilepsy are not currently consistently investigated or treated for cerebrovascular risk factors. We discuss how abnormalities of neurovascular unit function, namely, changes in regional cerebral blood flow and blood brain barrier disruption, may be caused by occult cerebrovascular disease but present clinically as late-onset epilepsy. We describe novel magnetic resonance imaging methods to detect abnormal neurovascular unit function in subjects with LOE and controls. We hypothesise that occult CVD may cause LOE as a result of neurovascular unit dysfunction.

1. Introduction

Late-onset epilepsy (LOE) is defined as epilepsy that first occurs after 60 years of age, and is considered by family doctors to be rare [1], despite the fact that it accounts for over a third of all incident epilepsy [2]. LOE occurs in approximately 4% of stroke patients [3], but importantly, LOE can present without a history of overt cerebrovascular disease (CVD), yet LOE confers a subsequent threefold increased risk of stroke [4]. It is widely assumed that LOE is often attributable to otherwise occult CVD. However, at least in the UK, patients with LOE tend to be prescribed anticonvulsant medication, but the opportunity that LOE presents as a marker of increased stroke risk may be lost if a presentation of LOE does not prompt clinicians to screen for other vascular risk factors and initiate appropriate vascular secondary prevention measures, for which there is a strong case [4, 5].

Occult CVD may be detected on brain imaging but by definition does not manifest otherwise clinically. Structural imaging markers of occult CVD are thought to include cortical or subcortical infarcts, white matter hyperintensities, leukoaraiosis (LA), cerebral atrophy, and brain microbleeds (BMBs) which are a marker particularly of cerebral microangiopathy, and strongly associated with hypertension [6]. However, between 72 and 94% of occult infarcts are subcortical, yet epilepsy derives from the cortex. If occult CVD is aetiologically important in LOE then markers of CVD would be expected to have a more diffuse anatomical distribution than described previously. Subcortical lesions in isolation would not be expected to cause the disruption of corticocortical or subcorticocortical circuits that would be a necessary substrate for epileptogenesis. Markers of functional rather than structural integrity may then be necessary to resolve this apparent discrepancy. For example, a corollary is seen in patients with frontal lobe cognitive dysfunction where structural lesions on MRI are confined anatomically to subcortical regions. In this group, frontal lobe hypometabolism measured using FDG-PET correlated with subcortical lacunes and white matter lesions [7]. We hypothesise that occult CVD may cause LOE via neurovascular unit dysfunction, namely, producing changes in cerebral blood flow (CBF) and/or disruption of the blood brain barrier (BBB). We present evidence for and against this

hypothesis and describe novel MRI methods for detecting neurovascular unit dysfunction in subjects with LOE and control participants.

2. The Neurovascular Unit and Neurovascular Coupling

The structural and functional integrity of the central nervous system depends on coupling between neural activity and (CBF), and regulation of transport across the (BBB). These two critical processes rely on the coordinated activity of a "neurovascular unit" comprising the cerebral endothelium, neurones, and glial cells. In the normal healthy state the increase in CBF produced by brain activity, termed functional hyperaemia, is an example of the close interaction between the neurones, glia, and vascular cells. Neurovascular coupling (NVC) can be defined as the relationship between the neural response which can be measured by a variety of methods and the associated vascular response, that is, change in CBF.

3. Assessing Neurovascular Unit Function

Functional MRI can help assess the functional capacity of cerebral blood vessels to respond to neuronal activation [8], using the Blood Oxygen Level Dependent (BOLD) signal. However, the BOLD signal is physiologically complex, depending on the relative change in CBF and oxygen metabolism (CMRO2). A relatively new technique using simultaneous arterial spin labelling (ASL) and BOLD allows quantification of these component parts.

ASL provides a quantitative measurement of CBF [9]. The BOLD signal is sensitive to deoxyhaemoglobin and is dependent on changes to CBF and CMRO2, which both change during neuronal activity [10]. A calibrating procedure is employed, which may consist of asking patients to hold their breath to induce hypercapnia (excess carbon dioxide in the blood). This causes CBF to increase and it is assumed that CMRO2 does not change, so isolating the CBF component of the BOLD signal. Using simultaneous BOLD and ASL imaging allows the calculation of a calibration factor which relates BOLD signal change to changes in CBF [8]. Patients then perform a task which increases cortical neuronal activity and oxygen demand. CBF change is measured using ASL again, and the calculated calibration factor enables CMRO2 to be calculated from the BOLD signal change [8]. Measurements of CBF can then be compared with CMRO2 during the task. It may be possible to see that CMRO2 becomes uncoupled from CBF which may indicate that the blood vessels cannot deliver the increases in blood flow required. This reduction in functional capacity may suggest occult ischaemia.

Studies show an association between reduced regional CBF (rCBF) and occult infarcts. In a study of 246 clinically neurologically normal patients, 32 (13.0%) patients were found to have occult lacunar infarcts. Of the 34 patients aged over 60, 7 (20.6%) were found to have occult lacunar infarcts. Patients with occult lacunar infarcts have significantly reduced rCBF in both right and left frontotemporal regions compared to patients without occult lacunar infarcts ($P < .05$) [11]. Furthermore nine patients (mean age 63.4, range 58–67) with occult infarcts were found to have reduced rCBF in all cortices (significant in the temporal and parietal cortices, $P < .05$) and a nonsignificant reduction in rCMRO2 globally compared to nine controls without occult infarcts, however, patients with epilepsy were not specifically excluded [12]. These findings suggest a diffuse vascular encephalopathy, which may result in a reduced functional capacity of the blood vessels and subsequent ischaemia.

Patients with both LOE and LA have significantly reduced regional CMRO2 (rCMRO2) in all cortices (frontal, temporal, parietal, and occipital) compared to controls, indicating hypometabolism in these regions ($P < .05$) [13]. These patients also have significantly reduced rCBF in all cortices compared to controls ($P < .05$) [13]. However, these results may have been confounded as no measure of carotid artery stenosis was made, which affects CBF measurements [14]. Reduced rCBF and rCMRO2 may indicate either a degenerative or vascular underlying process [13]. If the cortical neurones are degenerating their demand for oxygen reduces resulting in hypometabolism and reduced blood flow. On the other hand, damage to cortical blood vessels may result in reduced blood flow, therefore reducing oxygen delivery to the tissues and inducing hypometabolism. Both vascular and degenerative processes may be present in older patients.

4. A Preliminary Investigation of Neurovascular Coupling in Patients with Late-Onset Epilepsy

With relevant ethical and research governance approvals, we undertook an initial pilot clinical study in subjects with LOE and conventional vascular risk factors (aged 60 or over at onset, with at least 2 seizures of presumed partial onset), and control subjects with (RF+) or without (RF−) vascular risk factors. We excluded subjects with a history of clinically overt transient ischaemic attack or stroke, focal motor or sensory signs, known aetiology for epilepsy or acute symptomatic seizures, cognitive dysfunction sufficient to interfere with daily activities, or any other active, significant medical condition likely to complicate assessment.

Six participants were scanned using a 3T MRI scanner (Siemens Trio, Erlangen, Germany). The body coil was used for signal transmission and an 8−channel phased array head coil was used for signal collection. The MRI protocol comprised precerebral extracranial and intracranial time of flight angiography, high resolution T1 and T2 weighted images, T2* and fluid attenuated inversion recovery (FLAIR) anatomic images, and a pulsed arterial spin labelling (ASL) sequence (Q2TIPS). Simultaneous blood oxygenation level dependent (BOLD) contrast functional MRI (fMRI) was also performed, with the participant performing a breath-hold paradigm (6 cycles of breath holding on inspiration for 15 s followed by normal breathing for 40 s) and a combined visual and motor paradigm (8 cycles of bilateral hand squeezing of foam pads for 20 s followed by 20 s rest, cued with a flashing

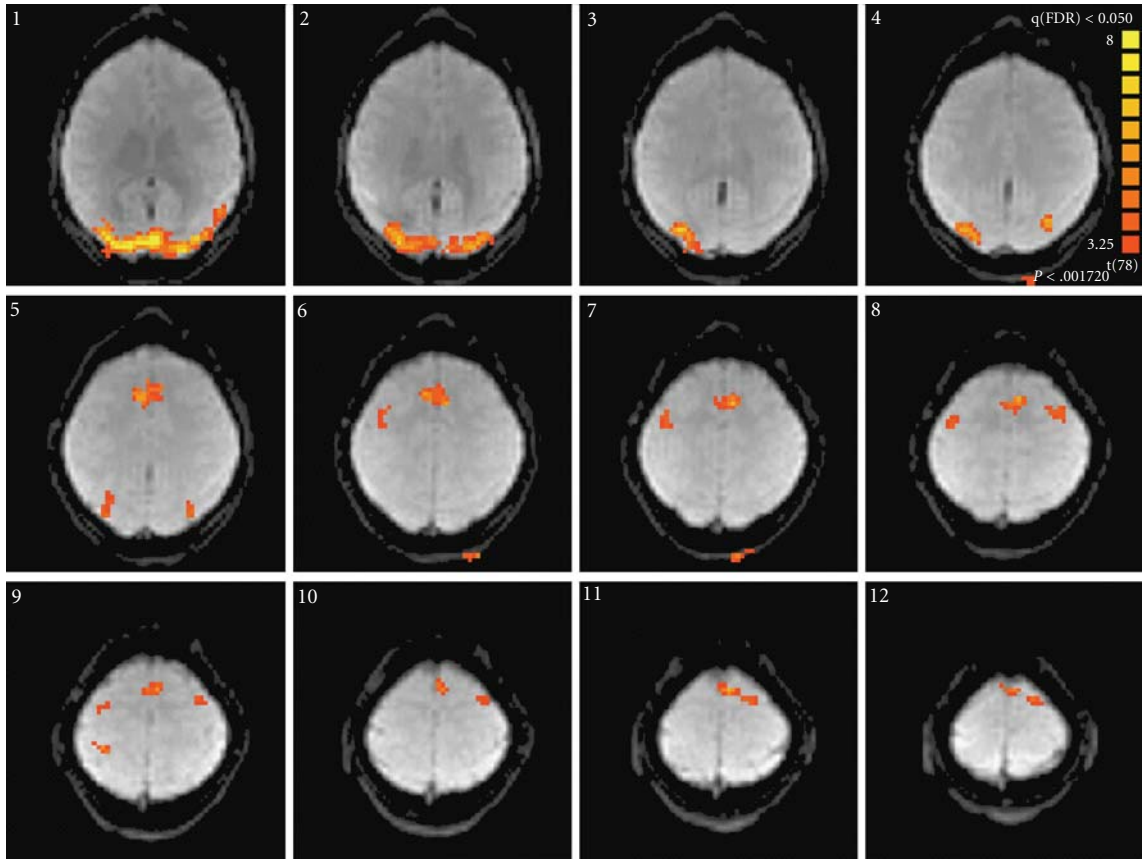

Figure 1: Regions of activation for the combined motor and visual task in a healthy volunteer, presented at a false detection rate of $P < .05$.

visual display). Custom written MATLAB programs (The MathWorks Inc., MA) were used to generate CBF and BOLD images using an appropriate kinetic model [9]. Standard analysis within BrainVoyager was used to identify regions that were significantly active (false detection rate $P < .05$) during the combined visual and motor task (Figure 1). CBF and BOLD time courses during both the motor task and breath hold were recorded within these regions using the model previously described [8].

Data were available for 3 subjects with LOE, and 3 controls (1 RF+, 2 RF−). 1 patient and 1 control (RF+) had mild white matter hyperintensities; all LOE subjects and 1 control (RF+) had reduced cortical volume compared to the other 2 controls (RF−); no other structural lesions were identified. Only one participant had extracranial or intracranial stenosis (RF+ control, 40% stenosis at origin of right internal carotid artery). Average whole brain (mean 35.5 mL blood/min/100 g tissue, range 30.3 to 39.3), grey matter (mean 49.6, range 42.6 to 55.3) and white matter (mean 21.0) perfusion was similar across all participants. During the combined visual and motor task, all subjects showed significant activation in the visual cortex, whereas motor cortex activation was more variable, presumably due to different performance levels on the task. Therefore, responses were recorded from the visual cortex only. BOLD and CBF responses to breath hold were very variable, to the extent that they could not be used reliably to calibrate the BOLD signal during activation. Future work should consider the use of gas-induced hypercapnia [15] or hyperoxia [16, 17] for calibration as, while they are more difficult to administer, they are better controlled than breath hold [18]. The BOLD and CBF responses showed differences in timing between the groups, with the RF+ control and the LOE subjects showing a later peak in the BOLD response compared to RF−controls (Figure 2). The finding of reduced cortical volumes among LOE subjects and the RF+ control compared to RF−controls probably reflects otherwise occult cerebrovascular disease given these participants' vascular risk factor burden.

This initial work demonstrates the feasibility of simultaneous ASL perfusion and BOLD measures in LOE patients, albeit with limited interpretation possible in this pilot study. Further work will be needed to explore potential impairment of NVC in LOE in addition to the apparent structural changes probably attributable to otherwise occult cerebrovascular disease.

5. Neurovascular Coupling and Epilepsy

Epilepsy is an abnormal state which places supranormal demands on the cerebral autoregulatory mechanisms consequent upon an enormous increase in CMRO2 following interictal and ictal events [19]. Normal NVC mechanisms

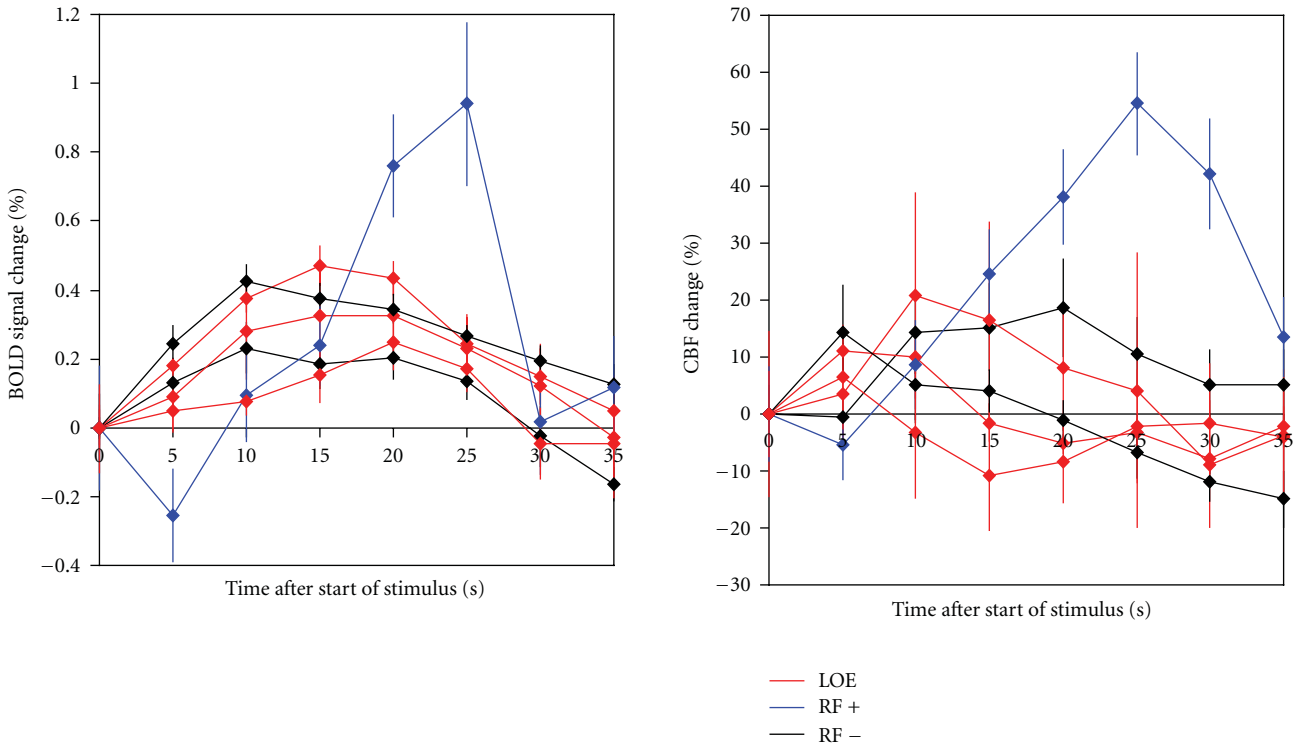

Figure 2: BOLD (a) and CBF (b) responses in participants' visual cortices. CBF is measured in mL blood/min/100 g tissue. Times are in seconds from the start of the motor task, that is, visually-cued hand-squeezing began at time 0 and lasted 20 seconds, followed by 20 seconds of rest. Error bars represent the standard error over the 8 cycles.

may not be relevant to the epileptic brain. It has been long debated whether or not CBF is adequate to meet the increased metabolic demands of epilepsy. Originally, based on histological similarities between ischaemic and epileptic brain damage, it was proposed that the cell damage following status epilepticus was caused by cerebral hypoxia. However, subsequent work refuted this theory, finding a greater increase in CBF relative to CMRO2, that cellular damage differs between status epilepticus and hypoxic injury, that seizures induce increases rather than reduction in venous oxygenation, and evidence of oxidation in the mitochondrial transport chain, NADH and cytochrome oxidase, increases in tissue pO2, and evidence of tissue injury in the absence of hypoxia [19].

6. How Might Loss of NVU Integrity in CVD Be Linked to Epileptogenesis?

There are conceivably several mechanisms linking disruption of NVU integrity—in terms of either an altered relationship between neural activity and CBF, or dysregulation of transport across the BBB—and epileptogenesis in the context of CVD (Figure 3). Cerebral amyloid angiopathy (CAA), a neurovascular degenerative disorder resulting in progressive neurovascular unit dysfunction and in some cases associated with seizures, is briefly discussed as a potentially useful case study in this area.

6.1. Changes in CBF. The notion that haemodynamic alterations might localise and predict the onset of seizures is not new but advances in imaging, including BOLD fMRI, has refocused attention on this area. Recently, changes in BOLD signal have been observed to precede scalp EEG epileptic spikes, raising the possibility that BOLD signal change is due to an event "invisible" to the scalp EEG, or that an abrupt haemodynamic change is responsible for the epileptic discharge [20]. However, whether it is hypoperfusion, hyperperfusion, or indeed the transition between the two states that might theoretically be important is not straightforward to determine. A study of 40 patients with complex partial seizures using 133Xe CT imaging at rest and during a light stimulation procedure found a significant increase in rCBF in the region of the suspected epileptic focus in nonlesional patients [21]. Middle cerebral artery blood flow velocity assessed with transcranial Doppler ultrasonography during simultaneous EEG recording, reveals asymmetric perfusion increases closely related to onset and cessation of EEG seizure activity during simple partial motor seizures [22]. Another study using perfusion CT to measure rCBF with EEG correlation found increased rCBF during subtle status epilepticus but regional hypoperfusion in postictal patients [23].

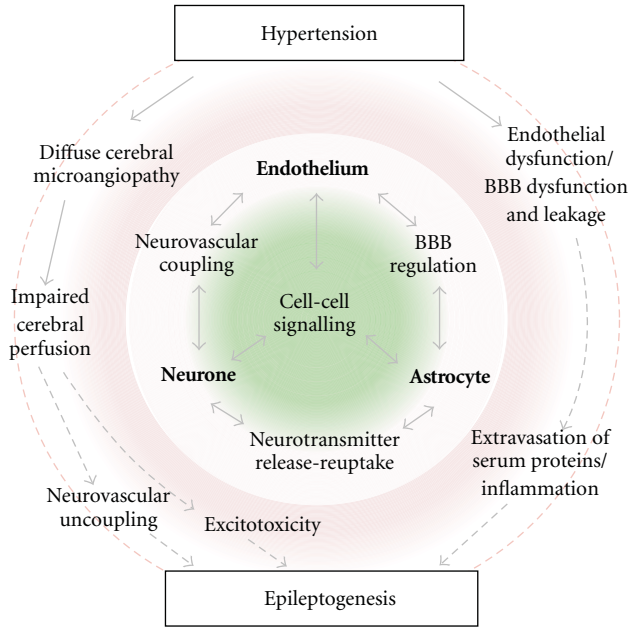

Figure 3: Proposed model of epileptogenicity in occult CVD. The central green/white circle depicts the elements of the healthy neurovascular unit. The outer red/white circle depicts possible sequelae of hypertension, a key determinant of CVD. Structural and functional integrity of the neurovascular unit may be compromised by a diffuse cerebral microangiopathy and endothelial and BBB dysfunction with BBB leakage. Potential mechanisms leading to epileptogenesis might then include impaired cerebral perfusion and neurovascular uncoupling, excitotoxicity occurring as a consequence of ischaemia, or extravasation of serum proteins and inflammation.

Indeed, postictal (or Todd's) paresis has been found, using perfusion MRI, to be accompanied by a reversible global hemispheric hypoperfusion, indicating transient but marked cerebrovascular dysfunction in postictal paresis [24]. In this instance, discrimination from emerging stroke is clearly important to avoid potentially harmful interventions such as thrombolysis. The occurrence of early onset seizures after acute ischaemic stroke has been related to the severity of stroke, with thrombolysis arguably reducing the occurrence of late-onset seizures after stroke, perhaps through improved reperfusion of the ischaemic brain regions [25]. Intriguingly, seizures occurring during thrombolytic therapy for acute ischaemic stroke and heralding dramatic recovery have been attributed to cerebral reperfusion and/or hyperperfusion [26].

An experimental model of stroke-induced epilepsy may shed light on how reduced rCBF producing ischaemia leads to LOE. The model uses glutamate excitotoxic injury to produce an infarct surrounded by an ischaemic penumbra. The ischaemic neurones survive the glutamate injury and produce spontaneous recurrent epileptiform discharges [27] which may be due to their increased basal levels of intracellular calcium [28]. However, this model uses 2-day-old rats and may not be appropriate for modelling LOE in occult CVD. An adult animal model of occult CVD is therefore needed to investigate the mechanisms of epileptogenesis which may be more applicable to LOE patients.

6.2. BBB Dysfunction. The microvasculature is abnormal in cerebral small vessel disease (cSVD), with loss of smooth muscle cells, vessel wall thickening, luminal narrowing, and increased vessel stiffness. These changes may contribute to the attenuation of vasomotor reactivity in response to hypercapnia or acetazolamide seen in cSVD [29], and consequently lead to an impairment of NVC. Such impairment of NVC appears to be specific for cSVD [30]. Recently BBB breakdown has received considerable attention as a cause of cSVD. BBB breakdown may lead to ischaemia, LA and lacunar infarcts [31]. Mild chronic hypertension may damage cerebrovascular endothelium in small vessels leading to thickening of the arterial wall and narrowing of the lumen, resulting in ischaemia (LA if ischaemia occurs in white matter) or infarction. Alternatively, the damage to the arterial wall may progress, causing disintegration and a leak of blood [31]. BBB leak may be visualised as small areas of low signal on T2*-weighted MR images which may be deposits of haemosiderin, a breakdown product of haemoglobin, usually indicating a BMB [32].

Seiffert and colleagues created a model of BBB breakdown-induced epilepsy by perfusing a section of adult rat somatosensory cortex with serum [33]. 77% of slices from treated cortices developed increased excitability compared to sham-operated controls. As the changes in firing rate were only evident four days after treatment, the authors suggest that an accumulation of albumin in the extracellular space due to BBB leak is required for epileptogenesis. More recent work suggests that BBB breakdown may lead to changes in astrocyte gene expression in astrocytes, which predicts impaired uptake of extracellular potassium [34]. The increased extracellular K+ may facilitate the conduction of excessive neuronal discharges, resulting in epilepsy [35]. However, the results of these animal experiments may not be applicable to human patients with epilepsy. Furthermore, to determine whether BBB breakdown in this model is truly occult, the motor cortex could be perfused with serum and the animals' motor function observed.

Novel MRI techniques to assess BBB opening could complement functional MRI to offer a fascinating insight into neurovascular unit function in terms of metabolism, neurovascular response, and BBB integrity. For example, there is increasing interest in the use of dynamic contrast-enhanced MRI in a range of conditions, including ageing and cerebral microvascular disease [36]. The prospect of applying this technique in patients with LOE is appealing.

6.3. Cerebral Amyloid Angiopathy: A Case Study in Neurovascular Unit Disruption and Epileptogenesis. Cerebral amyloid angiopathy (CAA) is a disorder caused by the accumulation of amyloid in cerebral vessels which leads to progressive dysfunction of the neurovascular unit, failure of vascular reactivity, smooth muscle cell loss, and eventual breakdown of vessel integrity [37]. CAA is associated with BMBs and recurrent lobar intracerebral haemorrhage. It is an increasingly recognised disorder in the elderly and can

be associated with recurrent seizures. Other manifestations include white matter disease, cortical infarcts, and cognitive dysfunction. Transient neurological events characterised by spread of symptoms to contiguous body areas during episodes, in keeping with seizures, have been described in CAA [38]. Seizures have also been reported in CAA by other workers [39]. CAA-associated vascular inflammation has also been described in a subset of CAA patients presenting with cognitive decline and seizures [40]. Further studies of neurovascular unit dysfunction in CAA and the potential relationship with epileptogenesis may prove valuable.

7. Conclusion

Occult CVD may cause LOE via neurovascular unit dysfunction, namely, producing changes in (CBF) and/or disruption of the (BBB). We have demonstrated the feasibility of a novel MRI technique to investigate NVC, reflecting underlying neurovascular unit integrity, in this population. Further studies will be important given the likely increasing burden of CVD and its complications in an ageing population. Increasing recognition of entities such as CAA is likely to provide further opportunities for research in this area. At the current time, conventional imaging techniques remain the mainstay of the identification of otherwise occult CVD, and it is evidence such as this that should prompt screening for other vascular risk factors and the initiation of appropriate vascular secondary prevention measures.

Acknowledgments

L. M. Gibson received a generous award from the Wolfson Foundation in order to fund an intercalated degree in Neuroscience, during which initial work on the hypothesis and pilot study detailed above was completed. This work has been presented internationally and published in abstract form [41, 42]

References

[1] I. Craig and R. C. Tallis, "General practitioner management of adult-onset epilepsyanalysed," *Care Elderly*, vol. 3, pp. 69–72, 1991.

[2] R. Tallis, G. Hall, I. Craig, and A. Dean, "How common are epileptic seizures in old age?" *Age and Ageing*, vol. 20, no. 6, pp. 442–448, 1991.

[3] J. Burn, M. Dennis, J. Bamford, P. Sandercock, D. Wade, and C. Warlow, "Epileptic seizures after a first stroke: the Oxfordshire community stroke project," *British Medical Journal*, vol. 315, no. 7122, pp. 1582–1587, 1997.

[4] P. Cleary, S. Shorvon, and R. Tallis, "Late-onset seizures as a predictor of subsequent stroke," *The Lancet*, vol. 363, no. 9416, pp. 1184–1186, 2004.

[5] C. L. M. Sudlow, "Epilepsy and stroke," *The Lancet*, vol. 363, no. 9416, pp. 1175–1176, 2004.

[6] C. Cordonnier, R. Al-Shahi Salman, and J. Wardlaw, "Spontaneous brain microbleeds: systematic review, subgroup analyses and standards for study design and reporting," *Brain*, vol. 130, no. 8, pp. 1988–2003, 2007.

[7] B. R. Reed, J. L. Eberling, D. Mungas, M. Weiner, J. H. Kramer, and W. J. Jagust, "Effects of white matter lesions and lacunes on cortical function," *Archives of Neurology*, vol. 61, no. 10, pp. 1545–1550, 2004.

[8] R. B. Buxton, K. Uludağ, D. J. Dubowitz, and T. T. Liu, "Modeling the hemodynamic response to brain activation," *NeuroImage*, vol. 23, supplement 1, pp. S220–S233, 2004.

[9] L. M. Parkes and P. S. Tofts, "Improved accuracy of human cerebral blood perfusion measurements using arterial spin labeling: accounting for capillary water permeability," *Magnetic Resonance in Medicine*, vol. 48, no. 1, pp. 27–41, 2002.

[10] P. Jezzard and R. B. Buxton, "The clinical potential of functional magnetic resonace imaging," *Journal of Magnetic Resonance Imaging*, vol. 23, no. 6, pp. 787–793, 2006.

[11] S. Kobayashi, K. Okada, and K. Yamashita, "Incidence of silent lacunar lesion in normal adults and its relation to cerebral blood flow and risk factors," *Stroke*, vol. 22, no. 11, pp. 1379–1383, 1991.

[12] H. Nakane, S. Ibayashi, K. Fujii et al., "Cerebral blood flow and metabolism in patients with silent brain infarction: occult misery perfusion in the cerebral cortex," *Journal of Neurology Neurosurgery and Psychiatry*, vol. 65, no. 3, pp. 317–321, 1998.

[13] J. De Reuck, D. Decoo, P. Boon, K. Strijckmans, P. Goethals, and I. Lemahieu, "Late-onset epileptic seizures in patients with leukoaraiosis: a positron emission tomographic study," *European Neurology*, vol. 36, no. 1, pp. 20–24, 1996.

[14] R. A. Trivedi, H. A. L. Green, J. U-King-Im et al., "Cerebral haemodynamic disturbances in patients with moderate carotid artery stenosis," *European Journal of Vascular and Endovascular Surgery*, vol. 29, no. 1, pp. 52–57, 2005.

[15] T. L. Davis, K. K. Kwong, R. M. Weisskoff, and B. R. Rosen, "Calibrated functional MRI: mapping the dynamics of oxidative metabolism," *Proceedings of the National Academy of Sciences of the United States of America*, vol. 95, no. 4, pp. 1834–1839, 1998.

[16] P. A. Chiarelli, D. P. Bulte, R. Wise, D. Gallichan, and P. Jezzard, "A calibration method for quantitative BOLD fMRI based on hyperoxia," *NeuroImage*, vol. 37, no. 3, pp. 808–820, 2007.

[17] J. A. Goodwin, R. Vidyasagar, G. M. Balanos, D. Bulte, and L. M. Parkes, "Quantitative fMRI using hyperoxia calibration: reproducibility during a cognitive Stroop task," *NeuroImage*, vol. 47, no. 2, pp. 573–580, 2009.

[18] D. P. Bulte, K. Drescher, and P. Jezzard, "Comparison of hypercapnia-based calibration techniques for measurement of cerebral oxygen metabolism with MRI," *Magnetic Resonance in Medicine*, vol. 61, no. 2, pp. 391–398, 2009.

[19] T. H. Schwartz, "Neurovascular coupling and epilepsy: hemodynamic markers forlocalizing and predicting seizure onset," *Epilepsy Current*, vol. 7, no. 4, pp. 91–94, 2007.

[20] C. S. Hawco, A. P. Bagshaw, Y. Lu, F. Dubeau, and J. Gotman, "BOLD changes occur prior to epileptic spikes seen on scalp EEG," *NeuroImage*, vol. 35, no. 4, pp. 1450–1458, 2007.

[21] J. Valmier, J. Touchon, and M. Baldy-Moulinier, "Interictal regional cerebral blood flow during non specific activation test in partial epilepsy," *Journal of Neurology Neurosurgery and Psychiatry*, vol. 52, no. 3, pp. 364–371, 1989.

[22] L. Niehaus, U. C. Wieshmann, and B. U. Meyer, "Changes in cerebral hemodynamics during simple partial motor seizures," *European Neurology*, vol. 44, no. 1, pp. 8–11, 2000.

[23] R. Wiest, F. von Bredow, K. Schindler et al., "Detection of regional blood perfusion changes in epileptic seizures with dynamic brain perfusion CT-A pilot study," *Epilepsy Research*, vol. 72, no. 2-3, pp. 102–110, 2006.

[24] S. Rupprecht, M. Schwab, C. Fitzek, O. W. Witte, C. Terborg, and G. Hagemann, "Hemispheric hypoperfusion in postictal paresis mimics early brain ischemia," *Epilepsy Research*, vol. 89, no. 2-3, pp. 355–359, 2010.

[25] J. De Reuck and G. Van Maele, "Acute ischemic stroke treatment and the occurrence of seizures," *Clinical Neurology and Neurosurgery*, vol. 112, no. 4, pp. 328–331, 2010.

[26] L. H. Rodan, R. I. Aviv, D. J. Sahlas, B. J. Murray, J. P. Gladstone, and D. J. Gladstone, "Seizures during stroke thrombolysis heralding dramatic neurologic recovery," *Neurology*, vol. 67, no. 11, pp. 2048–2049, 2006.

[27] D. A. Sun, S. Sombati, and R. J. DeLorenzo, "Glutamate injury-induced epileptogenesis in hippocampal neurons: an in vitro model of stroke-induced "epilepsy"," *Stroke*, vol. 32, no. 10, pp. 2344–2350, 2001.

[28] D. A. Sun, S. Sombati, R. E. Blair, and R. J. DeLorenzo, "Long-lasting alterations in neuronal calcium homeostasis in an in vitro model of stroke-induced epilepsy," *Cell Calcium*, vol. 35, no. 2, pp. 155–163, 2004.

[29] C. Terborg, F. Gora, C. Weiller, and J. Röther, "Reduced vasomotor reactivity in cerebral microangiopathy: a study with near-infrared spectroscopy and transcranial Doppler sonography," *Stroke*, vol. 31, no. 4, pp. 924–929, 2000.

[30] M. L. Schroeter, S. Cutini, M. M. Wahl, R. Scheid, and D. Yves von Cramon, "Neurovascular coupling is impaired in cerebral microangiopathy—an event-related Stroop study," *NeuroImage*, vol. 34, no. 1, pp. 26–34, 2007.

[31] J. M. Wardlaw, P. A. G. Sandercock, M. S. Dennis, and J. Starr, "Is breakdown of the blood-brain barrier responsible for lacunar stroke, leukoaraiosis, and dementia?" *Stroke*, vol. 34, no. 3, pp. 806–812, 2003.

[32] G. Roob and F. Fazekas, "Magnetic resonance imaging of cerebral microbleeds," *Current Opinion in Neurology*, vol. 13, no. 1, pp. 69–73, 2000.

[33] E. Seiffert, J. P. Dreier, S. Ivens et al., "Lasting blood-brain barrier disruption induces epileptic focus in the rat somatosensory cortex," *Journal of Neuroscience*, vol. 24, no. 36, pp. 7829–7836, 2004.

[34] Y. David, L. P. Cacheaux, S. Ivens et al., "Astrocytic dysfunction in epileptogenesis: consequence of altered potassium and glutamate homeostasis?" *Journal of Neuroscience*, vol. 29, no. 34, pp. 10588–10599, 2009.

[35] U. Heinemann, S. Gabriel, R. Jauch et al., "Alterations of glial cell function in temporal lobe epilepsy," *Epilepsia*, vol. 41, supplement 6, pp. S185–S189, 2000.

[36] P. A. Armitage, A. J. Farrall, T. K. Carpenter, F. N. Doubal, and J. M. Wardlaw, "Use of dynamic contrast-enhanced MRI to measure subtle blood-brain barrier abnormalities," *Magnetic Resonance Imaging*, 2010. Epub ahead of print.

[37] G. J. Zipfel, H. Han, A. L. Ford, and J. M. Lee, "Cerebral amyloid angiopathy progressive disruption of the neurovascular unit," *Stroke*, vol. 40, no. 3, supplement, pp. S16–S19, 2009.

[38] S. M. Greenberg, J. P. G. Vonsattel, J. W. Stakes, M. Gruber, and S. P. Finklestein, "The clinical spectrum of cerebral amyloid angiopathy: presentations without lobar hemorrhage," *Neurology*, vol. 43, no. 10, pp. 2073–2079, 1993.

[39] K. Karabatsou, B. R. F. Lecky, N. G. Rainov, J. C. Broome, and R. P. White, "Cerebral amyloid angiopathy with symptomatic or occult subarachnoid haemorrhage [1]," *European Neurology*, vol. 57, no. 2, pp. 103–105, 2007.

[40] C. Kinnecom, M. H. Lev, L. Wendell et al., "Course of cerebral amyloid angiopathy-related inflammation," *Neurology*, vol. 68, no. 17, pp. 1411–1416, 2007.

[41] L. M. Gibson, L. M. Parkes, and H. C. A. Emsley, "Occult cerebrovascular disease in late-onset epilepsy: a literature review and novel hypothesis," in *Proceedings of the 18th Meeting of the European Neurological Society*, Nice, France, June 2008, (poster).

[42] L. M. Gibson, L. M. Parkes, and H. C. A. Emsley, "Occult cerebrovascular disease in late-onset epilepsy: a literature review and novel hypothesis," *Journal of Neurology*, vol. 255, supplement 2, p. 102, 2008.

Hindawi Publishing Corporation
Cardiovascular Psychiatry and Neurology
Volume 2011, Article ID 646958, 9 pages
doi:10.1155/2011/646958

Research Article

Slice Cultures as a Model to Study Neurovascular Coupling and Blood Brain Barrier In Vitro

Richard Kovács, Ismini Papageorgiou, and Uwe Heinemann

Institute for Neurophysiology, Charité-Universitätsmedizin Berlin, Oudenarder Strasse 16, 13347 Berlin, Germany

Correspondence should be addressed to Richard Kovács, richard.kovacs@charite.de

Received 30 September 2010; Accepted 24 December 2010

Academic Editor: Alon Friedman

Proper neuronal functioning depends on a strictly regulated interstitial environment and tight coupling of neuronal and metabolic activity involving adequate vascular responses. These functions take place at the blood brain barrier (BBB) composed of endothelial cells, basal lamina covered with pericytes, and the endfeet of perivascular astrocytes. In conventional *in vitro* models of the BBB, some of these components are missing. Here we describe a new model system for studying BBB and neurovascular coupling by using confocal microscopy and fluorescence staining protocols in organotypic hippocampal slice cultures. An elaborated network of vessels is retained in culture in spite of the absence of blood flow. Application of calcein-AM either from the interstitial or from the luminal side resulted in different staining patterns indicating the maintenance of a barrier. By contrast, the ethidium derivative MitoSox penetrated perivascular basal lamina and revealed free radical formation in contractile cells embracing the vessels, likely pericytes.

1. Introduction

Proper function of the central nervous system requires a meticulously controlled interstitial environment. Since its composition largely differs from that of blood plasma, its maintenance relies on selective filtering and active transport processes at the blood brain barrier (BBB). In order to keep pace with the energetic demand of neuronal activity, cerebral blood flow is tightly regulated by multiple and only partially understood mechanisms termed as neurovascular coupling. The structural substrate for BBB and neurovascular coupling is the neurovascular unit composed of tight junction coupled endothelial cells, capillary basal lamina covered with smooth muscle cells (SMCs)/pericytes, and the endfeet of perivascular astrocytes [1].

Studies on BBB and neurovascular coupling are frequently done *in vivo* although the exact control of systemic effects is difficult. Accordingly, the conclusions which can be drawn need careful interpretation. Studies on acute brain slices gave us new insights on the regulation of capillary microcirculation [2–5] as well as on consequences of BBB disruption [6, 7]. However, brain slices represent acutely injured tissue with severed BBB and ongoing cell damage that might negatively interfere with the mechanisms of neurovascular coupling [8, 9].

Widely used *in vitro* models of BBB are based on different cocultures of endothelial cells and astrocytes [10]. However, such models dismiss the intimate influence of the surrounding nervous tissue, pericytes, and perivascular microglia on the development and function of BBB.

Organotypic brain slice cultures [11, 12] gained popularity after the invention of Stoppini's method of culturing on a membrane surface [13]. Although slice cultures retain the cellular diversity of the CNS, most of the studies focused exclusively on the neuronal compartment. One of the few exceptions was a promising approach for modeling BBB by cultivating brain slices on top of confluent endothelial cell cultures [14, 15]. We wondered whether functional and structural properties of the neurovascular unit and BBB are maintained within slice cultures and thus offer the possibility to study neurovascular coupling and transport processes at the BBB *in situ*.

Moser and colleges were the first to describe the survival of endothelial cells and vessel-like structures in organotypic slice cultures from rat cortex [16]. More recently, intactness of basal laminae, expression of structural components like tight junction and transport proteins as well as ensheathment of the vessels by GFAP positive astrocytes were demonstrated by immunofluorescence in slice cultures from mice [17, 18]. Thus, structural criteria of BBB seem to be fulfilled in this preparation.

Here we sought to characterize the functional intactness of the neurovascular unit and BBB in hippocampal slice cultures. We developed fluorescent staining protocols allowing for selective labeling of perivascular astrocytes, SMCs, pericytes, and endothelial cells in parallel with measurements of intracellular calcium concentration ($[Ca^{2+}]_i$) in astrocytes, as well as of contraction and reactive oxygen species (ROS) formation in pericytes or in SMCs. We used a combination of bulk and bolus staining methods taking advantage of the selective permeability of the BBB for different dyes.

2. Materials and Methods

Slice cultures were prepared and maintained as described previously [19]. Briefly, 7- to 8-day-old Wistar rat pups were decapitated, the brains were removed and submerged in ice-cold minimal essential medium (MEM) gassed with carbogen (95% O_2, 5% CO_2). Hippocampal slices (400 μm, McIllwain Tissue Chopper, Mickle Laboratories, Guildford, UK) were cut and placed on a culture plate insert (MilliCell-CM, Millipore, Eschborn, Germany). Slice cultures were used for experiments between 3 to 21 days *in vitro*. Culture medium (containing: 50% MEM, 25% Hank's Balanced Salt Solution, 25% Horse Serum, pH 7.4; all from Gibco, Eggenstein, Germany) was replaced three times a week.

Slice cultures were transferred to the recording chamber mounted on an epifluorescent microscope (Olympus BX51WI, Olympus-Europe GmbH, Hamburg, Germany) and were superfused with ACSF (5 mL/min, 30°C), containing (in mM): NaCl 129, KCl 3, NaH_2PO_4 1.25, $MgSO_4$ 1.8, $CaCl_2$ 1.6, $NaHCO_3$ 26, and glucose 10 (pH 7.4). For induction of epileptiform activity, Mg^{2+} was omitted from the perfusion and $[K^+]_o$ was slightly elevated to 5 mM.

Local field potential recordings were performed in area CA3 of slice cultures by using a MultiClamp 700B amplifier (Axon CNS, Molecular Devices, Sunnyvale, California, USA). Fluorescence recordings were performed with a spinning disk confocal microscope (Andor Revolution, BFIOptilas GmbH, Gröbenzell, Germany) equipped with an EMCCD camera (Andor iXonEM+) and a PIFOC fast-piezo z-scanner (Physik Instrumente, Berlin, Germany). Fluorescence was obtained by a 60x water immersion objective (N.A.: 0.9), laser intensity below the objective was below 10 μW for the 491 nm and <50 μW for the 561 nm laser line. In order to minimize photobleaching and interaction of illumination with ROS formation, exposure time was kept short (80–120 ms) and acquisition rate for time series reduced to one z-scan per 3 s for rhod-2 and one z-scan per 20 s for calcein/MitoSox. To avoid movement artifacts due to tissue swelling and apparent movement of the vessels, for each time point 8–12, z-planes were obtained (0.6–1.2 μm steps), containing the whole vessel. At the beginning and at the end of an experiment, a high resolution z-scan (0.3 μm steps) was acquired for volume rendering and 3D reconstruction of the vessels and surrounding astrocytes.

Slice cultures were bulk stained either with MitoSox, (5 μM, 10–60 min) or rhod-2 AM (5 μM, 10–60 min) and calcein-AM (4 μM, 10–60 min) in the incubator at 36°C. All dyes were prepared in DMSO (0.1% in final solution) immediately before each experiment. A bolus of calcein-AM (400 μM, freshly diluted in ACSF from the 4 mM DMSO stock) was applied either in the vicinity of the vessel or into the vessel lumen via a patch pipette and a Picospritzer (50 ms pulses, 7 psi; Toohey Comp. Fairfield, New Jersey, USA). Rhodamine-123 was solved in EtOH, diluted in ACSF to 50–100 μM and either applied as a bolus locally or allowed to leak out from the tip of the pipette.

Crosstalk of MitoSox and calcein fluorescence with tissue auto-fluorescence originating from lipofuscin was controlled in a subset of unstained slice cultures prior to application of the dyes. The nitric oxide (NO) donor S-Nitroso-N-acetyl-DL-penicillamine (SNAP, 100–200 μM) was freshly prepared for each application and was given to the perfusion [20]. SNAP was from ALEXIS Corporation (Lausen, Switzerland); all other chemicals were from Sigma-Aldrich (Taufkirchen, Germany).

Data evaluation and 3D reconstruction were carried out with the acquisition software Andor IQ (BFIOptilas GmbH, Gröbenzell, Germany) and with ImageJ (Wayne Rasband, NIH, USA). Changes in fluorescence over time were evaluated for each fluorescence channel in manually delineated regions of interests (ROI) and are presented as $\Delta f/f_0$ in percent where f_0 represents the average fluorescence from the first 1-2 min of a recording.

Colocalization was analyzed after thresholding for the background noise in selected ROIs containing the vessel, by using the JACoP-plugin [21]. Pearson's and Manders' coefficients were used as a measure of colocalization where value 1 corresponds to complete colocalization and -1 or 0 to anti-colocalization for Pearson's and Manders' coefficients (M_1, M_2), respectively. M_1 and M_2 values represent the fraction of the pixels from the green fluorescence channel overlapping the red fluorescence channel and vice versa. Paired Student's two-tailed t-test was used for comparison between two groups. Statistical significance was defined as $P < .05$. The data are presented as mean ± S.E.M.

3. Results

3.1. Vessels in Organotypic Hippocampal Slice Cultures. By using DIC videomicroscopy, we found an elaborated network of branching voids in hippocampal slice cultures, representing the remainders of vessels down to the capillary level (~5 μm diameter). The distribution closely resembled that of the hippocampus *in situ* [22] but numerous solitary vessels ending blind at both ends were also present. Larger vessels entered the hippocampus from the fissure and went

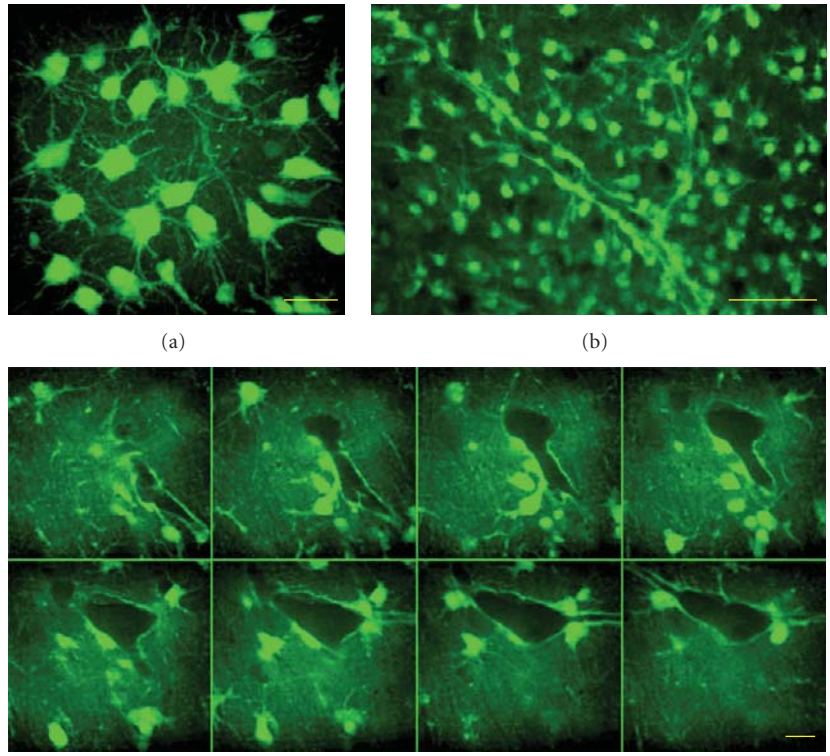

(a) (b)

(c)

Figure 1: Calcein labeling of astrocytes in hippocampal slice cultures. (a) Representative 3D reconstruction of calcein labeled astrocytes in the stratum radiatum of a hippocampal slice culture after short-term (~10 min) bulk staining with calcein-AM. (b) Lower magnification (20x objective) image of calcein labeled astrocytes in the stratum lacunosum moleculare. Note the subset of astrocytes covering a large vessel. (c) Representative series of confocal images from a vessel (1.2 μm steps). Calcein-labeled astrocytes and fine astrocytic processes were present in the neuropil but no calcein fluorescence could be observed within the lumen of the vessel. Astrocytic endfeet completely ensheathed the vessel. Scale bars represent 10 μm in (a, c) and 100 μm in (b).

along the border between the dentate gyrus and stratum lacunosum moleculare of the CA1 and CA3 giving rise to collaterals penetrating the stratum radiatum and pyramidale. In the stratum pyramidale and oriens blind ending solitary voids overwhelmed, as the branching vessels outreach the plane of cutting. Although vessels were present in the whole depth of the slice cultures (~250 μm), only the vessels in the upper 50 μm were used in the present study for imaging reasons. The number of vessels decreased with time in culture as described previously for slice cultures of mice [17]. Nevertheless, fragmentary vessels were still present after three weeks in culture.

3.2. Ca^{2+}-Imaging in Perivascular and Parenchymal Astrocytes. Short-term (~10 min) bulk staining of slice cultures with calcein-AM led to an almost exclusive labeling of astrocytes and microglia (Figures 1(a) and 1(b)), whereas calcein accumulation in neurons occurred only after >40 min staining. Astrocytes and microglia could be easily distinguished in the upper 50 μm of the slice cultures as the latter showed filopodial movements and accumulated calcein in vesicles rather than in the cytosol unlike astrocytes (see also Figure 3(c)). Vessels were completely ensheathed by cell bodies and endfeet of astrocytes (Figure 1(c)). Endfeet often originated from astrocytes located in the parenchyma in distances of up to ~30 μm. The selectivity of calcein-AM for astrocytes allowed us to compare Ca^{2+} transients in parenchymal and perivascular astrocytes by colabeling of slice cultures with the AM ester form of the calcium sensitive red fluorescent probe, rhod-2 (Figures 2(a) and 2(b)). Although rhod-2 AM accumulates in mitochondria due to its net positive charge, there is still a significant amount of dye de-esterified and captured in the cytosol [23]. Astrocytes with or without contact to the vessels (perivascular and parencyhmal) were identified prior to Ca^{2+}-imaging by 3D reconstruction of the calcein-labeled astrocytic network. As an example of activity-dependent changes in astrocytic $[Ca^{2+}]_i$, low-Mg^{2+} induced epileptiform activity associated Ca^{2+} transients in astrocytes are shown in Figure 2(c). Neither the duration (15.1 ± 2.5 s versus 15.8 ± 1.4 s) nor the relative amplitude ($25.9 \pm 10.6\%$ versus $23.2 \pm 6.2\%$) of the Ca^{2+} transients were different between perivascular and parenchymal astrocytes ($n = 48$ and 52 astrocytes from 5 cultures). Occasionally, Ca^{2+} transients in parenchymal astrocytes were synchronized with the transients in perivascular astrocytes. Taken into account their strategic role in neurovascular coupling, this suggests that perivascular astrocytes translate Ca^{2+} signals from a larger astrocytic network to the vascular unit.

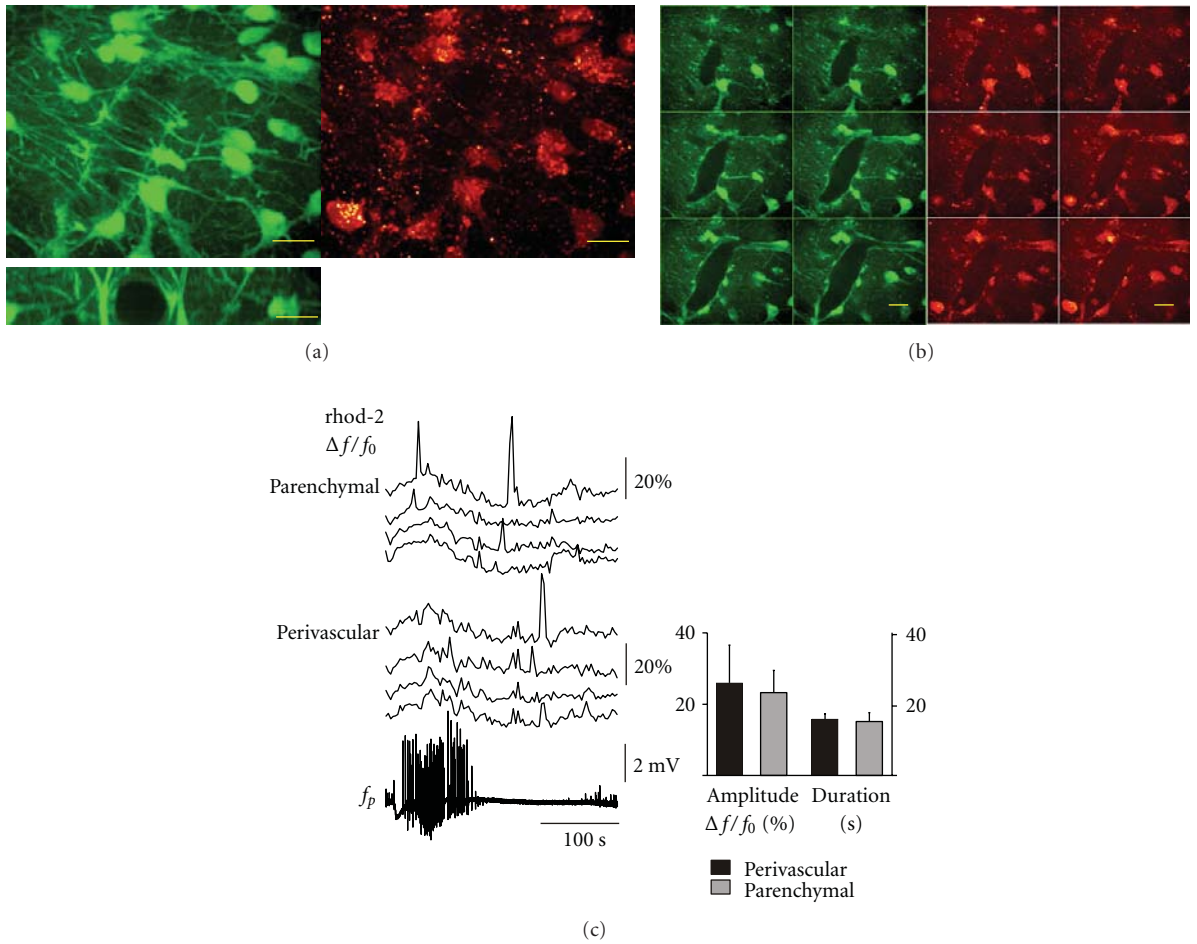

Figure 2: Ca^{2+}-imaging in perivascular and parenchymal astrocytes. (a) 3D reconstruction of the astrocytic network covering a vessel after colabeling the slice culture with calcein-AM (green fluorescence channel) and rhod-2 AM (red fluorescence channel). Note the considerable cytosolic rhod-2 fluorescence besides the presence of the rhod-2 labeled mitochondria in the neuropil. The excerpt on the left shows the cross-section of the same vessel. (b) Z-series of confocal images (1.2 μm steps) from the same vessel were used to distinguish between perivascular and parenchymal astrocytes, that is, with or without contact to the wall of the vessel. Scale bars in (a) and (b) represent 10 μm. (c) Comparison of $[Ca^{2+}]_i$ transients between perivascular and parenchymal astrocytes during low Mg^{2+}-ACSF induced epileptiform activity. Seizure-like events (lower trace: field potential) were associated with slight elevation of astrocytic $[Ca^{2+}]_i$ and were followed by large amplitude $[Ca^{2+}]_i$ transients. There were no statistical differences in amplitude or duration of $[Ca^{2+}]_i$ transients between perivascular and parenchymal astrocytes.

3.3. Diffusion Barrier around the Vessel Lumen in Slice Cultures. Remarkably, neither calcein-AM nor rhod-2 AM were able to stain cells below the basal membrane in slice cultures bulk stained for ~10 min. Even after one-hour staining the fluorescence of both, rhod-2 and calcein remained significantly lower within a vessel as compared with the surrounding astrocytes (Figure 3(a)). By contrast, endothelial cells and pericytes showed bright calcein labeling if calcein-AM was pressure applied into the lumen after penetration with a patch pipette (Figure 3(b)). This implicates the presence of a barrier preventing or delaying diffusion of the dye into the vessel in case of the bulk staining.

Calcein-AM application into a vessel led to an immediate rise of the fluorescence within the lumen, followed by a slow redistribution into the cellular elements of the vessel within a restricted area (Figure 3(b)). By contrast, application of calcein-AM at a random location into the stratum pyramidale resulted in a widespread (>50 μm) rise in fluorescence in astrocytes neurons and microglia (Figure 3(c)). In a subsequent set of experiments, we puffed a bolus of the membrane permeable mitochondrial marker, rhodamine-123 into the vessel in slice cultures previously bulk-stained with calcein-AM in the incubator (10 min). After intraluminal bolus application, rhodamine-123 fluorescence rose rapidly in mitochondria of endothelial cells and putative pericytes/SMCs (see below) but not in astrocytes adjacent to the wall of the vessel (Figures 4(b) and 4(c)). Although perforation of the vessel with the patch pipette disrupted the BBB, the leakage of rhodamine-123 from the lumen was minimal suggesting resealing of the membrane around the neck of the pipette.

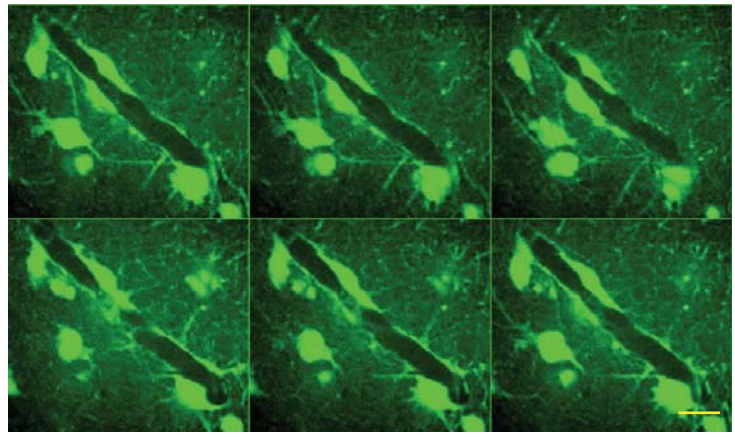

(a)

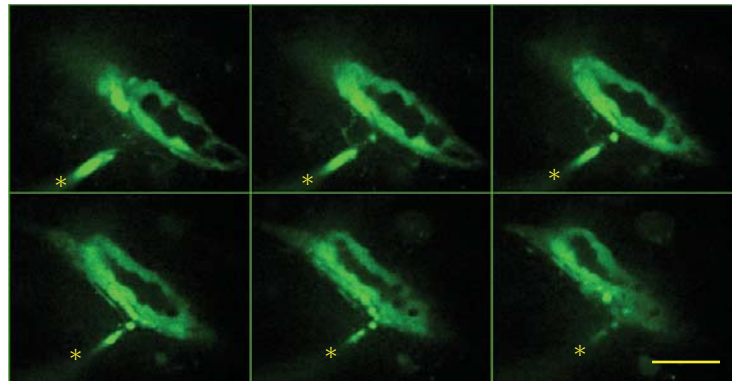

(b)

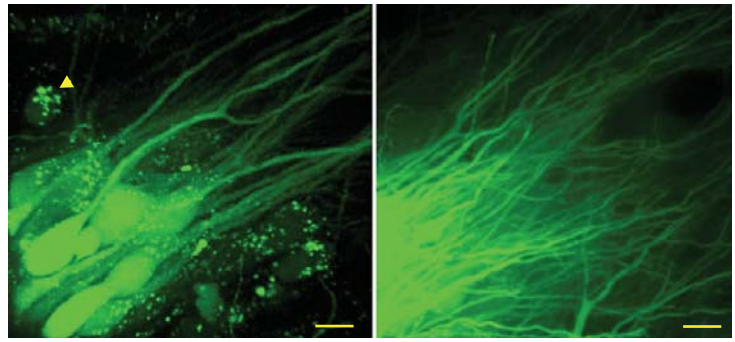

(c)

Figure 3: Diffusion barrier around the vessel lumen in slice cultures. (a) Z-series of confocal images (1.2 μm) from a vessel after long-term (60 min) bulk staing with calcein-AM in the incubator. Note that calcein fluorescence below the astrocytic endfeet is almost absent, indicating a diffusion barrier and/or powerful extrusion mechanisms in endothelial cells. (b) Z-series of confocal images (1.2 μm) from a vessel after bolus application of calcein-AM into the lumen of a vessel. Endothelial cells showed bright calcein fluorescence, whereas no fluorescence was observed in astrocytes outside of the vessel. The asterisks on the consecutive images represent the application pipette. (c) Bolus application of calcein-AM into the stratum pyramidale resulted in a neuronal/astrocytic/microglial labeling up to 80 μm distance from the application place (left). Arrowhead marks a microglial cell containing calcein in vesicles. Calcein within neuronal processes can travel for several 100 μm (right). Scale bars represent 10 μm.

The restriction of calcein fluorescence within the boundaries of a vessel in case of bolus application and the exclusion of the dye from the vessels in case of bulk staining clearly indicated the presence of a vascular diffusion barrier related to BBB in slice cultures.

3.4. Vasomotility in Slice Cultures. An important observation in the previous experiments was that pressure application into the lumen invariably led to vasoconstriction, indicating the presence of contractile cells, that is, SMCs or pericytes. Fortunately, these cells could be selectively labeled with

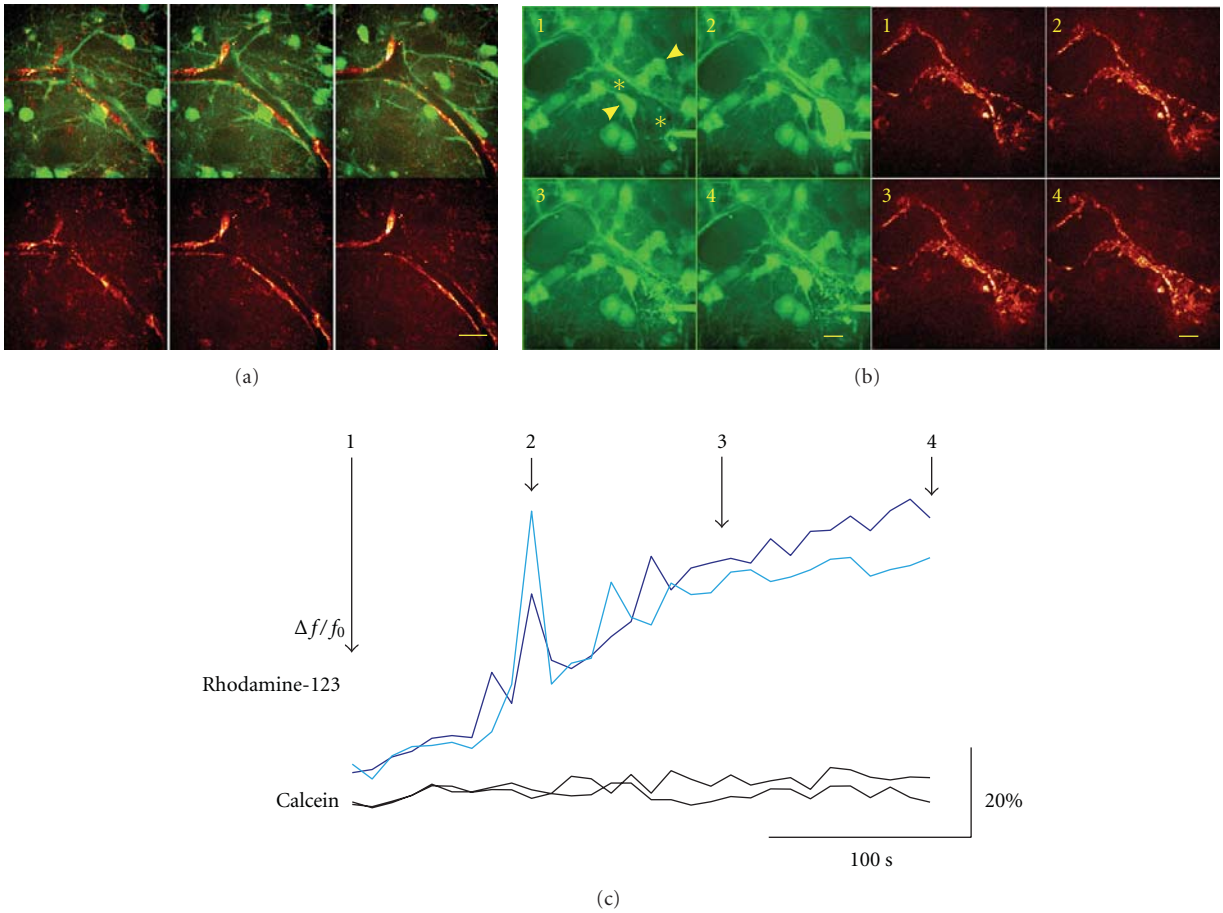

Figure 4: Mitochondrial free radical formation in pericytes/smooth muscle cells. (a) Representative Z-series of confocal images (1.2 μm) of a vessel double labeled with calcein-AM (green fluorescence channel—upper pictures) and MitSox (red fluorescence channel). MitoSox revealed free radical formation in spindle-shaped contractile cells associated with the wall of a vessel. MitoSox was anti-colocalized with calcein in pericytes/smooth muscle cells indicating low free radical formation in astrocytic endfeet. (b) 3D reconstruction of a vessel double labeled with calcein/MitoSox. The pictures are examples taken at four time points (as marked in (c)) during bolus application of rhodamine-123 into the intraluminal space. Both, calcein and rhodamine-123 fluorescence are represented in the green fluorescence channel (left) whereas the red fluorescence channel (right) corresponds to MitoSox labeling. After penetration of the vessel with the pipette, the lumen becomes slightly fluorescent due to leakage of rhodamine-123. Intraluminal rhodamine-123 fluorescence rapidly increased during bolus application, followed by redistribution of the dye into mitochondria within the vessel. No rise in the rhodamine-123 fluorescence was observed in the surrounding astrocytes. MitoSox almost completely colocalized with rhodamine-123 revealing mitochondrial origin of free radicals in pericytes/smooth muscle cells. Note the contraction of the vessel as a consequence of the increased intraluminal pressure. Scale bars represent 10 μm. (c) Changes in calcein (black traces) and rhodamine-123 (blue traces) fluorescence during bolus application of rhodamine-123 as measured in perivascular astrocytes (calcein, marked with arrowheads in (b)) and within the vessel lumen (rhodamine-123, marked with asterisks in (b)). Note that in spite of the physical contact of the astrocytic endfeet with the vessel wall, no rhodamine-123 appeared in astrocytes, further substantiating the presence of a diffusion barrier related to BBB.

another fluorescence probe in slice cultures. Bulk staining with MitoSox, a mitochondrially targeted fluorescent probe for superoxide radicals led to intense labeling of contractile cells associated with vessels, likely SMCs and pericytes (Figures 4(a) and 4(b)). Several SMCs covered the wall of larger vessels whereas solitary spindle-shaped cells were associated with small diameter (<10 μm) vessels, appearing frequently at branching points with two lengthy processes embracing the capillary. MitoSox fluorescence in SMCs and pericytes showed a dotted pattern, which is expected for a mitochondrially targeted dye. A similar dotted pattern was observed in the surrounding neuropil, but with significantly lower intensity (Figure 4(a)). In order to prove that those organelles are mitochondria, we applied a mitochondrial marker, rhodamine-123 to the immediate vicinity of the pericytes. Rhodamine-123 is a positively charged, membrane permeable fluorescent probe which can be loaded into cells via a patch pipette in cell-attached or whole cell mode and accumulates in mitochondria maintaining a negative membrane potential (~160 mV) against the cytosol [23]. After establishing the contact, MitoSox positive organelles become heavily stained with rhodamine-123

(Pearsons' coefficient: 0.5 ± 0.1, M_1 (rhodamine-123 to MitoSox): 0.55 ± 0.05M_2 (MitoSox to rhodamine-123): 0.69 ± 0.05) and showed typical mitochondrial movements (wiggling and directed "run and stop" sequences), thus verifying that MitoSox fluorescence originated from mitochondria (Figure 4(b)). When slice cultures were colabeled with MitoSox and calcein-AM, MitoSox was anticolocalized with calcein at the vessels (Pearson's coefficient: −0.12 ± 0.05; $n = 14$). MitoSox is an ethidium derivative, which is essentially nonfluorescent in its reduced form and its fluorescence increases when oxidized, mainly by superoxide [24]. Differences in the intensity of MitoSox fluorescence between astrocytes and putative pericytes or SMCs might represent either differences in rate of oxidation by ROS or differences in the rate of dye accumulation. Occasionally, sudden rise in MitoSox fluorescence occurred in microglial cells after more than 40 min perfusion with dye-free ACSF. This indicates that oxidation of MitoSox by ROS, rather than the accumulation of its reduced form, is responsible for the MitoSox fluorescence in our preparation. Consequently, intense MitoSox fluorescence in SMCs and in pericytes is caused by a higher mitochondrial ROS formation as compared to the surrounding astrocytes/neuropil. Differences in the Manders' coefficients M_1 (calcein to MitoSox): 0.042 ± 0.006 and M_2 (MitoSox to calcein): 0.34 ± 0.04 correspond to slight ROS formation in astrocytes but no calcein uptake into pericytes or SMCs.

Mechanical stimulation or increasing intraluminal pressure elicited a contraction of SMCs and pericytes leading to vasoconstriction (Figure 4(b)). On the other hand, application of the powerful vasodilatator, NO (SNAP, 100–200 μM, $n = 6$) did not cause vasodilatation. This suggested that capillaries in slice cultures are maximally dilated in absence of blood flow. Nevertheless, SMCs and pericytes still retained their contractile activity for several weeks in culture, which allows the use of slice cultures as a tool for studying neurovascular coupling *in vitro*.

4. Discussion

In the present study, we characterized the structural and functional properties of the neurovascular unit and the BBB *in vitro* in hippocampal slice cultures. We developed fluorescence staining protocols allowing for selective labeling of different cell types of the neurovascular unit. Capillaries and vessels survived and retained their organotypic structure in culture and importantly, their lumen was segregated from the interstitium by a diffusion barrier related to BBB. Vasomotion mediated by pericytes or SMCs was also present even after three weeks in culture. Perivascular astrocytes, astrocytic endfeet, pericytes, and SMCs can be identified and selectively monitored by using our staining protocols and are accessible for electrophysiological recordings. Similarly to acute slices, pH, pO_2, $[K^+]_o$, and $[Ca^{2+}]_o$ are easily manipulated in slice cultures whereas the major disadvantage of acute slices, the ongoing cell damage, is negligible after a few days in culture [19]. Thus, slice cultures offer a unique possibility to study the neurovascular unit and the BBB *in vitro*.

4.1. BBB in Slice Cultures. Intactness of BBB can be hardly studied in acute slices, as the preparation opens the vessels and eliminates their function as barrier [25]. By contrast, vessels reseal in slice cultures leading to formation of small enclosures of interstitial fluid. Intactness of basal lamina and the presence of tight junctional as well as transport proteins on endothelial cells were recently reported in slice cultures from mice [17, 18]. By applying calcein-AM either from the parenchymal or from the luminal side, we were able to show that these structures operate as a barrier. The BBB in slice cultures excluded calcein-AM and rhod 2-AM but not MitoSox from the vessels. The absence of calcein and rhod-2 fluorescence in endothelial cells, pericytes, and SMCs might be related to the fact that AM-esters of calcium dyes and especially of calcein are substrates of multidrug transport proteins, also expressed on the vessels in slice cultures [18, 26]. Thus slow diffusion of these dyes through the basal lamina might be counterbalanced by the activity of multidrug transport proteins at the luminal surface of BBB, finally leading to intraluminal accumulation of the nonfluorescent AM-esters.

Currently, we could not assert that tightness of BBB in slice cultures corresponds to that found *in vivo*. Nonetheless, the conditions and the cellular components necessary for the development of BBB are more close to the *in vivo* situation than in case of cocultures of endothelial cells and astrocytes [1]. Accordingly, the tightness of the artificial BBB in the combined slice culture—endothelial cell culture model, is exceedingly high [14, 15].

It is to note that the selectivity of calcein-AM for astrocytes in case of a short term bulk staining is characteristic for slice cultures, whereas in acute slices both neurons and glia were stained when applying the same protocol. One possible explanation might be a difference in esterase activity between neurons and astrocytes in culture. Alternatively, an up-regulation of multidrug transport proteins on neurons in slice culture might delay accumulation of calcein-AM.

4.2. Neurovascular Coupling and Vascular ROS Formation in Slice Cultures. Pressure application of different dyes into the lumen of a vessel revealed the presence and functional intactness of contractile cellular elements, namely, pericytes and SMCs in slice cultures. At present, we could only elicit vasoconstriction but no vasodilatation in our model. The most likely explanation is that vessels in cultures are maximally dilated in absence of blood flow and shear stress. Intraluminal dye application increases shear stress thereby leading to vasoconstriction indicating intact autoregulation of vascular tone. Alternatively, the NO-cGMP signalling pathway in pericytes/SMCs might be also altered in culture. Nevertheless, our experiments were carried out in the presence of 95% O_2, which also favor vasoconstriction rather than vasodilatation [27]. Whether vasodilatation can be induced in preconstricted vessels awaits further investigation.

In vivo studies on pericytic regulation of microcirculation have to take into account that capillaries passively follow

upstream changes in blood flow [9]. The absence of blood flow is an advantage of slice cultures, since only the active contractile responses are represented by changes in capillary diameter.

To our knowledge, this study is the first description of selective labeling of brain capillary pericytes and vascular SMCs with MitoSox. Free radical signaling is important in regulation of vasomotility [8, 28] and increased ROS formation was suggested to be involved in obstruction of microcirculation after hypoxia-reperfusion [29]. Oxygen glucose deprivation is frequently investigated in slice cultures but less attention was paid to the vascular compartment [30]. Besides their acute effects on SMCs and pericytes, oxygen glucose deprivation might cause lasting alterations of vascular function, which can be followed for weeks in culture. Understanding the mechanisms underlying free radical formation in the neurovascular unit might lead to improvement of neuroprotective strategies in stroke.

Most studies on pericytic ROS formation focus on pathological up-regulation of cytosolic NADPH oxidase activity [31]. In our preparation, mitochondria seem to significantly contribute to ROS formation in pericytes and SMCs. An interesting coincidence can be found with the study of Dai and colleagues who showed that cochlear pericytes can be selectively visualized *in vivo* by using the NO sensitive fluorescent probe DAF-2 [32]. They hypothesized that pericytes express neuronal NO synthase, and the resulting NO in addition to NO from endothelial cells leads to the intensive labeling of pericytes. Our findings offer an alternative explanation. DAF-2 fluorescence might be also influenced by increased superoxide and peroxynitrite formation, as DAF-2 reacts with oxidative derivatives of NO, rather than NO itself [20]. Consequently, the more intense labeling of pericytes with DAF-2 as compared to endothelial cells might indicate elevated ROS formation in addition to NO.

Pericytic ROS formation might also negatively interfere with the tightness and function of BBB [33]. ROS mediated deregulation of neurovascular coupling and BBB breakdown are of high clinical relevance occurring in different neurological disorders like epilepsy and Alzheimer's disease [34]. Initial BBB breakdown and subsequent angiogenesis might contribute to the progression of certain epilepsies [34, 35]. Amyloid deposits around capillaries and within degenerating pericytes were described in early onset familial Alzheimer's disease. Pericytes represent a clearance pathway for β-amyloid, but in turn, β-amyloid might impair pericytic control of vascular diameter in a free radical dependent manner [36]. An additional advantage of slice cultures is that they allow for pretreatment either with protective substances [37] or with pathogens like β-amyloid [30].

As diseases affecting the neurovascular unit seem to share some common mechanisms, future studies will take advantage of the possibility for selective monitoring of Ca^{2+}-signaling in astrocytic endfeet as well as contraction and ROS formation in pericytes/SMCs.

Acknowledgments

This work was supported by the Deutsche Forschungsgemeinschaft (SFB TR3) to R. Kovács and I. Papageorgiou and by the Hertie Foundation and NeuroCure Cluster of Excellence to UH.

References

[1] S. Banerjee and M. A. Bhat, "Neuron-glial interactions in blood-brain barrier formation," *Annual Review of Neuroscience*, vol. 30, pp. 235–258, 2007.

[2] M. Zonta, M. C. Angulo, S. Gobbo et al., "Neuron-to-astrocyte signaling is central to the dynamic control of brain microcirculation," *Nature Neuroscience*, vol. 6, no. 1, pp. 43–50, 2003.

[3] C. Iadecola, "Neurovascular regulation in the normal brain and in Alzheimer's disease," *Nature Reviews Neuroscience*, vol. 5, no. 5, pp. 347–360, 2004.

[4] S. J. Mulligan and B. A. MacVicar, "Calcium transients in astrocyte endfeet cause cerebrovascular constrictions," *Nature*, vol. 431, no. 7005, pp. 195–199, 2004.

[5] J. A. Filosa, A. D. Bonev, S. V. Straub et al., "Local potassium signaling couples neuronal activity to vasodilation in the brain," *Nature Neuroscience*, vol. 9, no. 11, pp. 1397–1403, 2006.

[6] E. Seiffert, J. P. Dreier, S. Ivens et al., "Lasting blood-brain barrier disruption induces epileptic focus in the rat somatosensory cortex," *Journal of Neuroscience*, vol. 24, no. 36, pp. 7829–7836, 2004.

[7] Y. David, L. P. Cacheaux, S. Ivens et al., "Astrocytic dysfunction in epileptogenesis: consequence of altered potassium and glutamate homeostasis?" *Journal of Neuroscience*, vol. 29, no. 34, pp. 10588–10599, 2009.

[8] H. Girouard and C. Iadecola, "Neurovascular coupling in the normal brain and in hypertension, stroke, and Alzheimer disease," *Journal of Applied Physiology*, vol. 100, no. 1, pp. 328–335, 2006.

[9] J. A. Filosa, "Vascular tone and neurovascular coupling: considerations toward an improved *in vitro* model," *Front Neuroenergetics*, vol. 2, article 16, 2010.

[10] M. Gumbleton and K. L. Audus, "Progress and limitations in the use of in vitro cell cultures to serve as a permeability screen for the blood-brain barrier," *Journal of Pharmaceutical Sciences*, vol. 90, no. 11, pp. 1681–1698, 2001.

[11] B. H. Gahwiler and F. Hefti, "Guidance of acetylcholinesterase-containing fibres by target tissue in co-cultured brain slices," *Neuroscience*, vol. 13, no. 3, pp. 681–689, 1984.

[12] M. Frothscher and B. H. Gahwiler, "Synaptic organization of intracellularly stained CA3 pyramidal neurons in slice cultures of rat hippocampus," *Neuroscience*, vol. 24, no. 2, pp. 541–551, 1988.

[13] L. Stoppini, P. A. Buchs, and D. Muller, "A simple method for organotypic cultures of nervous tissue," *Journal of Neuroscience Methods*, vol. 37, no. 2, pp. 173–182, 1991.

[14] S. Duport, F. Robert, D. Muller, G. Grau, L. Parisi, and L. Stoppini, "An in vitro blood-brain barrier model: cocultures between endothelial cells and organotypic brain slice cultures," *Proceedings of the National Academy of Sciences of the United States of America*, vol. 95, no. 4, pp. 1840–1845, 1998.

[15] C. M. Zehendner, H. J. Luhmann, and C. R. W. Kuhlmann, "Studying the neurovascular unit: an improved blood-brain barrier model," *Journal of Cerebral Blood Flow and Metabolism*, vol. 29, no. 12, pp. 1879–1884, 2009.

[16] K. V. Moser, R. Schmidt-Kastner, H. Hinterhuber, and C. Humpel, "Brain capillaries and cholinergic neurons persist in organotypic brain slices in the absence of blood flow," *European Journal of Neuroscience*, vol. 18, no. 1, pp. 85–94, 2003.

[17] K. Bendfeldt, V. Radojevic, J. Kapfhammer, and C. Nitsch, "Basic fibroblast growth factor modulates density of blood vessels and preserves tight junctions in organotypic cortical cultures of mice: a new in vitro model of the blood-brain barrier," *Journal of Neuroscience*, vol. 27, no. 12, pp. 3260–3267, 2007.

[18] R. S. Camenzind, S. Chip, H. Gutmann, J. P. Kapfhammer, C. Nitsch, and K. Bendfeldt, "Preservation of transendothelial glucose transporter 1 and P-glycoprotein transporters in a cortical slice culture model of the blood-brain barrier," *Neuroscience*, vol. 170, no. 1, pp. 361–371, 2010.

[19] R. Kovács, R. Gutiérrez, A. Kivi, S. Schuchmann, S. Gabriel, and U. Heinemann, "Acute cell damage after low Mg-induced epileptiform activity in organotypic hippocampal slice cultures," *NeuroReport*, vol. 10, no. 2, pp. 207–213, 1999.

[20] R. Kovács, A. Rabanus, J. Otáhal et al., "Endogenous nitric oxide is a key promoting factor for initiation of seizure-like events in hippocampal and entorhinal cortex slices," *Journal of Neuroscience*, vol. 29, no. 26, pp. 8565–8577, 2009.

[21] S. Bolte and F. P. Cordelières, "A guided tour into subcellular colocalization analysis in light microscopy," *Journal of Microscopy*, vol. 224, no. 3, pp. 213–232, 2006.

[22] A. Andreasen and G. Danscher, "Optical slicing and 3-D characterization of hippocampal capillaries in the rat visualized by autometallographic silver enhancement of colloidal gold particles," *Histochemical Journal*, vol. 29, no. 10, pp. 775–781, 1997.

[23] R. Kovács, J. Kardos, U. Heinemann, and O. Kann, "Mitochondrial calcium ion and membrane potential transients follow the pattern of epileptiform discharges in hippocampal slice cultures," *Journal of Neuroscience*, vol. 25, no. 17, pp. 4260–4269, 2005.

[24] K. M. Robinson, M. S. Janes, and J. S. Beckman, "The selective detection of mitochondrial superoxide by live cell imaging," *Nature Protocols*, vol. 3, no. 6, pp. 941–947, 2008.

[25] K. Jandová, D. Päsler, L. L. Antonio et al., "Carbamazepine-resistance in the epileptic dentate gyrus of human hippocampal slices," *Brain*, vol. 129, no. 12, pp. 3290–3306, 2006.

[26] I. Manzini and D. Schild, "Multidrug resistance transporters in the olfactory receptor neurons of Xenopus laevis tadpoles," *Journal of Physiology*, vol. 546, no. 2, pp. 375–385, 2003.

[27] G. R. J. Gordon, H. B. Choi, R. L. Rungta, G. C. R. Ellis-Davies, and B. A. MacVicar, "Brain metabolism dictates the polarity of astrocyte control over arterioles," *Nature*, vol. 456, no. 7223, pp. 745–750, 2008.

[28] C. Capone, G. Faraco, J. Anrather, P. Zhou, and C. Iadecola, "Cyclooxygenase 1-derived prostaglandin E2 and EP1 receptors are required for the cerebrovascular dysfunction induced by angiotensin II," *Hypertension*, vol. 55, no. 4, pp. 911–917, 2010.

[29] M. Yemisci, Y. Gursoy-Ozdemir, A. Vural, A. Can, K. Topalkara, and T. Dalkara, "Pericyte contraction induced by oxidative-nitrative stress impairs capillary reflow despite successful opening of an occluded cerebral artery," *Nature Medicine*, vol. 15, no. 9, pp. 1031–1037, 2009.

[30] J. Noraberg, F. R. Poulsen, M. Blaabjerg et al., "Organotypic hippocampal slice cultures for studies of brain damage, neuroprotection and neurorepair," *Current Drug Targets: CNS and Neurological Disorders*, vol. 4, no. 4, pp. 435–452, 2005.

[31] B. Lassègue and R. E. Clempus, "Vascular NAD(P)H oxidases: specific features, expression, and regulation," *American Journal of Physiology*, vol. 285, no. 2, pp. R277–R297, 2003.

[32] M. Dai, A. Nuttall, Y. Yang, and X. Shi, "Visualization and contractile activity of cochlear pericytes in the capillaries of the spiral ligament," *Hearing Research*, vol. 254, no. 1-2, pp. 100–107, 2009.

[33] P. Ballabh, A. Braun, and M. Nedergaard, "The blood-brain barrier: an overview: structure, regulation, and clinical implications," *Neurobiology of Disease*, vol. 16, no. 1, pp. 1–13, 2004.

[34] H. Shalev, Y. Serlin, and A. Friedman, "Breaching the blood-brain barrier as a gate to psychiatric disorder," *Cardiovascular Psychiatry and Neurology*, vol. 2009, Article ID 278531, 7 pages, 2009.

[35] X. E. Ndode-Ekane, N. Hayward, O. Gröhn, and A. Pitkänen, "Vascular changes in epilepsy: functional consequences and association with network plasticity in pilocarpine-induced experimental epilepsy," *Neuroscience*, vol. 166, no. 1, pp. 312–332, 2010.

[36] C. Iadecola, L. Park, and C. Capone, "Threats to the mind: aging, amyloid, and hypertension," *Stroke*, vol. 40, no. 3, supplement, pp. S40–S44, 2009.

[37] R. Kovács, S. Schuchmann, S. Gabriel, O. Kann, J. Kardos, and U. Heinemann, "Free radical-mediated cell damage after experimental status epilepticus in hippocampal slice cultures," *Journal of Neurophysiology*, vol. 88, no. 6, pp. 2909–2918, 2002.

Hindawi Publishing Corporation
Cardiovascular Psychiatry and Neurology
Volume 2011, Article ID 169580, 7 pages
doi:10.1155/2011/169580

Research Article

A Novel Algorithm for the Assessment of Blood-Brain Barrier Permeability Suggests That Brain Topical Application of Endothelin-1 Does Not Cause Early Opening of the Barrier in Rats

D. Jorks,[1,2,3] D. Milakara,[1,2,4] M. Alam,[5] E. J. Kang,[1,6] S. Major,[1,2,6] A. Friedman,[7] and J. P. Dreier[1,2,3,6]

[1] *Department of Experimental Neurology, Charité University Medicine Berlin, 10098 Berlin, Germany*
[2] *Center for Stroke Research Berlin, Charité University Medicine Berlin, Charitéplatz 1, 10117 Berlin, Germany*
[3] *Bernstein Center for Computational Neuroscience Berlin, 10115 Berlin, Germany*
[4] *Department of Neuroradiology, Charité University Medicine Berlin, 10098 Berlin, Germany*
[5] *Department of Neurosurgery, Hannover Medical School, 30625 Hannover, Germany*
[6] *Department of Neurology, Charité University Medicine Berlin, 10098 Berlin, Germany*
[7] *Departments of Physiology, Neurosurgery, and Biomedical Engineering, Ben-Gurion University of the Negev, Beersheva 84105, Israel*

Correspondence should be addressed to D. Jorks, de-vi-le.jorks@charite.de

Received 30 October 2010; Accepted 27 January 2011

Academic Editor: Daniela Kaufer

There are a number of different experimental methods for *ex vivo* assessment of blood-brain barrier (BBB) opening based on Evans blue dye extravasation. However, these methods require many different steps to prepare the brain and need special equipment for quantification. We here report a novel, simple, and fast semiquantitative algorithm to assess BBB integrity *ex vivo*. The method is particularly suitable for cranial window experiments, since it keeps the spatial information about where the BBB opened. We validated the algorithm using sham controls and the established model of brain topical application of the bile salt dehydrocholate for early BBB disruption. We then studied spreading depolarizations in the presence and the absence of the vasoconstrictor endothelin-1 and found no evidence of early BBB opening (three-hour time window). The algorithm can be used, for example, to assess BBB permeability *ex vivo* in combination with dynamic *in vivo* studies of BBB opening.

1. Introduction

Blood-brain barrier (BBB) disruption has been investigated in a multitude of experimental studies on cerebral pathologies. These include ischemic stroke, epilepsy, spreading depolarizations (SD) in otherwise healthy naïve tissue [1–4], or effects of detergents such as bile salts [5]. However, the knowledge on the early time course of BBB disruption is limited in these conditions. It is of particular interest for future clinical prevention and treatment of brain disorders associated with BBB impairment to characterize the early phase of BBB opening for the following reasons.

(i) From that moment on, damage of brain tissue can aggravate due to blood components that can now enter the brain without restriction.

(ii) Secondary effects associated with BBB opening such as edema and cerebral hemorrhage may limit the application of early therapies to a certain time window. This, for example, seems to apply to systemic thrombolysis with recombinant tissue plasminogen activator (rt-PA) in ischemic stroke which is limited to the 4.5-hour time window.

(iii) The onset of disruption marks the time point when drugs that are normally kept from entering the brain become

able to cross the barrier. This may be relevant for neuroprotective treatment that has been shown to be most effective when given either before or early after an initial insult. If a given neuroprotectant does not normally pass through the barrier but only crosses the barrier after disruption, it is important to determine whether BBB opening occurs early enough for the neuroprotectant to have a sufficient effect on its target in the parenchyma yet.

Even less is known about early BBB opening in gradually developing focal ischemia since most animal models of focal ischemia are designed to replicate severe sudden onset ischemic events in humans occurring after embolic or thrombotic occlusion of a large vessel. Gradually developing focal ischemia, however, is of similar importance for human stroke. It may, for example, occur in patients with delayed cerebral ischemia after aneurismal subarachnoid hemorrhage or in vasculitides, and so forth.

Here, we compared early BBB opening in rats at three hours in (i) the brain topical endothelin-1 (ET-1) model of focal cerebral ischemia, (ii) SDs propagating through healthy naïve cortex, (iii) the topical bile salt dehydrocholate (DHC) model, and (iv) a sham control. For this purpose we developed a simple, semiquantitative algorithm to assess BBB disruption using the target to background ratio. We chose the brain topical ET-1 model, since it allowed us to induce a gradually developing focal ischemia by titrating the constrictive effect of different concentrations of ET-1 on the cerebral vasculature. This results in features such as the absence of a terminal SD, clearly different to the classical and widely distributed model of middle cerebral artery occlusion. Instead, the brain topical ET-1 model is characterized by clusters of recurrent, prolonged SDs that ride on an ultraslow negative potential shift and lead to a persistent depression of brain electrical activity [6, 7]. Despite the absence of terminal SD, histological assessment indicated previously neuronal death in the cortex exposed to ET-1 [8]. Interestingly, we did not find evidence of early BBB disruption in cortex exposed to ET-1 in the present study in contrast to cortex exposed to DHC that served as a positive control.

2. Materials and Methods

2.1. Animals. Male Wistar rats ($n = 28$; 250–350 g) were anaesthetised with 100 mg/kg body weight thiopental-sodium (Trapanal, BYK Pharmaceuticals, Konstanz, Germany) intraperitoneally, tracheotomised, and artificially ventilated (Effenberger Rodent Respirator, Effenberger Med.-Techn. Gerätebau, Pfaffing/Attel, Germany).

After cannulation of the left femoral artery and vein both vessels were continuously infused with saline solution at 1 mL/h. Body temperature was maintained at $38.0 \pm 0.5^{\circ}$C using a heating pad. At all times during the experiments, mean arterial pressure (MAP; RFT Biomonitor, Zwönitz, Germany) and end-expiratory partial pressure of carbon dioxide (Heyer CO_2 Monitor EGM I, Bad Ems, Germany) were monitored, whereas arterial partial pressure of oxygen (paO_2), carbon dioxide ($paCO_2$), and pH were measured serially using a Compact 1 blood gas analyser (AVL Medizintechnik GmbH, Bad Homburg, Germany).

An open cranial window was implanted as reported previously [9–11]. First, a parietal craniotomy of 7×4 mm was performed using a saline-cooled drill. Then, wax and dental cement (Paladur) were used to build the outer rim of the cranial window. After removal of the dura mater, an inflow tube was inserted in the wax rim to later superfuse the brain cortex with artificial cerebrospinal fluid (aCSF). ACSF containing (mmol/L) K^+ 3, Na^+ 152, Ca^{2+} 1.5, Mg^{2+} 1.2, HCO_3^- 24.5, Cl^- 135, glucose 3.7, and urea 6.7 was equilibrated with a special gas mixture in order to yield physiological pH and partial gas pressures. A second small drill hole in the temporal bone served to later elicit SD by subdural application of potassium chloride (KCl, 150 mmol/L).

Two glass microelectrodes were positioned at the window site in a cortical depth of 300 μm below surface to record the intracortical electrocorticogram (ECoG). Alternate current (AC)-ECoG (bandpass: 0.5–45 Hz) and direct current (DC)-ECoG of each electrode were obtained using a differential amplifier (Jens Meyer, Munich, Germany).

2.2. Experimental Protocols. After surgery, the recording was started, and the cranial window was first superfused with aCSF for one to one and a half hours to obtain baseline parameters. In all four groups, 1 mL of 2% Evans blue was then slowly administered intravenously for five minutes.

Shortly thereafter, DHC (2 mmol/L in aCSF) was applied brain topically in the DHC group (group 1, $n = 8$), while in the sham-operated control group (group 2, $n = 6$), physiological aCSF was applied continuously for the whole period of measurement. In animals of the ET-1 (Sigma-Aldrich inc., Steinheim, Germany) group (group 3, $n = 7$), ET-1 was administered brain topically in stepwise increases from 10^{-8} to 10^{-7} to 10^{-6} mmol/L at one-hour intervals as described previously [11]. In group 4 ($n = 5$), physiological aCSF was applied brain topically in the recording window, while SDs were induced manually with a droplet of KCl in a remote window at three different time points. From the remote window, the SDs propagated to the naïve recording window equipped with the microelectrodes.

Three hours after the potentially BBB compromising events and approximately seven hours after the start of the head surgery (Figure 1), rats of all groups were sacrificed by decapitation. Brains were then extracted, rinsed carefully with saline solution, and preserved in cold 4% paraformaldehyde (PFA) solution for at least 48 hours. Each brain was later cut into five coronal slices of 2 mm thickness at and around the window area. Pictures of all slices were taken at 96 dots per inch (dpi) resolution (1040×1392 pixel) as 48-bit RGB images (16 bits per channel) using a digital microscope camera (magnification $\times 10$) (Leica DFC300 FX Digital Color Camera, Leica Microsystems AG, CH-9435, Heerbrugg, Switzerland).

2.3. Image Processing. In brief, brain slice images were imported as Matlab variables: three-dimensional matrices with the third dimension containing the three color components of the RGB color model, while the other two dimensions represent width and length of the image. In the

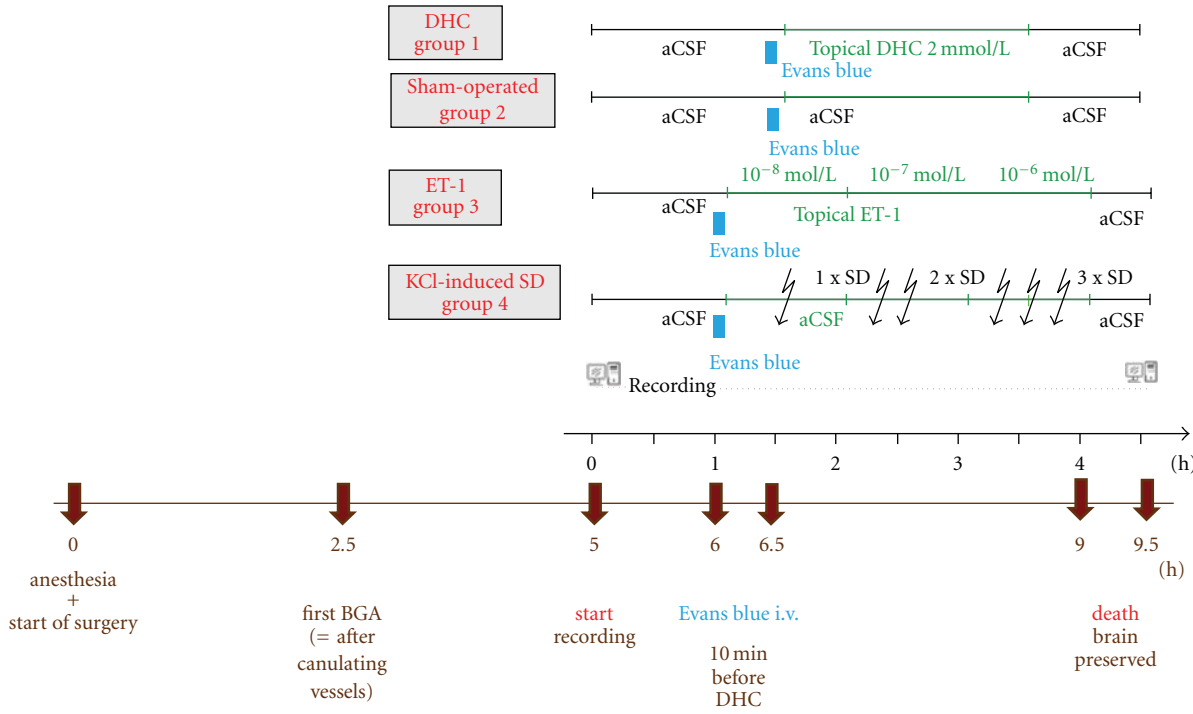

Figure 1: Experimental protocols. For a better overview, the important time points of the experimental protocols are visualized here. The black time line shows the recording period starting at the end of surgery. The brown time line shows the overall experimental time starting from anesthesia until death of the animals. BGA = blood gas analysis.

algorithm, the blue channel is selected from the RGB image which renders the variables two-dimensional for further calculations. Both, the three- and two-dimensional variables are stored in the unsigned integer 16 bit (uint16) format. The minimum intensity of each image was arbitrarily set to zero and the maximum intensity to 2^{16}, the maximum value of the uint16 format. The term filter used in the algorithm does not refer to technical but image filters. Those are selecting mechanisms depending on intensities and gradients (first derivatives of intensities) or using the "canny method" for edge detection succeeded by contour interpolation. Thresholds for the image filters were adjusted manually depending on the image quality. The filters were used to distinguish brain from background of the image. Pixel values were set to "one" when representing brain and to "zero" when representing background. The information of the thus-generated binary mask stores the location of the brain. This spatial information can easily be accessed later by matrix multiplication. The target to background ratio (TBR) was calculated by dividing the median intensity of the window area (target) by the corresponding value of the contralateral hemisphere (background). Both intensity values were normalized to an ipsilateral remote area. The algorithm is further explained in Section 3.

2.4. Data Analysis. Data were analyzed by comparing absolute changes of the DC-ECoG potential and relative changes in Evans blue dye extravasation. Statistical tests are mentioned more specifically in the results section. A P-value of $< .05$ was considered statistically significant. Data in text and figures are given as median value as well as first and third quartiles in parentheses.

3. Results

3.1. Evaluation Method of Evans Blue Dye Extravasation. BBB disruption was assessed by calculating the TBR of relative Evans blue dye extravasation in the cranial window region compared to the corresponding region of the contralateral hemisphere.

The digital images of all slices (five per brain) were imported into Matlab variables and screened manually for one representative slice of each rat brain that contained the region of the cranial window. The chosen slices were then further processed using the custom-made Matlab routine as described (see also Figure 2 for the algorithm used). The location of the brain was identified within the picture by filters and displayed through a binary mask. The image was then cropped (cutout image) down to the outermost "brain pixel" identified by the filter process. The upper 20% (value chosen manually) of the cutout brain image were defined as the region of interest (ROI) that approximately represented the area between the upper cortical surface and the ventricles. The routine provided a 50×50 pixel square ($\sim 0.3\ mm^2$, blue square in Figure 3(c)) within the ROI of the ipsilateral hemisphere (hemisphere with the cranial window) and a corresponding equally sized square (white square in Figure 3(c)) within the ROI of the contralateral hemisphere.

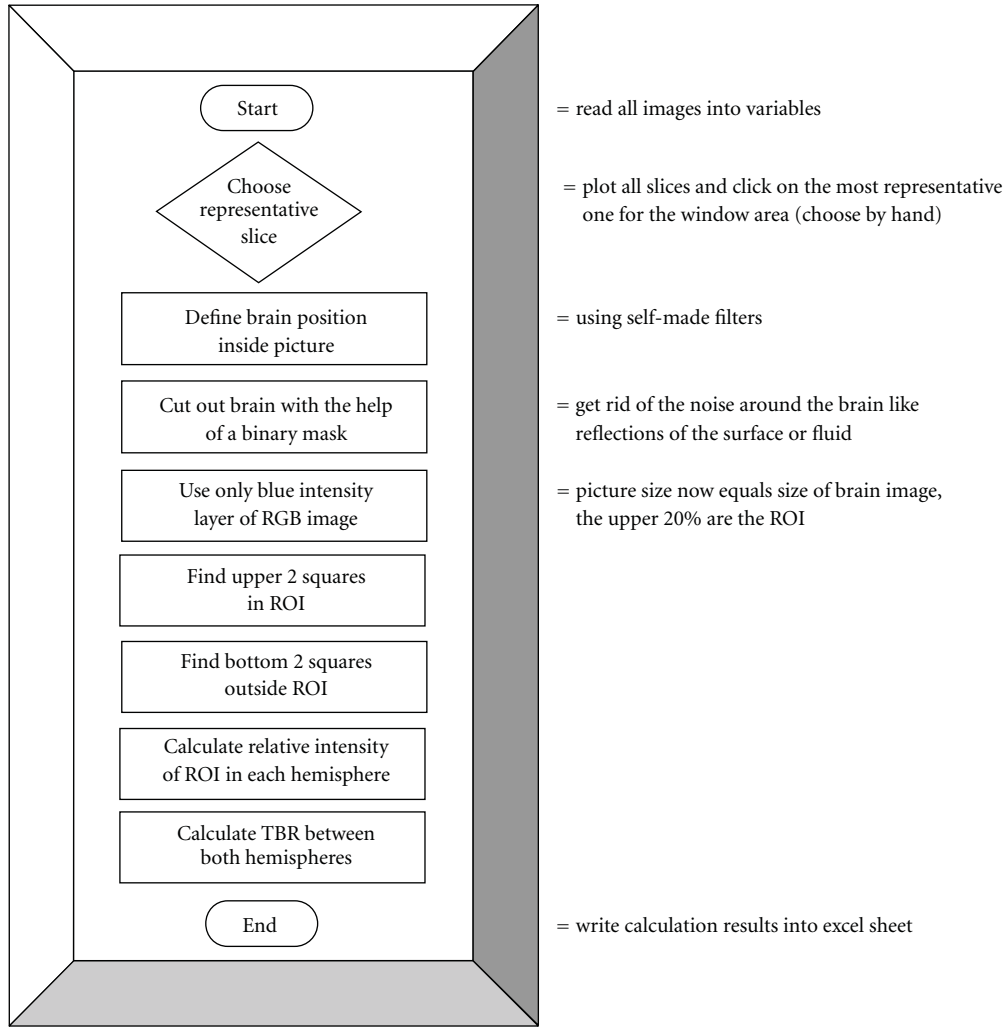

Figure 2: Algorithm.

Furthermore, the algorithm delivered two corresponding equally sized squares in the bottom region of the image (one bottom square in each hemisphere), clearly outside the ROI that were used to normalize the median intensities to yield a relative value for each side. The size of the four squares (50 by 50 pixels) was chosen according to the width of the cranial window (~4 mm) and thickness of the rat cortex. The initial location of the first square was user-selected according to the center of the cranial window area. This position was stored using distance values from the edges of the mask.

Since RGB is an additive color model, the blue channel of the images represents best the amount of blue dye (Evans blue). Therefore, the relative median blue intensities of both, the ipsilateral (blue square in the upper right hemisphere of Figure 3(c) = target) and the contralateral side (corresponding white square in the upper left hemisphere of Figure 3(c) = background) were used to calculate the TBR. As a visual control the routine plotted all four squares (blue and white ones) found in the image (Figure 3(c)).

3.2. DHC Induced Early BBB Opening Was Detected by the Novel Algorithm. The systemic variables measured in this study were mean arterial pressure, arterial pCO_2, arterial pO_2, and pH. Mean arterial pressure above 75 mmHg, arterial pO_2 between 90 and 130 mmHg, arterial pCO_2 between 35 and 45 mmHg, and arterial pH between 7.35 and 7.45 were accepted as being physiological [8]. Those systemic variables remained within normal limits throughout the preparation and experiments in the four experimental groups.

We first evaluated the brains of eight DHC-treated (group 1) and six sham-operated rats (group 2), since it was shown previously that topical application of DHC is a robust method for early BBB disruption [5]. These two groups served as positive and negative controls for BBB opening, respectively, in order to determine whether our fast algorithm would be able to detect the leakage of Evans blue into the brain tissue.

Brain topical application of DHC led to a significant increase in Evans blue extravasations compared to the sham

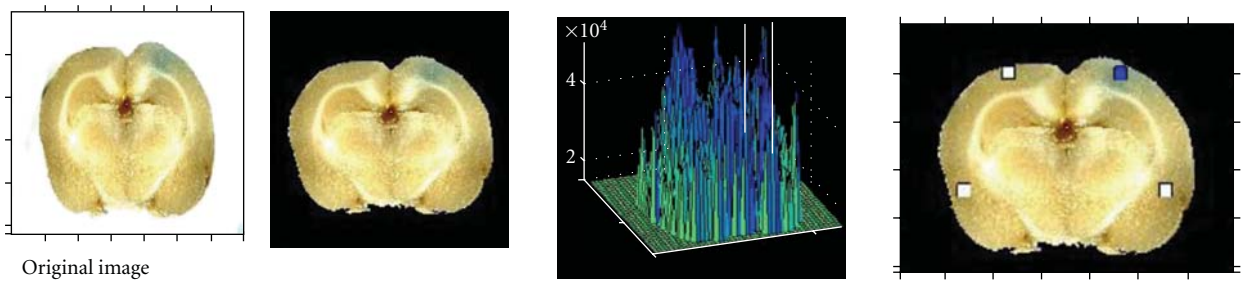

Figure 3: Steps of the algorithm. This figure shows how an original picture, taken by a digital camera, is processed using the Matlab routine. (a) First, the brain was identified within the picture, and a mask was created to reduce the background noise. (b) Then, the blue layer of the picture was analyzed, and the intensity scale was adjusted. (c) The four squares were chosen, and the target to background ratio was calculated.

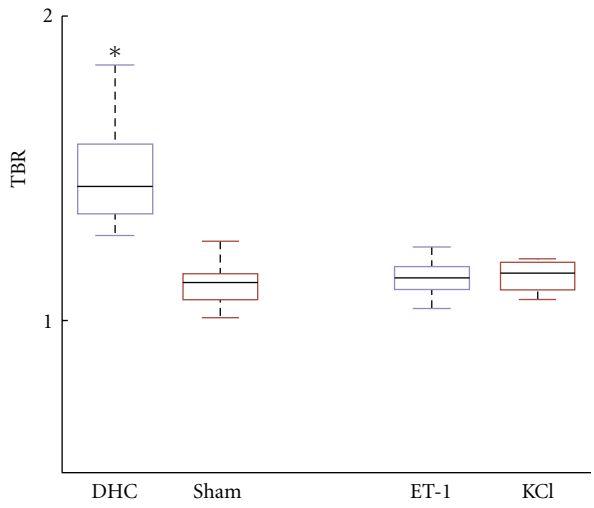

Figure 4: BBB opening. DHC-treated cortex shows significant (*) Evans blue leakage in contrast to the three other groups (Kruskal-Wallis ANOVA on ranks test with Dunn's post hoc analysis, $P < .05$).

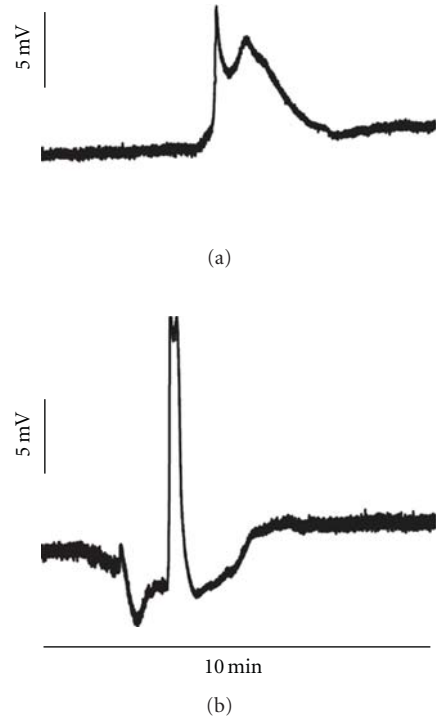

Figure 5: SDs in presence and absence of ET-1. (a) shows a typical SD in the cortex exposed to ET-1, while (b) demonstrates a typical SD in naïve cortex. Note the difference in duration and shape of the SDs. It has been suggested that ET-1 induces conditions of an ischemic penumbra. In the ischemic penumbra, SDs are typically prolonged.

operated group (Kruskal-Wallis ANOVA on ranks test with Dunn's post hoc analysis, $P < .05$, Figure 4). DHC did not induce SDs. Neither brain topical application of ET-1 (group 3, $n = 7$) nor SDs propagating through the naïve window area (group 4, $n = 5$) led to any changes in Evans blue extravasations compared to the sham-operated animals at this early time point (Figure 4).

In group 3, topical application of ET-1 induced 4 (2–6) SDs with an amplitude of −13.6 (−18.2–(−11.9)) mV and a duration of 104 (71–215) s, while, in group 4, 7 (7–9) SDs occurred with an amplitude of −13.7 (−16.8–(−9.2)) mV and a duration of 46 (35–50) s. The duration of SDs was significantly longer in presence of ET-1 ($P = .018$, Mann-Whitney rank sum test) [6] (Figure 5).

4. Discussion

We developed a novel, simple, and fast algorithm to assess BBB disruption *ex vivo*. Using this algorithm, we confirmed previous findings that brain topical application of the bile salt DHC causes early BBB opening. Neither ET-1-induced SDs nor SDs propagating in naïve cortex led to early BBB opening within the three-hour time window.

Our *ex vivo* algorithm is based on Evans blue dye extravasations. Evans blue, discovered in 1885 by Paul Ehrlich [12], binds to albumin with high affinity. This large complex of serum protein and vital dye cannot cross the intact BBB. Methods already exist to assess *ex vivo* Evans blue leakage

from the cerebral vasculature into the brain tissue. However, these methods include several time-consuming steps to prepare the animal brain, and they also require special equipment for quantification. Therefore, they are more costly and time-consuming. This applies to the commonly used method of Katayama and colleagues [13], for example, which is outlined briefly in [4]. At first, Evans blue is injected intravenously in a 2% solution in saline (3 mL/kg body weight) either before or shortly after an insult. Perfusion with physiological saline of the deeply anesthetized animal is necessary to remove the dye inside the vessels at the end of the experiment. After sacrificing the animal and extraction of the brain, either whole hemispheres or brain samples from each side are chosen, weighed, and soaked overnight in potassium hydroxide at 37°C. The alkaline solution is then neutralized by adding phosphoric acid and acetone and shaken vigorously. Thereafter, the solution is centrifuged three times at 3500 rpm for 15 minutes and the absorbance of the extracted solution is measured using a spectrophotometer. Quantitative calculation of the dye content in the brain is then performed based on external standards.

In our current study, we aimed at an easier, less time- and resources-consuming, semiquantitative *ex vivo* BBB evaluating method, since our experimental paradigm did not require absolute quantification. Our results show that this fast and inexpensive new algorithm is specific enough to identify early BBB disruption, verified by the DHC-model [5]. It is, however, not absolutely quantitative but only suitable for relative measurements. Therefore, we suggest its use once there is need of evidence for whether BBB opened or not in a given region compared to the contralateral hemisphere. For an absolute quantification, we are in favor of the method described by Katayama and colleagues [13]. On the other hand, a clear advantage of our method over that of Katayama and colleagues is that the spatial information is better preserved where exactly in the tissue the BBB disruption did occur. Thus, our method is suitable in particular for the *ex vivo* assessment of BBB opening in cranial window experiments in comparison to sham controls.

In vivo technology for the detection of BBB opening provides the advantage that dynamics of BBB opening can be studied. For this purpose, MR imaging is suitable as well as CT technology [14, 15]. Moreover, PET solutions have been discussed. For the specific purpose of cranial window experiments, an elegant method for the evaluation of BBB opening *in vivo* is fluorescent imaging of molecules with different molecular weights such as Lucifer Yellow using a CCD camera [16]. This method combines a high spatial with a high temporal resolution. Our algorithm can be used as a simple procedure to confirm the *in vivo* findings with another method *ex vivo*.

4.1. ET-1-Induced SDs as well as SDs Propagating in Naïve Tissue Do Not Lead to Significant Early BBB Opening. In 1993, Stanimirovic and colleagues reported that ET-1 increased cerebrovascular endothelium permeability in cultures derived from human brain capillary endothelial cells [17]. They suggested that this effect of ET-1 is due to receptor-specific activation of protein kinase C and intracellular calcium mobilization. Narushima and colleagues consequently showed in dogs that a single dose (40 pmol/animal) of ET-1 administered intracisternally led to enhanced fluorescein entry into the cerebrospinal fluid [18]. This effect was reversible by preadministration of the selective endothelin type A receptor (ET_A) antagonist S-0139. Matsuo and colleagues showed that S-0139 administration decreased brain edema and albumin extravasation in a rat ischemia model, where the ischemia was not induced by ET-1 but due to middle cerebral artery filament occlusion [19]. This study suggested that ET-1 is released in the wake of focal ischemia in general and is involved via ET_A receptors in the delayed BBB disruption following focal ischemia. Cerebral ischemia and reperfusion injury seem to induce dynamic changes in the BBB permeability [20, 21]. Initial very slight changes are assumed to be reversible and less harmful. After a refractory period of more than three and less than five hours, a more marked and persistent BBB disruption develops which may interfere with therapies such as thrombolysis, shows side effects such as vasogenic edema, and is thus a target for therapeutic intervention [20, 21].

Our data suggest that there is no significant BBB disruption in the first few hours after topical administration of ET-1. The prolongation of SDs under ET-1 in contrast to SDs in naïve tissue indicated that the vasoconstrictor ET-1 produced conditions of an ischemic penumbra consistently with previous findings [6, 8]. Hence, it is very likely that we could have detected BBB disruption at a time point later than three hours, since focal ischemia is associated typically with BBB disruption in a delayed fashion after the third hour [22–24]. Thus, the lack of early BBB disruption in response to ET-1 provides in fact an argument that the BBB disruption induced by ET-1 in previous studies *in vivo* may have been secondary to ET-1-induced vasoconstriction and ischemia rather than due to a direct effect of ET-1 on the barrier. However, we cannot exclude that very subtle permeability changes escaped our BBB evaluating algorithm or that an increase in permeability occurs for smaller molecules than the albumin-Evans-blue complex.

We neither found an early BBB opening after SDs propagating in naïve healthy tissue. This seems to contradict previous data in which matrix metalloproteinase (MMP)-9 was demonstrated to contribute to BBB permeability, edema formation, and vascular leakage after mechanically induced SDs in rats [4]. According to that study, MMP-9 activation occurred within the matrix of cortical blood vessels as early as 15 to 30 minutes and started within neurons more than three hours after SD induction. The authors reported an early BBB opening at three hours after SD induction, where BBB permeability was evaluated by quantification of vascular leakage of Evans blue dye using the method of Katayama and colleagues [13]. It is possible that our algorithm was not sensitive enough to detect a subtle early BBB opening. On the other hand, we used a less invasive method for SD induction (droplets of KCl at 150 mmol/L in a remote window) rather than a mechanical injury by pin prick. This might have influenced the time course of BBB opening.

Acknowledgments

This study was supported by grants of the Deutsche Forschungsgemeinschaft (DFG DR 323/2-2), the Bundesministerium für Bildung und Forschung (Center for Stroke Research Berlin, 01 EO 0801 and Bernstein Center for Computational Neuroscience Berlin 01GQ1001C B2), and the Kompetenznetz Schlaganfall to Dr. J. P. Dreier.

References

[1] M. Asahi, K. Asahi, J.-C. Jung, G. J. Del Zoppo, M. E. Fini, and E. H. Lo, "Role for matrix metalloproteinase 9 after focal cerebral ischemia: effects of gene knockout and enzyme inhibition with BB-94," *Journal of Cerebral Blood Flow and Metabolism*, vol. 20, no. 12, pp. 1681–1689, 2000.

[2] M. Asahi, T. Sumii, M. E. Fini, S. Itohara, and E. H. Lo, "Matrix metalloproteinase 2 gene knockout has no effect on acute brain injury after focal ischemia," *NeuroReport*, vol. 12, no. 13, pp. 3003–3007, 2001.

[3] J. Klohs, J. Steinbrink, R. Bourayou et al., "Near-infrared fluorescence imaging with fluorescently labeled albumin: a novel method for non-invasive optical imaging of blood-brain barrier impairment after focal cerebral ischemia in mice," *Journal of Neuroscience Methods*, vol. 180, no. 1, pp. 126–132, 2009.

[4] Y. Gursoy-Ozdemir, J. Qiu, N. Matsuoka et al., "Cortical spreading depression activates and upregulates MMP-9," *Journal of Clinical Investigation*, vol. 113, no. 10, pp. 1447–1455, 2004.

[5] E. Seiffert, J. P. Dreier, S. Ivens et al., "Lasting blood-brain barrier disruption induces epileptic focus in the rat somatosensory cortex," *Journal of Neuroscience*, vol. 24, no. 36, pp. 7829–7836, 2004.

[6] A. I. Oliveira-Ferreira, D. Milakara, M. Alam et al., "Experimental and preliminary clinical evidence of an ischemic zone with prolonged negative DC shifts surrounded by a normally perfused tissue belt with persistent electrocorticographic depression," *Journal of Cerebral Blood Flow and Metabolism*, vol. 30, no. 8, pp. 1504–1519, 2010.

[7] J. P. Dreier, "The role of spreading depression, spreadingdepolarization and spreading ischemia in neurological disease," *Nature Medicine*. In press.

[8] J. P. Dreier, J. Kleeberg, M. Alam et al., "Endothelin-1-induced spreading depression in rats is associated with a microarea of selective neuronal necrosis," *Experimental Biology and Medicine*, vol. 232, no. 2, pp. 204–213, 2007.

[9] U. Lindauer, A. Villringer, and U. Dirnagl, "Characterization of CBF response to somatosensory stimulation: model and influence of anesthetics," *American Journal of Physiology*, vol. 264, no. 4, part 2, pp. H1223–H1228, 1993.

[10] J. P. Dreier, J. Kleeberg, G. Petzold et al., "Endothelin-1 potently induces Leão's cortical spreading depression in vivo in the rat: a model for an endothelial trigger of migrainous aura?" *Brain*, vol. 125, no. 1, pp. 102–112, 2002.

[11] D. Jorks, S. Major, A. I. Oliveira-Ferreira, J. Kleeberg, and J. P. Dreier, "Endothelin-1(1-31) induces spreading depolarization in rats," *Acta Neurochirurgica Supplement*, vol. 110, pp. 111–117, 2011.

[12] P. Ehrlich, *Das Sauerstoff-Bedürfnis des Organismus Eine Farbenanalytische Studie*, Hirschwald, Berlin, Germany, 1885.

[13] S. Katayama, H. Shionoya, and S. Ohtake, "A new method for extraction of extravasated dye in the skin and the influence of fasting stress on passive cutaneous anaphylaxis in guinea pigs and rats," *Microbiology and Immunology*, vol. 22, no. 2, pp. 89–101, 1978.

[14] O. Tomkins, O. Friedman, S. Ivens et al., "Blood-brain barrier disruption results in delayed functional and structural alterations in the rat neocortex," *Neurobiology of Disease*, vol. 25, no. 2, pp. 367–377, 2007.

[15] N. Hjort, O. Wu, M. Ashkanian et al., "MRI detection of early blood-brain barrier disruption: parenchymal enhancement predicts focal hemorrhagic transformation after thrombolysis," *Stroke*, vol. 39, no. 3, pp. 1025–1028, 2008.

[16] O. Prager, Y. Chassidim, C. Klein, H. Levi, I. Shelef, and A. Friedman, "Dynamic in vivo imaging of cerebral blood flow and blood-brain barrier permeability," *NeuroImage*, vol. 49, no. 1, pp. 337–344, 2010.

[17] D. B. Stanimirovic, R. McCarron, N. Bertrand, and M. Spaiz, "Endothelins release Cr from cultured human cerebromicrovascular endothelium," *Biochemical and Biophysical Research Communications*, vol. 191, no. 1, pp. 1–8, 1993.

[18] I. Narushima, T. Kita, K. Kubo et al., "Contribution of endothelin-1 to disruption of blood-brain barrier permeability in dogs," *Naunyn-Schmiedeberg's Archives of Pharmacology*, vol. 360, no. 6, pp. 639–645, 1999.

[19] Y. Matsuo, S. I. Mihara, M. Ninomiya, and M. Fujimoto, "Protective effect of endothelin type A receptor antagonist on brain edema and injury after transient middle cerebral artery occlusion in rats," *Stroke*, vol. 32, no. 9, pp. 2143–2148, 2001.

[20] A. Y. Jin, U. I. Tuor, D. Rushforth et al., "Reduced blood brain barrier breakdown in P-selectin deficient mice following transient ischemic stroke: a future therapeutic target for treatment of stroke," *BMC Neuroscience*, vol. 11, article 12, 2010.

[21] R. Jin, G. Yang, and G. Li, "Molecular insights and therapeutic targets for blood-brain barrier disruption in ischemic stroke: critical role of matrix metalloproteinases and tissue-type plasminogen activator," *Neurobiology of Disease*, vol. 38, no. 3, pp. 376–385, 2010.

[22] T. Kuroiwa, P. Ting, H. Martinez, and I. Klatzo, "The biphasic opening of the blood-brain barrier to proteins following temporary middle cerebral artery occlusion," *Acta Neuropathologica*, vol. 68, no. 2, pp. 122–129, 1985.

[23] R. Pluta, A. S. Lossinsky, H. M. Wisnieuwski, and M. J. Mossakowski, "Early blood-brain barrier changes in the rat following transient complete cerebral ischemia induced by cardiac arrest," *Brain Research*, vol. 633, no. 1-2, pp. 41–52, 1994.

[24] L. Belayev, R. Busto, W. Zhao, and M. D. Ginsberg, "Quantitative evaluation of blood-brain barrier permeability following middle cerebral artery occlusion in rats," *Brain Research*, vol. 739, no. 1-2, pp. 88–96, 1996.

Hindawi Publishing Corporation
Cardiovascular Psychiatry and Neurology
Volume 2011, Article ID 175364, 11 pages
doi:10.1155/2011/175364

Hypothesis

Intercellular Interactomics of Human Brain Endothelial Cells and Th17 Lymphocytes: A Novel Strategy for Identifying Therapeutic Targets of CNS Inflammation

Arsalan S. Haqqani and Danica B. Stanimirovic

Institute for Biological Sciences, National Research Council, Ottawa, ON, Canada K1A 0R6

Correspondence should be addressed to Arsalan S. Haqqani, arsalan.haqqani@nrc.ca

Received 13 November 2010; Accepted 15 March 2011

Academic Editor: Daniela Kaufer

Leukocyte infiltration across an activated brain endothelium contributes to the neuroinflammation seen in many neurological disorders. Recent evidence shows that IL-17-producing T-lymphocytes (e.g., Th17 cells) possess brain-homing capability and contribute to the pathogenesis of multiple sclerosis and cerebral ischemia. The leukocyte transmigration across the endothelium is a highly regulated, multistep process involving intercellular communications and interactions between the leukocytes and endothelial cells. The molecules involved in the process are attractive therapeutic targets for inhibiting leukocyte brain migration. We hypothesized and have been successful in demonstrating that molecules of potential therapeutic significance involved in Th17-brain endothelial cell (BEC) communications and interactions can be discovered through the combination of advanced membrane/submembrane proteomic and interactomic methods. We describe elements of this strategy and preliminary results obtained in method and approach development. The Th17-BEC interaction network provides new insights into the complexity of the transmigration process mediated by well-organized, subcellularly localized molecular interactions. These molecules and interactions are potential diagnostic, therapeutic, or theranostic targets for treatment of neurological conditions accompanied or caused by leukocyte infiltration.

1. Leukocyte Infiltration in CNS Disorders

The central nervous system (CNS) has long been regarded as an "immune privileged" organ, being both immunologically inert and immunologically separated from the peripheral immune system [1]. Current data, however, indicates that the CNS is both immune competent and actively interactive with the peripheral immune system [2]. In physiological conditions, a limited number of peripheral immune cells cross the blood-brain barrier (BBB) and enter the CNS in a process called "immune surveillance" [1]. Many neurological diseases are associated with a much higher rate of leukocyte trafficking into the CNS, resulting in leukocyte infiltration and leukocyte-mediated neuronal damage. CNS inflammation is a major contributor to the diverse forms of brain injury seen in cerebral ischemia, multiple sclerosis, cerebral infection, and epilepsy [3–5].

A growing body of recent evidence shows that infiltration of a subset of IL-17-producing T-lymphocytes into the CNS contributes to the pathogenesis of multiple sclerosis, and cerebral ischemia. In multiple sclerosis these cells are CD4+ T helper 17 (Th17) lymphocytes that have CNS-homing properties and mediate the immune response directed at the myelin sheath. Gyulveszi and coworkers recently demonstrated that the CNS tropism of Th17 cells is driven by IL23, since T cells defective in IL-23 signaling fail to accumulate in the CNS in the mouse model of experimental autoimmune encephalomyelitis (EAE) [6]. These findings are consistent with the report by Prat and colleagues, showing that IL-23-stimulated Th17 lymphocytes promote BBB disruption *in vitro* and in the EAE, efficiently penetrate the BBB, kill neurons, and promote further CNS inflammation through CD4+ lymphocyte recruitment [7].

In experimental ischemic stroke, T-lymphocytes are localized to the infarction boundary zones [8] and contribute to the development of secondary inflammatory brain injury [9]. More recently, Shichita et al. have shown that in mice subjected to a transient middle cerebral artery occlusion an initial infiltration of IL-23-producing macrophages is followed by subsequent recruitment/activation of IL-17-producing $\gamma\delta$T lymphocytes [10]. These T cells concomitantly increase downstream proinflammatory and neurotoxic factors and the infarct size after focal cerebral ischemia [10]. Thus, as in multiple sclerosis, IL17-producing T cells activated by IL-23 are believed to "home-in" towards the CNS and induce injury during cerebral stroke.

2. Molecular Mechanisms of Leukocyte Migration through the Endothelial Layer

The endothelial lining of brain capillaries exhibits a specialized phenotype, commonly referred to as the blood-brain barrier (BBB). These endothelial cells (ECs) function as a restrictive gate to control the composition of extracellular fluid in the central nervous system (CNS), selectively restricting and/or controlling the access of blood-borne molecules to the brain [11]. The brain capillary endothelium exhibits unique anatomical and biochemical features, including tight junctions (TJ) that form a physical barrier for a majority of hydrophilic molecules larger than 500 Da, low pinocytic activity, and the *polarized* expression of transporters that control both brain influx and efflux of molecular substrates [11].

The *luminal* surface of BEC (i.e., the side accessible to the blood) contains a thick glycocalyx, which is enriched in proteins and glycoproteins involved in key BBB functions, including the transport of solutes and macromolecules, BEC permeability, vasoreactivity, and interactions with circulating cells and platelets [12–15]. Under inflammatory conditions, luminal adhesion molecules in the glycocalyx directly interact with leukocytes during the highly-regulated, multistep transmigration process involving tethering and rolling, activation, arrest, and diapedesis [16, 17]. These steps are mediated by surface adhesion molecules and cytokines on both leukocytes and BEC and the avidity of interactions among different intercellular interacting molecular pairs. The initial low-affinity contacts, leading to tethering and rolling, slow down the flowing leukocytes and are mediated by the binding of selectins on the glycocalyx of BEC to their paired ligands on leukocytes. Firm adhesion (arrest) of the leukocytes is mediated by the binding of cell adhesion molecules (CAMs) on EC to their respective integrins on the leukocyte surface. ICAM1 and VCAM1 are two well-known CAMs that are overexpressed on brain EC in response to inflammatory insults. ICAM1 can pair with either $\alpha L\beta 2$ (LFA1, CD11a/CD18) or $\alpha M\beta 2$ (Mac1, CD11b/CD18) integrins, while VCAM1 interacts with $\alpha 4\beta 1$ (VLA4, CD49d/CD29) integrin on leukocytes [18].

Leukocyte diapedesis from the luminal surface of BEC to its abluminal side is the last step in the transmigration process and is the least well understood. The step has been traditionally believed to take place through the paracellular route, that is, through the TJ of BEC [19]. A number of intercellular interacting pairs (IIPs), including JAM1-JAM1, JAM1-LFA1, PECAM1-PECAM1, and CD99-CD99, have been identified between BEC TJ and leukocytes [20]. However, the paracellular migration route has been repeatedly challenged by histological and electron microscopy studies demonstrating that leukocytes can migrate through the transcellular pathway, that is through the BEC themselves, leaving the TJ morphologically intact [17, 18, 21]. While it is likely that the leukocyte migration occurs through both pathways [17], the details of the molecular events involved in either of the pathways remain limited.

3. Therapies against Leukocyte Migration into the Brain: Successes and Failures

Inhibiting the interactions between the migrating leukocytes and the BEC is an attractive therapeutic approach for inhibiting tissue inflammation. A target is usually a molecule that is essential in the transmigration process and is easily accessible to therapy. The IIPs discussed above are some of the key players in different stages of the leukocyte transmigration process and are also blood-accessible molecules, that is, present on either the surface of leukocytes or the luminal membranes of BEC. Blocking antibodies against the selected leukocyte-brain BEC IIPs have already been developed and used in preclinical studies and clinical trials.

Two IIPs have been primarily targeted for the inhibition of CNS inflammation: VCAM1-VLA4 interactions or ICAM1-LFA1 interactions. Blocking antibodies and other drug molecules against the $\alpha 4$-integrin part of VLA4 have been shown to inhibit or reverse the EAE in various animal models (summarized in [18]). These findings led to the development of a humanized monoclonal anti-$\alpha 4$-integrin antibody, Natalizumab, which was evaluated in two randomized, double-blind, placebo-controlled trials in patients with multiple sclerosis. The results of the trials demonstrated a large benefit for patients taking Natalizumab, including a 42% reduction in the risk of sustained disability progression and a 68% reduction in relapse rate [22]. The drug was initially approved by FDA in 2004, but was subsequently withdrawn after it was linked with few cases of progressive multifocal leukoencephalopathy (PML) when combined with immunomodulatory treatment [22, 23]. However, after a review of safety information, the drug was returned to the market in 2006 because its clinical benefits outweighed the risks involved. While Natalizumab has proven to be very successful in controlling the disease, some limitations due to side effects have been reported, including elevated lymphocyte, basophil, and eosinophil counts, with 5% of drug recipients showing circulating nucleated erythrocytes [23]; these side effects are likely due to widespread functions of $\alpha 4$ integrin in the hematopoietic system [18, 23].

Blocking antibody therapies targeting ICAM1 and LFA1 have also been developed. *In vitro* studies using these antibodies have consistently shown that the ICAM1-LFA1 interaction is important for T-cell adhesion and diapedesis across brain endothelium (summarized in [18]). However,

these therapies have produced highly conflicting results in CNS inflammation *in vivo*. While some studies have shown a beneficial outcome of blocking either ICAM1 or LFA1, others could not find a significant inhibition or even showed worsening of the outcome and early mortality in the EAE animal models [18, 24]. Furthermore, clinical trails using humanized anti-LFA1 (Rovelizumab, LeukArrest) and anti-ICAM1 (Enlimomab) antibodies have shown lack of efficacy or serious side effects. Another anti-VLA1 antibody (Efalizumab) has been approved for the therapy of psoriasis, a non-CNS inflammatory disorder [25]. Thus, while the role of ICAM1-LFA1 interaction is controversial in CNS inflammation, this interaction plays an important role (similar to VCAM1-VLA4 interaction) in peripheral, non-CNS inflammation.

4. Unmet Needs and the Hypothesis

4.1. Discovery of Novel, Specific Targets. Currently, only a limited number of molecules on leukocytes and the BBB are known or known to interact. For example, ICAM1-LFA1 and VCAM1-VLA4 pairs have been known for more than two decades and are still pursued as the main targets for inhibiting interactions between endothelium and leukocytes in the brain. Targeting these interactions alone does not provide complete protection, suggesting that other adhesion molecules may "compensate" when these interactions are blocked [26]. From problems associated with the functional redundancy of leukocyte-BEC molecular interactions and the inhibition of peripheral immune system function with current treatments, an important need has emerged to discover molecules specifically involved in the adhesion and diapedesis of specific subsets of leukocytes through the BBB that are less important in the overall immune system competency. With emerging evidence of the role of the IL-23-induced IL-17-producing T cells in the pathogenesis of multiple sclerosis and cerebral ischemia, there is a need for identification of more specific molecules on these subpopulations of leukocytes, which confer their brain-tropism, to develop more cell-selective targets. Further, there is a need to identify cell-specific (and human-specific) molecules as targets on brain EC to minimize non-specific side effects of current drugs (described above). We propose that human brain EC and human brain tropic T-cells should become key models to discover novel targets implicated in neuroinflammatory cell recruitment and migration.

5. Hypothesis

Using advanced methods that combine membrane and submembrane proteomics and glycoproteomics with methods of in silico interactomics, a novel set of intercellular interactions between human brain endothelial cells and human CNS-homing T cells, can be identified and exploited as therapeutic targets for preventing brain inflammation caused by recruitment of peripheral inflammatory cells.

6. Testing the Hypothesis

The flow chart of proposed strategy to test the above hypothesis is shown in Figure 1. The *first phase* of the strategy includes the development of appropriate methods for membrane and submembrane proteomics and glycoproteomics and appropriate model system(s) for testing the hypothesis, including the generation and curation of database(s) of relevant known protein-protein and protein-carbohydrate interactions. The *second phase* involves the application of membrane and submembrane proteomic methods to the selected model system to identify protein and glycoprotein changes induced in endothelial cells and CNS-tropic lymphocytes under pathological conditions (i.e., inflammation or ischemia). In the *third phase*, intercellular interacting pairs (IIPs) between brain BEC and CNS-tropic lymphocytes, with potential roles in leukocyte-endothelium contact or communication (i.e., interactions among secreted proteins and cell surface proteins), are identified using *in silico* interactomics. Finally, *validation* of the role of identified IIPs in leukocyte adhesion/transmigration is accomplished using *in vitro* assays and biological readouts. Elements and phases of this strategy, and preliminary results obtained in method and approach development, are described in detail below.

6.1. Phase 1: Development and Validation of Methods

6.1.1. Membrane and Submembrane Proteomics Methods. Proteins present on cell membranes, facing the extracellular environment, are the main site of contacts between BEC and leukocytes during adhesion and diapedesis. The contact site on BEC is mainly the luminal membrane (glycocalyx), which consists of a complex mixture of proteins, glycoproteins, and other molecules. Since BEC have "polarized" membranes, that is, molecules on the luminal and abluminal membranes are different, there is also a need to couple submembrane fractionation with proteomics to identify the differences between the various fractions. Analyzing membrane molecules has usually been difficult, especially using proteomics. Traditional 2D gel-based proteomic methods lack the sensitivity, reproducibility, and the ability to analyze the complete spectrum of membrane proteins, due to inherent limitation of the technology (summarized in [27]). A quantitative and reproducible method for analyzing glycosylated proteins on a global scale has been lacking.

Over the last 5 years, technological growth in the proteomics field has led to the development of advanced nanoLC-MS-based systems that are composed of highly reproducible and sensitive nanoflow ultra HPLC systems (e.g., nanoAquity), coupled with sensitive and high mass-accuracy MS instruments (e.g., Orbitrap) [28]. We and others have also developed bioinformatics software that analyze nanoLC-MS data, allowing the quantification of thousands of proteins and glycoproteins in multiple biological samples [29]. In addition, the recent development of hydrazide capture technology [30, 31] has enabled selective enrichment of glycoproteins from cells and tissues for large-scale identification, using nanoLC-MS-based quantitative proteomics.

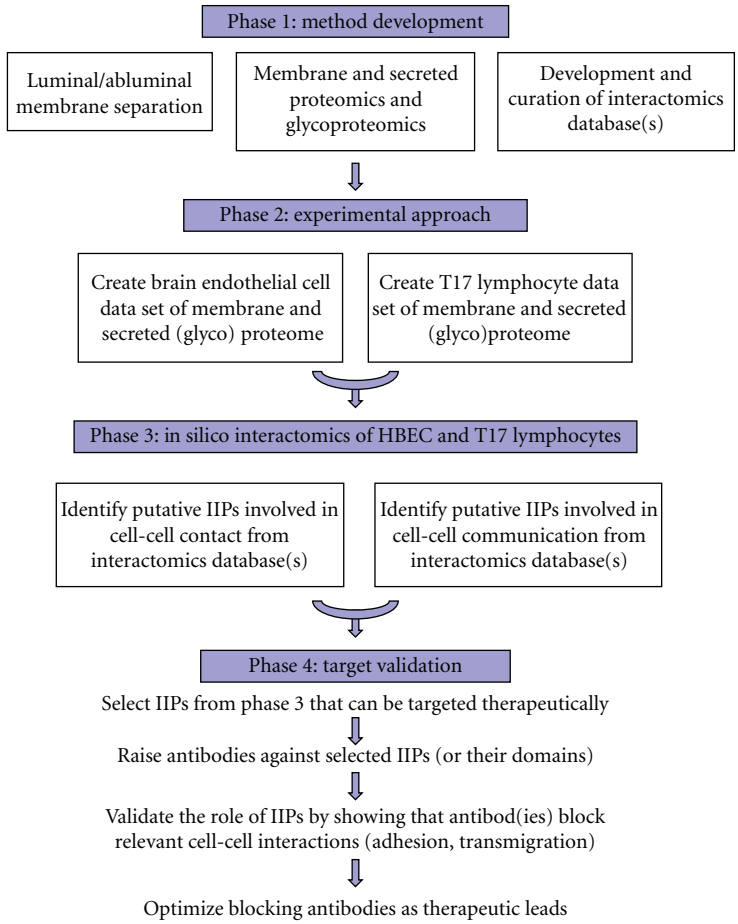

Figure 1: Schematic flowchart of the proposed approach to identify protein-protein interactions between Th17 lymphocytes and brain endothelial cells that are functionally implicated in the recruitment of inflammatory/immune cells across the blood-brain barrier.

Recently, we also described methods to enrich for various membrane fractions (e.g., luminal, abluminal) from human BEC and other cells, and coupled this with hydrazide capture and quantitative nanoLC-MS-based proteomics [28, 30]. This combination of submembrane isolation methods and advanced proteomics and glycoproteomics technology is needed to discover novel proteins and glycoproteins on the surfaces of BEC and T cells.

6.1.2. Intercellular Interactomics Data Base(s). Proteomics and other genomics methods generate overwhelming data sets of molecules that become difficult to follow up. Since validating entire "lists" becomes costly and time consuming, a single-factor/reductionist approach is often undertaken to select (or "cherry pick") a couple of molecules for further evaluation. As a result, a significant portion of disease-implicated molecules are simply overlooked. Thus, there is a need for development and application of alternative methodology to identify the overlooked molecules, which may include novel and more specific targets. Systems biology is the field of biology that aims to provide a more "holistic" view by examining the network of interactions between multiple molecules, pathways, cells, and characteristics of the tissue, as they converge to determine the disease implication of the molecules [32]. Since molecular interactions are the fundamentals of systems biology, a large amount of effort has been invested into generating protein-interaction databases through large-scale experimental interactomics and curation of the scientific literature [33]. We propose to use the curated protein-protein interaction databases and systems biology approaches, to identify which molecules actually interact between BEC and brain-specific lymphocytes. This *in silico* interactomics methodology has a potential to identify novel IIPs as therapeutic targets for CNS inflammation.

Protein interactions have traditionally been measured using immunoprecipitation and yeast two-hybrid systems. However, high-throughput techniques have also been developed that identify affinity pull-down complexes using advanced proteomics [34], and systematically constructed double-knockout strains in yeast have proven to be useful for constructing a large-scale view of molecular interaction networks [35]. As a result, a number of publicly available protein-protein interaction databases currently exist, including BIND, Human Protein Reference Database, HiMAP, BioGRID, and EcoCyc. Utilizing these existing databases and datasets, we reconstructed an in-house database consisting of more than a million molecular interactions. For the current study, we limited the interactions to immunoprecipitation

and affinity pull-down assays in mammalian systems to reduce the incidence of false interactions. The resulting mammalian protein-protein interaction database (mPPI-db) consists of more than 200,000 nonredundant interactions, and was used for the discovery of novel IIPs between human brain endothelial cells (BEC) and lymphocytes using the experimental approaches described below.

6.2. Phase 2: Experimental Models and Their Validation

6.2.1. Activated Human BEC. Brain endothelium undergoes significant changes in response to inflammation and becomes more receptive to interactions towards immune cells. This "activation" of the endothelium is characterized by molecular and physical changes in the luminal glycocalyx. Because proposed studies are focused on BEC-lymphocyte interactions relevant for human disease, to test the hypothesis we used the hCMEC/D3 human brain endothelial cell line as a stable human *in vitro* model of the BBB [36]. The cells were grown in EBM-2 media (Lonza, Walkersville, MD) supplemented with 2% FBS and were activated under serum-free conditions using various inflammatory insults, including TNFα/INFγ, IL-1β, or simulated ischemia/reperfusion conditions as previously described [26, 37, 38]. Although lymphocyte transmigration process *in vivo* occurs in post-capillary venules, there are currently no *in vitro* BBB models that specifically distinguish endothelium from capillaries and venules; most models, including the one used in these studies are mixed population of endothelial cells originating from both. The hCMEC/D3 have been demonstrated to be valid for studies of BBB function, responses of brain endothelium to inflammatory and infectious stimuli, and the interaction of brain endothelium with lymphocytes or other cells [26, 36]. From the activated cells, proteins from luminal (apical) and abluminal (basolateral) membranes and from cellular and secreted fractions were isolated using recently described methods [28], enriched for glycoproteins using hydrazide capture [30], and analyzed using nanoLC-MS-based quantitative proteomics to identify differentially expressed molecules [39]. In total, more than 4500 unique proteins and glycoproteins were identified in the human BEC, with about 650 present on each the luminal and abluminal membranes. In addition, about 25–30% of all the proteins responded significantly to the inflammatory insults, several of which were well-known indicators of BEC activation. Upregulation of surface adhesion molecules on luminal membranes (including ICAM1, VCAM1) changes in several TJ proteins [19] and integrins, including β1, β2, α4, αL, αM were observed. A number of proteins involved in *intra*cellular signaling and downstream pathways were also detected, including those involved in the recruitment of the "transmigratory cup" machinery [20] to the luminal membranes, for example, ezrin, moesin, radixin, and other cytoskeletal proteins, suggesting that the cells have been "primed" for the anticipated process of leukocyte adhesion. Furthermore, about 20% of the proteins were associated with BEC-alone or BEC activation as found by large-scale literature mining. These results validate adequate activation of hCMEC/D3 cells with inflammatory insults and suggest the validity of the model for further discovery of BEC-Th17 IIPs.

The majority of the cellular, membrane, and secreted proteins identified (>75%) were not previously described to be associated with BEC, BBB, luminal or abluminal membranes, CNS inflammation or leukocyte trafficking; 50 of these molecules were surface adhesion molecules that have not been previously reported in BEC in response to inflammation. Thus, the use of advanced proteomic and glycoproteomic tools led to identification of a large number of novel molecules in the luminal glycocalyx and other cellular compartments of human BEC.

6.2.2. Brain-Homing T Cells. The same advanced tools were also utilized to discover novel molecules in leukocytes. T cells with encephalo-tropism were generated by activation of lymphocytes, isolated from multiple sclerosis patients, with IL-23 as recently described [7]. These IL-17-producing T-helper (i.e., Th17) cells were utilized for further analysis, which included isolation of cellular and secreted proteins and performing label-free proteomics/glycoproteomics to identify molecular changes. More than 2850 cellular, 1875 membrane and 450 secreted proteins and glyoproteins were identified in the IL-23-activated Th17 cells. These included the key glycoproteins IL-17, IL-22, INFγ, and TNFα in the secreted fraction, validating the adequate activation of the cells. Well-known membrane glycoproteins involved in endothelium adhesion, such as LFA1, Mac1, and VLA4, were also detected in the activated Th17 cells. Furthermore, a number of proteins involved in *intra*cellular signaling and downstream pathways were also identified, including paxilin, talin, vinculin, Arp2/3, wasp, and cytoskeletal proteins. Since these proteins are involved in cell migration and projection—including formation of podosome-like structures for invasion—the Th17 cells appear to be primed for the anticipated attachment, adhesion, and diapedesis process. The majority of the molecules (>80%) identified in the activated Th17 cells (in both membrane and secreted fractions) were not described in the literature in association with T lymphocytes, inflammation, or leukocyte trafficking. These newly Th17-associated molecules include 10 additional integrins and more than 200 additional adhesion molecules, suggesting the potential importance of new molecular interactions and interacting pairs between Th17 and BEC.

The summary of the experimental approach used to generate membrane and secreted proteome data sets from human BEC and brain-tropic Th17 lymphocytes is shown in Figure 2.

6.3. Phase 3: Constructing Intercellular Networks between hBEC and T Cells. A computational approach was undertaken to construct intercellular interaction networks of stimuli-responsive molecules identified in human BEC and Th17 cells. This involved searching for each protein-protein interaction from the mPPI-db in the two proteomic datasets, such that one interactant is in the BEC and the other in the Th17 dataset. The resulting network consisted of more than 9000 interactions and was referred to as the master IIP network, since it represented all possible IIPs between the two

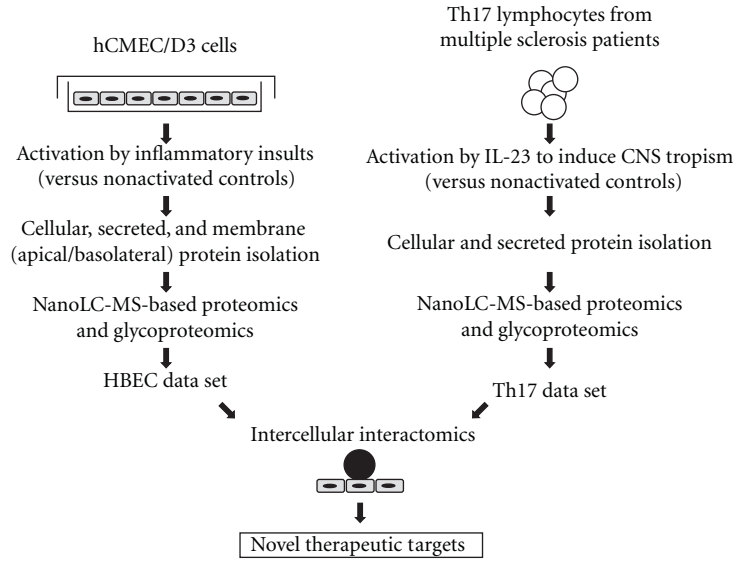

Figure 2: Schematic representation of the experimental approach used for described studies. Immortalized human brain endothelial cell line, hCMEC/D3 was exposed to various inflammatory cytokines or oxygen-glucose deprivation to identify differentially expressed proteins in response to these stimuli in luminal and abluminal membranes as well as in secreted proteins. Th17 lymphocytes derived from MS patients were exposed *in vitro* to IL-23 to induce their CNS tropism and to identify proteins regulated by this treatment. Respective databases of regulated proteins in inflammation-primed brain endothelial cells (BEC) and CNS-tropic Th17 lymphocytes were subjected to in sillico interactomics analyses to map putative protein-protein interactions that may contribute to Th17 cell adhesion and transmigration across the blood-brain barrier (BBB).

datasets. However, most of these IIPs are unlikely to occur *in vivo*, since the intercellular pathological and physiological interactions and communications between T cells and BEC are limited to only accessible molecules, that is, surface and secreted molecules. To reduce the complexity of the master network and identify more relevant IIPs, we limited the interactions to cell-cell "*contacts*" and "*communications.*" The intercellular "contacts" consist of interactions between BEC and Th17 surface molecules, whereas intercellular "communications" consist of interactions between BEC secreted and Th17 surface molecules, and vice versa. For surface molecules, only proteins containing extracellular membrane domains were included. Furthermore, only molecules that were expressed under activated conditions were included. These criteria significantly reduced the master IIP network and produced a more relevant network of cell-cell contacts (Figure 3) and communications (Figure 4) between T cells and brain endothelium during leukocyte trafficking.

6.4. Identification of Novel IIPs between Human BEC and T Cells

6.4.1. Cell-Cell Contacts. A network of cell-cell contact points between human BEC and Th17 cells was generated to identify potential IIPs involved in the adhesion and diapedesis processes (Figure 3). The network shows interactions between molecules on membranes of Th17 with molecules on either luminal membranes or in the TJ of BEC. In addition, it shows the molecules on the abluminal membrane of BEC that can interact with Th17 surface molecules. It is apparent from the network (Figure 3) that many more IIPs are identified than there are currently known in the literature. Great number of molecules showed a high degree of interactions, that is, they interacted with more than one protein and with as many as 18 proteins. If accurate, these results suggest that interactions between T cells and the glycocalyx of endothelium are likely much more complex, involving a significantly larger number of molecules than previously believed.

More than 180 interacting pairs (IIPs) were detected between 116 Th17 membrane proteins and 62 human BEC glycocalyx proteins. About half of the molecules (55%) have been previously associated in the literature with endothelium or T-lymphocytes in general, but very few have been implicated specifically with either BBB, Th17 cells, or BEC-T cell adhesion/diapedesis. This suggests that many of the molecular changes in brain endothelium in response to inflammation are common with changes in other endothelia, and similar is true for Th17 and T cells. Some of identified IIPs between human BEC glycocalyx and Th17 membranes included VCAM1-VLA4, ICAM1-LFA1, ICAM1-Mac1, P-selectin-PSGL1, and E-selectin-ESL1, respectively (Figure 3, table insert). Most of the molecules involved in these IIPs had high number of intercellular interactions in the network. While connection points or "nodes" like these with high numbers of interactions in the network can potentially be used to locate potential targets to interrupt interaction between cells, more often they indicate very common, redundant, or nonselective interactions and consequently may lead to drug side effects [40]. The network however suggests that the remaining IIPs are novel and perhaps more specific to human BEC-Th17 interactions.

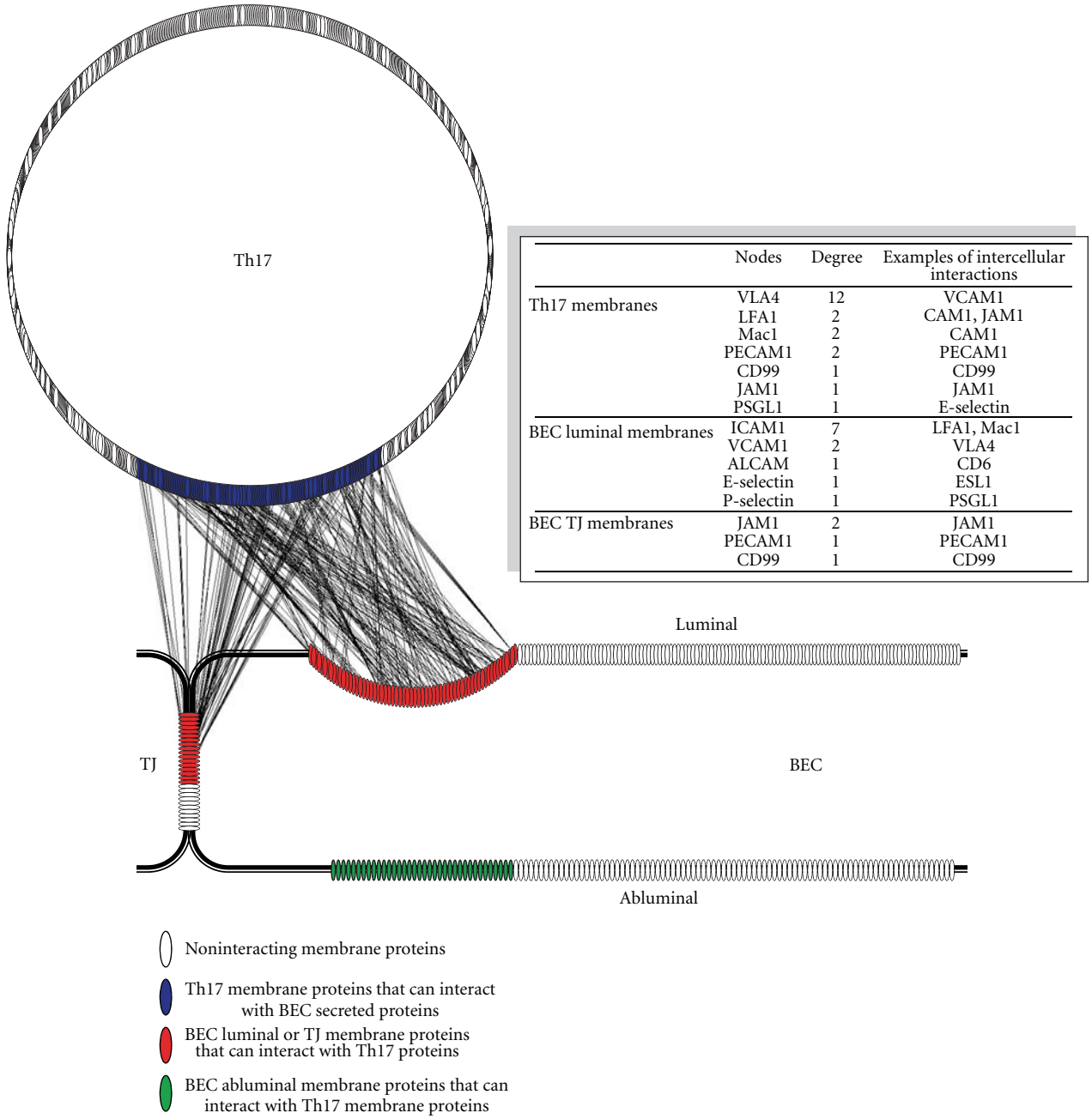

	Nodes	Degree	Examples of intercellular interactions
Th17 membranes	VLA4	12	VCAM1
	LFA1	2	CAM1, JAM1
	Mac1	2	CAM1
	PECAM1	2	PECAM1
	CD99	1	CD99
	JAM1	1	JAM1
	PSGL1	1	E-selectin
BEC luminal membranes	ICAM1	7	LFA1, Mac1
	VCAM1	2	VLA4
	ALCAM	1	CD6
	E-selectin	1	ESL1
	P-selectin	1	PSGL1
BEC TJ membranes	JAM1	2	JAM1
	PECAM1	1	PECAM1
	CD99	1	CD99

Figure 3: Shown is a visual depiction of the intercellular interaction network between proteins identified in Th17 lymphocytes and hCMEC/D3 brain endothelial cells using approach described in Figure 2. Each identified protein is represented by an oval; noninteracting proteins are shown in white, membrane proteins identified in Th17 lymphocytes that can interact with luminal membrane proteins of brain endothelial cells (BEC) are shown in blue, BEC luminal membrane- and tight junction proteins that can interact with Th17 membrane proteins are shown in red, and BEC abluminal proteins that can interact with Th17 membrane proteins are shown in green. Proteins were identified using membrane and subcellular proteomics and glycoproteomics and their interactions were catalogued using protein-protein databases as described in the text (each interaction is shown as a line connecting interacting proteins). *Insert*: the table shows a list of known proteins identified from the interactome network. Nodes represent the proteins or connection points in the membranes of Th17 and BEC in the network, and degree is the number of *intercellular* connections per node. Examples of these intercellular interactions are shown in the Table.

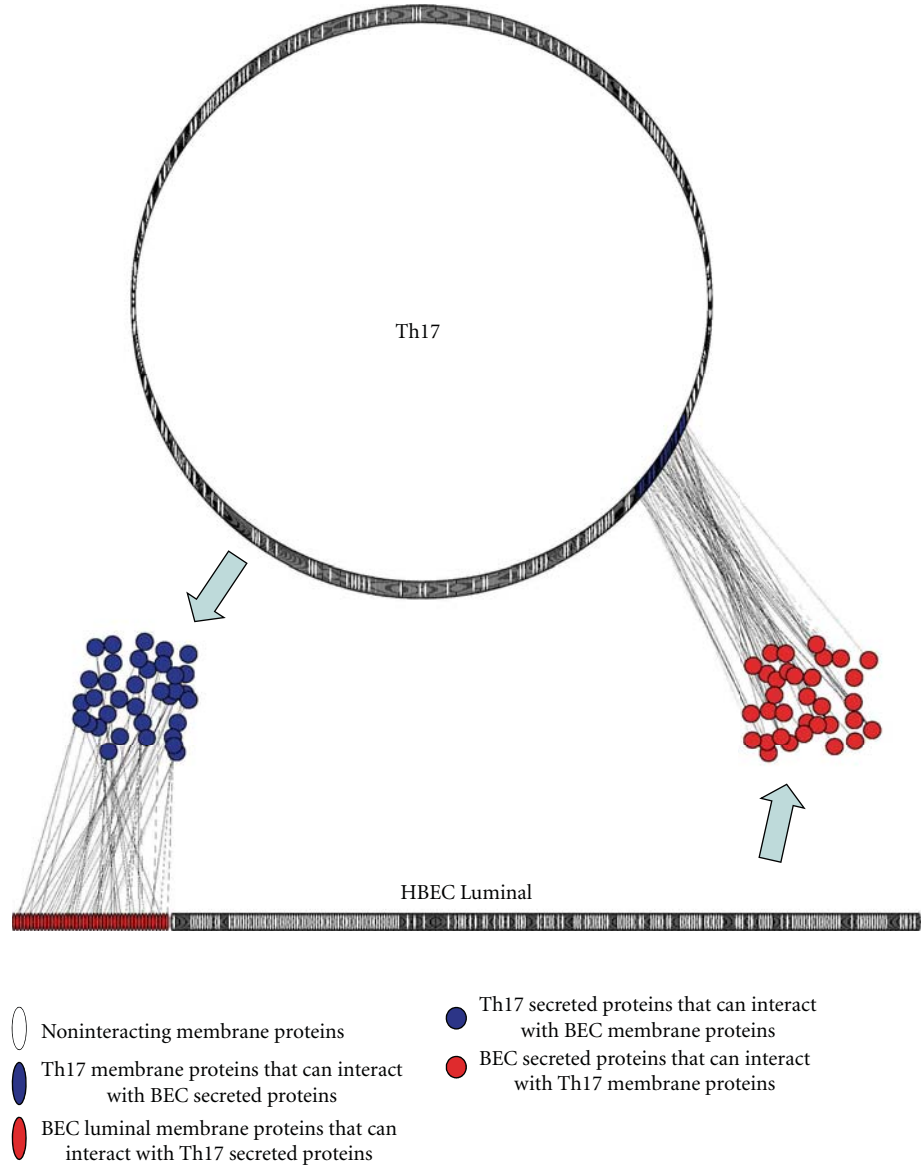

Figure 4: Extracellular signaling (communication) between Th17 and BEC. Shown is a visual depiction of the intercellular interaction network between proteins secreted by either Th17 lymphocytes or BEC and their interacting membrane counterparts expressed on the other cell type. All identified membrane proteins are represented by ovals, whereas secreted proteins are represented as circles: in red are luminal BEC membrane proteins that interact with secreted T17 proteins (in blue circles); in blue are membrane T17 proteins that interact with secreted BEC proteins (in red circles). Proteins were identified using membrane and subcellular proteomics and glycoproteomics and their interactions were catalogued using protein-protein databases as described in the text (each interaction is shown as a line connecting interacting proteins).

Not unexpectedly, IIPs between human BEC TJs and Th17 membranes were also discovered (Figure 3), consistent with the postulated mechanisms of leukocyte diapedesis. During the paracellular diapedesis process, leukocytes may encounter homophilic interactions with TJ molecules, creating zipper-like contacts that replace the interendothelial junction [18]. Corroborating this and further validating the generated interactome network, we detected the known IIPs JAM1-LFA1, JAM1-JAM1, PECAM1-PECAM1, and CD99-CD99 pairs between the BEC TJs and the Th17 membranes, respectively. More than 50 additional IIPs between TJs and Th17 membranes were also identified, many of which have not been previously associated in this context.

Finally, 113 IIPs between human BEC abluminal membranes and Th17 membranes were also identified (Figure 3). These are of significance since they might be involved in the diapedesis process through the transcellular pathway. In the final stages of this process, the transmigrating leukocytes need to transverse the abluminal membrane to enter the perivascular space and thus may recruit these IIPs.

Taken together, the cell-cell contact network provides new insights into the complexity of the adhesion and diapedesis processes and underscores that the intercellular interactions involved are likely not limited to just a few well-known IIPs, but rather extend to dozens of well-organized, cell-domain-localized molecular interactions.

6.4.2. Cell-Cell Communication. A network of cell-cell paracrine communications between human BEC and Th17 cells was also generated (Figure 4) to identify extracellular signals potentially involved in the cross-talks during leukocyte recruitment, adhesion, and diapedesis. The network shows the signals released from one cell which interact with their known receptors on the other cell's surface (Figure 4), depicting the potential cross-talk between leukocytes and the BBB during inflammation. Most of the signaling molecules identified were cytokines, chemokines, hormones, and/or growth factors. While the majority of the paracrine signaling molecules were not previously associated in the literature with leukocyte-BBB communication, several expected interacting pairs were also detected. These included MCP1, RANTES, and CCL19 cytokines in the BEC secretome and their respective receptors on the Th17 surface. Likewise, IL17, IL22, and others were detected in the Th17 secreted milieu and their receptors on the BEC glycocalyx. More than 25 additional extracellular signaling molecules from BEC were found to have receptors on Th17. Some of these receptors are known to be involved in T-cell recruitment/activation during the process of transmigration. Furthermore, more than 30 signals from Th17 were found to have receptors on human BEC, some of which are involved in receptor-mediated endocytosis/transcytosis. Overall, it was apparent that the paracrine communication between leukocytes and BBB under inflammatory conditions involves a large number of complex soluble ligand-receptor interactions which might lead to "priming" of the receptive cell for the anticipated diapedesis/transmigration process.

6.5. Phase 4: Validation of IIPs That Can Be Targeted Therapeutically. Validation of human BEC-T17 IIPs that may be suitable for the development of (blocking) therapeutic approaches could be done using various approaches. We propose that, after selection of potentially important interactions based on various bioinformatics algorithms that determine "strengths" of interactions in silico, potentially "drugable" interactions could be identified based on predetermined set of criteria including target molecule expression in brain vessels *in vivo*, accessibility from systemic compartment, brain/disease specificity, and so forth. In previous studies that compared the expression of proteins identified by 2D-gel and ICAT proteomics in BBB model(s) *in vitro* [38] and those identified using ICAT proteomics in laser-captured microvessels from animals *in vivo* [41], we identified and validated using immunochemistry and enzyme assays 19 commonly expressed proteins. In another proteomics study that identified more than 40 lipid-raft-specific proteins in human BEC *in vitro*, the expression of majority of these proteins has been confirmed in brain vessels in human brain tissue sections *in vivo* [26, 42, 43]. Most notably, activated leukocyte cell adhesion molecule (ALCAM) identified in these studies has been shown to promote leukocyte trafficking across the BBB through homotypic interaction with leukocytes; inhibition of this interaction reduced the severity and delayed the time of onset of experimental autoimmune encephalomyelitis in animal model. These studies provide validation that some of identified BEC-Th17 cell-cell interactions could be successfully targeted *in vivo* to inhibit leukocyte migration across the BBB.

The systematic validation of the role of BEC-Th17 cell-cell interactions catalogued by methods described above in facilitating leukocyte transmigration could be achieved using a high-throughput antibody development approach that targets the relevant epitopes of interacting molecules. For example, this can be done using antibody display approaches (phage or ribosome display) or *in vivo* immunization against expressed epitopes of interacting molecules. Resulting antibody "libraries" could then be screened for antibodies with interaction blocking properties using various *in vitro* assays (Surface Plasmon Resonance—SPR, ELISA etc.) or biological readouts that determine biological functions of the antibodies, for example, an efficacy in inhibiting leukocyte adhesion to brain endothelial cells or leukocyte transmigration across *in vitro* BBB models. Antibodies efficacious in modulating and inhibiting leukocyte adhesion and transmigration across the *in vitro* BBB model simultaneously validate the physiological or pathological role of identified IIPs. Identified "function-blocking" antibodies *in vitro*, could proceed into testing in various animal models, including EAE model [26]. The resulting lead molecule(s) could become amenable for further development as diagnostic, therapeutic, or theranostic for the treatment of neurological conditions accompanied, or caused by, leukocyte/lymphocyte infiltration. As a proof of concept for such an approach, we have generated a library of anti-ICAM-1 single-domain (VhH) antibodies from an immunized llama phage-displayed library, among which two antibodies displayed high affinity and ICAM-1 blocking activity in leukocyte adhesion assays (unpublished). One of these antibodies is currently being developed as molecular imaging agent for vascular inflammatory activation in stroke. Current advances in antibody engineering enable generation of bispecific antibodies that could simultaneously target more than one interacting molecule involved in the process of T-cell brain entry.

The proof of concept for clinical translation of proposed approach has already been achieved with Natalizumab antibody, showing that the inhibition of leukocyte recruitment into the brain by antibody that blocks one of molecular interactions between leukocytes and BEC resulted in clinically successful control of inflammatory brain disease. The hypothesis and experimental approach described in this paper provide the opportunity to identify and clinically target other important leukocyte-BEC interactions that are more specific/selective for brain-tropic leukocyte subsets.

7. Conclusions

To develop new therapies for inhibiting CNS inflammation, there is a need to identify novel interacting molecules between CNS-homing T cells and activated BEC. Currently only a limited number of molecules on leukocytes and BEC are known or known to interact. We have hypothesized here, and have been successful in demonstrating, that interacting molecules of potential therapeutic significance can be discovered through the combination of advanced membrane/submembrane proteomic and interactomic methods. A number of novel protein-protein interactions identified between BEC luminal and Th17 membrane molecules by these methods are key targets for inhibiting various stages of T-cell entry into brain, including T cell/BEC attachment, firm adhesion, and diapedesis. In addition, formation of specialized domain, including recruitment of the "transmigratory cup" complex at luminal membranes in BEC and evidence of podosome-associated molecules on the activated T cells, not only suggests that the cells are preparing and ready for interactions, but also identifies these structures as important therapeutic targets. Furthermore, interactions identified between BEC tight junction and Th17 membrane molecules are key therapeutic targets for inhibiting the paracellular diapedesis route. The identified TJ molecules may also be involved in the transcellular process since Muller and coworkers recently showed that the membrane from a parajunctional reticulum of interconnected vesicles, containing JAM1, PECAM1, and CD99, is recruited to surround the transcellularly migrating leukocytes and aids in the process [44]. Interactions identified between BEC abluminal and Th17 membrane molecules are also interesting as therapeutic targets since they may be involved in the final stages of the diapedesis process (by either route). Finally, intercellular paracrine signaling between T cells and BEC is also considered an important target for inhibiting recruitment and activation of the leukocytes. Collectively, identification of novel human BEC-Th17 IIPs not only allows more in-depth understanding of the interactions and communications between CNS-homing T cells and activated BEC, but also allows discovery of novel targets for therapy at different stages of the CNS inflammation.

The combination of advanced methodologies described here also has other applications. The use of emerging membrane/submembrane proteomic and glycoproteomic methods is applicable to other systems to allow identification of blood-accessible luminal and secreted targets. The intercellular interactomics has applications in understanding the complex interactions and communications among the various cell types in other systems.

The significance of the molecules discovered by the advanced "omic" methodologies described here also goes beyond the scope of this hypothesis. Novel molecules identified on the luminal surfaces of the activated BEC are also attractive targets for molecular imaging-based diagnosis of inflammatory insults in the brain since they are blood-accessible. Molecules identified in IL-23 stimulated Th17 cells may clarify the mechanism of tropism of these cells toward the CNS. Furthermore, secreted signaling molecules from BEC and T cells also target other cell types, including cells in the neurovascular unit, as well as in the peripheral tissues. It would be interesting to further elaborate these intercellular networks to decipher the complex communications within the CNS, as well as between the CNS and the peripheral environment.

Acknowledgments

The authors thank Dr. Alexandre Prat, Centre hospitalier de l'Université de Montréal (CHUM), for providing IL-23-activated Th17 cells. They also thank Christie Delaney and James Mullen for their technical assistance.

References

[1] M. J. Carson, J. M. Doose, B. Melchior, C. D. Schmid, and C. C. Ploix, "CNS immune privilege: hiding in plain sight," *Immunological Reviews*, vol. 213, no. 1, pp. 48–65, 2006.

[2] R. M. Ransohoff, P. Kivisäkk, and G. Kidd, "Three or more routes for leukocyte migration into the central nervous system," *Nature Reviews Immunology*, vol. 3, no. 7, pp. 569–581, 2003.

[3] B. V. Zlokovic, "The blood-brain barrier in health and chronic neurodegenerative disorders," *Neuron*, vol. 57, no. 2, pp. 178–201, 2008.

[4] P. F. Fabene, M. G. Navarro, M. Martinello et al., "A role for leukocyte-endothelial adhesion mechanisms in epilepsy," *Nature Medicine*, vol. 14, no. 12, pp. 1377–1383, 2008.

[5] G. J. del Zoppo, "Inflammation and the neurovascular unit in the setting of focal cerebral ischemia," *Neuroscience*, vol. 158, no. 3, pp. 972–982, 2009.

[6] G. Gyulveszi, S. Haak, and B. Becher, "IL-23-driven encephalo-tropism and Th17 polarization during CNS-inflammation in vivo," *European Journal of Immunology*, vol. 39, no. 7, pp. 1864–1869, 2009.

[7] H. Kebir, K. Kreymborg, I. Ifergan et al., "Human TH17 lymphocytes promote blood-brain barrier disruption and central nervous system inflammation," *Nature Medicine*, vol. 13, no. 10, pp. 1173–1175, 2007.

[8] M. Schroeter, S. Jander, O. W. Witte, and G. Stoll, "Local immune responses in the rat cerebral cortex after middle cerebral artery occlusion," *Journal of Neuroimmunology*, vol. 55, no. 2, pp. 195–203, 1994.

[9] G. Yilmaz, T. V. Arumugam, K. Y. Stokes, and D. N. Granger, "Role of T lymphocytes and interferon-γ in ischemic stroke," *Circulation*, vol. 113, no. 17, pp. 2105–2112, 2006.

[10] T. Shichita, Y. Sugiyama, H. Ooboshi et al., "Pivotal role of cerebral interleukin-17-producing gammadelta T cells in the delayed phase of ischemic brain injury," *Nature Medicine*, vol. 15, no. 8, pp. 946–950, 2009.

[11] D. J. Begley and M. W. Brightman, "Structural and functional aspects of the blood-brain barrier," *Progress in Drug Research*, vol. 61, pp. 39–78, 2003.

[12] S. Weinbaum, X. Zhang, Y. Han, H. Vink, and S. C. Cowin, "Mechanotransduction and flow across the endothelial glycocalyx," *Proceedings of the National Academy of Sciences of the United States of America*, vol. 100, no. 13, pp. 7988–7995, 2003.

[13] S. Weinbaum, J. M. Tarbell, and E. R. Damiano, "The structure and function of the endothelial glycocalyx layer," *Annual Review of Biomedical Engineering*, vol. 9, pp. 121–167, 2007.

[14] A. W. Vorbrodt, D. H. Dobrogowska, A. S. Lossinsky, and H. M. Wisniewski, "Ultrastructural localization of lectin receptors on the luminal and abluminal aspects of brain microblood vessels," *Journal of Histochemistry and Cytochemistry*, vol. 34, no. 2, pp. 251–261, 1986.

[15] J. Vogel, M. Sperandio, A. R. Pries, O. Linderkamp, P. Gaehtgens, and W. Kuschinsky, "Influence of the endothelial glycocalyx on cerebral blood flow in mice," *Journal of Cerebral Blood Flow and Metabolism*, vol. 20, no. 11, pp. 1571–1578, 2000.

[16] B. Rossi and G. Constantin, "Anti-selectin therapy for the treatment of inflammatory diseases," *Inflammation and Allergy—Drug Targets*, vol. 7, no. 2, pp. 85–93, 2008.

[17] B. Engelhardt and H. Wolburg, "Mini review: transendothelial migration of leukocytes: through the front door or around the side of the house?" *European Journal of Immunology*, vol. 34, no. 11, pp. 2955–2963, 2004.

[18] C. Coisne, R. Lyck, and B. Engelhardt, "Therapeutic targeting of leukocyte trafficking across the blood-brain barrier," *Inflammation and Allergy—Drug Targets*, vol. 6, no. 4, pp. 210–222, 2007.

[19] S. M. Stamatovic, R. F. Keep, and A. V. Andjelkovic, "Brain endothelial cell-cell junctions: how to "open" the blood brain barrier," *Current Neuropharmacology*, vol. 6, no. 3, pp. 179–192, 2008.

[20] E. S. Wittchen, "Endothelial signaling in paracellular and transcellular leukocyte transmigration," *Frontiers in Bioscience*, vol. 14, pp. 2522–2545, 2009.

[21] J. Greenwood, R. Howes, and S. Lightman, "The blood-retinal barrier in experimental autoimmune uveoretinitis: leukocyte interactions and functional damage," *Laboratory Investigation*, vol. 70, no. 1, pp. 39–52, 1994.

[22] B. A. Brown, "Natalizumab in the treatment of multiple sclerosis," *Therapeutics and Clinical Risk Management*, vol. 5, no. 3, pp. 585–594, 2009.

[23] R. M. Ransohoff, "Natalizumab and PML," *Nature Neuroscience*, vol. 8, no. 10, p. 1275, 2005.

[24] C. T. Welsh, J. W. Rose, K. E. Hill, and J. J. Townsend, "Augmentation of adoptively transferred experimental allergic encephalomyelitis by administration of a monoclonal antibody specific for LFA-1α," *Journal of Neuroimmunology*, vol. 43, no. 1-2, pp. 161–167, 1993.

[25] C. L. Leonardi, "Efalizumab in the treatment of psoriasis," *Dermatologic Therapy*, vol. 17, no. 5, pp. 393–400, 2004.

[26] R. Cayrol, K. Wosik, J. L. Berard et al., "Activated leukocyte cell adhesion molecule promotes leukocyte trafficking into the central nervous system," *Nature Immunology*, vol. 9, no. 2, pp. 137–145, 2008.

[27] A. S. Haqqani, J. F. Kelly, and D. B. Stanimirovic, "Quantitative protein profiling by mass spectrometry using isotope-coded affinity tags," *Methods in Molecular Biology*, vol. 439, pp. 225–240, 2008.

[28] A. S. Haqqani, J. J. Hill, J. Mullen, and D. Stanimirovic, "Methods to Study Glycoproteins at the Blood-Brain Barrier Using Mass Spectrometry," in *Methods in Molecular Biology: The Blood-Brain and Other Neural Barriers*, S. Nag, Ed., The Humana Press, 2011.

[29] A. S. Haqqani, J. F. Kelly, and D. B. Stanimirovic, "Quantitative protein profiling by mass spectrometry using label-free proteomics," *Methods in Molecular Biology*, vol. 439, pp. 241–256, 2008.

[30] J. J. Hill, M. J. Moreno, J. C. Y. Lam, A. S. Haqqani, and J. F. Kelly, "Identification of secreted proteins regulated by cAMP in glioblastoma cells using glycopeptide capture and label-free quantification," *Proteomics*, vol. 9, no. 3, pp. 535–549, 2009.

[31] H. Zhang, X. J. Li, D. B. Martin, and R. Aebersold, "Identification and quantification of N-linked glycoproteins using hydrazide chemistry, stable isotope labeling and mass spectrometry," *Nature Biotechnology*, vol. 21, no. 6, pp. 660–666, 2003.

[32] S. M. Studer and N. Kaminski, "Towards systems biology of human pulmonary fibrosis," *Proceedings of the American Thoracic Society*, vol. 4, no. 1, pp. 85–91, 2007.

[33] K. A. Pattin and J. H. Moore, "Role for protein-protein interaction databases in human genetics," *Expert Review of Proteomics*, vol. 6, no. 6, pp. 647–659, 2009.

[34] M. Pellegrini, D. Haynor, and J. M. Johnson, "Protein interaction networks," *Expert Review of Proteomics*, vol. 1, no. 2, pp. 239–249, 2004.

[35] A. H. Y. Tong, M. Evangelista, A. B. Parsons et al., "Systematic genetic analysis with ordered arrays of yeast deletion mutants," *Science*, vol. 294, no. 5550, pp. 2364–2368, 2001.

[36] B. B. Weksler, E. A. Subileau, N. Perrière et al., "Blood-brain barrier-specific properties of a human adult brain endothelial cell line," *FASEB Journal*, vol. 19, no. 13, pp. 1872–1874, 2005.

[37] D. Stanimirovic, A. Shapiro, J. Wong, J. Hutchison, and J. Durkin, "The induction of ICAM-1 in human cerebromicrovascular endothelial cells (HCEC) by ischemia-like conditions promotes enhanced neutrophil/HCEC adhesion," *Journal of Neuroimmunology*, vol. 76, no. 1-2, pp. 193–205, 1997.

[38] A. S. Haqqani, J. Kelly, E. Baumann, R. F. Haseloff, I. E. Blasig, and D. B. Stanimirovic, "Protein markers of ischemic insult in brain endothelial cells identified using 2D gel electrophoresis and ICAT-based quantitative proteomics," *Journal of Proteome Research*, vol. 6, no. 1, pp. 226–239, 2007.

[39] A. S. Haqqani, J. F. Kelly, and D. B. Stanimirovic, "Quantitative protein profiling by mass spectrometry using label-free proteomics," *Methods in Molecular Biology*, vol. 439, pp. 241–256, 2008.

[40] T. Hase, H. Tanaka, Y. Suzuki, S. Nakagawa, and H. Kitano, "Structure of protein interaction networks and their implications on drug design," *PLoS Computational Biology*, vol. 5, no. 10, Article ID e1000550, 2009.

[41] A. S. Haqqani, M. Nesic, ED. Preston, E. Baumann, J. Kelly, and D. Stanimirovic, "Characterization of vascular protein expression patterns in cerebral ischemia/reperfusion using laser capture microdissection and ICAT-nanoLC-MS/MS," *FASEB Journal*, vol. 19, no. 13, pp. 1809–1821, 2005.

[42] A. Dodelet-Devillers, R. Cayrol, H. J. Van et al., "Functions of lipid raft membrane microdomains at the blood-brain barrier," *Journal of Molecular Medicine*, vol. 87, no. 8, pp. 765–774, 2009.

[43] R. Cayrol, A. S. Haqqani, I. Ifergan, A. Dodelet-Devillers, and A. Prat, "Isolation of human brain endothelial cells and characterization of lipid raft-associated proteins by mass spectroscopy," *Methods in Molecular Biology*, vol. 686, pp. 275–295, 2011.

[44] Z. Mamdouh, A. Mikhailov, and W. A. Muller, "Transcellular migration of leukocytes is mediated by the endothelial lateral border recycling compartment," *Journal of Experimental Medicine*, vol. 206, no. 12, pp. 2795–2808, 2009.